Characterization of mutations identified in patients historically diagnosed with type 1 Von Willebrand disease

Nasher H. Alyami

Thesis Submitted for the Degree of Doctor of Philosophy

Faculty of Medicine, Dentistry and Health

Department of Cardiovascular Science

Haemostasis Research Group

March 2014

Dedication

This research work is dedicated to my late father, who gave me a solid foundation for my chosen career. Also to my great mother, my brothers and sisters for their prayers, love, support and encouragement throughout my study. To my devoted wife for her support and patience. To my Lovely children Ibraheem, Lorin, Hamad and Zaid.

Acknowledgement

In the name of Allah Most Gracious and Most Merciful, first of all, i would like to express my sincere gratitude and thanks to my supervisors, Prof. Anne Goodeve and Dr. Daniel Hampshire for their advice, help and encouragement, for their contributions in preparing my project and for their valuable and impressive comments during the course of my project and during thesis writing.

I would also like to express special thanks to Dr. Ian Peak and Dr. Martina Daly for their advice and guidance during my project.

I am deeply indebted to my colleague Ashley Cartwright for his continuous advice, support and helpful discussion especially in the expression aspect during my laboratory work.

I must also express my thanks to my colleagues of Hemostasis Research Group; Dr. Vincenzo Leo, Mr. Essa Sabi, Mr. Ahmed Mofti and Mr. John Anson for their kindness and support during the period of my project.

I wish particularly to thank others, who have helped me in my project especially Core Facility technicians Mr. Steve Haynes and Mrs. Helen for their technical support and assistance. Also, I would like to express my thanks to Dr. Colin Gray for his assistant during confocal microscopy.

Moreover, I would like to acknowledge Saudi Arabia Government presented by Ministry of Health for giving me the scholarship opportunity and sponsoring my PhD study.

Finally, I have to express my joy and happiness to my entire family members and all my friends in Sheffield and in Saudi Arabia.

Abstract

von Willebrand disease (VWD) is the most common autosomal congenital bleeding disorder in humans results from either quantitative deficiencies in the level of plasma glycoprotein von Willebrand factor (VWF) (type 1 and type 3) or qualitative deficiencies (type 2). Type 1 VWD the commonest VWD variant is characterized by mucocutaneous bleeding and a partial quantitative deficiency of plasma VWF. Previous analysis of an EU VWD1 family cohort undertook mutation scanning and sequencing of the *VWF* gene in 150 index cases (IC), but failed to detect mutations in ~33% IC. Single nucleotide polymorphisms (SNP) within primer annealing sites leading to lack of mutant allele amplification or insensitivity of mutation scanning methods may explain this failure. In this study, *VWF* 18 IC were re-analysed where phenotype suggested that mutations may have been missed using newly designed primers free of SNP underneath their annealing sites and direct sequencing.

Mutational analysis of 18IC led to the identification of heterozygous mutations in four families; missense mutations c.6811T>G; p.W2271G (in compound heterozygosity with c.2811G>A;p.R854Q) and c.3469T>C;p.C1157R (in compound heterozygosity with c.1614del;p.S539Lfs*38), silent mutation c.4146G>T;p.L1382= and splice mutation c.1432+1G>T (in compound heterozygosity with c.2446C>T;p.R816W).

p.W2271G, p.C1927R and p.C1157R mutations affect fully conserved residues, predicted to be damaging by *in silico* analysis, p.L1382= predicted to alter splicing exonic enhancer (ESE) and c.1432+1G>T predicted to produce a null allele. These identified mutations appeared to be segregated with disease phenotype. Mutations were missed due to insensitivity of mutation analysis method (c.6811T>G) and SNP within primer annealing sites (c.3469T>C and c.1432+1G>T). In addition to the mutations identified, *in vitro* expression of two previously identified changes was also undertaken (the two mutations were c.2771G>A;p.R924Q and c.5779T>C;p.C1927R and were found in one IC).

In vitro expression data indicates that missense mutations p.C1157R, p.C1927R and p.W2271G located in D3 and D4 assemblies resulted in in significantly reduced secretion of VWF levels with significantly increased intracellular retention, abnormal intracellular storage and abnormal multimers, but p.R924Q showed normal expression. Also, reduced secretion in p.W2271G and p.C1927R appeared to be due to dominant-negative mechanism. p.L1382= revealed a significant defect of secreted VWF which may be due to its impact on mRNA translation rate. Silent change may contribute to VWF deficiency through alteration protein folding or

destroying splicing regulatory elements (SRE) that mediates exon skipping resulting in truncated protein. The expression of p.S539Lfs*38 resulted to significant defect of secreted VWF due to nonsense mediated decay (NMD). Results raised from *in vitro* expression found to be correlated with phenotypes observed in patients with identified mutations. This study has provided insight into the pathogenicity of type 1 VWD.

Contents

Abstract I

List of tables IX

List of figures XII

List of Abbreviations XVI

1. Introduction 1

1.1. Epidemiology and clinical features of von Willebrand disease 1

1.2. History of von Willebrand disease 1

1.3. The molecular biology of von Willebrand factor 2

1.3.1. The *VWF* gene 2

1.3.2. The VWF protein 3

1.4. Biosynthesis of VWF 6

1.4.1. Dimerisation 6

1.4.2. Glycosylation of VWF in ER 8

1.4.4. VWF multimerisation 10

1.5. Functional domains of VWF 11

1.6. Storage and function of von Willebrand factor 11

1.6.1. Platelet plug formation 11

1.6.2. Binding with FVIII 12

1.7. Cleavage of HMW multimers 14

1.8. Diagnosis of von Willebrand disease 14

1.8.1. Clinical diagnosis of von Willebrand disease 15

1.8.2. Laboratory diagnosis of VWD 16

1.8.2.1. Screening tests for diagnosing VWD 16

1.8.2.2. Specific laboratory studies 17

1.8.2.2.1. VWF antigen assay (VWF:Ag) 17

1.8.2.2.2. VWF ristocetin co-factor activity (VWF:RCo) 17

1.8.2.2.3. FVIII activity (FVIII:C) 18

1.8.3. Laboratory tests for VWD classification 18

1.8.3.1. VWF multimeric analysis 18
1.8.3.2. Ristocetin-induced platelet aggregation (RIPA) 18
1.8.3.3. VWF:FVIII binding assay (VWF:FVIIIB) 19
1.8.3.4. VWF-collagen binding assay (VWF:CB) 19
1.8.3.5. The ratio of VWF pro-peptide to mature VWF (VWFpp/VWF:Ag) 19
1.8.3.6. Molecular analysis of *VWF* gene 20
1.8.3.7 Factors that make diagnosis of type 1 VWD difficult 20
1.9. Classification of von Willebrand disease 20
1.9.1. Type 3 VWD 22
1.9.2. Type 2 von Willebrand disease 23
1.9.2.1. Type 2A VWD 23
1.9.2.2. Type 2B VWD 25
1.9.2.3. Type 2M VWD 25
1.9.2.4. Type 2N VWD 26
1.9.3. Type 1 VWD 26
1.9.3.1. Type 1 VWD mutational cohort studies 27
1.9.3.1.1. The European Union study on type 1 VWD 28
1.9.3.1.2. Reasons for failure to detect mutations 30
1.9.3.1.2.1. Missed mutations 30
1.9.3.1.2.2. Misdiagnosis of type 1 VWD 31
1.9.3.1.2.3. Heterozygous copy number variation (CNV) 31
1.9.3.1.2.4. Other genetic loci may contribute to VWD 32
1.9.3.1.2.5. Single nucleotide polymorphism within *VWF* 35
1.9.3.2. Type 1 VWD mutation mechanisms 35
1.9.3.2.1. Reduced secretion and intracellular retention of VWF 36
1.9.3.2.2. Clearance of VWF in plasma 36
1.9.3.2.3. Increased susceptibility to proteolytic cleavage 37
1.10. Environmental and genetic factors affect level of VWF 37
1.11. Aim of study 38

2. Materials and methods 41
2.1. Materials 41
2.1.1. Patient population and samples 41
2.1.2. Chemicals, reagents, kits and enzymes 41
2.1.3. Primers 42
2.2. Methods 42
2.2.1. PCR primer design and SNP check 42
2.2.2. Polymerase chain reaction (PCR) amplification of *VWF* 43
2.2.2.1. Conventional PCR 44
2.2.2.2. DNA amplification of *VWF* 44
2.2.2.3. Long-range PCR 45
2.2.2.4. Agarose gel electrophoresis 45
2.2.3. PCR product purification 46
2.2.4. DNA sequencing analysis 47
2.2.4.1. Principle of DNA sequencing 47
2.2.4.2. Sequence analysis 48
2.2.4.2.1. Staden sequence analysis 48
2.2.5. Prediction of the effect of amino acid substitutions on protein function 48
2.2.6. *In silico* splice-site prediction 49
2.2.7. *In silico* prediction of exonic splice enhancers and silencers 49
2.2.8. Multiple sequence alignment (Evolutionary Conservation) 49
2.2.9. Model structure of the protein 50
2.2.10. Graphical codon usage analysis 50
2.2.11. Nomenclature and numbering of *VWF* sequence 50
2.2.12. Generation of VWF mutant plasmids 51
2.2.12.1. VWF expression plasmid 51
2.2.12.1.2. Structure of pcDNA3.1/Hygro (-) 52
2.2.12.2. Transformation into NM554 *E.coli* competent cells 54
2.2.12.3. Mutagenic primer design 54

2.2.12.4. Transformation of XL10-Gold ultracompetent cells 56
2.2.12.5. Purification of plasmid DNA using mini-prep 57
2.2.12.5.1 DNA sequence alignment 58
2.2.12.6. Preparation of glycerol stock 58
2.2.12.7. Measurement of plasmid DNA concentration using the NanoDrop spectrophotometer 58
2.2.12.8. Purification of large scale plasmid DNA using maxi-prep 59
2.2.13. *In vitro* expression of *VWF* mutants 60
2.2.13.1. Culture of HEK293T cells 60
2.2.13.2. Cell thawing 60
2.2.13.3. Passaging HEK293T cells 61
2.2.13.4. Cell counting 61
2.2.13.5. Transient transfection and *in vitro* expression using Lipofectamine LTX 61
2.2.13.5.1. Inhibition of proteosome activity of transfected HEK293T cells 64
2.2.13.6. Collection of cell culture supernatant and cell lysate 64
2.2.14. Measurement of expressed VWF using ELISA 64
2.2.14.1. Principle of ELISA 64
2.2.14.2. ELISA Procedure 65
2.2.14.3. ELISA data analysis 67
2.2.15. Statistical analysis 67
2.2.16. Multimer analysis 68
2.2.17. Immunofluorescence analysis 68
2.2.17.1. Immunofluorescence staining 68
3. Sequence re-analysis of VWF in the EU-MCMDM-1VWD study 71
3.1. Introduction 71
3.2. Primer design and SNP screen 74
3.3. PCR optimisation 76
3.3.1. Specific exon optimisation 76
3.3.1.1 Exon 28 76

3.4. Confirmation of *VWF* amplification 77
3.5. *VWF* amplification and sequencing 79
3.6. Identified VWF mutations and polymorphisms 79
3.6.1. Mutation result in family P5F1 80
3.6.1.1. Linkage and mutation analysis in family P5F1 83
3.6.1.2. p.W2271G protein prediction and multiple species alignment 85
3.6.2. Mutation analysis in P9F18 family 86
3.6.2.1. Linkage analysis and mutation study in family P9F18 88
3.6.2.2. p.C1157 protein predictions and multiple species alignment 90
3.6.3. Mutation analysis in family P10F5 91
3.6.3.1. Linkage analysis and mutation study in family P10F5 92
3.6.3.2. *In silico* splice-site prediction 94
3.6.4. Splice mutation c.1432+1G>T and linkage analysis in P10F8 family 95
3.6.4.1. Review of linkage analysis and mutation in P10F8 family 98
3.6.4.2. *In silico* splice site prediction 100
3.6.5. Confirmation of the presence of mutations previously identified 100
3.6.5.1. Mutation analysis in family P9F14 100
3.6.5.1. Linkage analysis and mutation study in family P9F14 101
3.6.5.2. *In silico* predictions 103
3.7. Discussion 105
4. *In vitro* expression of type 1 VWD candidate mutations 118
4.1. Introduction 118
4.2. Results 121
4.2.1. Confirmation of wild type VWF cDNA sequence 121
4.2.2. Efficiency of site-directed mutagenesis and transformation 122
4.2.3. Mutagenesis 123
4.2.4. *In vitro* expression of recombinant VWF containing the candidate mutations 125
4.2.5. Quantitative analysis of supernatant and cell lysates following transfection of HEK293T cells with rVWF-WT and mutant plasmid (rVWF-G2271) 126

4.2.5.1. Multimer analysis of expressed mutation 128

4.2.5.1.1. Multimer analysis for the p.W2271G VWF protein secreted from HEK293T cells. 129

4.2.5.2. Immunofluorescence staining and confocal microscopy imaging of expressed mutations 130

4.2.5.2.1. Confocal microscopy of p.W2271G 131

4.2.5.2.2. Confocal microscopy of p.W2271G to determine retention of VWF in the ER..... 133

4.2.6. *In vitro* expression of recombinant VWF containing the candidate mutations p.R924Q and p.C1927R 135

4.2.6.1. Quantitative analysis of supernatant and cell lysates following transfection of HEK293T cells with rVWF-WT and mutant plasmid (rVWF-Q924) 135

4.2.6.1.1. Multimer analysis for the p.R924Q VWF protein secreted from HEK293T cells.... 137

4.2.6.2. Quantitative analysis of supernatant and cell lysates following transfection of HEK293T cells with rVWF-WT and mutant plasmid (rVWF-R1927) 140

4.2.6.3. Quantitative analysis of supernatant and cell lysates following transfection of HK293T cells with rVWF-WT and mutant plasmid rVWF [R1927;Q924]..... 142

4.2.6.3.1. Multimer analysis for the rVWF-R1927 and rVWF [R1927;Q924] rVWF protein secreted from HEK293T cells..... 144

4.2.6.3.2. Confocal microscopy of p.C1927R and p.[C1927R;R924Q] 145

4.2.6.3.3. Confocal microscopy of p.C1927R and p.[C1927R:R924Q] to determine retention of VWF in the ER..... 148

4.3. Discussion 151

4.3.1. *In vitro* expression of p.W2271G..... 151

4.3.2. *In vitro* expression of p.C1927R 154

4.3.3. *In vitro* expression of p.R924Q..... 155

4.3.4. *In vitro* expression of p.[R924Q;C1927R]..... 158

4.3.5. Conclusion 159

5. *In vitro* expression of non-type 1 VWD..... 161

5.1. Introduction..... 161

5.2. Results..... 163

5.2.1. Mutagenesis 163

5.2.2. *In vitro* expression of recombinant VWF containing the candidate mutations p.C1157R and p.S539Lfs*38 164

5.2.3. Quantitative analysis of supernatant and cell lysates following transfection of HEK293T cells with rVWF-wild-type and mutant plasmid (rVWF-R1157) 164

5.2.3.1. Multimer analysis for the p.C1157R VWF protein secreted from HEK293T cells 166

5.2.3.2. Confocal imaging of p.C1157R 167

5.2.3.2.1. Confocal microscopy of p.C1157R to determine retention of VWF in the ER 169

5.2.4. Quantitative analysis of supernatant and cell lysates following transfection of HEK293T cells with rVWF-wild-type and mutant plasmid (rVWF-L539fs) 171

5.2.4.1. Multimer gel analysis for the p.S539fs VWF protein secreted from HEK293T cells . 175

5.2.4.2. Confocal imaging of p.S539fs 176

5.2.5. Quantitative analysis of supernatant and cell lysates following transfection of HEK293T cells with rVWF-wild-type and mutant plasmids rVWF [R1157];[L539fs 178

5.2.5.1. Multimer analysis for the rVWF [R1157];[L593fs] protein secreted from HEK293T cells 180

5.2.5.2. Confocal imaging of p.[S539fs];[C1157R] 181

5.3. Discussion 183

5.3.1. *In vitro* expression of p.C1157R 183

5.3.2. *In vitro* expression of c.1614del; p.S539Lfs*38 186

5.3.3. *In vitro* co-expression of p.[S539fs];[C1157R] 189

6. *In vitro* characterisation of silent mutation associated with type 1 VWD 193

6.1. Introduction 193

6.1.1. Effect of synonymous mutation on normal splicing pathway 194

6.1.2. Effect of synonymous mutation on translation rate and protein folding 197

6.1.3. Hypothesis and aims 198

6.2. Results 199

6.2.1. Graphical codon usage 199

6.2.2. Location of p.L1382= in VWF 200

6.2.4. *In vitro* expression of *rVWF* harbouring the candidate mutation p.L1382= 203

6.2.4.1. Quantitative analysis of the expressed rVWF-WT and mutant plasmid (c.4146G>T; rVWF-L1382) transfected into HEK293T cells 203

6.2.4.2. Multimer analysis of wild-type and c.4146G>T; p.L1382= VWF secreted from HEK293T cells 205

6.2.4.3. Confocal microscopy imaging of c.4146 206

6.2.4.3.1. Confocal microscopy of c.4146G>T; p.L1382= 206

6.2.5. Quantitative analysis of the expressed rVWF-WT and hypothetical mutant plasmid (rVWF-c.4146G>A; p.L1382=) transfected into HEK293T cells 208

6.2.5.1. Multimer analysis of wild-type and c.4146G>A; p.L1382= rVWF protein secreted from HEK293T cells 210

6.2.5.2. Confocal microscopy of c.4146G>A; p.L1382= 211

6.2.6. Quantitative analysis of the expressed rVWF-WT and mutant plasmid (rVWF-c.4146G>C; p.L1382=) transfected into HEK293T cells 213

6.2.6.1. Multimer analysis of wild-type and c.4146G>C; p.L1382= rVWF protein secreted from HEK293T cells 215

6.2.6.2. Confocal microscopy of c.4146G>C; p.L1382= 216

6.3. Discussion 218

6.3.1. *In vitro* expression of c.4146G>T;p.L1382= 218

6.3.2. *In vitro* expression of c.4146G>A and c.4146G>C mutants 219

7. Discussion 225

7.1. Future work 229

8. References 236

9. APPENDICES 262

List of tables

Table 1.1	Genes associated with variation in the level of VWF and their location……	33
Table 1.2	List of studies conducted on mice demonstrated VWF variability ……	34
Table 2.1	Preparation of the pWhitescript mutagenesis control reaction……	56
Table 2.2	Summary of transfection method……	63
Table 3.1	Phenotypic data for 18 ICs……..	73
Table 3.2	List of candidate missed and previously mutations identified in this study…	80
Table 3.3	List of 20 known heterozygous SNP in IC P5F1II:3……..	81
Table 3.4	Phenotypic data for family P5F1…….	84
Table 3.5	Prediction methods used for amino acid substitution with prediction score...	85
Table 3.6	List of 23 known heterozygous SNP in the IC P9F18I:1……	87
Table 3.7	Identified SNP underlying the primer annealing sites for the VWF exon 26 Primers…….	88
Table 3.8	Phenotypic data for family P9F18……...	89
Table 3.9	Prediction methods used for amino acid substitution with prediction score and range of scores for each tool…….	90
Table 3.10	List of 27 known heterozygous SNP in IC P10F5II:2……	91
Table 3.11	Phenotypic data for family P10F5……...	93
Table 3.12	In silico prediction of effect of c.4146G>T in splice regulatory elements….	94
Table 3.13	List of 22 known heterozygous SNP in IC P10F8II:1……	96
Table 3.14	Initial phenotypic data for family P10F8……	97
Table 3.15	Identified SNP underlying the primer annealing site for the VWF exon 12 Primer……	97
Table 3.16	The new SNP markers used for linkage analysis……	98
Table 3.17	Phenotypic data for family P10F8 after modification…….	99
Table 3.18	In silico prediction tools to determine the effects of c.1432+1G>T……...	100
Table 3.19	Phenotypic data for family P9F14……...	102
Table 3.20	In silico prediction tools to determine the effects of c.1533+1G>T……...	104
Table 4.1	List of SNP identified in full length VWF cDNA……...	122
Table 4.2	The mean values and standard deviation of secreted VWF:Ag levels for WT and mutant plasmids rVWF-G2271……	127

Table 4.3	The mean values and standard deviation of retained VWF:Ag levels for WT and mutant plasmids rVWF-G2271……	127
Table 4.4	The mean values and standard deviation of secreted VWF:Ag levels WT and mutant plasmids rVWF-Q924……	136
Table 4.5	The mean values and standard deviation of retained VWF:Ag levels for WT and mutant plasmids rVWF-Q924……	136
Table 4.6	The mean values and standard deviation of secreted VWF:Ag levels for WT and mutant plasmids rVWF-R1927…….	141
Table 4.7	The mean values and standard deviation of retained VWF:Ag levels for WT and mutant plasmids rVWF-R1927…….	141
Table 4.8	The mean values and standard deviation of secreted VWF:Ag levels WT and mutant plasmids rVWF-R1927+R924Q……	143
Table 4.9	The mean values and standard deviation of retained VWF:Ag levels for WT and mutant plasmids rVWF-R1927+R924Q……	143
Table 4.10	List of publications relevant to p.R924Q variant……	158
Table 5.1	The mean values and standard deviation of secreted VWF:Ag levels wild-type and mutant plasmids rVWF-R1157……	165
Table 5.2	The mean values and standard deviation of retained VWF:Ag levels for wild-type and mutant plasmids rVWF-R1157…….....	165
Table 5.3	The mean values and standard deviation of secreted VWF:Ag levels wild-type and mutant plasmids rVWF-L539fs……...	172
Table 5.4	The mean values and standard deviation of retained VWF:Ag levels for wild-type and mutant plasmids rVWF-L539fs……	172
Table 5.5	The expression mean values of secreted and retained VWF using proteosome inhibitor in the heterozygous and homozygous states……	173
Table 5.6	The mean values and standard deviation of secreted VWF:Ag levels for WT and mutant plasmids rVWF-R1157 and L539fs……	179
Table 5.7	The mean values and standard deviation of retained VWF:Ag levels for both mutant plasmids rVWF-R1157 and L539fs……	179
Table 6.1	List of the possible mechanisms that could be involved in silent mutation…	193
Table 6.2	The mean values and standard deviation of secreted VWF:Ag levels for WT and mutant plasmids rVWF-L1382=……	204
Table 6.3	The mean values and standard deviation of retained VWF:Ag levels for WT and mutant plasmids (rVWF-L1382=……	204
Table 6.4	The mean values and standard deviation of secreted VWF:Ag levels for WT and mutant plasmids rVWF-c.4146G>A; p.L1382=……	209

Table 6.5 The mean values and standard deviation of retained VWF:Ag levels for WT and mutant plasmids rVWF-c.4146G>A; p.L1382=…… 209
Table 6.6 The mean values and standard deviation of secreted VWF:Ag levels for WT and mutant plasmids rVWF-c.4146G>C; p.L1382=…… 214
Table 6.7 The mean values and standard deviation of retained VWF:Ag levels for WT and mutant plasmids rVWF-c.4146G>C; p.L1382=…… 214
Table 6.8 Wobble hypothesis…….. 219

List of figures

Figure 1.1	Schematic representation of the VWF protein and encoding exons.....	4
Figure 1.2	Schematic representation showing the intracellular synthesis of HMW-VWF…….....	7
Figure 1.3	The role of VWF in platelet aggregation and clot formation……..	13
Figure 1.4	Flow chart showing the aim and plan of the study……..	40
Figure 2.1	Site directed mutagenesis (SDM) method……...	52
Figure 2.2	Map of pcDNA 3.1/Hygro used as expression vector…….	53
Figure 2.3	A schematic representation of the co-transfection protocol……	63
Figure 2.4	Diagram showing the principle of the ELISA technique……	66
Figure 2.5	Summary of double serial dilution……..	67
Figure 3.1	Flow chart shows the selection criteria for VWD IC recruited in this study..	72
Figure 3.2	Alignments between VWF and PVWF and mismatch locations (exon31)….	75
Figure 3.3	Amplification of exon 27 on a 1% agarose gel……...	77
Figure 3.4	Amplification of exon 32 on a 1% agarose gel……...	78
Figure 3.5	Amplification of exon 28 on a 1% agarose gel……...	78
Figure 3.6	Chromatogram of part of VWF exon 32 indicating mismatch sites between *VWF* and *VWFP*……	79
Figure 3.7	Heterozygous c.6811T>G point mutation in P5F1…….	82
Figure 3.8	Chemical structures of amino acids A (tryptophan) and B (glycine)……..	82
Figure 3.9	Sequence analysis results of family P5F1II:3…….	83
Figure 3.10	Pedigree of family P5F1 showing linkage analysis and mutation results…..	84
Figure 3.11	Schematic representation of the evolutionary conservation of p.W2271……	86
Figure 3.12	Heterozygous c.3469T>C point mutation in P9F18 family……	87
Figure 3.13	Pedigree of family P9F18……	89
Figure 3.14	Schematic representation of the evolutionary conservation of p.C1157…….	90
Figure 3.15	Heterozygous c.4146G>T point mutation in P10F5 family……	92
Figure 3.16	Pedigree of family P10F5……	93
Figure 3.17	The relative frequency values of normal codon CTG and mutant CTT……..	95
Figure 3.18	Sequence chromatogram analysis results of family P10F8…….	96
Figure 3.19	Initial pedigree of family P10F8…….	97

Figure 3.20	Revised pedigree of family P10F8……..	99
Figure 3.21	Pedigree of family P9F14……	102
Figure 3.22	Schematic representation of the evolutionary conservation of p.C1927…….	103
Figure 4.1	Sequence chromatographs to show introduction of novel variants into the cDNA VWF plasmid……	124
Figure 4.2	VWF standard ELISA curve……...	126
Figure 4.3	Expression of p.W2271G……	127
Figure 4.4	Multimer analysis of secreted p.W2271G……...	129
Figure 4.5	Intracellular storage of rWT and rVWF-G2271 mutant……..	132
Figure 4.6	Intracellular localisation of VWF in rWT and rVWF-G2271 mutant…….	134
Figure 4.7	Expression of p.R924Q……...	136
Figure 4.8	Multimer analysis of rVWF p.R924Q…….	137
Figure 4.9	Intracellular storage of rWT and rVWF-Q924 mutant……	139
Figure 4.10	Expression of p.C1927R…….	141
Figure 4.11	Expression of p.[C1927R;R924Q]……..	143
Figure 4.12	Multimer analysis of secreted p.C1927R (A) and p.[C1927R;R924Q] (B) Mutants……	144
Figure 4.13	Intracellular storage of rWT and r-VWF-R1927 mutant……	146
Figure 4.14	Intracellular storage of rWT and rVWF-R1927+Q924mutant……	147
Figure 4.15	Intracellular localisation of VWF in rWT and rVWF-R1927 mutant…….	149
Figure 4.16	Intracellular localisation of VWF in rWT and rVWF-R1927+Q924 mutant..	150
Figure 5.1	Sequence chromatographs show introduction of novel variants into the cDNA VWF plasmid……	163
Figure 5.2	Expression of p.C1157R…….	165
Figure 5.3	Multimer analysis of secreted p.C1157R……	166
Figure 5.4	Intracellular storage of rWT and rVWF-R1157 mutant…….	168
Figure 5.5	Intracellular localisation of VWF in rWT and rVWF-R1157 mutant……..	170
Figure 5.6	Expression of p.S539Lfs*38……...	172
Figure 5.7	*In vitro* expression of p.S539fs using proteosome inhibitor……...	174
Figure 5.8	Multimer analysis of secreted p.S539fs……..	175
Figure 5.9	Intracellular storage of rWT and rVWF-L539fs mutant…….	177
Figure 5.10	Expression of p.[C1157R];[S539fs]……	179
Figure 5.11	Multimer analysis of secreted rVWF-R1157 /rVWF-L539fs…….	180
Figure 5.12	Intracellular storage of rWT and rVWF-L539fs + R1157 mutants…….	182

Figure 6.1	Schematic representations of normal and defective DNA transcription and Translation……	195
Figure 6.2	Frequencies of triplet codon usage that encode leucine……..	199
Figure 6.3	Pymol model of the 3D structural location of p.L1382= in the VWF A1 Domain……	200
Figure 6.4	Sequence chromatographs shows introduction of silent variants into the cDNA VWF plasmid……	202
Figure 6.5	Expression of c.4146G>T;p.L1382=……...	204
Figure 6.6	Multimer analysis of secreted rVWF-c.4146G>T; p.L1382=…….	205
Figure 6.7	Intracellular storage of rWT and rVWF-L1382 mutant……..	207
Figure 6.8	Expression of c.4146G>A;p.L1382=……..	209
Figure 6.9	Multimer analysis of secreted rVWF c.4146G>A; p.L1382=…….	210
Figure 6.10	Intracellular storage of rWT and rVWF-c.4146G>A;L1382 Mutant…….	212
Figure 6.11	Expression of c.4146G>C;p.L1382=……..	214
Figure 6.12	Multimer analysis of secreted rVWF-c.4146G>C; p.L1382=……	215
Figure 6.13	Intracellular storage of rWT andrVWF- c.4146G>C;L1382 Mutant…..……..	217

Publications and presentations raised from this study

- Alyami N, Hampshire D, Goudemand J, Castaman G, Federici AB, Cartwright A, Peake I, Goodeve A on behalf of the EU-VWD & ZPMCB-VWD study groups. Previously Missed Mutations in the MCMDM-1VWD Type 1 von Willebrand Disease Study. Journal of Thrombosis and Haemostasis 2013; Volume 11, Supplement 2: Abstract PA 3.09-4. Poster presentation at the XXIV Congress of the International Society on Thrombosis and Haemostasis in Amsterdam, Netherlands, June 29-July 4, 2013.

- Alyami N, Hampshire D, Goudemand J, Castaman G, Federici AB, Peake I, Goodeve A. Missing Mutations in Type 1 von Willebrand Disease in the MCMDM-1VWD Study. Journal of Thrombosis and Haemostasis 2011. Oral presentation at the British Society of Haemostasis and Thrombosis and UKHCDO Annual Scientific Meeting in Brighton, UK, 3-5 October 2011.

- Alyami N, Hampshire D, Goudemand J, Castaman G, Federici AB, Peake I, Goodeve A on behalf of the EU-VWD & ZPMCB-VWD study groups. Missing Mutations in Type 1 von Willebrand Disease in the MCMDM-1VWD Study. Journal of Thrombosis and Haemostasis 2011; Volume 9, Supplement 2: Abstract P-TH-464. Poster Presentation at the XXIII Congress of the International Society on Thrombosis and Haemostasis in Kyoto, Japan, 2011.

- Alyami N, Goodeve, A. Previously missed mutations in the MCMDM-1VWD type 1 von Willebrand disease study. Oral presentation in 3rd Year Graduate Presentation Day, Sheffield Medical School, Sheffield, UK, 10th June 2013.

- Alyami N, Hampshire D, Peake I, Goodeve A. Missing Mutations in Type 1 von Willebrand Disease in the MCMDM-1VWD Study. Poster Presentation at the Medical School Research Meeting, Sheffield, UK, 11th -12th June 2012.

- Alyami N, Hampshire D, Peake I, Goodeve A. Molecular mechanisms in the pathogenesis of type 1 von Willebrand disease. Poster Presentation at the Medical School Research Meeting, Sheffield, UK, 20th -21st June 2011.

- Alyami N, Goodeve, A. Molecular mechanisms in the pathogenesis of type 1 von Willebrand disease Oral presentation in 1st Year Graduate Presentation Day, Sheffield Medical School, Sheffield, UK, 10th May 2011.

List of Abbreviations

α	Alpha
A	Adenine
AA	Amino acid
ABI	Applied Biosystems Inc
ABO	ABO blood group
aCGH	Array comparative genomic hybridisation
ADAMTS13	A disintegrin and metalloproteinase with a thrombospondin type 1 motif member 13
ADP	Adenosine 5'-diphosphate
AFM	Affected family member
Amp R	Ampicillin resistant
ANOVA	Analysis of variance
Approx	Approximately
APTT	Activated partial thromboplastin time
ATP	Adenosine tri-phosphate
AtT-20 cells	Pituitary adenoma cell line
ß	Beta
B	Blank
BGH pA	Bovine growth hormone polyadenylation
ß-ME	ß-mecraptoethanol
bp	Base pair
BOEC	Blood outgrowth endothelial cells
BRCA2	Breast and ovarian cancer gene
BS	Bleeding score
BSA	Bovine serum albumin
BTS	Blood transfusion services
C	Cytosine
C8	Cysteine 8
°C	Celsius
c.	Nucleotide alteration position using HGVS nomenclature
$CaCl_2$	Calcium chloride
CCD	Charge coupled device
cDNA	Coding DNA

cfu	Colony forming units
CGLC	Cysteine-Glycine-Leucine-Cysteine
CHARGE	Cohorts for heart and aging research genome epidemiology
CK	Cysteine knot
CLEC4M	C-type lectin domain family, member M
cm	Centimetre
cMV	Cytomegalo virus
CNX	Calnexin
CNV	Copy number variation
CO_2	Carbon dioxide
COS-7	Monkey kidney tissue culture cell line
CRT	Calreticulin
CSGE	Conformation sensitive gel electrophoresis
CVD	Cardio vascular disease
Cys	Cysteine
D	Domain of VWF
DAP	Diaminophenazine
DDAVP	Desmopressin
ddH_2O	Double deionized water
ddNTP	Didioxynucleotide triphosphate
Del	Deletion
dHPLC	Denaturing high pressure liquid chromatography
dH_2O	Deionized water
dGTP	Deoxyguanosine triphosphate
DMEM	Dulbecco's modified Eagle's medium
DNA	Deoxyribonucleic acid
dNTP	Deoxynucleotide triphosphate
DRD2	Dopamine receptor D2
dsDNA	Double strand DNA
dTTP	Thymidine triphosphate
dL	Decilitre
EB	Ethidium bromide
EB	Elution buffer
EBNA	Epstein-Barr virus nuclear antigen
EBS	Epidermolysis bullosa simplex
E.coli	Escherichia coli

*Eco*RI	*E.coli* endonuclease restriction enzyme
EDTA	Ethylenediamine tetra acetic acid
EJC	Exon-exon junction complex
ELISA	Enzyme linked immunosorbant assay
ER	Endoplasmic reticulum
ESE	Exonic splice enhancer
ESR1	Estrogen receptor gene
ESS	Exonic splice silencer
EU	European Union
Ex	Exon
Exo I	Exonuclease I
F	Family, Forward
f1 ori	Phage origin
FBS	Foetal bovine serum
F-CSGE	Fluorescent conformation sensitive gel electrophoresis
fs	Frameshift mutation
FUT3	Fucosyltransferase 3 gene
FVII	Factor VII
FVIII	Factor VIII
FVIII:C	Factor VIII coagulant activity
FVIII/VWF:Ag	Factor VIII to von Willebrand factor antigen ratio
FIX	Factor IX
G	Guanine
g	Gram
g	Gravitational force
GA	Golgi apparatus
GAIT	Genetic analysis of idiopathic thrombophilia
GCUA	Graphical codon usage analyser
Gly	Glycine
GP	Glycoprotein (platelet receptor)
GPCR	G-protein coupled receptor gene
GpIbα	platelet glycoprotein
GVGD	Align Grantham variation Grantham deviation
HC	Healthy control
HCl	Hydrochloric acid
HEK293T	Human embryonic kidney culture cell line

Het	Heterozygous
HEPES	Hydroxyethy-l-piperazine-1-ethanesulfonic acid sodium salt
HGNC	HUGO Gene Nomenclature Committee
HGVS	Human Gene Variation Society
H_2O_2	Hydrogen peroxide
Hom	Homozygous
hr	Hour
HSF	Human splice finder
H_2SO_4	Sulfuric acid
HUGO	Human Genome Organization
HMW	High molecular weight
IC	Index case
ISTH-SSC	Scientific and Standardization Committee of the International Society on Thrombosis and Haemostasis
Ins	Insertion
Int	Intron
IPTG	Isopropyl-1-thio-ß-D-galactopyranoside
ISE	Intronic splicing enhancer
IU/dl	International unit per decilitre
Kb	Kilobase
LB broth	Luria-Bertani broth
Leu	Leucine
LIA	Latex immunoassay
LR	Long range
M	Size marker
MCAD	Medium-chain acyl-CoA dehydrogenase
MCMDM-1VWD	Molecular and Clinical Markers for the Diagnosis and Management of Type 1 von Willebrand Disease
MDR1	Membrane-bound transporter gene
MES	MaxEntScan: scorsplice
Mg	Milligram
$MgCl_2$	Magnesium chloride
Min	Minute
miRNA	MicroRNA
mL	Millilitre
MLH1	mutL homolog 1 gene

MLPA	Multiplex-ligation-dependent probe amplification
mM	Milli molar
mRNA	Messenger RNA
Mut	Mutant
Mvwf	Mouse von Willebrand factor gene
ng	Nanogram
N	N terminal
N/A	Not applicable
n	Number
Na_2CO_3	Sodium carbonate
$NaHCO_3$	sodium bicarbonate
Na_2HPO_4	Sodium hydrogen phosphate
NCBI	National Centre for Biotechnology Information
NetGene2	Splice site prediction tool
NH_4	Ammonium
nm	Nanometre
NMD	Nonsense mediated decay
*Not*I	Nocardia otitidis-caviarum restriction enzyme
NRG1	Neuregulin gene
OH	Hydroxide
OD	Optical density
OPD	O-Phenylenediamine
P	Partner
p.	Protein substitution position using HGVS nomenclature
pA	Polyadenylation
PBS	Phosphate buffered saline
PC	Phase contrast
PCR	Polymerase chain reaction
PDI	Protein disulfide-isomerase
PFA	Platelet function assay
pH	Hydrogen ion
Plt	Platelet
pmol	Pico mole
pp	Pro-peptide
PolyPhen	Polymorphism phenotyping
PT	Prothrombin time

PTC	Premature termination codon
P2RY12	Purinergic receptor P2Y, G-protein coupled gene
R	Reverse
RGD	Arginine-Glycine-Asparagine-Serine motif
RIPA	Ristocetin induced platelet aggregation
RNA	Ribonucleic acid
rpm	Rotations per minute
Rs	Mutation reference number
rVWF	Recombinant VWF
SAP	Shrimp alkaline phosphatase
SCARA5	Scavenger receptor class A, member 5
SD	Standard deviation
SDM	Site-directed mutagenesis
SDS	Sodium dodecyl sulphate
Sec	Second
SIFT	Sorting intolerant from tolerant
-SH	Sulfhydryl group
SNP	Single nucleotide polymorphism
SO_4	Sulphate
SP	signal peptide
SSCP	single strand conformation polymorphism
STAB2	Stabilin-2 gene
STR	Short tandem repeat
STXBP5	Syntaxin binding protein 5 gene
STX2	Syntaxin 2 gene
SV40	Simian vacuolating virus 40
T	Thymine
Taq	Thermus aquaticus
TBE	Tris-borate EDTA
TC2N	Tandem C2 domains nuclear protein gene
TGN	Trans-Golgi network
TIL	Trypsin-inhibitor-lik
Tm	Melting temperature
tRNA	Transfer RNA
TTP	Thrombotic thrombocytic purpura
U	Unit

UFM	Unaffected family member
µg	Microgram
UK	United Kingdom
UKHCDO	United Kingdom Haemophilia Centre Doctors' Organisation
µl	Microlitre
µM	Micro molar
USA	United States of America
UTR	Un-translated region
UV	Ultra violet
v	Volume
Vis	Visible
VWD	von Willebrand Disease
VWF	von Willebrand factor gene
VWF	von Willebrand factor protein
VWF:Ag	VWF antigen
VWF:CB	VWF to collagen binding assay
VWF:FVIIIB	VWF-FVIII binding assay
VWF:FVIII	Ratio of VWF to FVIII
VWFpp	von Willebrand factor pro-peptide
VWFpp/VWF:Ag	Ratio of VWF pro-peptide to mature VWF
VWF:RCo	Ristocetin co-factor activity
VWF:RCo/VWF:Ag	Ratio between VWF:RCo/VWF:Ag
VWFP	von Willebrand factor pseudogene
w	Weight
WPB	Weibel-Palade body
WT	Wild-type
w/v	Weight/ volume
X-gal	5-bromo-4-chloro-3-indolyl-ß-D-galactopyranoside

DNA nucleotides and symbols

Nucleotide	Symbol
Adenine	A
Cytosine	C
Guanine	G
Thymine	T
Uracil	U

Amino acids and symbols

Amino acid	Symbol
Alanine	A
Cysteine	C
Aspartic acid	D
Glutamic acid	E
Phenylalanine	F
Glycine	G
Histidine	H
Isoleucine	I
Lysine	K
Leucine	L
Methionine	M
Asparagine	N
Proline	P
Glutamine	Q
Arginine	R
Serine	S
Threonine	T
Valine	V
Tryptophan	W
Tyrosine	Y

Chapter 1
Introduction

1. Introduction

1.1. Epidemiology and clinical features of von Willebrand disease

von Willebrand disease (VWD) has been identified as the most common autosomal congenital bleeding disorder in humans in the last two decades, with prevalence rates ranging between 0.1% and 1.3% in the population according to many epidemiological studies. VWD affects both genders, and occurrence across ethnic groups is approximately equal frequencies (Miller et al., 1987, Rodeghiero et al., 1987, Ruggeri and Zimmerman, 1987, Werner et al., 1993, Sadler et al., 2000, Bowman et al., 2010, Flood et al., 2011, Ghosh and Shetty, 2011).

Gene alterations lead to qualitative and quantitative abnormalities in the von Willebrand factor (VWF) protein in the plasma, and these result in VWD. The disease presents as excess mucocutaneous bleeding, which can be mild to severe depending on the VWD type, in the form of easy bruising, menorrhagia, epistaxis and bleeding post-surgery or trauma (Sadler et al., 2006).

Based on clinical characteristics and laboratory findings, VWD is classified into three primary types: type 1 VWD; type 2 VWD, which is further divided into four secondary subtypes (2A, 2B, 2M and 2N); and type 3 VWD (Sadler, 1994, Sadler et al., 2006).

1.2. History of von Willebrand disease

In 1926, a Finnish physician named Dr. Erik von Willebrand described the first case of VWD in several members of families from Föglo in the Finnish Aland Islands. These individuals presented with significant mucocutaneous bleeding, including easy bruising, menorrhagia and epistaxis. Initially, von Willebrand thought that the bleeding was due to abnormal platelet function, and he described it as “pseudohaemophilia” (von Willebrand, 1926, Ginsburg and Bowie, 1992). In 1950, a reduction in the level of plasma coagulation factor VIII (FVIII) in mucocutaneous bleeding was observed (Graham, 1959, Sadler, 1998). Larrieu and Soulier then found low levels of FVIII and prolonged bleeding times in pseudohemophilia patients, and they proposed the name von Willebrand disease for this condition (Alexander and Goldstein, 1953, Larrieu and Soulier, 1953). In 1963, Salzman demonstrated *in vitro* a decreased adhesiveness of platelets to glass from the blood of patients with VWD. He found that this was normalized with normal plasma (Salzman, 1963, Larrieu et al., 1968, Meyer and Larrieu, 1970). During the 1960s, cases of VWD reported from several countries indicated that the disease was distributed worldwide, and it was defined as an autosomal heritable haemorrhagic disease characterized by a prolonged bleeding time, decreased activity of FVIII, decreased platelet adhesion and a

progressive increase of FVIII activity after the infusion of plasma and FVIII concentrate (Nilsson and Holmberg, 1979). Most cases of types 1, 2A and entirally all 2B and 2M are inherited as autosomal dominant while types 2N and 3 are inherited as autosomal recessive disorders. Many studies suggested that the impaired haemostasis in VWD was due to the lack of a certain plasma protein called VWF. When this factor was infused, it corrected the prolonged bleeding time and increased the level of FVIII. At the Congress of the International Society of Haematology in Rome in 1958 it was asserted that a previously unknown factor in blood had been discovered (Blomback, 1958, Blomback et al., 1964). Then in 1970, through the use of newly developed immunoassays and laboratory techniques, VWF, the carrier of FVIII, was detected, isolated and identified as the cause of VWD. At that time, it was recognized as being distinct from blood coagulation FVIII (Weiss et al., 1973, Ruggeri and Zimmerman, 1980). In 1971, Zimmerman developed an immunologic technique using a polyclonal antibody against VWF and FVIII to distinguish between VWD and haemophilia A (Zimmerman et al., 1971), and in 1985, the *VWF* was cloned by several groups in the United States (Ginsburg et al., 1985, Sadler, 1998). VWF is a large multimeric plasma glycoprotein with a high molecular weight that plays an important role in primary haemostasis. Zimmerman *et al* (1986) detected the VWF multimers after electrophoresis of purified VWF in 5% of polyacrylamide gels (Zimmerman et al., 1986). Mancuso *et al* (1989) reported the genomic structure of *VWF* in 1989 (Mancuso et al., 1989), and in 2001, A disintegrin-like and metalloprotease domain (reprolysin type) with thrombospondin type 1 motifs (ADAMTS13) that cleaves multimeric VWF was discovered (Fujikawa et al., 2001).

1.3. The molecular biology of von Willebrand factor

1.3.1. The *VWF* gene

Many studies showed that the large multimeric VWF is encoded by a large gene located at the tip of the short arm of chromosome 12 at 12p13.3 (Ginsburg et al., 1985, Verweij et al., 1985). *VWF* consists of 52 exons that extend over approximately 178 kb of DNA (Figure 1.1A). The *VWF* exons vary in size between 40 base pairs (bp), the smallest being exon 50, and 1,400 bp, the largest being exon 28 (Mancuso et al., 1989), while the introns range in size from 97 bp to almost 19,900 bp. The length of encoded VWF mRNA is 9 kb.

Two factors have, to date, made the analysis of the *VWF* gene both demanding and complicated. One factor is the large size of the *VWF* gene. The other is the presence of an unprocessed partial pseudogene copy that is located on chromosome 22. This pseudogene is highly similar to the *VWF* gene and corresponds to exons between 23 and 34 with slight sequence variation, estimated at 3%, from the chromosome 12 locus (Figure 1.1A). So, during polymerase chain reaction (PCR), care must be taken to ensure that the amplification is for the true *VWF* sequence

and not for the sequence of the *VWF* pseudogene *(VWFP*) (Mancuso et al., 1991, Laffan et al., 2004). Moreover, the presence of single nucleotide polymorphisms (SNP) within primer sequence annealing sites could mask heterozygous genetic defects and could lead to missing mutation.

1.3.2. The VWF protein

The primary translation pre-pro-VWF product consists of 2813 amino acids (AA) with a 22 AA signal peptide, a 741 AA large pro-peptide (VWFpp) and a 2050 AA mature VWF molecule that starts with residue 764 and ends with residue 2813. These are secreted as mature VWF multimers formed from single VWF subunits that contain all the binding sites that are needed to perform its function (Figure 1.1C) (Titani et al., 1986). The first *VWF* exon contains 250 base pairs and is non-coding. The next 15 exons of *VWF* encode the pro-peptide of VWF, while the mature multimers of VWF are encoded by exons 18-52 (Mercier et al., 1991). The VWF pro-peptide and mature VWF subunit contain four types of repeating domains found in two to five copies, and each is arranged from the amino to the carboxyl ends in the following order: D1-D2-D'-D3-A1-A2-A3-D4-B1-B2-B3-C1-C2-CK (Figure.1.1A) (Shelton-Inloes et al., 1986). These domains are essential for the different functions of VWF, including platelet adhesion and aggregation in addition to other binding functions with other proteins, such as GpIbα, FVIII and collagen. Domains from D' to CK comprise the mature VWF, while the VWF pro-peptide consists of D1 and D2 domains. A significant amount of cysteine is present in VWF, which accounts for 243 of 2813 AA in the pro-VWF product (8.3%). It has been found that all VWF domains contain abundant amounts of cysteine except the three A domains, which have only six cysteines and are considered to be cysteine poor regions. The secreted protein has cysteine residue linked monomers held together by intra-and inter- subunit disulfide bonds to form multimers (Marti et al., 1987, Dong et al., 1994, Sadler, 2009). Also, in the updated annotation of VWF structure, no new cysteines have been identified, but 8 cysteines now lie in gaps between domains and in domains boundaries. These include 8 cysteine residues found between D1-D2, D2-D3, D3-A1, A3-D4 (D4N) and between D4 and C1 (Figure 1.1B) (Zhou et al., 2012).

In order to assign the whole VWF sequence and due to the presence of gaps between VWF domains, the structure was updated and re-annotated to cover these gaps that contain cysteine residues. Based on sequence repeats, homologies and number of cysteine residues, additional modules were added to D domains and VWF expression at acidic pH mimicking the conditions that occur in the Golgi followed by examination using electron microscopy. The updated structure consists of three A domains, six C domains, five D domains and a terminal CK domain, while B domains are eliminated. D domains consist of modules that include cysteine 8

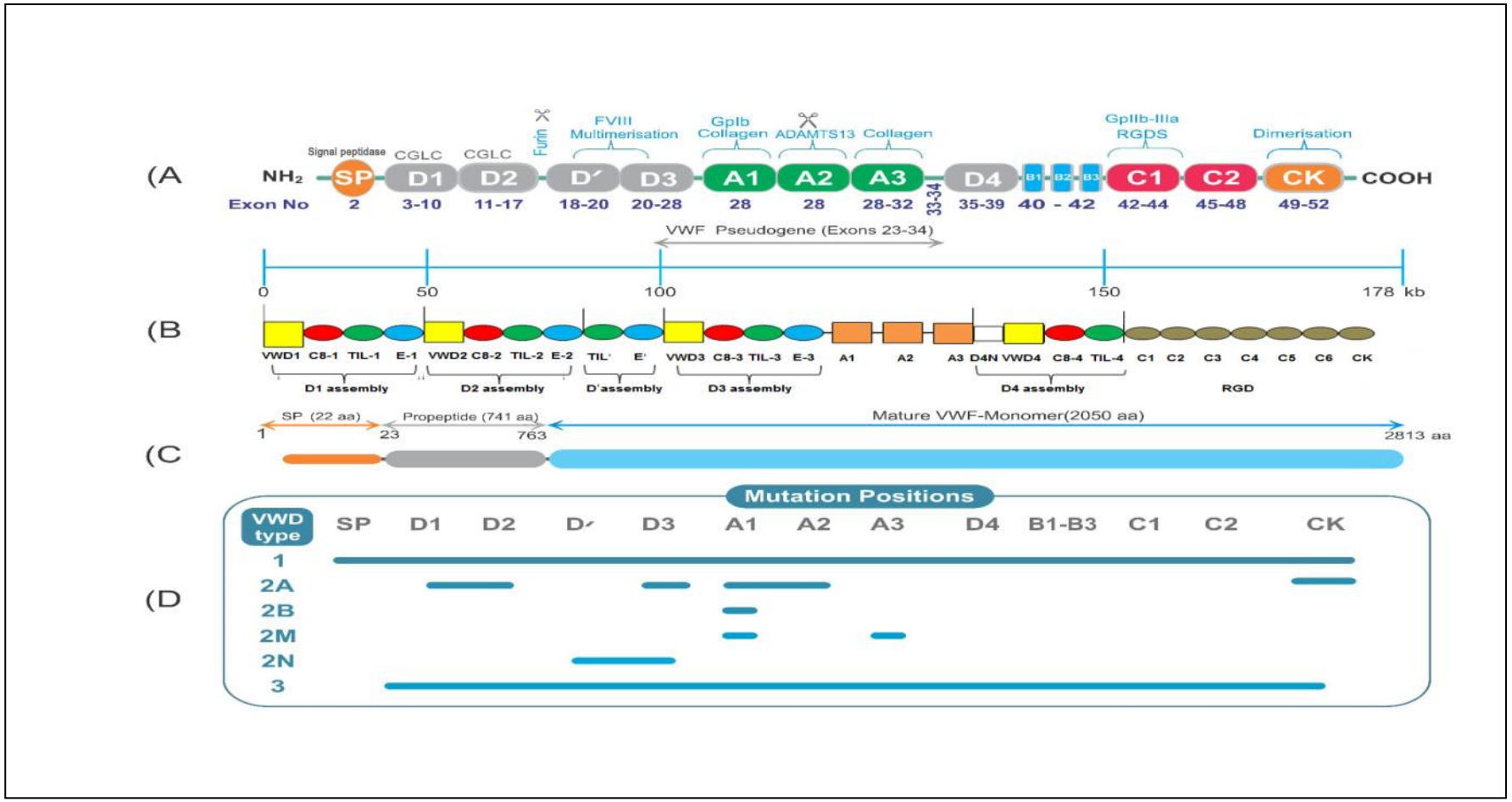

Figure 1.1: Schematic representation of the VWF protein and encoding exons. **A**): Shows the original functional domains of VWF, exons encoded by each domain and the size of the entire *VWF* (178 kb). VWF consists of several repeated domains A, B, C and D. **B**): Shows the VWF protein updated and re-annotated functional domains. The revised domains consist of four D assembly domains, three A domains and six C domains where B domains are eliminated. Additional multiple modules include cysteine 8 (C8) domains, trypsin-inhibitor-like (TIL) domains and E repeats that follow each TIL

domain. The D4N module which contains eight cysteines is found between A3 and VWD4 domains. The Arg-Gly-Asp (RGD) sequence is found within C4 domain. Vertical lines represent boundaries of domain assemblies. **C**): Shows the 2813 amino acids of pre-pro-VWF, of which the first 22 AA comprise the signal peptide (SP), the following 741 AA comprise the pro-peptide (VWFpp) which consists of D1 and D2 domains and disulphide isomerase-like sites (CGLC) and the final 2050 AA represent the mature VWF. **D**): Represents mutation distribution and location in each domain that have been identified in VWD types 1, 2 and 3. Mutations were found in all domains in type 1 and 3, while type 2 VWD varies based on the subtype (Wagner et al., 1987, Mancuso et al., 1989, Ruggeri, 2001, Goodeve, 2010, Zhou et al., 2012).

(C8) domains, trypsin-inhibitor-like (TIL) domains that contain five highly conserved disulfide bonds and E repeats follow each TIL domain. D domain assemblies 1-3 are subdivided into multiple modules; VWD, C8, TIL and E in each, while VWD4 is similar but lacks segment E and has an additional D4N module which makes a bridge between A3 and VWD4 by a disulphide bond. D' is a small domain containing only TIL and E modules (Figure 1.1B). The VWC4 domain carries the VWF RGD motif (Zhou et al., 2012). This updated structure enables identification of additional disulfides bonds in the additional modules.

1.4. Biosynthesis of VWF

The synthesis of VWF has been studied extensively, and it has been found that VWF is synthesised exclusively in two types of cell: endothelial cells and megakaryocytes. VWF from both sites has the same structure, and the processing of VWF at these sites seems to be similar. Many studies have examined the processing of VWF, in terms of assembly, secretion and expression, and found that it is complex (Jaffe et al., 1974, Nachman et al., 1977). VWF forms high molecular weight multimers and is packaged in secretary vesicles: Weibel-Palade bodies (WPB) in endothelial cells and alpha-granules in megakaryocytes (Wagner et al., 1982, Sporn et al., 1985). VWF is released from Weibel-Palade bodies to the circulation either basally or following stimulation (Giblin et al., 2008). In order to explore the effect of mutant VWF on its synthesis, storage and secretion, blood outgrowth endothelial cells (BOEC) were isolated from peripheral blood of type 1 and 2 VWD patients followed by measuring the level of released VWF and mRNA before and after stimulation. As a result, the level of released VWF was found to be decreased in patients with type 1 VWD and type 2M VWD which reflects the defect in VWF synthesis while synthesis and secretion were normal in patients with type 2A accompanied with functional defects (Starke et al., 2013a).

1.4.1. Dimerisation

VWF processing, namely glycosylation and dimerization, takes place in the endoplasmic reticulum (ER), while multimerisation occurs in the Golgi apparatus (GA). Pre-pro VWF undergoes an extensive series of intracellular and post-translational modifications to regulate its synthesis, prior to release and exit of VWF from the ER (Figure 1.2). Initially, the released mRNA is translated to synthesize a VWF product of 2813 AA (pre-pro-VWF polypeptide), which includes a 22 AA signal peptide, a large pro-peptide of 741 AA and a mature VWF subunit of 2050 AA that is released from the original molecule during intracellular biosynthesis. This primary product is translocated from the ribosome into the endoplasmic reticulum, where signal peptidase cleaves and removes the signal peptide domain, converting it into the pro-VWF monomer (Figure 1.2). After removal of the signal peptide, the pro-VWF monomer is folded

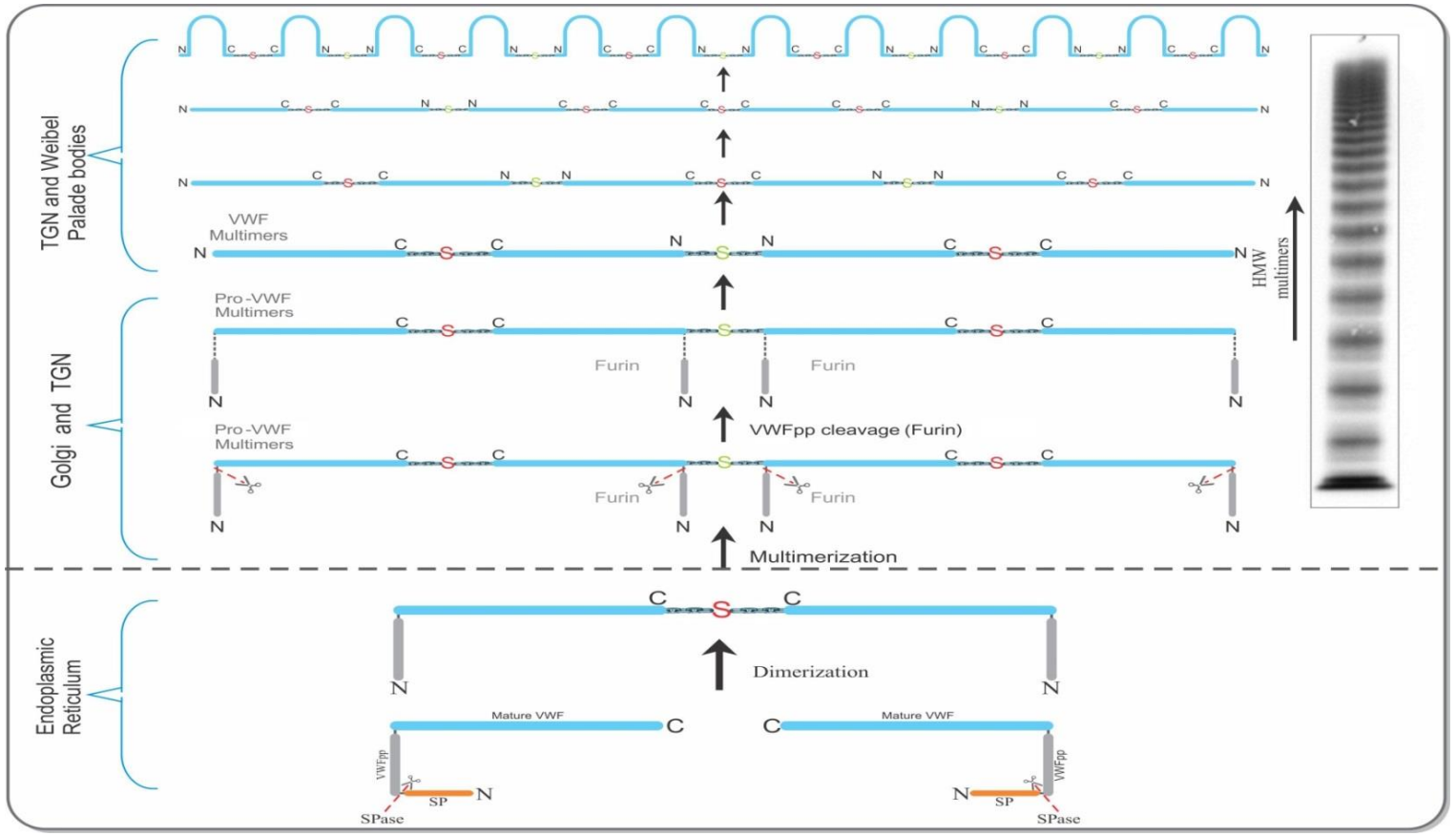

Figure 1.2: Schematic representation showing the intracellular synthesis of HMW-VWF. Initially, VWF is synthesised as a pre-pro-VWF product of 2813 AA. This product is translocated into the ER where SP is removed forming the pro-VWF which subsequently forms C-terminal dimers. The pro-VWF dimers exit from the ER to the Golgi complex and trans-Golgi network (TGN) where pro-VWF forming head to head bridges followed by cleavage of VWFpp by Furin occurs. In the Golgi and TGN, dimers form a bridge of disulphide bonds between each other which leads to the assembly of HMW-VWF multimers. Both VWFpp and mature VWF multimers are released to Weibel-Palade bodies in either endothelial cells or platelet α-granules (Rehemtulla and Kaufman, 1992, Rosenberg et al., 2002, Michaux et al., 2006, Sadler, 2009).

and disulfide bonds are formed between the adjacent VWF monomers via cysteine knot (CK) or their carboxyl terminal regions domains at residues p.C2671 to p.C2813, forming tail-to-tail dimers (Mayadas and Wagner, 1992, Katsumi et al., 2000, Sadler, 2009). The D4-CK domains are cysteine rich and the last 151 amino acids of the mature VWF subunit following the C6 domain (from the updated domain structure) seem to be essential to the completion of the process of dimerisation. They are involved in tail-to-tail dimerisation and are needed to achieve efficient dimerisation. However, *in vitro* expression studies showed that dimerisation fails when using recombinant VWF that lacks some of these 151 AA, degrading in the ER (Marti et al., 1987, Voorberg et al., 1991, Schneppenheim et al., 1996, Yadegeri et al., 2013).

These sequences within the CK domain may play a role in retaining the monomers in the ER until they are either degraded or dimerised. Furthermore, there is some evidence that the last 90 AA in the CK domain play a role in the dimerisation of VWF due to their similarity to the CK superfamily of proteins, which have a high tendency to dimerise, usually by forming disulfide bonds (McDonald and Hendrickson, 1993, Desseyn et al., 1997). *In vitro* expression studies using mutated recombinant *VWF* have been conducted to study the effect of several mutations in the CK domains in VWF dimerisation. Several mutations in the carboxyl terminal region, including p.C2362F, p.C2773R, p.C2739Y and p.A2801D, have been identified and found to disrupt VWF dimerisation and cause defective formation. The p.C2773R mutation that was identified through the carboxyl terminal domains has been found to impair dimerisation in addition to causing abnormal HMW multimers (Schneppenheim et al., 1996, Hommais et al., 2006b, Tjernberg et al., 2006). The large pro-peptide VWF is also not needed for dimerisation because expression of a mutated recombinant mature *VWF* with the pro-peptide deleted results in normal secretion of a dimeric VWF, which indicates that VWFpp is not needed for dimerisation or for the exit of the VWF protein from the ER but is required for multimerisation (Verweij et al., 1987, Wise et al., 1988, Haberichter et al., 2000).

1.4.2. Glycosylation of VWF in ER

Glycosylation is defined as the addition of high-mannose carbohydrate side chains glycans to VWF in order to facilitate and regulate the release of VWF from the ER to the GA. After the removal of the signal peptide and prior to tail-to-tail dimerisation, the pro-VWF is also extensively modified and glycosylated in the ER. The VWF post-translational glycosylation is found to have an effect on VWF structure and function. It is essential for dimerisation, regulates folding and preserves protein structure, and is required for release of VWF from ER to GA (Kornfeld and Kornfeld, 1985, Wagner et al., 1986, Lenting et al., 2010). Moreover, it protects VWF from intracellular destruction and degradation which prolongs the protein half-life. In

addition, it has an effect on circulating VWF survival. Individuals with blood group O who lack glycosyl-transferase encoded by the *ABO* gene that protects VWF from clearance have lower plasma levels of VWF compared to those with AB blood group who have transferase-enzyme. It was suggested that the absence of ABO glycosyl-transferase influences the cleavage susceptibility of VWF by ADAMTS13 and contributes to reduced levels of plasma VWF in individuals who lack this allele (Bowen, 2003). There are several glycosylation carbohydrate sites, which are located on VWF, and these glycans account for almost 20% of the total mass of the VWF (McKinnon et al., 2010). Glycosylation is divided into two types; N-linked glycosylation where glycans are added to asparagine residues on VWF present in the Asn-X-Ser/Thr/Cys sequence (X indicates any amino acid) and O-linked glycosylation where glycans are added to either serine or threonine residues in VWF (Lenting et al., 2010). There are sixteen N-linked glycosylation sites, twelve of which are located in mature VWF and the remainder in VWF pro-peptide (Titani et al., 1986, McKinnon et al., 2010). The distribution of these side chains is not equal along the VWF protein. There is a large gap in the central region, and most of these sites are located on either the amino or carboxyl terminal ends of each VWF subunit (Titani et al., 1986, McKinnon et al., 2010). N-linked glycans are distributed between VWF residues 856-2791 and O-linked glycans distributed between VWF residues1247-2299 (Lenting et al., 2010). Furthermore, the ABO blood group oligosaccharides are present on plasma VWF as a part of the N-linked glycosylation oligosaccharides (Matsui et al., 1992). An *in vitro* expression study performed by Wanger *et al*.1986 reported that glycosylation is needed to achieve proper dimerisation and multimerisation. They found that adding tunicamycin to the endothelial cells in the culture medium in order to inhibit the N-linked glycosylation resulted in an accumulation of pro-VWF in the ER and impaired dimerisation (Wagner et al., 1986). These findings suggest that dimerisation occurs after glycosylation. Moreover, an experimental study that mutated the VWF N- linked glycosylation binding sites followed by transfection in human embryonic kidney (HEK293T) cells found reduced VWF secretion and prevention of VWF dimer formation and multimer assembly (McKinnon et al., 2010). There are twelve O-linked glycosylation sites, ten of which are located in mature VWF, where sialyalated T-antigen was reported to account for 70-90% and ABH antigen found to account for approximately 1% of glycosylation sites. It has been proposed that O-linked glycans influence VWF survival by an unknown mechanism that may be due to cleavage susceptibility by ADAMTS13. Until now the role of O-glycans on VWF function is still poorly understood, but Gallinaro *et al* (2008) showed a strong influence of ABO blood group on VWF clearance where the half-life of VWF in group O individuals is shorter (10 hr) compared to non-group O (26 hr). (Gallinaro et al., 2008). However, knowledge of O-glycan addition has improved our understanding about the exact effect of glycosylation on VWF function (van Schooten et al., 2007, Canis et al., 2010, McGrath et al., 2010).

1.4.3. Folding of VWF in the ER

Apart from glycosylation and dimerisation, proper folding of VWF is required to release pro-VWF from the ER to the Golgi. In the ER, proteins are checked for proper folding and misfolded proteins are selected and destroyed by the proteasome complex (Hampton, 2002). Many mutations that may affect the secretion of VWF or the destruction of misfolded protein in the ER have been identified in patients with VWD. p.C1157F and p.C1234W mutants were found to cause intracellular retention and abnormal multimerisation (Hommais et al., 2006a). It has been proposed that the p.C1149R mutation identified in families diagnosed with type 1 VWD caused intracellular retention and decreased secretion (Bodo et al., 2001a, Eikenboom et al., 2009). Impaired processing of VWF in the ER during intracellular biosynthesis may contribute to the symptoms observed in patients with VWD.

1.4.4. VWF multimerisation

Following the translation of mRNA, signal peptide cleavage, initial glycosylation and tail-to-tail dimerisation in the ER, multimerisation, further glycosylation and proteolytic cleavage of VWFpp dimer also takes place in the Golgi apparatus. The pro-VWF dimers are transported from the ER to the Golgi complex and polymerise to build large chains of VWF linked by additional disulfide bonds. The D1 and D2 assemblies that represent the VWF pro-peptide contain two CGLC sequences. p.C159-G-L-C162 and p.C521-G-L-C524 residues are found in each domain with vicinal cysteine motifs, which resemble the active sites of the protein disulfide isomerase (PDI) enzymes which catalyse the formation of intracellular disulfide bonds during VWF synthesis and secretion in the ER. These isomerase-like enzymes enhance and promote pro-VWF association and the formation of head-to-head multimers through intermolecular disulfide bonding between adjacent D3 domains near to the amino-termini of the pro-VWF dimers (Sadler, 2009). This association results in the production of multimers of more than 20 million daltons in size (Figure 1.2). Also, prior to multimerisation when the pro-VWF dimers are released from the ER into the Golgi, galactose and sialic acid are added to form secondary carbohydrate complexes (Mayadas and Wagner, 1992, Rehemtulla and Kaufman, 1992, Ruggeri, 1999, Rosenberg et al., 2002). The results of various studies suggest that VWFpp plays a critical role in VWF biosynthesis, particularly during protein multimerisation. A study conducted by Mayadas and Wanger (1989) indicated that the pro-peptide is needed to regulate multimerisation of the dimers expressed either as full length VWF or as independent expression of pro-peptide and mature VWF (Mayadas and Wagner, 1989). Following head-to-head multimerisation through the D3 domains of the dimers, proteolytic removal of the 741AA of VWFpp occurs in the Golgi network. Either a membrane associated calcium-dependent endoprotease enzyme or paired basic amino acid cleaving enzyme (Furin) catalyses cleavage of

the VWFpp at position p.R763-S764 to produce two fragments: mature multimers of 2050 AA plus the VWF pro-peptide consisting of 741 AA (Figure 1.2) (Mayadas and Wagner, 1992). Intracellularly and before secretion, the cleaved VWF pro-peptide remains non-covalently linked with the mature VWF-multimers within two storage sites; endothelial WPB and platelet alpha granules. However, both proteins are dissociated when secreted from the cell into the plasma (van de Ven et al., 1990, Bosshart et al., 1994, Sadler, 2009). Many laboratories have used the ratio of secreted VWFpp/VWF:Ag and FVIII/VWF:Ag to evaluate synthesis and measure the rate of VWF clearance. Increased pro-peptide to antigen ratios suggest a clearance defect (Haberichter et al., 2006, Haberichter et al., 2008, Sztukowska et al., 2008, Eikenboom et al., 2013b). The stored VWF is regularly secreted at the site of vascular injury to promote platelet adhesion, aggregation and response to inflammation.

1.5. Functional domains of VWF

The pre-pro-VWF consists of various homologous domains, including signal peptide (SP), three A domains, six C domains and four D assemblies, with the partial D' assembly (Figure 1.1A and B) (Ginsburg et al., 1985, Mancuso et al., 1989, Zhou et al., 2012). During intracellular processing, the SP and VWFpp, which consist of D1 and D2 assemblies, are removed, leaving the mature VWF, which is responsible for the major function of VWF required during vascular injury. Mature VWF has various binding functions due to the presence of different domains (Figure 1.1A and B). VWF exists as various sizes of multimers with variable molecular weights of VWF, but the most active forms of VWF have the highest molecular weight multimers (HMW) due to the presence of higher numbers of active binding sites for platelet GpIb. These support the functional domains and the capacity to bind sub-endothelium and platelets (Sadler, 1998). These domains are key to VWF carrying out its functions, which include binding with various proteins, such as collagen and FVIII in addition to platelets and any genetic defects within these domains may alter the function (Ruggeri, 1999).

1.6. Storage and function of von Willebrand factor

1.6.1. Platelet plug formation

High molecular weight (HMW) VWF multimers, which hemostatically are the most effective forms, are synthesized and stored in various tissues. Some VWF stored in the WPB in endothelial cells and in platelet granules, but approximately 10% of endothelial VWF stored. The mature form of VWF is secreted directly into the circulating plasma or sub-endothelial matrix (Ruggeri, 2001). One of the most important functions of VWF is to interact with platelets in order to bring about adhesion and subsequent aggregation upon vascular injury. At sites of vascular injury, VWF promotes and mediates the interaction between exposed sites of sub-endothelium and the platelet membrane via the platelet glycoproteins and thereby supports

adhesion and platelet aggregation. Following blood vessel (BV) injury and under high shear stress conditions, conformational changes of VWF occur facilitating VWF-platelet binding and thereby platelet adhesion and aggregation.

Within mature VWF, two domains, A1 and A3, are responsible for binding with collagen (Figure 1.1A). A3 is the major binding site for type I and III collagen, which also binds to A1, while type VI collagen is involved in binding with A1 domain only. Flood *et al* (2012), reported mutations located in the A1 domain associated with bleeding characterized by a selective reduction in the binding to type VI collagen but not types I and III such as p.R1399H, p.S1387I and p.Q1402P. The exposed immobilised VWF which binds via its A3 domain to exposed collagen of the BV wall. Binding of VWF to exposed collagen results in a shape change, exposing the VWF A1 domain, this interacts with the platelet glycoprotein GpIbα (Figure 1.3). The interaction between VWF and platelet receptor GpIbα is the only interaction that occurs in unactivated platelet. This interaction between immobilised VWF and GpIbα is required for the initiation of platelet adhesion and further aggregation (Savage et al., 1996, Nichols et al., 2008b, Reininger, 2008).

Following initial interaction between VWF A1 domain with GPIbα, further activation of platelet surface complex receptors, such as GPIbβ and GPIbIX engage VWF and collagen and thereby result in adhesion (Kenny et al., 2002). Following the initial adhesion of VWF and platelets, other domains of VWF bind to other platelet receptors and platelet aggregation subsequently result in thrombus formation. GpIbα complex binding induces the platelet surface expression of the GPIIb/IIIa (integrin $\alpha_{IIb}\beta_3$) platelet receptor, which rapidly binds with high affinity to the circulating VWF RGDS (Arg-Gly-Asp-Ser) sequence that is located within the C-terminal end of the C4 domain at position 1744 to 1746. The GPIIb/IIIa receptor also binds to fibrinogen to further enable platelet-platelet interactions. Platelet binding with circulating immobilised VWF results in platelet aggregation and initiation of the coagulation pathway (Figure 1.3) and formation of a platelet plug through activation of thrombin, converting fibrinogen to insoluble fibrin strands. (Weiss et al., 1991, Beacham et al., 1992, Reininger, 2008).

1.6.2. Binding with FVIII

One of the most important functions of VWF is to carry FVIII and protect it from degradation caused by proteolytic proteins in the plasma and thereby prolong the survival of FVIII and localize it to the site of vascular injury (Rodeghiero, 2002, Keeney et al., 2008) (Figure 1.1A).

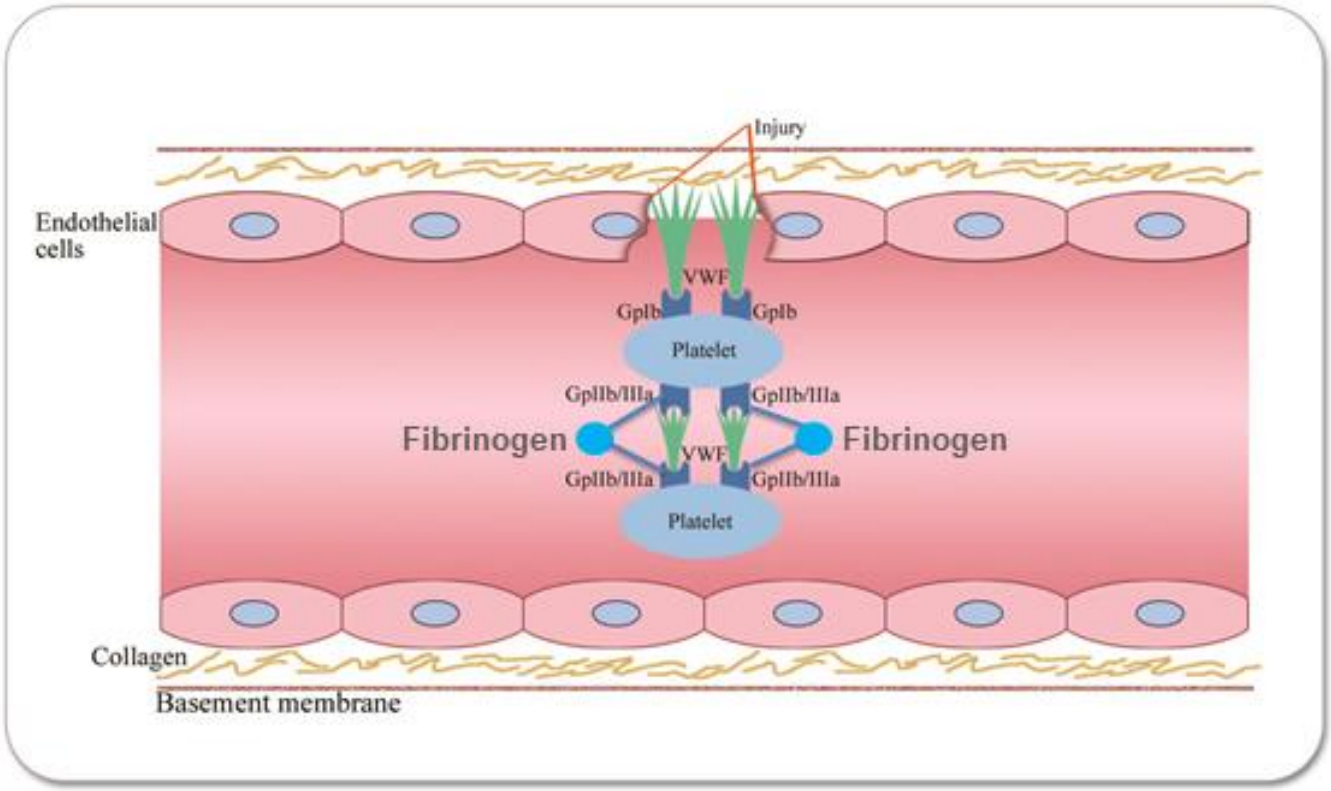

Figure 1.3 Diagram showing the role of VWF in platelet aggregation and clot formation. Following blood vessel injury, VWF which adheres to sub-endothelial collagen is released. Platelets passing to the site of endothelial damage bind to VWF via platelet GpIb receptors resulting in the adhesion of platelets to the damaged sites. The primary binding of platelets to exposed VWF induces the activation of platelet GpIIb/IIIa receptors which enables VWF to form a bridge between adjacent platelets leading to platelet aggregation and thrombus formation. (Ruggeri, 1999, Nichols et al., 2008b, Reininger, 2008). Also, Platelets bind to fibrinogen via GpIIb/IIIa receptors, thus lead to clot formation.

HMW-VWF is not essential for this function (Zimmerman and Ruggeri, 1987, Ruggeri, 1999). The D' and D3 domains are the regions responsible for the binding of VWF to FVIII, and missense mutations that occur in this region can impair this binding and cause type 2N VWD (Nishino et al., 1989, Mazurier et al., 2001, Sadler et al., 2006). Also, many mutations located in the D3 region may result in type 2A(IIE) VWD (Hommais et al., 2006a, Schneppenheim et al., 2010).Many studies have shown that the half- life of FVIII in the presence of normal quantities of VWF is significantly higher than when less than normal amounts are present or in its absence. *In vitro* studies have shown that the half-life of FVIII in the absence of VWF is significantly lower (2.5 hr) than when VWF levels are normal (8-12 hr) (Cattaneo et al., 1994, Noe, 1996). The binding domain D'-D3, which is located within the first 272 amino acid residues of the mature subunit, was identified as the binding site of VWF for factor VIII (Vlot et al., 1996).

1.7. Cleavage of HMW multimers

HMW-VWF is cleaved by the ADAMTS13 enzyme which cuts VWF multimers into smaller fragments reducing platelet aggregation and clot formation. The cleavage site of VWF is located within the A2 domain at residues p.Y1605-M1606 (Figure 1.1A) (Zheng et al., 2001). Some mutations in this domain result in type 2A VWD due to either impaired multimer assembly or due to increased susceptibility of VWF to cleavage by ADAMTS13 which can impair secretion (IIA group I) or enhance proteolysis (IIA group II) (Zimmerman et al., 1986, Lyons et al., 1992). Also, the p.Y1584C mutation in this domain results in increased susceptibility of VWF to cleavage and mild intracellular retention in type 1 VWD patients (Bowen, 2004).

In contrast, mutations in the *ADAMTS13* gene results in reduce quantity in circulation alter the binding of ADAMTS13 to VWF and lead to accumulation of HMW-VWF, induce platelet aggregation and lead to thrombotic thrombocytic purpura (TTP) and thereby microvascular thrombus formation (Moake et al., 1986, Levy et al., 2001).

1.8. Diagnosis of von Willebrand disease

Three main pillars must be taken into consideration when diagnosing type 1 VWD: a personal history of significant and multiple bleeding symptoms, a positive family history and a low level of VWF in the plasma. Since VWD is a highly heterogeneous bleeding disease, diagnosis is complicated and these pillars together contribute to the accurate diagnosis of VWD. The bleeding symptoms apparent in VWD patients vary, even within the same family, and usually depend on the severity of the disease as well as the VWD type or subtype. Some patients only bleed when there is a haemostatic challenge. Individuals diagnosed with type 1 VWD may have no bleeding symptoms, whilst those with type 3 VWD may have a severe bleeding tendency.

Moreover, the presence of mild bleeding symptoms in healthy individuals may complicate the diagnosis and lead to a false positive diagnosis. However, using a bleeding score (BS) to evaluate bleeding may help and support the accuracy of diagnosis. Also, accurate diagnosis and classification of VWD is important in order that the disease can be managed correctly via treatment of bleeding or preventive therapy.

1.8.1. Clinical diagnosis of von Willebrand disease

Clinical diagnosis plays an essential role in the accurate diagnosis of VWD and aims to avoid misdiagnosis as well as false-positive diagnosis. In the past, many studies were performed to evaluate bleeding symptoms among patients with different types of VWD, but there were no clear guidelines for evaluating the bleeding in those patients (Silwer, 1973, Federici, 2004). The history of mucocutaneous bleeding symptoms throughout a patient's life should be used as an initial clinical evaluation tool for a patient who is suspected as having VWD as well as looking at the patient's family history in terms of a bleeding disorder.

International multicenter studies have now established a BS, which is based on a quantitative analysis of the number and severity of mucocutaneous bleeding symptoms. The purpose of the BS is to provide a measure of the bleeding symptoms in VWD cases and to compare the relationship between both clinical and laboratory findings and thereby verify the accuracy of diagnosis (Tosetto et al., 2006, Tosetto et al., 2007, Bowman et al., 2008). The BS also helps to predict the occurrence of future bleeding in some circumstances, especially during tooth extraction or surgery, and it helps to identify patients who need preventive therapy (Tosetto et al., 2007). The final BS is derived by summing all haemorrhagic symptoms based on their severity and ranged from 0 to 3 where 0 represents the absence of bleeding even after particular procedures, such as dental or surgical, through 1, 2 and 3 for varying degrees of bleeding to more than 3, which indicates the presence of significant bleeding that requires medical intervention. This particular score is highly sensitive and used to evaluate the severity of bleeding in response to haemostatic challenges. A BS score higher than three is considered abnormal (Eikenboom et al., 2006, Tosetto et al., 2006, Tosetto et al., 2007, Bowman et al., 2008). The BS is reached through the clinician filling in a simple questionnaire to evaluate patients bleeding symptoms. The initial questionnaire used to assess the severity of bleeding was time consuming for both physicians and patients, so this questionnaire has been modified and certain details that had little direct effect on the score have been removed (Bowman et al., 2008, Rodeghiero et al., 2010). Tosetto *et al*. reported that the BS was significantly higher in index cases and affected family members when compared to both unaffected family members and controls (Tosetto et al., 2006). Recently, BS was revised for diagnosis of bleeding disorder in children to distinguish between children with and without a bleeding disorder. Children

usually have less exposure to bleeding challenges but have specific bleeding symptoms such as umbilical stump bleeding. circumcision and cephalohematoma that are not present in adults (Montgomery, 2005). The bleeding symptoms are scored from 0 (no abnormal bleeding symptoms) to 3 (severe bleeding) (Rodeghiero et al., 2010, O'Brien, 2012).

1.8.2. Laboratory diagnosis of VWD

The diagnosis of VWD does not depend on one particular test but on various assays to evaluate the levels, structure and function of VWF. According to Laffan *et al.*'s (2004) guidelines on the diagnosis of VWD, laboratory tests are categorized into screening tests for the initial assessment, specific tests to confirm the presence of VWD and more advanced tests to distinguish between particular types and subtypes of VWD and to identify genetic defects (Laffan et al., 2004). Due to variability in bleeding symptoms among VWD patients, laboratory tests play an essential role in the diagnosis and classification of VWD. Some physiological and pathological factors, such as stress, age, infection and pregnancy may influence the level of VWF, causing it to fluctuate. Hence, these investigations should be repeated at least two times with concordant results under different conditions especially in patients suspected of having type 1 VWD, to avoid any false results.

1.8.2.1. Screening tests for diagnosing VWD

A group of laboratory tests are used for the initial evaluation and diagnosis of bleeding and haemorrhagic disorders, which may include bleeding time, platelet count, activated partial thromboplatsin time (APTT) and prothrombin time (PT) (Sadler et al., 2000, Laffan et al., 2004). These results vary depending on the type of VWD and its severity. Skin bleeding time (BT) evaluates the ability of blood to form blood clots to stop bleeding via making small incision in skin. It was not considered a suitable screening test for primary haemostasis but should be considered in specific circumstances in the investigation of patients with bleeding disorders if other tests have not demonstrated a defect. The clinical utility of BT is limited due to its low sensitivity, low specificity, invasive and poorly reproducibility as it is prolonged in some platelet disorders, this test is now rarely used and has been replaced by the more sensitive platelet function closure time assay (PFA-100 and PFA-200), which however is not very sensitive in type 1 VWD (Tosetto et al., 2007). This test tends to be normal in patients with type 2N VWD but may be abnormal in patients with the other types of VWD (Schlammadinger et al., 2000). Thrombocytopenia is generally observed only in type 2B VWD and in some variants of type 2A such as p.R1374H, while the platelet count remains within the normal range in patients with other types of VWD. Prothrombin time is within normal limits in all types of VWD, while APTT is usually normal or mildly abnormal but variably prolonged in patients

with type 3 VWD and severe type 2N due to decreases in the level of circulating FVIII. These two tests are generally used as screening tests to detect the level and activity of coagulation factors, such as FVIII, FIX and FVII, and to diagnose haemophilia, and they are still used widely to diagnose any suspicion of a bleeding disorder. The detection of APTT within the normal range should not exclude VWD nor prevent any follow-up diagnosis (Sadler et al., 2000).

1.8.2.2. Specific laboratory studies

These tests are used to confirm a VWD diagnosis and to screen for VWD. The following assays evaluate the level and function of VWF:

1.8.2.2.1. VWF antigen assay (VWF:Ag)

This test measures the proportion of VWF protein (VWF:Ag) in the plasma and is considered to be one of the most important confirmatory tests of VWD. The levels of VWF in the plasma can increase or decrease in the same individual depending on several factors. Its levels increase after stress, infections, in pregnancy and with age, while levels are lower among the blood group O population. VWF levels are invariably decreased in type 1 VWD and absent or below the detection limit in type 3, while low or normal levels can be observed in type 2 VWD variants (Sadler et al., 2000). Levels of VWF are evaluated in the laboratory using immunological methods, such as latex immunoassay (LIA) and enzyme linked immunosorbant assay (ELISA) (Favaloro, 2001, Laffan et al., 2004, Castaman et al., 2010b). The normal level is approximately 48-167 IU/dL. Reference ranges are based on an average from a pool of blood samples with different blood groups.

1.8.2.2.2. VWF ristocetin co-factor activity (VWF:RCo)

VWF ristocetin co-factor activity (VWF:RCo) is a standard test that can be used to evaluate VWF function due to its ability to associate and interact with the GpIbα after the addition of the antibiotic ristocetin via platelet agglutination methods (Castaman et al., 2003, Laffan et al., 2004). Addition of ristocetin stimulates binding of VWF to platelets. Results are based on the presence of normal multimeric structures. Results with reduced values indicate a loss of HMW multimers. In type 1 VWD, VWF:RCo and VWF:Ag levels are reduced equally and the ratio between VWF:RCo/VWF:Ag is approximately normal, while in types 2A and 2M the ratio of VWF:RCo to VWF:Ag is significantly decreased and values of VWF:Ag and VWF:RCo below the detection limit in type 3 (Sadler et al., 2000, Lethagen, 2007). The normal range is approximately 47-194 IU/dL.

1.8.2.2.3. FVIII activity (FVIII:C)

This test investigates the activity of FVIII in plasma. This is measured by either a clotting assay based on the APTT test using factor VIII deficient plasma or by a chromogenic assay (Laffan et al., 2004). The level of FVIII in plasma is directly proportional to the level of VWF because the half-life of FVIII is dependent on the level of VWF. Therefore, FVIII is significantly reduced or absent in type 3 VWD due to a severe lack of VWF, and is generally < 10 IU/dL or may even be undetectable on rare occasions. FVIII coagulant activity (FVIII:C) is also reduced in type 2N due to poor binding by VWF, and variable activity has been reported in other types of VWD based on the levels of VWF in the plasma (Table 1.2) (Sadler et al., 2000). The normal range is approximately 57-198 IU/dL.

1.8.3. Laboratory tests for VWD classification

Additional laboratory methods are widely available to facilitate the identification, classification and subtyping of VWD types and subtypes. They include the following assays:

1.8.3.1. VWF multimeric analysis

When VWD has been diagnosed, VWF multimeric analysis is used to determine the presence or absence of HMW-VWF multimers and to identify any abnormalities in multimer structure. Thus, the disease type can be classified. In this discriminating test, patient plasma is electrophoresed through 1 to 1.5% medium resolution agarose gels. A normal pattern of HMW multimers, including low, intermediate and high molecular weights, is found in type 1 VWD, while a mildly abnormal structure is observed in a small proportion in this type, and an absence of multimers is observed in type 3 VWD. Also, HMW multimers are generally normal in types 2N and 2M VWD in contrast with types 2A and 2B VWD, in which they may be completely or partially absent. This test is useful for the sub-typing of type 2A and identification of type 2M VWD (Laffan et al., 2004, Schneppenheim and Budde, 2005). Technically, this test is difficult to perform, and good quality multimer analysis can only be produced in a limited number of laboratories.

1.8.3.2. Ristocetin-induced platelet aggregation (RIPA)

The ristocetin-induced platelet aggregation (RIPA) screening test at a low dose of ristocetin is used to distinguish between type 2B and other VWD variants (Frontroth et al., 2010). The RIPA evaluates the strength of VWF interaction with platelets after ristocetin in variable concentrations (~0.5-1.3 mg/ml) has been added to platelet-rich plasma samples. Aggregation is observed in type 2B VWD with the lowest concentration of ristocetin (~0.5 mg/ml), but

aggregation reduced in other types compared to normal plasma. Also, aggregation at this concentration is absent in other VWD types and normal individuals (Laffan et al., 2004). However, this test is used exclusively to identify type 2B and is not sensitive enough for the diagnosis and subtyping of other VWD variants.

1.8.3.3. VWF:FVIII binding assay (VWF:FVIIIB)

This is an ELISA based assay particularly used to evaluate the binding affinity of VWF for FVIII. VWF with endogenous FVIII is captured onto an ELISA plate, followed by removal of endogenous FVIII using a high concentration solution of calcium chloride. Next, recombinant FVIII is added, and binds to the immobilized VWF. Then, ELISA or a chromogenic assay are used in turn to quantify VWF:Ag and bound exogenous FVIII. A markedly decreased affinity is reported in type 2N. This lower affinity distinguishes type 2N VWD from mild to moderate forms of haemophilia A (Sadler et al., 2000, Laffan et al., 2004, Caron et al., 2009).

1.8.3.4. VWF-collagen binding assay (VWF:CB)

This ELISA based technique investigates and evaluates the binding affinity of VWF to collagen. This assay depends upon the presence or absence of VWF with a HMW multimer structure much as does the VWF:RCo assay, where strong binding is achieved with HMW VWF (Neugebauer et al., 2002). The presence of mutations within VWF in the A3 domain may also affect the binding affinity of VWF to collagen (Ribba et al., 2001). The normal range of this assay is very similar to those for the VWF:Ag and VWF:RCo assays (66-226 IU/dL).

1.8.3.5. The ratio of VWF pro-peptide to mature VWF (VWFpp/VWF:Ag)

This test investigates the ratio of the VWF pro-peptide (VWFpp) to VWF:Ag in patients with type 1 VWD in order to evaluate the survival of VWF in the plasma. These two proteins are found dissociated and circulating independently in the plasma. The half-life of VWFpp, which circulates as a homodimer, is 2-3 hours, while mature VWF has a half-life of 8-12 hours (Borchiellini et al., 1996, Haberichter et al., 2006). The normal ratio of pro-peptide to mature VWF is expected to be one. This ratio is increased in individuals with mutations which lead to reduced survival or increased clearance of VWF such as p.R1205H. This is possibly due to normal VWF secretion and normal levels of pro-peptide but reduced levels of mature VWF due to an increased rate of clearance (Haberichter et al., 2008). This ratio may help in the identification of a number of patients with type 1 VWD having mutations enhanced VWF clearance that results in short half-life (Eikenboom et al., 2013a).

1.8.3.6. Molecular analysis of *VWF* gene

VWF analysis can be performed in order to help diagnose and classify VWD. Some mutations in *VWF* are specific to particular VWD subtypes. Moreover, the detection of genetic defects, including missense mutations, deletions and insertions can make the molecular mechanism of VWD easier to comprehend and can help clarify VWD pathogenesis as well as facilitate the diagnosis and subtyping of VWD cases (Laffan et al., 2004). The presence of missense mutations associated with type 2 VWD in particular VWF domains has given rise to recommendations to analyse specific regions. It is better to start with these domains but a further search in other domains may be required (Keeney et al., 2008). The first of these being exons 17-27 in type 2N and exon 28 in type 2A, 2B and 2M and exons 1-52 in type 3. Mutations that are found in type 1 are mostly missense and located throughout *VWF* (Cumming et al., 2006, Goodeve et al., 2007, James et al., 2007). All exons should be sequenced when there were no mutations identified or dosage analysis can be applied to detect large deletion or duplication within *VWF*.

1.8.3.7 Factors that make diagnosis of type 1 VWD difficult

The diagnosis of VWD is based on the presence of low levels of VWF in the patient's plasma in addition to the presence of bleeding symptoms in patients and family members. The diagnosis of VWD is difficult due to various physiological and environmental reasons. Firstly, a slightly low level of VWF is often found in blood group O individuals, who may be difficult to distinguish from patients who have classic type 1 VWD. Also, incomplete penetrance of *VWF* mutations in different families and variable expressivity in the same family result in variable levels of VWF (Tosetto et al., 2007). Furthermore, low levels of VWF are often associated with the presence of mild bleeding disorders, but this does not necessarily indicate VWD and can lead to false positive diagnosis (Sadler, 2007). Levels of VWF increase spontaneously in response to stress, infections, pregnancy, and exercise and also with age, which may hide the true level of VWF, lead to less bleeding and thereby cause misdiagnosis of VWD. Finally, the reduced sensitivity of tests used to diagnose type 1 VWD and variability in bleeding symptoms make the diagnosis difficult because of variable expressivity and mutation penetrance. However it may contributes to difficulties of properly differentiation between patients with mild type 1 VWD and healthy individuals who have VWF levels close to the lower end of normal range (Eikenboom et al., 2006).

1.9. Classification of von Willebrand disease

Various classifications of VWD have been reported based upon the VWF phenotypic analysis and the severity of the bleeding among VWD patients and the initial classifications were

complex (Holmberg and Nilsson, 1972, Ruggeri and Zimmerman, 1987). In 1972, Holmberg and Nilsson categorized the disorder into two main groups, one with normal VWF antigen plasma concentration and another with structurally abnormal VWF antigen. This was done using the crossed immuneelectrophoresis technique (Holmberg and Nilsson, 1972). In 1987, when the molecular structure and function of VWF was known, Ruggeri *et al* (1987) offered a definitive classification of the disease based upon the structural and functional abnormalities of VWF. This classification was mainly based on the VWF multimer patterns in order to distinguish various types of VWD using agarose gel electrophoresis. Limited phenotype data provided minimal information about the molecular mechanisms that lead to various types of VWD. Moreover, this categorization led to the emergence of many disease subtypes that clinicians found difficult to use for diagnosis and treatment of VWD patients (Ruggeri and Zimmerman, 1987, Schneppenheim et al., 2001b).

Thus, in 1994, a simplified, easier to use phenotypic classification based on the clinical and laboratory characteristics of VWD, including its molecular aspects, was proposed by Sadler. This was accepted by the International Society on Thrombosis and Haemostasis Scientific and Standardisation Committee on von Willebrand Factor (ISTH SSC on VWF). Accordingly, VWD is currently classified into three main, or primary, types based on laboratory findings and family data. These three types are: partial quantitative deficiency (type 1), qualitative deficiency (type 2) and total quantitative deficiency (type 3). Type 2 VWD is further subdivided into four sub, or secondary, types: 2A, 2B, 2M and 2N, depends upon the pathophysiological mechanism. In certain circumstances, tertiary information that includes the name of the place that indicates a remarkable phenotype such as a "Vicenza" mutation or a VWF multimer pattern that in turn indicates that a particular disease mechanism, such as 2A (IIC) or (IIE) can be used (Sadler et al., 2006).

The previous classification restricted VWD to *VWF* mutations, implying that mutations within the gene were the predominant cause of VWD. In 2006, with increased knowledge of the pathophysiology of VWD, VWD classification was reviewed, re-evaluated and progressed by the ISTH SSC on VWF to incorporate new ideas on the disease (Sadler et al., 2006). Two amendments to the 1994 classification were introduced. Firstly, that VWD is not only caused by *VWF* mutations due to many patients having shown no identified mutation and it thus being a possibility that other genetic defects contribute to the disease phenotype. Secondly, that normal quantity and quality of plasma VWF can be observed in type 1 VWD patients who presumably bleed despite the presence of a mutation in *VWF*. This may due to the incomplete penetrance and variable expressivity of some *VWF* mutations (Sadler et al., 2006). Moreover, recent studies on type 1 VWD identified patients with slight multimer abnormalities that do not impede VWF function (Goodeve et al., 2007, James et al., 2007). This new version of the classification aimed

to facilitate and enable procedures for diagnosis and treatment to provide the best care for VWD patients.

1.9.1. Type 3 VWD

Type 3 VWD is the rarest of all the VWD types and accounts for less than 5% of all VWD cases with a very low frequency amongst the population, there being only 0.5 case per one million individuals in Scandinavian countries (Mannucci et al., 1984). However, in communities where consanguineous partnerships are common such as Iran, Arabic and Indian population, the frequency can be as high as 6 cases per million people (Sadler et al., 2000, Ghosh and Shetty, 2011). This type is most prevalent within Middle Eastern populations, especially the Arab and Iranian population, while it is least prevalent within Southern European populations (Weiss et al., 1982, Berliner et al., 1986, Lak et al., 2000). Type 3 VWD is the most clinically severe form of VWD and is characterised by undetectable VWF in the plasma and platelets as well as a secondary reduction in the level of FVIII, leading to the impairment of both primary and secondary haemostasis. It is inherited as an autosomal recessive trait. Patients with homozygous or compound heterozygous forms usually present with severe haemorrhagic symptoms, including epistaxis, bleeding following surgical procedures, menorrhagia, and mucocutaneous and arthropathic bleeding, at an early stage in their lives due to a severe reduction in FVIII (Nichols and Ginsburg, 1997, Federici, 2004), while heterozygous relatives occasionally present with mild haemorrhagic symptoms. A large number of mutations responsible for this type have been reported as being distributed throughout the whole *VWF* locus, including the coding and non-coding (splice sites) sequences (Figure 1.1D). These mutations are highly variable among various populations and mostly impair VWF production and cause a null allele phenotype. The genetic abnormalities associated with type 3 VWD include nonsense, large deletion, splice site, small deletion and small insertion, all of which result in frameshift. These mutations account for almost 80% of mutations, while missense mutations account for the remaining 20% (Zhang et al., 1994, Baronciani et al., 2003, Bowman et al., 2013). The large deletions involve the removal of one or more exons of *VWF* sequence and are mainly associated with type 3 VWD. Expression studies have shown that large deletions may impair VWF multimerisation and cause a reduction in VWF secretion. Deletions in type 3 are usually out of frame which causes a truncated protein to be made which is degraded through nonsense mediated decay. A study conducted by Allen *et al*. reported that a number of type 3 missense mutations cause intracellular retention of VWF because mutations disrupt VWF multimerisation and thus affect VWF folding (Allen et al., 2000b). Moreover, gene conversion between *VWF* and *VWFP*, where the pseudogene sequence introduces a null mutation, is considered to be a mechanism associated with type 3 VWD (Gupta et al., 2008, Sutherland et al., 2009b).

1.9.2. Type 2 von Willebrand disease

Type 2 VWD represents the qualitative defects of VWF that affect its function. Up to 25% of all VWD patients have type 2 VWD. According to the most recent classification, type 2 VWD is subdivided based on the structural and functional defects that alter the binding of VWF to FVIII or to platelets or collagen and therefore alter platelet adhesion. Various types of mutations, nearly all missense and others such as in-frame deletions and insertions, are associated with the disease phenotype in the majority of patients.

1.9.2.1. Type 2A VWD

This is the commonest variant of type 2 VWD, being found in almost 75% of all type 2 VWD patients and is mostly inherited as autosomal dominant although some variants are inherited as autosomal recessive (Schneppenheim et al., 2010). Type 2A is a qualitative defect that affects the function of VWF due to an absence or a reduction in HMW-VWF multimers. This impairs VWF binding to the platelet binding site on GpIbα. Patients with this type usually present mild to moderate bleeding symptoms with normal or reduced levels of VWF:Ag and FVIII:C activity and an abnormal functional assay as a significantly decreased level of VWF:RCo is observed in addition to reduced VWF:RCo/VWF:Ag ratio (Nichols and Ginsburg, 1997, Meyer et al., 2001, Schneppenheim and Budde, 2005). The majority of mutations that contribute to this variant are missense, and are mainly (82%) located in the A1 and A2 domains of VWF encoded by exon 28, although few mutations have also been identified in the D3 domain in type 2A(IIE) (Meyer et al., 1997, Schneppenheim et al., 2010). About 8% of mutations are found in the pro-peptide domains and a further 8% of mutations are found in the C-terminal domains (Figure 1.1D). (Hilbert et al., 1995, Meyer et al., 1997, Sadler et al., 2006). These mutations lead to the emergence of the disease and cause structural and functional changes to the VWF through two main mechanisms. Firstly, they impair the assembly of large VWF multimers, causing the secretion of small or intermediate multimers, which reduce the binding to platelets or other receptors (Zimmerman et al., 1986, Lyons et al., 1992). More than 70 mutations have been identified, of which 64 of 70 are missense in various VWF domains impairing normal VWF multimer assembly and secretion, leading to less HMW (VWF) multimers in plasma and platelets (http://www.vwf.group.shef.ac.uk/ accessed November, 2012) (Hampshire and Goodeve, 2011). Many studies have identified various types of mutations mostly are missense and rarely small deletion, large deletion and insertion in different domains that impair or prevent VWF multimerisation, alter intracellular transportation can lead to intracellular retention of VWF. Homozygous or compound heterozygous mutations that occur in the pro-peptide D2 domain encoded by exons 11-17 impair multimer assembly in the ER due to abnormal formation of disulphide bonds and prevent multimerisation and intracellular transport, thereby

producing small multimers or dimers and the presence of a fine smear around the central bands that lack the ability to react with platelets. This is inherited as autosomal recessive, and was originally named type 2A(IIC) VWD (Ruggeri et al., 1982, Batlle et al., 1986, Schneppenheim et al., 1995). Other types of heterozygous mutations located in the CK domain can impair the assembly of dimers in the ER and prevent the dimerisation of pro VWF. These mutations lead to the secretion of small multimers that lack normal function in addition to absence of triplet satellite bands normally results from ADAMTS13 cleavage. This multimer pattern was initially referred to as VWD type 2A(IID) which exhibit dominant inheritance (Kinoshita et al., 1984, Schneppenheim et al., 1996, Budde, 2008). The 2A(IIE) phenotype is characterized by the lack of large VWF multimers. This subtype is inherited as autosomal dominant and often caused by heterozygous mutations leading to loss or gain of cysteine residues in the D3 domain that can impair multimerisation and further multimer assembly due to interfering with the formation of disulfide bonds in the Golgi and secretion of oligomers only. These mutations produce smeary multimer patterns characterized by absence of the outer proteolytic bands (Zimmerman et al., 1986, Meyer et al., 2001, Schneppenheim et al., 2001b, Schneppenheim et al., 2010).

The second mechanism is characterised by impaired VWF assembly and secretion in addition to increased sensitivity of VWF to the cleaving protease represented by ADAMTS13, which is caused by mutations located in the A2 domain. Mutations in the A2 domain can lead to increased proteolysis by ADAMTS13 and impair multimer assembly due to abnormal folding caused by mutation (Sadler et al., 2006, Nichols et al., 2008b). These mutations markedly interfere with VWF folding and make the p.Y1605-M1606 bond in the A2 domain accessible to the cleaving protease. Based on this mechanism, this pattern has been divided into two mutation groups. The hallmark of group I, which has an effect on the A2 domain folding, is the presence of mutations that enhance proteolysis and mainly impair multimer assembly and impair intracellular transport or secretion, whereas group II mutations have normal multimerisation and secretion of VWF, but multimer destruction can occur in plasma due to enhanced susceptibility of HMW-VWF to cleavage that results from extracellular proteolysis by ADAMTS13 following secretion (Zimmerman et al., 1986, Lyons et al., 1992). Jacobi *et al* (2012) have reported several mutations identified in type 2A patients that do not fit into either group I or II categories. These mutations result from complex mechanisms that include intracellular retention and degradation of VWF, loss of WPB formation and regulated storage which is associated with severe reduced secretion and abnormal multimer assembly in mutations involve cysteine residues (Jacobi et al., 2012).

1.9.2.2. Type 2B VWD

This is the rarest subtype accounting for less than 5% of all VWD cases and is characterized by an increased affinity of VWF for the platelet GpIbα binding site, which may be associated with reduced HMW multimers in the plasma as a result of increased cleavage by ADAMTS13 (Keeney and Cumming, 2001, Sadler et al., 2006). This type is inherited mostly as autosomal dominant with a few cases being recessively inherited but not confirmed by mutation analysis (Donner et al., 1987). Mutations responsible for this type cause conformational changes that render the GPIbα receptor exposed and enable VWF to bind to platelet GpIbα spontaneously (Sadler et al., 2006). The majority of the mutations that are responsible are missense mutations that are located within or adjacent to the VWF A1 domain (Figure 1.1D) (Sadler et al., 2006, Goodeve, 2010). These mutations stabilise the A1 domain bound conformation and thereby enhance the binding of VWF to the platelets (Randi et al., 1991, Huizinga et al., 2002). Although many studies have reported that almost 25 missense and one duplication mutations are associated with type 2B VWD, four mutations are considered to be the most common (http://www.vwf.group.shef.ac.uk/ accessed November 2012). Frequent variants are located within the A1 domain and are responsible for almost 90% of this form of VWD (Ginsburg and Sadler, 1993, Nichols and Ginsburg, 1997, Meyer et al., 2001).

1.9.2.3. Type 2M VWD

Type 2M VWD is dominantly inherited, and bleeding symptoms vary from mild to severe (Nitu-Whalley et al., 2000, Sadler et al., 2006). This subtype is caused by mutations that alter the binding of VWF to platelet or to the subendothelium, which has an essentially normal range of HMW multimers. (Meyer et al., 2001, Schneppenheim et al., 2001b, Sadler et al., 2006). The function of VWF in this subtype is indicated by a significant decrease in VWF:RCo levels in companion with VWF:Ag. Impaired binding of VWF to platelets decreases the cleavage of VWF by ADAMTS13 and prevents degradation of the VWF subunits, resulting in the preservation of the HMW multimers but loss of HMW-VWF is relatively observed (Mancuso et al., 1996, Budde, 2008). Most of the detected mutations that alter platelet binding and are responsible for type 2M VWD are missense or in-frame deletions located in the A1 domain encoded by exon 28 (Figure 1.1D) (Rabinowitz et al., 1992, Meyer et al., 2001). Moreover, mutations found in the A3 domain may cause type 2M VWD by reducing the binding of VWF to collagen and thereby reducing platelet adhesion. They include p.L1696R, p.S1731T, p.W1745C, p.S1783A, p.H1786D and p.P1824H (Ribba et al., 2001, Flood et al., 2012, Legendre et al., 2013).

1.9.2.4. Type 2N VWD

Type 2N VWD, which is recessively inherited, was initially described as the 'Normandy' type of VWD because the first patient with this subtype was born in this area of France. Type 2N is characterised by the markedly reduced binding affinity of VWF to pro-coagulant FVIII and reduced FVIII levels in the plasma along with normal or mildly reduced levels of the VWF:Ag and VWF:RCo (Mazurier et al., 1990b, Mazurier et al., 2001). Multimers are often normal, but some patients with type 2N have multimer defects, which can include ultra-high MWM or an absence of HMW multimers (Jorieux et al., 1998, Allen et al., 2000a). Type 2N VWD is clinically similar to mild haemophilia A, which can lead to misdiagnosis. Patients usually present with musculoskeletal bleeding symptoms due to decreased levels of FVIII (Mazurier, 1992). However, a differential test measuring the binding of FVIII to VWF (VWF:FVIIIB), is currently used to distinguish between these disorders and also to identify type 2N VWD. Type 2N is the result of mutations located in the FVIII binding site of VWF. These lie between Ser764 and Arg1225 residues and cover the domain D' and part of D3 domain (exons 18-27), which impair VWF binding to FVIII and subsequently is classified as type 2A (Figure 1.1D) (Nishino et al., 1989, Mazurier et al., 1990a, Sadler et al., 2006). Three genetic mechanisms are involved in this subtype: homozygosity, which is less common and involves both alleles having the same 2N missense mutation; compound heterozygosity, where two different 2N missense mutations are found one on each allele; and compound heterozygosity, where in addition to a 2N missense mutation on one allele there is a null mutation of the second (Mazurier et al., 2001, Schneppenheim and Budde, 2005). To date, almost 28 missense mutations have been reported as the genetic cause of type 2N VWD, and it has been found that almost 90% of the cases of this subtype result from three variants: p.R816W, p.T791M and p.R854Q (Mazurier and Meyer, 1996, Mazurier and Hilbert, 2005). The latter one, p.R854Q, is the most prevalent, occurring in the heterozygous form in 1% of the Caucasians population. *In vitro* expression studies have shown that this mutation, when found in the homozygous form, causes the least severe type 2N (Nishino et al., 1996, Castaman et al., 2010a). p.R854Q frequently occurs in the heterozygous form, and it can be co-inherited with other mutations, resulting in mixed or dual type 2N/other VWD types. Several mutations in the *VWF* D' domain have been identified in type 2N VWD patients, an example of them p.C788Y and p.C858F, These alterations, which induce conformational changes in the D' domain, reduce the binding of FVIII to VWF in addition to impairing normal VWF multimerisation and secretion (Jorieux et al., 2000)

1.9.3. Type 1 VWD

Type 1 VWD is the most common form of VWD with 70-80% of all patients diagnosed with VWD having type 1. It is characterised by a partial quantitative deficiency of VWF in the

plasma, and patients usually present with mild to moderate mucocutaneous bleeding symptoms including easy bruising, epistaxis, prolonged bleeding following surgery and dental extraction or cleaning, menorrhagia and postpartum bleeding. Musculoskeletal bleeding also occurs when FVIII is reduced secondary to reduced VWF. Bleeding symptoms are mostly associated with low levels of VWF and are observed more in adult females than males and children due to increased rates of exposure to haemostatic challenges. Menorrhagia is the most common bleeding symptom among women, while bruising and epistaxis are observed more in children (James and Lillicrap, 2006).

Type 1 VWD is mostly inherited as an autosomal dominant trait with reduced penetrance and variable expressivity, which complicates diagnosis, and more rarely inherited as autosomal recessive (Nichols and Ginsburg, 1997, Keeney and Cumming, 2001, Cumming et al., 2006, Goodeve et al., 2007). Reduced/incomplete penetrance of type 1 VWD mutations means that an individual with a known mutation within VWF does not display any phenotypic symptoms of disease, whereas the variable expressivity of a mutation means that individuals with a known mutation can express vastly different phenotypes. These could potentially be due to other polymorphisms or mutations that are inherited alongside them, meaning that both mutations would have to be present in order to result in a disease phenotype and that if only one is present, an individual does not present with bleeding symptoms. One of the changes in the updated VWD classification is the inclusion of type 1 VWD patients who have slightly decreased HMWM, which does not affect the relatively normal function of VWF levels (Sadler et al., 2006).

1.9.3.1. Type 1 VWD mutational cohort studies

Since 2000, three early multicentre studies have carried out analysis of groups of patients and their families diagnosed with type 1 VWD. These three studies were the MCMDM-1VWD study (Molecular and Clinical Markers for the Diagnosis and Management of type 1 von Willebrand Disease), which was conducted within the European Union, the UKHCDO study (United Kingdom Haemophilia Centre Doctor's Organisation), which was conducted in the UK, and the Canadian study (Cumming et al., 2006, Goodeve et al., 2007, James et al., 2007). Also, Swedish and American studies have been conducted and analysed group of patients diagnosed with type 1 VWD (Lanke et al., 2005, Flood et al., 2011). The genetic linkage between *VWF* and type 1 VWD was investigated in 31 Swedish families diagnosed with type 1 VWD according to ISTH criteria. As a result, genetic co-segregation to *VWF* was observed high in 87% of families because families who were non informative excluded from the study (Lanke et al., 2005). The aim of these studies was to improve our understanding of the molecular basis and pathogenesis of type 1 VWD. These three extensive studies recruited 305 IC from a number

of families who were historically diagnosed with type 1 VWD in addition to a large number of healthy controls. The outcome of these three studies was similar, with the highest proportion of identified mutations, 62-70%, being missense mutations, while other types of mutations, such as splice sequence mutations, transcription regulatory mutations, small deletions, insertions and nonsense mutations were also identified in lower proportions ranging from 2 to 16%. Almost 40% of families recruited in these studies were linked to *VWF* (Eikenboom et al., 2006). The majority of these mutations are located in the A1, A2 and D3 domains. The level of VWF was lower on average when a mutation was detected. However, to date, although these three studies failed to detect mutation in 35-40% of cases, they have identified almost 150 in total different mutations in the *VWF* gene as the main cause of VWD in 60-65% of IC and the online locus-specific database for von Willebrand disease (http://www.vwf.group.shef.ac.uk/) holds details of these mutations (Hampshire and Goodeve, 2011). Moreover, these studies reported that more than one candidate mutation was identified in 15-20% of cases (Cumming et al., 2006, Goodeve et al., 2007, James et al., 2007). These genetic abnormalities may alter the expression, processing and function of VWF.

1.9.3.1.1. The European Union study on type 1 VWD

The EU study (MCMDM-1VWD) which was co-ordinated from Sheffield, was designed with the aim of increasing knowledge about molecular mechanisms and the pathogenesis of type 1 VWD. It initially recruited a total of 154 IC with affected and unaffected family members from fourteen VWD treatment medical centres in nine European countries. Later, four IC were eliminated from the study; two because the multimers were not detected due to a very low level of VWF, one due to insufficient plasma sample and one because the DNA sample was insufficient for mutational analysis (Goodeve et al., 2007). A total of 150 IC who were historically diagnosed with type 1 VWD and their families, 278 affected members (AFM) and 312 unaffected members (UFM) plus 1166 healthy control (HC) samples were included in this study. The healthy controls' samples were analysed along with the VWD patients' samples in order to help understand the molecular basis of VWD. Every family recruited for this study contained one IC, as many affected and unaffected members as possible and a minimum of two generations. Extensive phenotypic and genotypic studies were performed. During recruitment, several coagulation tests were performed on all members of all the families and HC individuals to determine the individual phenotypes. In addition, to evaluate the severity of the bleeding, all family members were assessed using a detailed bleeding score questionnaire. Most of the patients had at least one bleeding symptom, while almost 80% presented with more than one symptom. Few individuals classified as UFM showed bleeding symptoms at recruitment (Tosetto et al., 2006). To assess the linkage between *VWF* and clinical and phenotypic data in

the recruited families, three different short tandem repeat markers were used to detect linkage between VWD and *VWF*. The GT_n repeat marker, which is located within the promoter region, and the $TCTA_n$ repeat (STR III) and $TCTA_n$ repeat (STR II), which are both located within intron 40, were used (Eikenboom et al., 2006). Within this study, VWD was linked to *VWF* in 70% of cases; of which complete co-segregation was achieved in 40% of IC and 30% was not linked to *VWF* plus 30% was non-informative.

Extensive amplification and sequencing of the entire coding region of *VWF* (exons 2-52) and the closely flanking intronic regions in addition to 2 kb of the 5' regulatory region was performed for mutational analysis in most IC. This cohort was analysed using various mutational scanning techniques including single-stranded conformation polymorphism (SSCP), conformation sensitive gel electrophoresis (CSGE), denaturing high-performance liquid chromatography (dHPLC) and direct DNA sequencing, which was used following screening to identify all mutations (Goodeve et al., 2007). As a result, 124 mutations were identified in 105 (70%) of the IC, 34% (54) of which were novel mutations. These identified mutations were mainly missense (80%), although others, including splice, nonsense/insertion and promoter, were found to a lesser degree. The mutations identified were located throughout *VWF*, most of them within the A domains. Almost 50% of IC showed incomplete penetrance. 10 to 15% of mutations resulted in null alleles, and more than one mutation was detected in 15% of IC. The most frequent candidate mutations identified were p.Y1584C and p.R1205H (Goodeve et al., 2007).

The analysed IC were divided into three groups based on the multimer pattern and the presence or absence of mutations. Group 1 represented the 57 IC (38%) who had abnormal multimers, a very low level of VWF:Ag with median ranges between 10 and 19 IU/dL and the median BS was 10. Abnormal multimers do not fit with the standard criteria for type 1 VWD diagnosis, however, these 'atypical' individuals were studied to ensure no mutations within the cohort were overlooked. The abnormal multimers showed as either a relative loss of high molecular weight VWF multimers, or abnormal satellite bands (Sadler 1994, Goodeve et al. 2007). The reduction of VWF levels was more in IC with more than one mutation compared to those with only one mutation. Mutations were found in 54/57 and the remaining 3 IC showed no mutation although having abnormal multimers, with one candidate mutation being reported in 45 IC and the remaining IC showing more than one candidate mutation. Complete co-segregation was seen in almost 60% of cases (Goodeve et al., 2007). Group 2 represented the 51 IC (34%) with normal multimers and identified mutations. Also, the IC in this group had moderate levels of VWF:Ag, ranging between 26 and 70 IU/dL and median BS was 8. 44 IC

each had one mutation identified, while two or more mutations were identified in 7 IC. Complete co-segregation was observed in 41% of cases (Goodeve et al., 2007).

The third group is the questionable group, and more research is needed due to the absence of mutations amongst the IC representing this group. Although the patients did bleed, the MCMDM-1VWD study failed to detect genetic alterations in 42 IC (28%) of the investigated 150 IC although the median BS was similar to other groups (median BS=8). These IC had normal multimers but no identified mutation even though the median level of VWF:Ag was 49 IU/dL, higher than levels in groups 1 and 2 but below the normal range (NR=50-200 IU/dL). Out of the 42 cases, eleven children aged 6-18 years showed no significant bleeding despite four of them having a reduced level of VWF. In contrast, out of the 31 cases that bled, 23 presented with a low level of VWF, 13 of which were not linked to *VWF*. Complete co-segregation was observed in only 19% of this group and incomplete co-segregation was observed in 45% of cases. Blood group O was predominant amongst this group and accounted for almost 76% of IC, while 63% of complete segregating IC and 89% of incomplete co-segregating IC had blood group O (Goodeve et al., 2007).

1.9.3.1.2. Reasons for failure to detect mutations

Although these three studies provided details about the molecular and genetic basic of type 1 VWD, they failed to detect the genetic alterations or mutations involved in VWD in 30-40% of VWD cases (Cumming et al., 2006, Goodeve et al., 2007, James et al., 2007). The failure of these studies to determine the cause of these genetic defects can be explained by the following:

1.9.3.1.2.1. Missed mutations

Mutations may have been missed in some families in the EU study that showed complete co-segregation. Several mutation analysis methods, including SSCP, CSGE, DHPLC and direct DNA sequencing, were used to sequence *VWF* exonic regions (Goodeve et al., 2007). However, these methods can lack sensitivity and thus may have missed mutations (Markoof et al., 1998, Whittock et al., 1999, Eng et al., 2001). Furthermore, mutations may have also been missed due to human error. Re-evaluation of patients within this group using direct sequencing could identify new mutations.

The *VWF* gene is a highly polymorphic gene, and mutations may be missed due to the presence of SNP located within sites of primer annealing that can lead to poor or mono-allelic amplification of the mutant allele. SNP within the primer sequence could mask a heterozygous genetic defect, and this could cause a mutation to be missed (Eikenboom et al., 1994, Thomas et al., 2006b, Hampshire et al., 2010). The primers used in the EU study were designed prior to the

availability of the complete *VWF* sequence using the limited knowledge of the sequence available in 2000. This limited knowledge lacked information on SNP that impact on molecular analysis (Goodeve et al., 2007). After re-designing primers free of SNP within their sequence, Thomas *et al*. (2006) and Hampshire *et al.* (2010) identified mutations in patients with type 1 and type 2 VWD whose previous mutation analysis was negative. Thus, reviewing the design of primers for SNP on a regular basis is recommended.

1.9.3.1.2.2. Misdiagnosis of type 1 VWD

Many environmental and genetic factors make the diagnosis of type 1 VWD difficult, and this may lead to misdiagnosis or false positive diagnoses of VWD, leading to an unexpected link to *VWF*. Furthermore, many studies have shown that other bleeding disorders may impair the function of VWF and result in bleeding symptoms similar to those of VWD (Cumming et al., 2006, Eikenboom et al., 2006). During the EU study, Daly *et al*. reported a novel genetic defect in *P2RY12* (c.520A>G; p.K174E) in a patient who was initially diagnosed with mild type 1 VWD and were found to have a locus heterogeneity that may contribute to bleeding symptoms (Daly et al., 2009). In this instance the mutation in P2RY12 is likely to explain the bleeding symptoms and hence this IC is likely to have a platelet defect disorder rather than type 1 VWD.

1.9.3.1.2.3. Heterozygous copy number variation (CNV)

It has been proposed that large deletions and duplications of *VWF* may be causative mutations in type 1 VWD; however, these mutations can be missed when present as large scale heterozygous deletions or duplications of either single or multiple exons within *VWF*. Heterozygous deletions of *VWF* in type 1 VWD were not detected using standard DNA sequencing/ mutation scanning techniques due to the presence of the wild-type allele, standard sequencing and scanning methods do not quantify exons present and so detection of heterozygous deletions is difficult. However, Sutherland *et al* (2009) detected a deletion involving exons 4-5 that was homozygous in type 3 individuals and heterozygous in type 1 individuals. This deletion was initially detected in homozygous type 3 individuals due to exons 4 and 5 failing to amplify during PCR analysis in 7 patients, leading to the detection of a deletion of exons 4-5. The deletion and breakpoints was confirmed using a PCR primer walking technique. A multiplex PCR was then designed around the breakpoints, to be able to screen patients that were homozygous and heterozygous for the deletion. This multiplex assay was used to screen 34 individuals in the UKHCDO type 1 VWD study for a heterozygous deletion of exon 4-5 and it was confirmed in 2 individuals, suggesting that heterozygous deletions may contribute to type 1 VWD (Sutherland et al., 2009a). Therefore, newly developed techniques capable of finding these alterations, such as multiplex ligation-dependent probe amplification

(MLPA), have been recommended (Sellner and Taylor, 2004, Cumming et al., 2006). Moreover, Cartwright *et al* (2013) reported that copy number variation (CNV) may contribute to type 1 VWD pathogenesis in the EU study. Large deletions of exons 4-5 (3 IC) and of exon 3, 32-34 and 33-34 were identified each in 1 IC, none of which had been previously identified in the EU study (Cartwright et al., 2013). MLPA could therefore be implemented as an initial screen for all types of VWD mutational analysis (Yadegari et al., 2011).

1.9.3.1.2.4. Other genetic loci may contribute to VWD

The presence of mutations or genetic alterations outside of *VWF* other than the ABO blood group locus could be a possible cause of VWD and may influence the survival of VWF in the plasma by increasing the rate of protein clearance (Casana et al., 2001, Eikenboom et al., 2006, James et al., 2007). ABO groups can affect VWF levels due to the different complexities of carbohydrate structures present on VWF between individuals with different blood group. ABO blood group system is based on A,B or H antigens on red blood cells and other carbohydrate structures. N-linked and O-linked carbohydrates can have A, B or H carbohydrates which are added during dimerisation, multimerisation and maturation of VWF in the ER and Golgi (Canis et al. 2010, Canis et al. 2012). *ABO* codes for a glycosyltransferase, which adds N-acetyl galactosamine to galactose of the H carbohydrate in A blood group; another galactose is added to the galactose of H antigen for blood group B and in people with O blood group nothing is added and the H antigen carbohydrate structure is unchanged. This is because there is a nucleotide deletion in *ABO*, which introduces a stop codon and leads to loss of function of the glycosyltransferase enzyme.

Smith *et al.* in the Cohorts for Heart and Aging Research Genome Epidemiology (CHARGE) study reported seven different candidate genes outside of *VWF* that demonstrate significant statistical associations with VWF:Ag levels in the plasma either through impaired gene expression or biosynthesis or by increasing the rate of VWF clearance. Syntaxin binding protein 5 (*STXBP5*) and syntaxin 2 (*STX2*) proteins associated with exocytosis and vesicular trafficking, while other genes such as stabilin-2 (*STAB2*), C-type lectin domain family, member M (*CLEC4M*) and scavenger receptor class A, member 5 (*SCARA5*) were significantly associated with level of VWF possibility due to increased VWF clearance (Smith et al., 2010, Rydz et al., 2013). Table 1.1 lists various genes that can influence the level of VWF in the plasma.

Table 1.1 Genes shown to be associated with variation in the level of VWF and their location adapted from Smith *et al* 2010.

Protein function	Encoded protein	Located on chromosome	Gene
Regulates exocytosis and neurotransmitter	Syntaxin-binding protein 5	6	***STXBP5***
Mediates uptake of ferritin- bound iron Ferritin receptor	Ferritin receptor	8	***SCARA5***
Express transferase enzymes with different glycosyltransferase properties, adding either N-acetyl galactosamine to the H antigen to convert to the A antigen or adding galactose to the H antigen converting it to into the B antigen. A mutation in the *ABO* gene can stop glycosyltransferase activity and prevent addition of a sugar group, leaving the H antigen (O blood group)	ABO protein	9	***ABO***
Transmembrane receptor protein which has been shown to have a number of functions in angiogenesis, lymphocyte homing, cell adhesion and receptor scavenging	Stabilin-2	12	***STAB2***
Syntaxins have been shown to function in the targeting and fusion of intracellular transport vesicles and in epithelial morphogenesis	Syntaxin-2	12	***STX2***
Not known	Tandem C2 domains nuclear protein	14	***TC2N***
Involved in the innate immune system response and recognition of bacteria and viruses	C-type lectin domain family 4, member M	19	***CLEC4M***

The Genetic Analysis of Idiopathic Thrombophilia (GAIT) study was a genome-wide linkage analysis on chromosomal loci that may influence the levels of VWF among 21 thrombophilic Spanish families. As a result, this study confirmed the presence of potential genetic loci additional to the *ABO* locus on chromosomes 1, 2, 5, 6 and 22 that influence VWF levels and may influence the risk of thromboembolic disease. This study interestingly indicated that the *ABO* locus has the major influence on circulating VWF levels, while *VWF* alone has only a limited influence (Souto et al., 2003). In addition to studies on humans, experimental studies performed to investigate *VWF* and potential other genetic loci in mice because the mouse model of VWD shows similar levels of VWF with incomplete penetrance and variable expressivity compared to humans. A number of studies were conducted in order to analyse the genotype and phenotype and to explain the variability in circulating VWF. These studies were able to identify a number of loci when cross breeding with specific mouse strains (Table 1.2).

Table 1.2 List of studies conducted on mice demonstrated VWF variability

Comments	Reference
Identification of one locus termed as modifier of VWF1, *Mvwf1* by cross breeding of RIIIS/J and CASA/Rk strains. This locus was accounted for 65% of the variability of circulating VWF levels. The modification effect in *Mvwf1* was suggested to be due to a mutation in *B4galnt2* which can influence VWF glycosylation	(Mohlke et al., 1996, Mohlke et al., 1999)
Identification of another locus within VWF on chromosome 6 termed *Mvwf2* which was able to explain 16% of VWF level variability. This point mutation was found to impair VWF secretion and synthesis	(Lemmerhirt et al., 2007)
Mvwf5 modifier which was found to impair binding of *cis*-regulatory elements in its promoter	(Shavit et al., 2009).
An additional two loci; *Mvwf3* and *Mvwf4* were identified and found to influence VWF levels when co-inherited with *Mvwf2*. Mouse *Mvwf4* was mapped to chromosome 13 and shared homology with a human genetic locus located at chromosome 5 and 6	(Lemmerhirt et al., 2007).
Mvwf6 showed homology to human genetic locus 12q 13.2 and *Mvwf7* modifiers from cross breeding C57BL/6J and WSB/EiJ mice strains which may regulate the level of VWF	(Shavit et al., 2009)

FUT3 (fucosyltransferase 3) encodes fucosyltransferase that required for adding the fucose to polysaccharides during Synthesis of Lewis antigen. *FUT3* encodes for the fucosyltransferase that adds fucose to the precursor molecule (Lewis antigen) where its absence may increases the rate of VWF clearance. Mutations found in *FUT3* were associated with a 10% reduction in the level of VWF (Hickson et al., 2009a). Individuals with Lewis negative genotype showed low levels of VWF compared to Lewis positive genotype while the level of VWF is higher in homozygous individuals carry Se allele than heterozygous ones (O'Donnell et al., 2002b, Cakir et al., 2004). Moreover, Stockley *et al* (2012) identified mutations in platelet G-protein coupled receptor (*GPCR*) genes which are co-inherited in patients with type 1 VWD recruited through the EU study and were found to be associated with the bleeding phenotype. The presence of mutation outside the *VWF* may lead to reduction of VWF level and can explain the disease phenotype observed in IC who showed no mutation in this study.

1.9.3.1.2.5. Single nucleotide polymorphism within *VWF*

Most SNP within *VWF* have no effect on the level of VWF, but two recent studies (Campos et al., 2011, Zabaneh et al., 2011) have shown that SNP located within *VWF* regions that encode the D' and D3 domains, the amino terminal domains of mature VWF may be strongly associated with levels of VWF either through an influence on clearance or on biosynthesis. In order to identify genetic variants associated with VWF levels in healthy individuals, the gene-centric Illumina Human Cardio Vascular Disease (CVD) BedChip was used. As a result, 48 SNP were identified in four genes; *ABO, VWF*, *ESR1*and *NRG1*. A combined effect of five *ABO* SNP and 2 *VWF* SNP located in exon 18 (c.2365A>G; p.T789A) and intron 20 (c.2685+498A>G) on the levels of VWF has been found. The *ABO* polymorphisms were found to be responsible for about 15% and *VWF* polymorphisms for an additional 2% of the variance of the VWF levels (Zabaneh et al., 2011). Also, Campos *et al*, (2011) have reported a significant association between VWF levels and 18 *VWF* SNP, of which 16 were intronic and 2 were silent exonic polymorphisms located in exons 18 (c.2385T>C; p.T795=) and 22 (c.2880G>A; p.R960=) which are within the D' and D3 domains (Campos et al., 2011).

1.9.3.2. Type 1 VWD mutation mechanisms

Mutations affect the level of VWF in various ways. Recent studies have reported a large number of mutations located within different domains that affect the level of VWF in patients diagnosed with type 1 VWD (Figure 1.1D) (Goodeve et al., 2007, James et al., 2007). Mutations can cause type 1 VWD through a number of mechanisms, including: reduced VWF secretion, an increased rate of VWF clearance (decreased survival) and slightly increased susceptibility to the

proteolytic cleavage enzyme ADAMTS13 (Haberichter et al., 2006, Sadler et al., 2006, Goodeve, 2010).

1.9.3.2.1. Reduced secretion and intracellular retention of VWF

Reduced secretion of VWF is considered to be the most common mechanism causing type 1 VWD. The mutations that affect gene expression may impair and disrupt the intracellular transport of VWF to the plasma thereby leading to a low level of VWF, causing an inherited dominant type 1 VWD. The EU study identified a number of missense mutations responsible for the pathogenicity in patients with type 1 VWD (Goodeve et al., 2007). An *in vitro* expression study conducted by Eikenboom *et a*l (2009) was performed to examine the pathogenicity of 14 missense mutations detected in patients diagnosed with type 1 VWD. Interestingly, seven homozygous missense mutations (p.G160W, p.N1661I, p.L2207P, p.C2257S, p.C2304Y, p.G2441C, and p.C2477Y) showed a severe deficiency of VWF in the plasma due to intracellular retention, aberrant multimer patterns indicating loss of HMW multimers and impaired secretion (Eikenboom et al., 2009). Moreover, expression study indicated that four heterozygous mutations (p.2287W, p.R2464C, p.G2518S and p.Q2520P) caused a mild reduction in secreted VWF. Normal secretion was reported for three benign missense mutations (p.G19R, p.P2063S and p.R2313H) (Eikenboom et al., 2009).

1.9.3.2.2. Clearance of VWF in plasma

Haberichter *et al*. (2006), (2008) reported that increased clearance of VWF in the plasma is an important mechanism in the pathogenesis of type 1 VWD. They used the ratio of VWFpp /VWF:Ag in patients with type 1 VWD to evaluate the survival of VWF in the plasma and found an increased ratio among patients with type 1 VWD with certain missense mutations and an increased clearance phenotype after the administration of 1-desamino-8-D-arginine vasopressin (DDAVP-desmopressin) (Haberichter et al., 2006, Haberichter et al., 2008). These findings suggest that an increase in the rate of clearance may be the cause of the low level of VWF in the plasma of affected cases. The most common type of mutation that represents the clearance phenotype is the Vicenza mutation (p.R1205H). According to EU and Canadian studies, this was the second most frequent mutation found in the index cases (IC), affecting almost 6% of them. When patients with this mutation were compared with healthy control individuals, the average half-life of VWF was significantly reduced (<2 hr), clearance after DDAVP infusion was greatly increased, there were lower levels of VWF in the plasma, and multimer structure was abnormal but more subtle than observed in type 2A VWD in some individuals (Casonato et al., 2002, Sadler et al., 2006, Goodeve et al., 2007, James et al., 2007, Budde et al., 2008a). The Vicenza subtype (p.R1205H) was previously classified as type 2M

VWD but is currently classified as type 1 VWD (Sadler et al., 2006). *In vitro* expression studies using r*VWF* have shown that normal secretion is achieved, indicating that the abnormal level is not due to a synthesis defect (Casonato et al., 2002). Other missense mutations, such as p.C1130F, p.W1144G and p.C1149R in the D3 domain and p.S2179F and p.C2671Y in the D4 and CK domains, have been associated with this phenotype and have been shown to cause accelerated clearance and low levels of plasma VWF post desmopressin infusion but to a lesser degree than the Vicenza mutation (Gavazova et al., 2002, Schooten et al., 2005, Haberichter et al., 2006). As a result of these studies, it appears that an increased rate of clearance is responsible for 5-15% of type 1 VWD cases.

1.9.3.2.3. Increased susceptibility to proteolytic cleavage

The most common mutation identified by these three cohort studies was the p.Y1584C variant, which was found in 10-25% of the IC of type 1 and < 2% of healthy individuals (Cumming et al., 2006, Goodeve et al., 2007, James et al., 2007). This mutation is associated with a low level of VWF, ranging between 25 and 40 IU/dL. It slightly increases the susceptibility of VWF to the proteolytic enzyme ADAMTS13 and also increases intracellular retention in affected individuals. Their defects result in impaired binding of VWF to the platelet receptors, thereby reducing platelet plug formation (O'Brien et al., 2003, Bowen and Collins, 2004, James et al., 2006, Sadler et al., 2006). Furthermore, this mutation can cause a slight reduction in survival or increased clearance though to a much lesser degree than the Vicenza mutation. It is located within the A2 domain and has phenotypic penetrance of approximately 70% (O'Brien et al., 2003). The presence of p.Y1584C in individuals with blood group O contributes to slightly increased clearance and susceptibility to ADAMTS13 cleavage (Davies et al., 2007, Davies et al., 2008).

1.10. Environmental and genetic factors affect level of VWF

Although type 1 VWD is the most common of the three VWD types, it is the most complicated to diagnose. The level of VWF may be affected by environmental as well as genetic factors. VWF levels and half-life were found to increase with age at a rate of about 10 IU/dL per decade (Kadir et al., 1999, Nossent et al., 2006). Also, VWF levels increase in response to infection, malignancy, stress, in pregnancy and estrogen treatment, while levels are significantly less in individuals with blood group O compared with individuals with other blood groups, with clearance being accelerated in the blood group O population (Gill et al., 1987, Shima et al., 1995, Kadir et al., 1999, Laffan et al., 2004, Franchini et al., 2007). A study conducted by Gill *et al.* (1987) showed that the average levels of VWF in individuals with blood group O were 25-35 % lower than the average levels in individuals with blood groups A, B and AB . The highest

mean level of plasma VWF was observed in individuals with blood group AB (123.3 IU/dL), but levels were lower in individuals with blood group A (116.9 IU/dL)) and B (105.9 IU/dL) respectively, while the lowest level of VWF was observed in individuals with blood group O (74.8 IU/dL). Also, individuals who have the AO genotype have a lower level of VWF when compared to those with the AA genotype (Shima et al., 1995, O'Donnell et al., 2002a). Moreover, Souto *et al.* (2000) reported that the level of VWF in AO and BO genotypes, where there is one O allele, was significantly lower than in AA, BB and AB genotypes, where there are no O alleles. The average level of VWF in individuals with one O allele (AO) was 2-5% lower than the average level in individuals with no O allele, that is the (AA) genotype (Souto et al., 2000). Various transferase enzymes specificities are encoded by *ABO* glycosyl-transferase alleles. Due to disruption of the allele by a single base pair deletion in individuals with blood group O, the enzyme is non-functional. The presence of sugar groups that are added in individuals with blood group A and B protects VWF from clearance and the clearance of VWF is more rapid due to their absence in blood group O (Castaman et al., 2009). The absence of ABO glycosyl-transferase thus increases the cleavage susceptibility of VWF by ADAMTS13 and contributes to its increased rate of clearance (Bowen, 2003, Davies et al., 2008). It has been shown that the half-life of VWF is influenced by blood group, which influences the rate of clearance of circulating VWF rather than its rates of synthesis and secretion. Nossent *et al* (2006) reported that the half-life of mature circulating VWF in individuals with blood group O (10 hr) is 2 hr lower compared to non-O (12 hr), while VWFpp was not influenced by blood groups because it does not carry ABO antigen (Nossent et al., 2006). Davies et al (2007) showed that the rate of VWF clearance in blood group O individuals who carry the p.Y1584C mutation is higher than those with blood group A who have the same mutation (Davies et al., 2007, Davies et al., 2008).

1.11. Aim of study

The EU study carried out mutational analysis on a group of patients who were historically diagnosed with type 1 von Willebrand disease along with a large number of HC. This cohort study has used various mutation analysis techniques with variable sensitivities. However, this study failed to detect mutations in almost 30% of IC (Goodeve et al., 2007).

The hypothesis being tested in the present study was that mutations in *VWF* have been missed in a proportion of type 1 VWD patients who have been analysed previously due to the insensitivity of mutation scanning methods used or due to the presence of single nucleotide polymorphisms (SNP) within primer annealing sites leading to lack of mutant allele amplification.

One of the initial aims of this study was to revise and screen all primers used during the EU study for the presence of SNP within primer sequences in addition to designing and optimising new primers when SNP were found to reside under historical primers.

The second aim was to re-analyse and re-sequence all 52 *VWF* exons in addition to approximately 50 bp into each end of each intron in 18 candidate index cases historically diagnosed as having type 1 VWD where point mutations were likely to have been missed either due to there being a SNP within primer binding sequences or to insensitivity of the mutation analysis previously undertaken.

A third aim was to perform *in silico* analysis to examine the predicted pathogenicity of any candidate type 1 and non-type 1 VWD mutations identified. In the case on non-type 1 VWD mutations, this was from a historical VWD diagnosis whereby the family (P9F18) was re-classified as a potential type 3 case. *In silico* analysis of the mutations was used to determine the effect of the mutations prior to in vitro analysis. The final aim was to transfect the mutagenized plasmid bearing recombinant mutant *VWF* cDNA (r*VWF*) into HEK293T mammalian cells and to perform *in vitro* expression of both newly detected and other selected mutations in order to determine the effect of any new candidate mutations on VWF structure and function.

Overall, this study aimed to increase knowledge about molecular mechanisms and the pathogenesis of type 1 VWD and to determine the mechanism by which candidate mutations exert an effect on VWF synthesis and secretion (Figure 1.4)

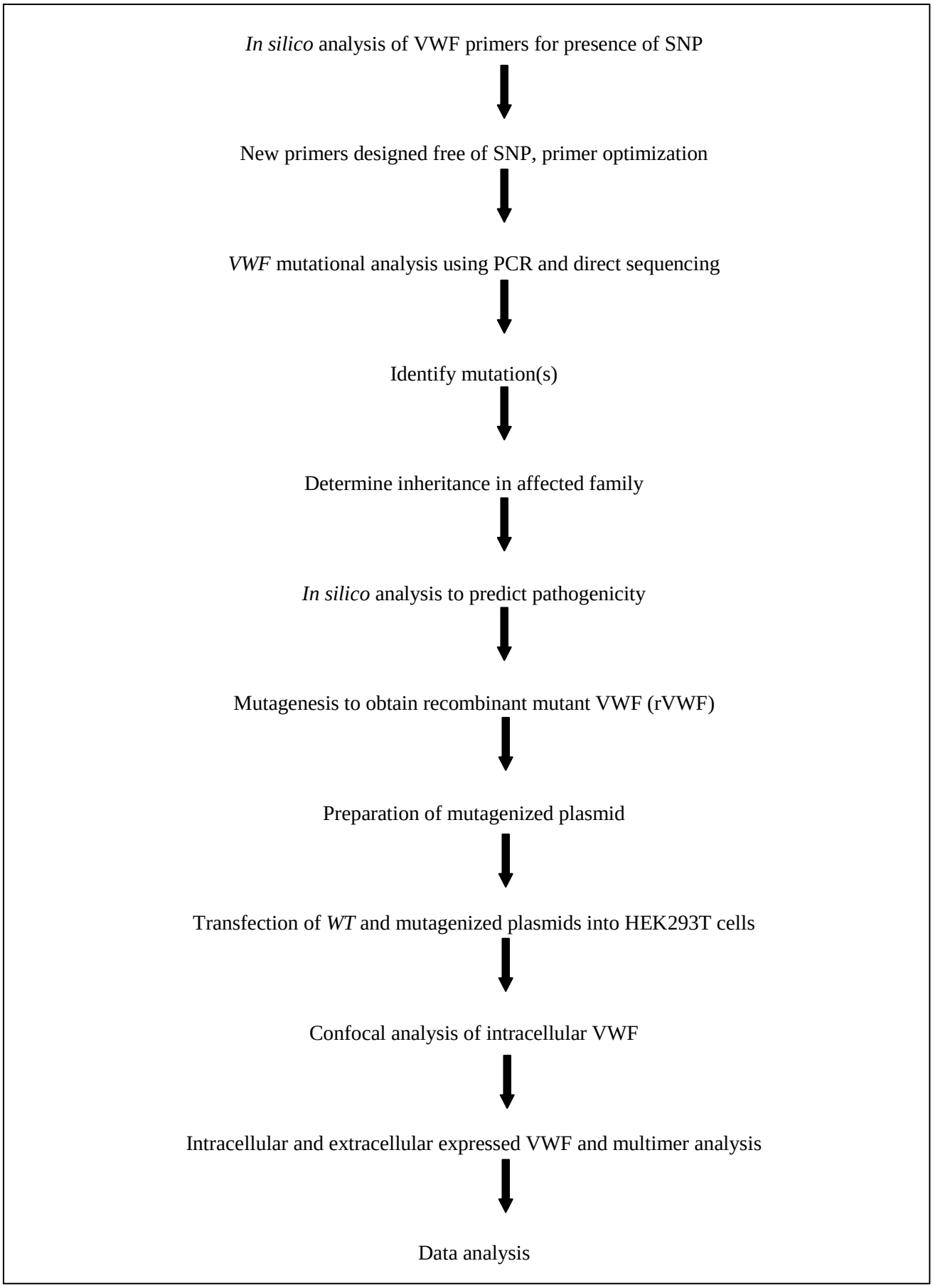

Figure 1.4 Flow chart showing the aim and plan of the study

2. Materials and methods

2.1. Materials

2.1.1. Patient population and samples

The MCMDM-1VWD study included 154 families who were selected from fourteen haemophilia centres in nine European countries and who were historically diagnosed with type 1 VWD and their families, 278 AFM, 312 UFM and 1166 HC (Goodeve et al., 2007). All these cases were diagnosed as type 1 VWD by standard criteria and guidelines created by ISTH-SSC on VWF (Sadler et al., 2006). Among all, *VWF* mutation was not identified in 42 index cases (IC). All individuals were recruited following informal consent.

Clinical and laboratory data as well as genotypic data on all IC were available. The clinical data included bleeding score (Tosetto et al., 2006), while laboratory data included test results for VWF antigen (VWF:Ag), FVIII coagulant activity (FVIII:C), ristocetin cofactor activity (VWF:RCo), platelet function assay (PFA-100 using ADP and epinephrine), ristocetin-induced platelet aggregation (RIPA), VWF-FVIII binding assay (VWF:FVIIIB), the ratio of VWF pro-peptide (VWFpp) to mature VWF (VWFpp/VWF:Ag) and VWF multimer pattern. Any VWF:Ag and VWF:RCo of 3 or less was listed as 3 IU/dL for mathematical purposes. In addition, genetically determined ABO blood group and platelet count results were included. Genomic DNA was extracted from citrated whole blood for all family members and stored at -20°C. Stored genomic DNA from the 18 IC and HC as well was utilised to search for mutations in the *VWF* gene. DNA samples for IC and HC had already been extracted from whole blood during the EU study were used in this study (Goodeve et al., 2007). HC samples were used for two purposes; first to optimise the amplification conditions for *VWF* exons. Second, they were analysed and sequenced alongside IC to compare their traces. Samples were obtained following informed consent.

Eighteen index cases (18 IC) out of 77 IC who were diagnosed as having type 1 VWD within the European Union study (MCMDM-1VWD) were selected for the study. IC selected for the current study either had no mutation detected (n=13) or had a *VWF* mutation detected that was insufficient to explain the patient's phenotype (n=5). Moreover, these selected cases had low levels of VWF and presented with significant bleeding.

2.1.2. Chemicals, reagents, kits and enzymes

Chemicals and reagents were supplied from various sources. They were used for DNA amplification, DNA electrophoresis, PCR product purification DNA sequencing, mutagenesis,

transfection and enzyme linked Immunosorbent assay (ELISA). PCR Master MixReddyMix® was purchased from Fisher Scientific (Loughborough, UK) while thin walled thermo-tube strips and domed cap strips were purchased from ABgene Ltd (Surrey, UK). The ExoSAP-IT kit was supplied by USB Corporation (Ohio, USA) while the agarose gel extraction kit, QIAprep Spin Miniprep Kit, QIAGEN® Plasmid Maxi Kits were purchased from QIAGEN Ltd. (Crawley, UK). The transfection reagents Lipofectamine LTX reagent was purchased from Invitrogen by Life Technologies (USA). The 5× passive lysis buffer (5× PLB) and Dual-Luciferase® Reporter Assay System were both from Promega Ltd. (USA). The QuickChange® Lightning site-directed mutagenesis kit was purchased from Agilent Technologies; Stratagene (USA). The antibodies used for ELISA were purchased from Enzyme Research (Swansea, UK), while standard VWF:Ag calibrator was purchased from Siemens Healthcare GmbH (Marburg, Germany).

2.1.3. Primers

PCR primer sequences were supplied by Eurofins MWG (Ebersberg, Germany). A number of oligonucleotide primers had already been prepared in previous studies while others were redesigned and supplied lyophilized and were re-constituted with deionized water (dH_2O) according to supplier's instructions to prepare a concentration of 100 pmol/µl (Eurofins MWG, Ebersberg, Germany). A 1 in 10 dilution was prepared with dH_2O to form a working stock solution for each primer to be used for PCR.

2.2. Methods

2.2.1. PCR primer design and SNP check

In this study, a set of primers were used to PCR amplify *VWF* essential regions including all 52 exons and closely flanking intronic regions in addition to 1.4 kb of intron 1. Some of these primers had previously been designed for the historical MCMDM-1VWD study and other previous studies. All of these primers were revised and screened for the presence of possible SNP within primer sequences in order to avoid amplification errors. Primers that showed no SNP underneath their annealing sites were utilised in *VWF* amplification, but primers which were found to have SNP within their sequences were re-designed. Because *VWF* is highly polymorphic and due to the presence of *VWFP* (pseudogene) which is similar to a large portion of *VWF*, care must be taken when designing the primers. Presence of SNP within primer sequences may lead to lack of amplification, while design of primers for exons 23-34 without including sequence mismatches with *VWFP* will cause amplification of the pseudogene in addition to the target gene. Therefore, designed primers did not include SNP underneath their annealing sites and included sequence mismatches with *VWFP*. Prior to publication of the full human gene sequence, this was not always possible due to lack of intron sequence. Also

designed primers were 50bp at least away from the target exon in order to amplify the exon and intronic flanking regions to include any splice-site defects.

Primers were checked for the presence of SNP underneath their annealing sites by two methods; first, a manual search to identify SNP within primer sequence through comparison with the genomic sequence ENSG00000110799 (HGNC symbol:*VWF*), accessed using the Ensembl genome browser (www.ensembl.org/index, last accessed May 2010). The *VWF* sequence was obtained from the National Center for Biotechnology information (NCBI). The nucleotide accession number was NC_000012.11 and protein accession number was NP_000543.2. Second, SNP were checked and identified within primer sequences by using the Manchester SNP check tool (http//ngrl.manchester.ac.uk/SNPCheckv2/snpcheck.htm, last accessed November 2010). In this way, the primer pair sequences were entered and checked for the presence of SNP in PCR primer binding sites.

All primers used either forward or reverse were attached to M13 tails except for primers used in long PCR and for DNA sequencing. M13 primers are universal primers used to facilitate DNA sequencing where single forward and single reverse primers are used to sequence target DNA. The sequence of M13 forward and reverse primers are listed in appendix 1.

Primers that had SNP within their sequences were re-designed by using online Primer3 software (www.bioinformatics.org.sms2, accessed May 2010). When designing primers, many criteria were taken into account. All primers were between 18-25 bases in length, had GC content between 45-60%, had no repeat of >3 of a single base, and avoided complementarities between forward and reverse primers. In addition to designing forward and reverse primers, Primer 3 calculated GC%, melting temperature (Tm), length of each primer and product size.

Due to the constraint of the small number of possible positions to design primers for the pseudogene region, it was not always possible to design primers following all of these criteria.

Primers used to amplify *VWF* exons 23-34 where *VWF* and *VWFP* are highly similar (97%), were designed manually to include sequence mismatches between gene and pseudogene at the 3' end (Mancuso et al, 1989; Mancuso et al, 1991). This was achieved by aligning *VWF* sequence against *VWFP* sequence using Clustal multiple sequence aligment available on the website (http://www.clustal.org/ last accessed January 2011). Occasionally, mismatches were introduced to confer maximum *VWF* specificity and to de-stabilise binding to *VWFP*.

2.2.2. Polymerase chain reaction (PCR) amplification of *VWF*

Essential regions of *VWF* and closely flanking intronic regions that required re-sequencing were amplified by performing PCR. PCR is a quick technique used to amplify a particular DNA

region to generate large quantities of target DNA with known sequence and length for a variety of applications. The PCR reaction takes place in a thermal cycler consisting of cycles of repeated heating and cooling providing suitable temperatures required for the reaction.

2.2.2.1. Conventional PCR

PCR is commonly performed in small reaction tubes with a buffered mixture containing forward and reverse oligonucleotide primers with sequence complementary to the target DNA, genomic DNA, *Taq* polymerase and deoxynucleoside triphosphate (dNTP). Three essential steps are required to achieve amplification; denaturating of the double stranded DNA, annealing of the primers to their template single stranded DNA and elongation of annealed primers in the presence of dNTP and *Taq* polymerase to generate a new DNA complementary to the target DNA. Some primer pairs used in this study required optimisation of conditions. These conditions included annealing temperature, number of cycles and $MgCl_2$ concentration. After completing the optimization, primers were used to amplify *VWF*.

2.2.2.2. DNA amplification of *VWF*

Every exon of *VWF* was amplified individually. The procedure was performed according to the standard method. The PCR mixtures used are shown in Appendix Table 2. Twenty seven µl of PCR master mix (ReddyMix) resulting in a final concentration of 1.5 mM $MgCl_2$ was mixed with 0.6 µl (10pmol/µl) of forward and reverse primers, 1.2 µl of dH_2O and 0.6 µl of genomic DNA (100ng/µl) results in a final reaction volume of 30 µl. The 100 pmol/µl stock primers were diluted with deionized water to prepare a concentration of 10 pmol/µl. The PCR ReddyMix master mix contained:1.25 units of thermoprime plus DNA polymerase, 75 mM Tris-HCl (pH 8.8 at 25°C), 20 mM $(NH_4)_2$ SO_4, 1.5 mM $MgCl_2$, 0.2 mM each of dATP, dCTP, dGTP and dTTP and and red dye for electrophoresis. PCR contained 1.5 mM $MgCl_2$ unless specified.

All reactions were undertaken in 0.2 ml Eppendorf tubes and PCR reactions were performed using a GeneAMP 9700 thermocycler (Applied Biosystems, Singapore). The thermal cycling steps to amplify *VWF* were programmed as shown in Appendix Table 3. The conventional PCR temperature cycling conditions used were; initial denaturation step at 94°C for 7 min, followed by amplification over 35 cycles starting with denaturation at 94°C for 1 min, primer annealing for 1 min at n°C based on primer Tm, extension at 72°C for 1 min and a final extension step for 7 min at 72°C (Appendix Table 3). The primer sequence, annealing temperatures, $MgCl_2$ concentration and cycles for previously designed primers are listed in Appendix Table 4.

2.2.2.3. Long-range PCR

In order to amplify exon 28, intron 1 and exon 1 which are each 1.4kb in size, long range PCR (LR-PCR) amplification was used. LR-PCR is similar to the standard method except that the Phusion Taq polymerase has a high 5'-3' polymerase activity in addition to 3'-5' proofreading ability was used. Exon 28 and its intronic flanking regions were amplified in a 50µl reaction containing 10µl HF buffer, 1µl mM dNTP, 2.5 µl (10 pmol/µl) of each primer, 0.5µl of phusion Taq polymerase and 31.5µl dH_2O. Two µl of template DNA (100ng/µl) was added to the reaction. The LR-PCR temperature cycling conditions used were; initial denaturation step at 98°C for 30 sec, followed by amplification for 32 cycles starting with denaturation at 98°C for 10 sec, primer annealing at 67°C for 30 sec based on primer Tm, extension at 72°C for 2 min and a final extension step for 10 min at 72°C. The LR-PCR reaction was performed using a GeneAMP 9700 thermocycler. Primers used to sequence the long range PCR exon 28 region are listed in Appendix Table 5. The estimated Tm was calculated using the Finnzymes online tool at: (http://www.finnzymes.fi/tm_determination.html, last accessed June 2011). The exon-intron 1 single amplicons was amplified using OneTaq Hot Start Master Mix in a 100 µl reaction containing 50µl OneTaq Hot Start 2X master mix with standard buffer, 2µl (10 pm/µl) of each primer, 42µl of dH_2O and 4 µl of 100ng/µl of DNA samples. The primer sequence, annealing temperatures, $MgCl_2$ concentration and cycles for exon-intron 1 are listed in Appendix Table 6. The thermocycling conditions used were similar to the routine PCR where initial denaturation was at 94°C for 30 sec, followed by amplification over 30 cycles starting with denaturation at 94°C for 30 sec, primer annealing at 58°C for the exon- intron 1 region for 55 sec or based on primer Tm, extension at 68°C for 1 min per kb and a final extension step for 5 min at 68°C.

2.2.2.4. Agarose gel electrophoresis

DNA amplification using specific primers was followed by agarose gel electrophoresis. To ensure that successful DNA amplification had been achieved and to determine the size of PCR products, agarose gel electrophoresis was employed. Electrophoresis on agarose gel is a standard method used to separate, identify and purify DNA fragments. DNA products are separated in the gel according to their size: smaller DNA fragments migrate faster through the gel and larger DNA fragments migrate slower. The location of nucleic acids within the gel was determined directly by staining with a low concentration of the intercalating dye Ethidium Bromide (EB) (3,8-diamino-5ethyl-6 phenylphennanthridinium bromide). To detect *VWF* integrity, DNA was electrophoresed on 0.7% to 2% agarose gel stained with EB based on the expected size of the DNA fragments that were compared with a size marker. The agarose gel was prepared by dissolving appropriate amounts of agarose powder in appropriate volumes of 1x Tris-Borate EDTA (TBE) buffer (8.9 mM Boric acid, 8.9mM Tris base, 0.2 mM EDTA pH

8.3). The suspension was heated in the microwave until the agarose completely dissolved and left until the solution had cooled to approximately 60°C. This was followed by adding EB to a final concentration of 10mg/ml into the agarose. The gel was left to solidify for almost one hour. Prior to electrophoresis, the gel was placed into the electrophoresis apparatus and overlaid with 1x TBE buffer. Five µl of each sample alongside DNA hyperladder (Bioline) with known size bands was mixed with 2µl loading dye containing bromophenol blue unless a PCR master mix already containing loading dye was used. It was loaded carefully in the gel wells. The power supply at a constant 100 volts was connected for 35-55 min so that the DNA migrated towards the anode. After completion of the electrophoresis, the gel was placed on the UV transilluminator (Bio-Rad laboratories Ltd, Hertfordshire, UK) at 302 nm and photographed to detect the quality and the size of DNA using a gel documentation system (ChemiDoc EQ camera Bio-Rad).

Various DNA standard size markers with different sizes were used in this study based on the DNA fragments that were electrophoresed. DNA size was evaluated by comparing with a standard size hyperladder. Hyperladders supplied by Bioline that contained fragments between 25 bp and 10 kbp were used. Hyperladder IV was the marker used generally in this study and included 9 regularly spaced fragments, ranging between 100 bp and 1000 bp (Appendix 7). Each band was an exact multiple of 100bp.

2.2.3. PCR product purification

There are various techniques used for DNA purification based on the requirement of the procedure. In this study, ExoSAP-IT (USB products, Ohio, USA) was used to purify PCR products prior to DNA sequencing. ExoSAP-IT is a quick method used for fast and efficient clean-up of PCR products prior to DNA sequencing. This method was used to remove unwanted primers and dNTP from PCR products. ExoSAP-IT reagent contains two different hydrolytic enzymes, exonuclease I which removes residual single-stranded primers and any extraneous single-strand DNA produced in the PCR and shrimp alkaline phosphatase which removes the remaining dNTP from the PCR mixture. PCR product purification was undertaken using a 1:10 dilution of ExoSAP-IT reagent. Thus, 6µl of PCR product, 4µl of dH_2O and 4µl of 1:10 ExoSAP-IT were mixed together in a PCR tube and followed by centrifugation at 700 g using an ALC microcentrifuge PK120 (Thermo Electron Corporation, France). This mixture was put in a thermocycler and incubated for 30 min at 37°C followed by enzyme inactivation at 80°C for a further 15 min.

2.2.4. DNA sequencing analysis

After completion of purification, samples were sent for automated DNA sequencing to the Core Genomic Facility at the School of Medicine, University of Sheffield. Direct DNA sequencing was used as a method for identification of sequence variants in *VWF* amplified fragments. Each successfully amplified fragment was directly sequenced in both directions using the BigDye terminator v3.1 (Applied Biosystems, Foster City, USA) on an ABI PRISM 3730 DNA analyser (Applied Biosystems, Japan). The output sequence was analysed using the Staden sequence analysis package (Staden, 1979, Staden, 1984) and FinchTV v1.4 software (Geospiza inc., Seattle, USA).

2.2.4.1. Principle of DNA sequencing

The process of determining the order of the nucleotide bases along a DNA strand is called DNA sequencing. This technique was developed in 1977 by Fredrick Sanger and is known as Sanger sequencing or the chain termination method (Sanger et al., 1977). This technique is similar to PCR and utilizes fluorescent 2'-3'-dideoxynucleotide triphosphate (ddNTP), molecules that differ from dNTP in having a hydrogen atom at carbon-3 rather than an OH group. These molecules terminate the DNA chain elongation because they cannot form a phosphodiester bond with the next deoxynucleotide during DNA elongation. In this technique, the amplified product from the PCR (DNA template) is added to a reaction tube containing Taq DNA polymerase, a primer that can hybridise at the desired location on a single strand of the DNA (as opposed to both strands in PCR), and all four nucleotide bases (A, T, C, G). In addition, small amounts of four fluorescently- labeled ddNTP (almost 1% of the dNTP concentration) A, T, C, G are added to the mixture. After the first deoxynucleotide is added to the growing complementary sequence, DNA polymerase moves along the template and continues to add bases. The strand synthesis reaction continues until a dideoxynucleotide is added, blocking further elongation (termination). After 45 cycles of the reaction, the resulting mixture will contain a series of fragments of different lengths depending on how many bases have been added to the chain before one ddNTP was attached and blocked further elongation. These fragments with various sizes are separated by capillary electrophoresis. A smaller fragment migrates faster, so the DNA molecules are separated according to their size. The fluorescent signal released from the labeled end of ddNTP during electrophoresis is detected and recorded by a charge coupled device (CCD). Each ddNTP has its own colour, so the order of the bases in the sequenced fragment can be detected. The 5' terminal base (ddNTP) of the shortest fragment that moves the fastest is the first base detected and larger products follow, thus the sequence can be read base by base.

2.2.4.2. Sequence analysis

2.2.4.2.1. Staden sequence analysis

In order to detect sequence variation and putative mutations or polymorphisms, the sequencing traces for *VWF* were checked and analysed using the Staden software package (Staden, 1979, Staden, 1984). Staden subtracts two traces from each other to show where these traces are similar or differ, indicated by peaks or troughs on the 'trace dif ' display. This program was used to analyse the released sequence data and align it with the wild-type *VWF*.

The reference sequence used in this study was ENSG00000110799 *VWF*. Sequences of IC and HC were imported into a blank Staden database (*VWF* sequence) as DNA reference sequence derived and saved from Ensembl website (http://www.ensembl.org/index.html). A blank database was created by importing the *VWF* reference sequence. The Ensembl sequence used was marked up with reported SNP and exons and introns were highlighted. A blank database was created first, and then IC and HC sequences were imported for each analysis. Two software files were selected from the Staden package. Pregap4 software was utilised to add the ab1 files of IC and HC to the blank database, while GAP4 was utilized in order to edit the sequence of *VWF*. Ab1 files of IC, HC (forward and reverse) and the copy of blank database files were added and run using pregap4 to allow all traces to be aligned to the reference sequence in the blank database. Forward and reverse control traces were selected as the reference sequence to be compared with traces of IC. This step was created each time when processing a single exon. To analyse the generated sequence, GAP4 software was used. It compares the traces of the gene sequence against traces of the control sequence and the reference traces. Next, GAP4 subtracts one trace from another to generate new traces that show the differences in the form of highlighted peaks or troughs. Every *VWF* exon sequence was analysed and evaluated individually.

2.2.5. Prediction of the effect of amino acid substitutions on protein function

To evaluate the possible pathogenicity underlying identified sequence variations, *in silico* prediction tools were used. Three different online tools were used to overcome weakness or defect in any of the tools (Houdayer et al., 2008)**.** The amino acid substitution online tools used are listed below:

Sorting Intolerant From Tolerant (SIFT) predicts whether an amino acid substitution affects protein function based on sequence homology and the physical properties of amino acids: http://sift.jcvi.org/.

Polymorphism Phenotyping (PolyPhen) tool predicts the possible effects of an amino acid replacement on the structure and function of a human protein using straightforward physical and comparative considerations: http://genetics.bwh.harvard.edu/pph/.

Align Grantham Variation Grantham Deviation (GVGD) predicts where missense substitutions in proteins of interest fall in a spectrum from enriched deleterious to enriched neutral: http://agvgd.iarc.fr/. Tools were accessed December 2010.

2.2.6. *In silico* splice-site prediction

mRNA splicing is defined as a process that allows removal of introns and joins exons together post- transcription in order to form mature mRNA. It has been suggested that the presence of genetic alterations located either within intronic sequence surrounding the splice site junction or exonic regions including missense, nonsense and silent mutations can potentially affect the splicing mechanisms (Cartegni et al., 2002, Zatkova et al., 2004). In an attempt to predict the potential effects of *VWF* alteration on splicing mechanisms, several different online *in silico* splice site prediction tools were used to overcome weaknesses and shortcomings in any of them. Also these tools were used to evaluate the pathogenicity of potential splice site modifications. These online tools included MaxEntScan: scorsplice (MES) (http://genes.mit.edu/burgelab/maxent/Xmaxentscan_scoreseq.html, Splice site prediction by neural network (http://fruitfly.org:9005/seq_tools/splice.html), NetGene2 splice prediction (http://www.cbs.dtu.dk/services/NetGene2/) and Human Splice Finder (HSF) (http://www.umd.be/HSF/). All these tools were accessed between December 2010 and May 2013.

2.2.7. *In silico* prediction of exonic splice enhancers and silencers

In order to predict the effect of exonic mutation on exonic splice enhancer (ESE), exonic splice silencer (ESS) and the possibility of creating a new splice sites, three bioinformatics online *in silico* prediction tools were used.

They include several online tools such as exonic splice enhancer (ESE) (http://www.umd.be/HSF/), Human Splice Finder (HSF) (http://www.umd.be/HSF/), and RESCUE-ESE (http://www.umd.be/HSF/). All tools were accessed between December 2010 and May 2013.

2.2.8. Multiple sequence alignment (Evolutionary Conservation)

To evaluate the amino acid sequence evolutionary conservation, the affected amino acid sequence of the VWF was aligned against orthologues. The purpose of this analysis was to

predict the possible impact of altered sequence on the VWF protein structure. It was undertaken through aligning different species and compares their protein sequence homology. Therefore, various species were selected to align and compare. The protein sequences for all species were created using FASTA format (*blastp:* http://blast.ncbi.nlm.nih.gov, last accessed January 2012). Multalin online tools for multiple sequence alignment were used to compare selected sequence homology (http://multalin.toulouse.inra.fr/multalin/, last accessed January 2012).

2.2.9. Model structure of the protein

To generate a model structure and show the model, 1SQ0 (VWF A1 domain) Protein Data Bank (PDB) file for crystal structure and PYMOL were used respectively. PYMOL is a programme used to visualize nucleic acids and proteins in graphic forms.

2.2.10. Graphical codon usage analysis

The graphical codon usage analyser (GCUA) tool which compares the frequency of use of two different triplet codons encoding the same amino acid was used (Nakamura et al., 2000). Codon usage data was collected from group of genes in thousand individuals.

2.2.11. Nomenclature and numbering of *VWF* sequence

Sequence variants were identified and numbered according to the recommendations and guidelines issued by both the International Society on Thrombosis and Haemostasis Scientific and Standardisation SubCommittee (ISTH-SSC) on VWF (Goodeve et al., 2011) as well as the Human Genome Variation Society (HGVS) (den Dunnen and Antonarakis, 2001). The name of *VWF* was utilised according to the guidelines of Human Genome Organization (HUGO) gene nomenclature committee (HGNC) which uses italicised Latin symbols for genes to distinguish them from proteins.

The first nucleotide (adenine) of the initiator methionine translation codon (ATG) at the beginning of exon 2 of *VWF* sequence was used as the protein start site and given the number +1. The numbering of exonic nucleotides started from this point while the previous nucleotide was numbered as -1. The numbering of the intronic regions started from the closest exonic nucleotide and was given a number prefixed with either a sign + or – depending on the sequence direction either 5' or 3'. The one letter code was used to denote amino acids. The sequence of VWF amino acids were numbered from the first translation initiation codon (methionine) as amino acid number 1 (Goodeve et al., 2001, Goodeve et al., 2011). The nucleotide alterations were prefixed with a letter (c.), while the protein substitutions were prefixed with a letter (p.). Moreover, in the presence of insertions or deletions, the number of involved nucleotides

followed the symbol ins or del respectively. The presence of * sign represents mutation that create stop codon (e.g p.A123*). The symbol fs* followed by number indicates a frameshift mutation causes creation of a stop codon after number of codons downstream of the mutation (e.g p.A123Cfs*20).

2.2.12. Generation of VWF mutant plasmids

Site-directed mutagenesis (SDM) was performed in order to create a specific nucleotide alteration in the recombinant vector that contained the wild-type human *VWF* cDNA. SDM is a quick, simple, efficient and accurate mutagenesis technique used to mutate vectors either small or large. SDM is based on PCR thermal cycling using a set of mutagenic primers, both of which contain the desired nucleotide change. Each primer was complementary to opposite strands of the plasmid to create the change in the wild-type plasmid. It also used a *PfuUltra* high fidelity DNA polymerase (Agilent Technologies, UK Ltd) which permits extension of the primer without strand displacement (Figure 2.1).

2.2.12.1. VWF expression plasmid

The pcDNA3.1/Hygro (-) expression plasmid (Life Technologies Ltd, Paisley, UK) (5.6 kb) containing full-length wild type human *VWF* cDNA (8.6 kb) was kindly provided by Prof. Reinhard Schneppenheim, Germany (Figure 2.2). The full length *VWF* cDNA originated from the *VWF*-PMT2 plasmid which was transferred to a pcDNA3.1/Hygro (-) expression plasmid. The *VWF* cDNA was introduced into the plasmid using two restriction enzymes, *Eco*RI and *Not*I. It produces almost 14 kb pcDNA3.1VWF plasmid (Schneppenheim et al., 2001a). This plasmid was used for expression of *VWF* in the HEK293T cell line.

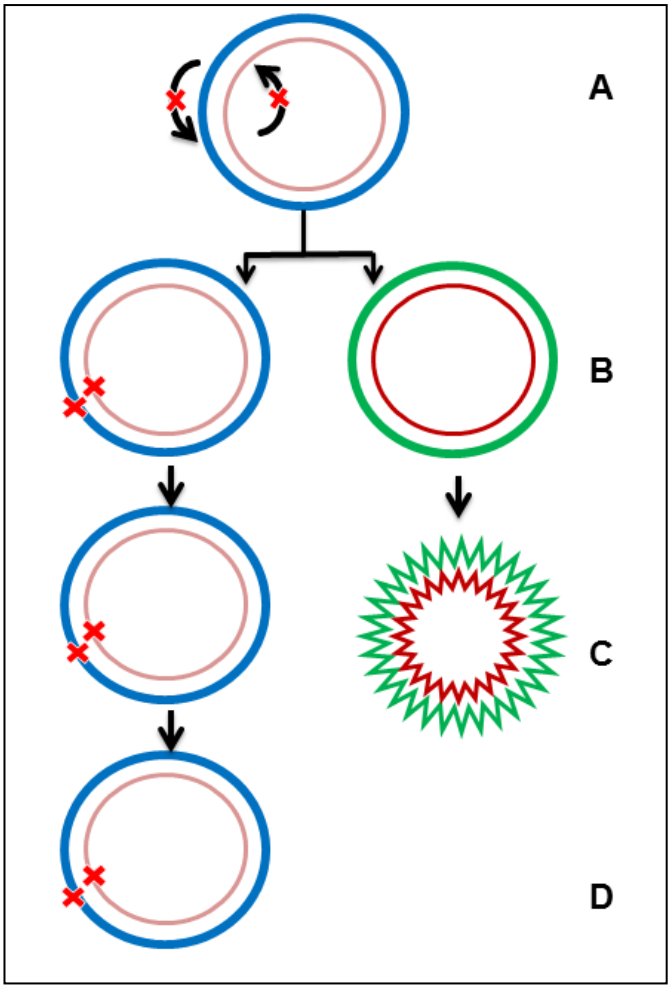

Figure 2.1 Site directed mutagenesis (SDM) method. A) The DNA plasmid contains the WT cDNA that is denatured using thermal cycling. **B)** A set of mutagenic primers containing the desired nucleotide change anneal to the plasmid and are extended using high fidelity *PfuUltr* - based DNA polymerase to introduce the desired change. **C)** As some intact parental DNA plasmid has not been mutagenized, *Dpn I* digests parental methylated and hemimethylated DNA but not the mutagenized sequence. **D)** Subsequently the mutated plasmids are transformed into ultracompetent *E.coli* cells for nick repair (adapted from QuikChange® Lighting Site-directed Mutagenesis kit, instruction manual).

2.2.12.1.2. Structure of pcDNA3.1/Hygro (-)

The VWF cDNA (8.6kb) was previously cloned into pcDNA3.1/Hygro (-) plasmid that is 5.6 kb in size. The pcDNA3.1 plasmid is designed to enable a high level of protein expression when transfected into mammalian cell line, either transiently or stably. Specifically, the plasmid backbone has a number of features enable high level protein expression in mammalian cell line (Figure 2.2), the presence of the human cytomegalovirus (P cMV) promoter driving high level expression of the VWF cDNA gene sequence inserted into multiple cloning site. The presence

of T7 promoter/priming site allows insertion of the gene of interest and facilitates cloning. The hygromycin resistance gene is used as a selection antibiotic to create stably transfected cell line, driven by the SV40 promoter/origin (SV40 ori) of replication. The SV40 promoter/ origin of replication is also used to drive expression of transfected plasmid in cells which contain the SV40 large T antigen. The bovine growth hormone polyadenylation (BGH pA) and SV40 early polyadenylation (SV40 pA) sites allow for correct transcription, translation and polyadenylation processing of plasmid mRNA insert sequence. The polyadenylation site used is determined by whether the mammalian cell lines used for transfection contain the SV40 large T antigen. Also, the phage origin (f1ori) enables production of a single-stranded copy of DNA. Finally, the presence of ampicillin resistance gene (β-lactamase) allows for the positive selection of E.coli bacteria (Amp R) containing plasmid after transformation of mutagenised VWF cDNA in order to determine the presence or absence of a mutation after small scale mini-preparation and extraction of plasmid DNA. During bacterial transformation the pUC origin (pUC ori) allows for replication of the plasmid in E.coli.

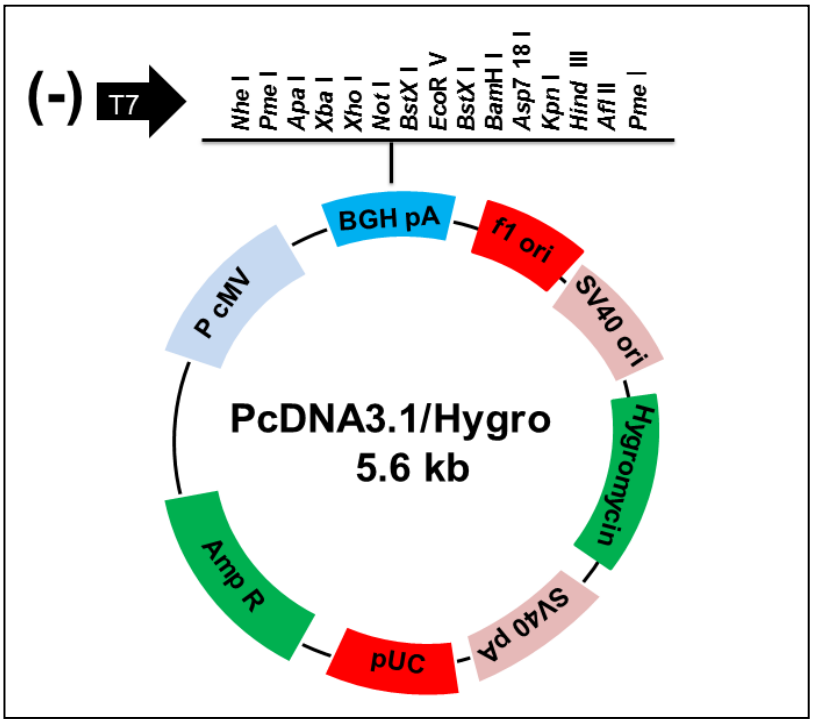

Figure 2.2 Map of pcDNA 3.1/Hygro used as expression vector

2.2.12.2. Transformation into NM554 *E.coli* competent cells

Competent cells are defined as bacterial cells that have the ability to uptake extracellular naked plasmid DNA from the surrounding media. The aim was to transfer plasmid containing full-length wild-type human *VWF* cDNA into *E.coli* NM554 competent cells. The purpose was to produce a large quantity of plasmid DNA containing full sequence of wild-type *VWF* cDNA in order to firstly ensure that the appropriate wild-type sequence was present within the plasmid and also to use the wild-type plasmid as a template during mutagenesis and to prepare it for transfection. Transformation of plasmid DNA into competent cells was carried out based on heat shock treatment. The NM554 competent cells kept frozen at -80 °C were thawed on ice for a few minutes prior to adding 100 µl of cells to a pre-chilled 14 ml polypropylene round-bottom reaction tube (Becton Dickinson Labware, Franklin Lakes, NJ. USA). Five µl of the recombinant plasmid was added and mixed gently with 100 µl NM554 competent cells. At the same time, 100 µl of competent cells only were added to another reaction tube to be used as a negative control. This was followed by incubating the reaction tubes on ice for 10 min. Then, they were heat shocked at 42°C in a water bath for 90 sec in order to enable membrane pores to be opened. The reaction tubes were kept immediately on ice for 2 min before addition of 100 µl of LB-broth alone without ampicillin (Merck KGaA, Darmstadt, Germany) to each tube and immediately incubated at 37 °C for 20 min with shaking at 200 rpm. 2.5% of LB broth (0.5% yeast extract, 1% tryptone and 1% NaCl) was prepared by dissolving 10 g of LB with 400 ml deionized water and autoclaved for one hour. Samples were plated onto LB-agar plates containing 50 mg/ml ampicillin and one plate was included without *E.coli* plating as a negative control. Ampicillin was prepared by dissolving 0.84 g of sodium bicarbonate and 0.5 g of ampicillin trihydrate (Sigma) into 10 ml of deionized water to prepare a solution of 1 M. The mixture was filtered through non-pyrogeneic syringe filter (Pall Corporation, Life Science, MI. USA), aliquoted in 1 ml tube and then stored at -20°C. 3.5% LB-agar was prepared by dissolving 11.1g LB-agar (Merck KGaA, Darmstadt, Germany) (0.5% yeast extract, 1% tryptone, 2% of agar and 1% NaCl) in 300 ml deionized water and autoclaving at 121°C for one hr. Following plating, plates were incubated inverted overnight at 37°C. After overnight incubation, plates were checked for the presence of colonies which were inoculated into LB-broth for plasmid DNA purification (Section 2.2.12.5).

2.2.12.3. Mutagenic primer design

The mutagenic oligonucleotide primers used in this study were designed individually based on the desired mutation. Eight pairs of primers were designed to introduce the respective mutation into the plasmid containing wild type *VWF* cDNA (Appendix Table 8). According to the manufacturer's recommendations, both of the forward and reverse mutagenic primers must

contain the desired nucleotide change, primers should be in length between 25-45 bases with ≥ 78°C melting temperature, they should have a GC content as minimum 40% and terminate with G or C bases. Primers were designed online using QuikChange primer design program at: www.aglient.com/genomics/qcpd (Accessed May, 2011). All designed primers were supplied lyophilized and were re-constituted with deionized water according to supplier's instructions to prepare a concentration of 100 pmol/µl. The optimised concentration of each oligonucleotide designed primer to be used during mutagenesis was 125 ng according to the mutagenesis protocol. The following equation was used in order to convert nanograms to picomoles: *X* pmoles of oligo = ng of oligo x 1000/ 330 x No of bases in the oligonucleotide primer.

The purpose of this technique was to introduce the respective mutation into the *VWF* construct to be expressed in the human embryonic kidney (HEK) 293T cells (LGC Standards, Middlesex, UK) and eventually to evaluate the level and structure of released VWF protein. Plasmids containing the desired mutations were created using QuikChange® Lightning site-directed mutagenesis kit (Agilent Technologies; Stratagene, USA). Mutagenesis was performed on the wild-type plasmid pcDNA 3.1 containing the full-length cDNA sequence for human *VWF*. Eight mutagenic primers used to introduce mismatches to wild-type are listed in Appendix 8.

Site-directed mutagenesis based on PCR was carried out in 50 µl reactions containing 5µl of reaction buffer, 1 µl of (125) ng of each forward and reverse oligonucleotide primer, 1 µl of dNTP mix and 1.5 µl of Quik solution reagent. A series of quantities of dsDNA template 10, 25, 50 and 100 ng were added to separate reactions in order to optimise the colony number following transformation. This was followed by adding 1 µl of QuikChange Lightning enzyme. ddH_2O was added to the reaction to reach a final volume of 50 µl.

A control mutagenesis reaction using pWhitescript mutagenesis plasmid was run alongside the sample reaction to evaluate the mutagenesis efficiency as indicated in table 2.1. The thermal PCR temperature cycling conditions used for both sample and control reactions were; initial denaturation step at 95°C for 2 min, followed by amplification over 18 cycles starting with denaturation at 95°C for 20 sec, primer annealing at 60°C for 10 sec, extension at 68°C for 7 min (30 sec/kb) and a final extension step for 5 min at 68°C. The mutagenesis PCR reaction was performed using a GeneAMP 9700 thermocycler. The PCR reaction was followed by adding 2 µl of *Dpn* I restriction enzyme directly to each reaction mixture and gently mixing using a pipette. *Dpn* I digests parental methylated and hemimethylated template DNA. The reaction mixture was immediately incubated at 37 °C in a water bath for 5 min to allow digestion of parental DNA. The treated PCR product were stored at -20 °C or used immediately for bacterial transformation.

Table 2.1 Preparation of the pWhitescript mutagenesis control reaction

Component	Volume
10x reaction buffer	5 µl
25 ng of pWhitescript 4.5 kb control plasmid (5 ng/µl)	5 µl
125 ng of oligonucleotide control primer 1 (100 ng/µl)	1.25 µl
125 ng of oligonucleotide control primer 2 (100 ng/µl)	1.25 µl
dNTP mix	1 µl
QuikSolution reagent	1.5 µl
QuikChange lightning enzyme	1 µl
ddH2O to bring the final reaction volume to 50 µl	34 µl

2.2.12.4. Transformation of XL10-Gold ultracompetent cells

The purpose of this reaction was to transform mutated plasmid (either sample and/or control reactions) following mutagenesis into highly efficient competent cells for nick repair. It was performed following mutagenesis and *Dpn* I digestion. The frozen XL10-Gold ultracompetent cells were gently thawed for 5 min on ice before addition of 45 µl of cells to a prechilled 14-ml BD Falcon polypropylene round-bottom tube. 2 µl of ß-mecraptoethanol (ß-ME) was mixed gently with the ultracompetent cells and incubated on ice for 2 min. ß-ME has been shown to increase transformation efficiency. This was followed by adding 2 µl of *Dpn* I-treated plasmid DNA from sample plasmid and pWhitescript control plasmid into the mixture. Also 1 µl of 0.01 ng/µl pUC18 control plasmid was added to another 45 µl XL10-Gold competent cells to determine the transformation efficiency of the competent cells. They were mixed gently and incubated on ice for 30 min before heat shocking in a water bath at 42 °C for 30 sec. Samples were kept on ice for 2 min immediately after heat shock and 500 µl of preheated NZY broth (10 g of NZ amine (casein hydrolysate), 5 g of NaCl and 5 g of yeast extract) at 42 °C in water bath was added into each reaction tube followed by incubating the tubes for one hr at 37 °C with shaking at 200 rpm. NZY broth (Fisher Scientific, USA) was prepared by dissolving 8.8 g of NZY powder in 400 ml deionised water and autoclaved at 121 °C for one hr. After the incubation period, 250 µl of each transformed sample was plated onto LB-agar plates containing 50 mg/ml ampicillin for mutagenesis samples. Plates were prepared by adding a 15 ml of LB-ampicillin agar to each plate. Also 10 µl of the pWhitescript mutagenesis control and 2.5 µl of pUC18 transformation control were plated onto LB-ampicillin agar plates containing 80µl/ml of 5-bromo-4-chloro-3-indolyl-ß-D-galactopyranoside (X-gal) and 20 mM isopropyl-1-thio-ß-D-galactopyranoside (IPTG).

Mutagenesis (pWhitescript) and transformation (pUC18) control plasmids were used to evaluate the mutagenesis and transformation efficiency respectively and also to ensure the synthesis of sufficient mutant DNA in the reaction. Plates for mutagenesis and pUC18 controls for blue-white colour screening were prepared by dissolving 4 µg of X-gal in 200 µl of IPTG. This mixture was added to 50 ml of LB-agar and 100 µl of 50 mg/ml of ampicillin (15 ml/plate). The IPTG was prepared by dissolving 0.476 g of IPTG in 100 ml deionised water. Following plating, transformation plates were incubated inverted at 37 °C for > 16 hr. After overnight incubation, plates were checked for the presence of colonies and selected colonies were isolated for plasmid DNA purification.

The efficiency of mutagenesis of the pWhitescript control plasmid and of transformation of the pUC18 control plasmid were evaluated by calculating the percentage of blue colonies from the transformation of pWhitescript and pUC18 control plasmids on agar plates containing IPTG and X-gal using this formula:

Number of blue colony forming units (cfu) / total number of colony forming units (cfu) X100

2.2.12.5. Purification of plasmid DNA using mini-prep

This test was performed to produce a small quantity of plasmid DNA in order to sequence the fragment of VWF cDNA that had the respective mutation to ensure the achievement of mutagenesis. It was carried out using the QIAprep Spin mini-prep kit protocol (QIAGEN Ltd, Crawley, UK). Four colonies from the transformed plates were picked and each was inoculated into 10 ml of LB-broth containing 50 mg/ml of ampicillin. It was followed by overnight incubation at 37 °C with shaking at 200 rpm. After overnight incubation, 1.5 ml of culture was transferred into an Eppendorf tube and centrifuged at 13,000 g for 3 min using an accuSpin™ Micro centrifuge (Fisher Scientific, Osterode, Germany). The supernatant was aspirated and this step was repeated twice more. The cell pellet was resuspended in 250 µl of suspension buffer P1 that contained RNase A and LyseBlue reagent. Following the addition of 250 µl of P2 buffer; the tubes were gently inverted and mixed several times until the solution turned blue. It was left for 5 min before adding 350 µl of neutralisation buffer N3 and tubes were also gently mixed by inversion several times until the solution became cloudy. Following centrifugation at 13,000 g for 10 min, the supernatant was applied to the QIAprep spin column. The column was centrifuged for one min at 13,000 g and the flow-through was discarded before washing the column with 0.5 ml PB buffer. Again, the column was centrifuged at 13,000 g for one min and the flow-through was discarded before adding 0.75 ml of the PE buffer that had 80 % ethanol to the column and centrifuged at 13,000 g for one min twice to remove the residual wash buffer. After discarding the flow-through, the QIAprep column was transferred into a clean 1.5 ml

Eppendorf tube for DNA elution by adding 50 µl of EB buffer to the column. The samples were kept at room temperature for one min to increase DNA yield followed by centrifugation for one min at 13,000 g. The plasmid DNA was submitted for DNA sequencing analysis to check for the occurrence of the desired mutation within the plasmid.

2.2.12.5.1 DNA sequence alignment

The released sequencing data (FASTA sequence) for *VWF* cDNA expression plasmid was aligned to the VWF cDNA reference sequence (Gene ID: ENSG00000110799) using NCBI BLAST software: http://blast.ncbi.nlm.nih.gov/Blast.cgi, last accessed, May 2011). This analysis was aim to detect any nucleotide(s) variation present in the expressed plasmid compared to the reference sequence pre and post mutagenesis and also to confirm the presence of desired nucleotide change. Also, all identified variants found in the wild-type expressed plasmid were checked for their effect on VWF structure and function using VWF database at: (www.ragtimedesign.com/vwf/polymorphism, last accessed May 2011).

2.2.12.6. Preparation of glycerol stock

The remaining quantity of cell culture used during mini-prep was used to make a long-term glycerol stock of bacterial cells to be used for maxi-prep or further plasmid DNA purification. A glycerol stock was prepared by adding 1.7 ml of the culture media into a fresh 2 ml screw-cap tube. It was centrifuged at 13,000 g for 3 min. After removing the supernatant, another 1.7 ml of cell suspension was added to the tube twice followed by centrifugation at 13,000 g for 3 min. The supernatant was aspirated and the cell pellet was resuspended in 200 µl of cell suspension, before adding another 1.1 ml of cell suspension to the tube. Finally, 0.3 ml of 80% glycerol was gently added to the tube containing the cell suspension before storing the glycerol stock at -80 °C.

2.2.12.7. Measurement of plasmid DNA concentration using the NanoDrop spectrophotometer

Nucleic acid and protein present in plasmid DNA preparations were quantified using a spectrophotometer and absorbance at 260 nm and 280 nm respectively. The plasmid DNA concentration was measured in the NanoDrop®- ND-1000 (Thermo Fisher Scientific, Inc., Wilmington), with readings taken at 260 nm and 280 nm. A sample volume of 1µl was used for the NanoDrop® after applying deionised water as a blank. The sample was pipetted onto the lower measurement pedestal. The sampling arm was closed and measurement was initiated using software on the PC. The average of three readings was taken as ng/µl. The ratio of A_{260}/

A_{280} should be between 1.6-1.8. A Ratio of 1.8 indicates the presence of pure DNA while a ratio below this range indicates the presence of impurities or protein contamination. The presence of organic solvents such as ethanol may lead to a lower ratio. Moreover the ratio of A_{260}/ A_{230} should be considered. A ratio of > 2 is indicative of pure DNA while a ratio below this value is indicative of protein or phenol contamination.

2.2.12.8. Purification of large scale plasmid DNA using maxi-prep

To produce a large quantity of plasmid DNA either wild type or mutant required during transfection experiments, large-scale plasmid DNA purification was carried out using the QIAgen maxi-prep purification kit (QIAGEN Ltd, Crawley, UK). A small quantity of cells from a glycerol stock was inoculated a large flask containing 250 ml of LB-broth and 50 mg/ml penicillin and was incubated in an orbital shaker at 37 °C overnight. After overnight incubation, the cell suspension was transferred in a Beckman 250 ml tube (Beckman, USA) and bacterial cells were harvested by centrifugation at 5000 g at 4 °C for 8 min using a Beckman J2-21M/E centrifuge with JA-14 rotor. The supernatant was carefully decanted and the cell pellets were resuspended in 10 ml of buffer P1 containing RNase A and LyseBlue reagents followed by pipetting up and down until no cell clumps remained. Ten ml of lysis solution P2 was added and the tube gently inverted several times until the solution colour turned blue and became viscous. After 5 min incubation, 10 ml of neutralising pre-chilled buffer P3 was added and the tube was inverted gently several times until the suspension became a white precipitate. It was followed by incubation on ice for 20 min, then centrifuged at 14,000 g for 30 min at 4 °C using the JA-14 rotor. The supernatant containing the lysate was carefully transferred to a fresh Beckman tube and again centrifuged at 14,000 g for 15 min at 4 °C. During centrifugation, a QIAGEN-tip 500 was equilibrated by applying 10 ml of QBT buffer and the column was allowed to empty by gravitonal flow. The supernatant containing the plasmid DNA was transferred to the equilibrated QIAGEN-tip and allowed to enter the resin layer by gravity flow. In order to remove all contaminants, the QIAGEN-tip was washed twice using 30 ml QC buffer. After washing, the QIAGEN column was placed into a Beckman 40 ml tube before elution. Plasmid DNA was eluted from the resin by addition of 15 ml QF elution buffer. The DNA was precipitated by adding 10.5 ml of room-temperature isopropanol to the eluted DNA followed by inversion and centrifugation at 12,000 g for 30 min at 4 °C using a JA-20 rotor. The supernatant was carefully discarded before the pellet was washed with 5 ml 70% ethanol. The solution was again centrifuged at 12,000 g (JA-20) for 10 min at 4 °C. Without disturbing the pellet, the supernatant was carefully discarded and the pellet was air-dried by allowing standing for 10 min at room temperature to remove excess ethanol. The DNA pellet was resuspended with 0.5-1 ml (based on pellet size) of sterile dH_2O. The concentration of plasmid DNA was measured using

NanoDrop as previously described in section 2.2.12.7. The plasmid DNA was submitted to sequencing to check the entire cDNA sequence for either the wild-type or to ensure the presence of the desired mutation only and no other nucleotide changes were found within the mutant plasmid. The entire VWF cDNA was sequenced using the 18 primers listed in Appendix 9. These primers were designed and supplied lyophilised and were re-constituted with deionised water according to supplier's instructions to prepare a concentration of 100 pmol/µl. The plasmid DNA was stored either at -20 or 2-6 °C.

2.2.13. *In vitro* expression of *VWF* mutants

In vitro expression helped to determine the mechanism by which identified mutations lead to the disease phenotype in the affected families from the MCMDM-1VWD cohort study. This was achieved by using transient transfection of mutant *VWF* plasmid in parallel with wild-type *VWF* plasmid in order to mimic the homozygous and heterozygous states. The transient transfection was conducted in human embryonic kidney cell line (HEK) 293T cells.

2.2.13.1. Culture of HEK293T cells

The cells were maintained in Dulbecco's modified Eagle's medium (DMEM + GlutaMAX) (Gibco Life Technology Ltd). 10% of heat inactivated foetal bovine serum (FBS) (Gibco Life Technology Ltd) was added to the medium to prepare full medium. GlutaMAX media was used to increase cell performance, minimize ammonia toxicity and also to increase the stability of media. Cells were split frequently for subcultures using 10% trypsin and phosphate buffered saline (PBS) (Life Technologies Ltd) and reached the desired confluence (70-90%) in almost 3 days when grown in 80 cm^3 flasks. Trypsin (10%) was prepared by adding 5 ml of trypsin-EDTA (PAA Laboratory Ltd, Germany) into 45 ml of PBS. HEK293T cells were incubated at 37°C with 5% CO_2 and 95% air in a humidified condition. Cells were split in an aseptic hood when they reached the desired confluency or when the colour of the medium changed from red to orange. The HEK293T cells were selected to be used for transient transfection of wild-type and mutant *VWF* because they do not express endogenous VWF.

2.2.13.2. Cell thawing

The HEK293T cells were removed from liquid nitrogen and cells were thawed on ice before being transferred into a Falcon tube and centrifuged for 5 min at 2000 g (Centaur 2, England). The supernatant was carefully discarded before re-suspending the pellet with 5 ml of full medium, followed by an additional spin at 2000 g for 5 min. Again the supernatant was discarded and the pellet was resuspended in 6 ml of full medium and then the mixture was

transferred to a flask containing 9 ml of full media. Cells were incubated at 37°C/5% CO_2 until they reached the required confluency.

2.2.13.3. Passaging HEK293T cells

All cell culture media including DMEM, PBS and trypsin were put into 37°C water bath for approximately 15 min prior to splitting the cells. Bottles were cleaned before being placed in the hood along with a pipette gun, pipettes and a waste jug. After checking the tissue culture flask for the presence of any infection, the old media was aspirated off the cells. This was followed by gently adding 10 ml of PBS to the flask and tilting to allow the media to wash over the cells without disturbing them. The PBS was aspirated before 2 ml of 10% trypsin-EDTA was added to the cells making sure that the cells were lightly covered by trypsin and incubated for approximately 5 min at 37^{o}C until the cells started to float and could easily be dislodged from the flask with light tapping. 6 ml of full media was added and pipetted up and down to make sure to collect all the cells from the bottom of the flask. One ml of the trypsinised medium was added into a new T75 cm^2 flask containing 14 ml of full media followed by incubation at 37 °C/5% CO_2.

2.2.13.4. Cell counting

HEK293T cells were counted and adjusted manually to $1.5x10^6$ in each plate using a haemocytometer (AC6000 Modified Fuchs Rosenthal Counting Chamber). Prior to counting, the cell suspension was trypsinised, centrifuged at 2000 g (Centaur 2, England) and followed by discarding the supernatant and adding of 6 ml of prewarmed full medium to the pellet. Prior to use, the haemocytometer and cover-slip were cleaned gently with ethanol. This was followed by adding 20 µl of cell suspension into the edge of the coverslip of one side to cover the counting area under the coverslip. Cells within the 4x4 (16 small squares) within one major square of the counting grid were counted using x10 objective on an inverted phase contrast microscope (Zeiss, Germany). The obtained number was multiplied by 10 which represent the number of cells per µl. Finally, the volume of cells required to be added to 8 ml of full media in one plate was determined by dividing $1.5x10^6$ /number of cells/µl.

2.2.13.5. Transient transfection and *in vitro* expression using Lipofectamine LTX

Lipofectamine™ LTX reagent (Invitrogen, UK) was used to transiently introduce full length wild-type and mutant plasmid DNA into HEK293T cell. Lipofectamine ™ LTX reagent is a highly efficient transfection reagent which is an animal-origin free formulation for the transfection of plasmid DNA into HEK293 cells with low cytotoxicity. Lipofectamine creates a complex with the plasmid DNA and forms a positively charged DNA-Lipofectamine complex

which binds with the cell surface membrane carrying a negative charge. The discrepancy in charges between the cell membrane and DNA-Lipofectamine complexes facilitates the entry of DNA into the cells by endocytosis.

The transient transfection of wild-type and mutant VWF constructs was undertaken in 10 cm^3 dishes using a plasmid concentration of 6µg in total. One day prior to transfection, a total of $1.5x10^6$ cells were plated into 10 cm^3 petri dishes containing 8 ml of complete media and cells. Cells were incubated for 24 hr at 37 °C/5% CO_2 until they reached approximately 50-80% confluency on the day of transfection. 24 hr following incubation of seeded cells, a master mix containing 50 µl of Lipofectamine, 2 µl of renilla (500 ng/µl), 6 µl of plasmid DNA (prepared from working concentration of 1000 ng/µl) was prepared and diluted with 1.2 ml of DMEM reduced serum media (Table 2.2). The transfection efficiency was assessed by transfecting cells with a Renilla luciferase plasmid (Promega, UK, Ltd; Southampton, UK). The expression level of transfection data was normalised to correct for transfection efficiency of the cells using Renilla. Also, Renilla was used to evaluate whether the expressed VWF quantity was a true reflection exactly of what was happening in the cells. The Renilla plasmid expresses a fluorescent protein which can be measured using luminometry. The mixture was allowed to stand in the hood at room temperature for 30 min then added drop-wise with gentle swirling into each dish. This was followed by incubating cells for 48 hr at 37 °C/5% CO_2 to allow expression of VWF. Moreover, to mimic the *in vivo* state of patients with these mutations, co-transfection of each mutation expressed in the study was carried out using three different co-transfection states (Figure 2.3). The first state was conducted to mimic the wild-type-homozygous state using only wild-type plasmid while in the second state, only mutant plasmid was transfected in order to mimic the mutant homozygous state. In the third state, a mixture of 50% wild-type and 50% of mutant plasmid was transfected in order to mimic the heterozygous state of the mutation (Table 2.2). For each experiment, transfection was undertaken in triplicate and repeated three times using a total of 6µg of plasmid DNA.

Table 2.2 Summary of transfection method

Reagent	Wild-type VWF homozygous	Mutant-VWF homozygous	Mutant and wild-type-VWF heterozygous
Volume of plating medium	8 ml	8 ml	8 ml
Cells per dish	$1.5x10^6$	$1.5x10^6$	$1.5x10^6$
Lipofectamine LTX reagent	50 µl	50 µl	50 µl
Plasmid DNA (1000 ng/µl)	6 µl of WT plasmid	6 µl of mutant plasmid	3 µl of WT+ 3 µl of mutant plasmid
Renilla (500 ng/µl)	2 µl	2 µl	2 µl
Dilution media (Reduced serum)	1.2 ml	1.2 ml	1.2 ml

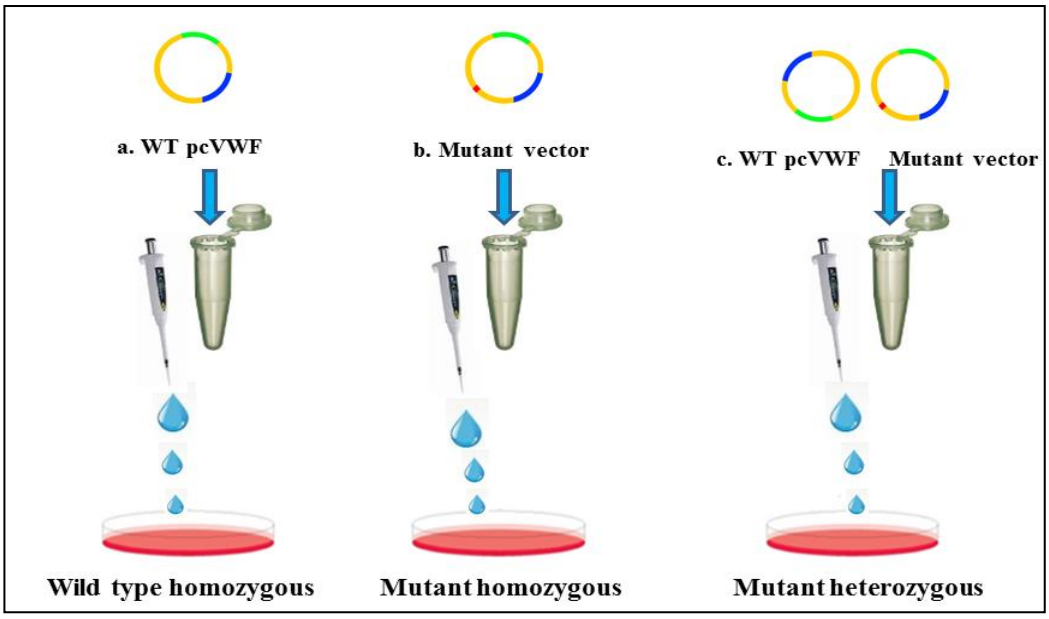

Figure 2.3: A schematic representation of the co-transfection protocol. A) Represents the transfection of wild type vector only to mimic the WT homozygous state. **B)** Represents the transfection of mutant vector alone to mimic the mutant homozygous state. **C)** In order to mimic the heterozygous state, a mixture of both wild type and mutant vectors was transfected.

2.2.13.5.1. Inhibition of proteosome activity of transfected HEK293T cells

Inhibition of the proteosome activity of transfected cells was undertaken for mutants showed low levels of expressed VWF. The severe reduction of expressed VWF was thought to be due degradation of mutant protein by proteosome complex. However, the obtained results following proteosome inhibition were compared to those results from normal transfection. Transfection was undertaken in 6 well plates using at cell density of 250,000 cells/ well in 2 ml of DMEM, plasmid concentration of 2.5 µg/ml in total, Renilla concentration of 1.5 µg/ml and 10 µl of Lipofectamine LTX. The transfection was similar to the normal transfection except for adding the inhibition solution 45 hr prior to harvesting. Each transfected well contain 2180 µl in total and the working concentration of proteosome inhibitor to be added was 25 µM. 5.3 µl of the inhibitor solution of 10 mM stock solution was added to each well three hr prior to harvesting. The cells were collected 48 hr post transfection for wild-type, homozygous and heterozygous states as previously described. The secreted and lysate VWF was measured using ELISA.

2.2.13.6. Collection of cell culture supernatant and cell lysate

Forty-eight hr post transfection; one ml of the supernatant media was collected from each plate and transferred to an Eppendorf tube while the remaining medium was collected into a fresh Falcon tube and stored at -20 °C for multimer analysis. This was followed by washing the cells attached to the plate with 2 ml of PBS buffer; media was allowed to wash gently over the cells without disturbing them. After removal of the PBS buffer from the plate, adherent cells were directly lysed using one ml of 1:5 diluted passive lysis 5X buffer (Promega, USA). This buffer was formulated to promote rapid lysis of cultured cells without the need for scraping adherent cells. Upon addition of the lysis buffer plates were rotated on a shaker at room temperature for 15 min at 100 rpm, and then one ml of lysates was transferred into an Eppendorf tube and kept at -20 °C for ELISA analysis. The cell lysates were centrifuged at 13,000 g for 10 min prior to ELISA assay to remove any cellular debris.

2.2.14. Measurement of expressed VWF using ELISA

Following transfection, the expressed VWF protein from the HEK293T transfected cells either in the supernatant or cell lysate was measured using a sandwich ELISA method.

2.2.14.1. Principle of ELISA

ELISA assay is used to measure the concentration of VWF. The coated polyclonal antibodies to VWF bound to solid phase are bound to VWF found in samples and reference plasma forming anti VWF-VWF complex and the remaining binding sites are blocked to block unbound sites to

avoid false positive results. The secondary detecting conjugated antibodies to VWF are added forming a sandwich complex with anti VWF-VWF (Figure 2.4). The peroxidase substrate O-Phenylenediamine (OPD) is added to the reaction to determine the activity of peroxidase. Peroxidase which is conjugated with the secondary antibody catalyses the reaction with OPD (colourless) via producing a soluble yellow product diaminophenazine (DAP) that can be measured and read spectrophotometrically at an optical density (OD) of 490 nm. The colour intensity produced was proportional to the concentration of VWF present (Figure 2.4).

2.2.14.2. ELISA Procedure

The capture antibody (Enzyme Research, Swansea, UK) was diluted 1/100 with coating buffer (50 mM carbonate coating buffer, pH 9.6) and 100 µl was added to each well of a 96 plate and incubated at 4 °C overnight. Coating buffer was prepared by dissolving 1.59 g of sodium carbonate (Na_2CO_3) and 2.93 g of sodium bicarbonate ($NaHCO_3$) in deionized water with the volume made up to one litre to produce a solution of 50 mM carbonate and pH was adjusted to 9.6. 24 hr after incubation, the coating antibody was discarded followed by adding 150 µl of blocking buffer to each well and incubated for one hr at room temperature in a wet box. Blocking buffer was prepared by dissolving 2 g of bovine serum albumin (BSA) (Sigm-RIA grade) in 200 ml of PBS to give a final concentration of 1% at pH of 7.4. This was followed by washing wells three times with wash buffer (PBS-Tween 0.1% v/v). Next, 100 µl of supernatants, lysates and VWF standard calibrator samples was added to the wells followed by incubation at room temperature for 90 min. In order to produce a standard curve, a 12 serial dilutions of standard calibrator (Siemens Healthcare GmbH, Marburg, Germany) starting from 1/5 down to 1/10240 was prepared in duplicate (Figure 2.5). Calibrator was diluted in HBS-BSA-T20 (100mM HEPES, 100mM NaCl, 1% w/v BSA, 0.1% v/v Tween-20, pH 7.2). After washing three times, 100 µl of 1/100 diluted detection antibody (Enzyme Research, Swansea, UK) diluted in HBS-BSA-T20 was applied to every well and incubated for 90 min at RT in humid box. The plate was washed three times followed by adding 100 µl of OPD substrate buffer (27 mM Citric acid, 97 mM Na_2HPO_4, pH 5.0) containing 6% hydrogen peroxide (H_2O_2) to each well to produce a coloured reaction. After the colour changed to yellow in a period between 5-10 minutes, the reaction was stopped by adding 100 µl of 2.5M sulphuric acid to all wells. The micro plate was read at wavelength of 490 nm using Varioskan Flash plate reader (Thermo Fisher Scientific, Loughborough, UK).

Moreover, to measure the luciferase activity and to determine the Renilla plasmid expression, the plate reader was also used at 490 nm. It was done by mixing 10 µl lysate samples of WT, homozygous and heterozygous with 25 µl of (1:50) dual-luciferase reporter in ELISA plate

(Promega, WI, USA). The plate was read at a wavelength of 490 nm using Varioskan Flash plate reader.

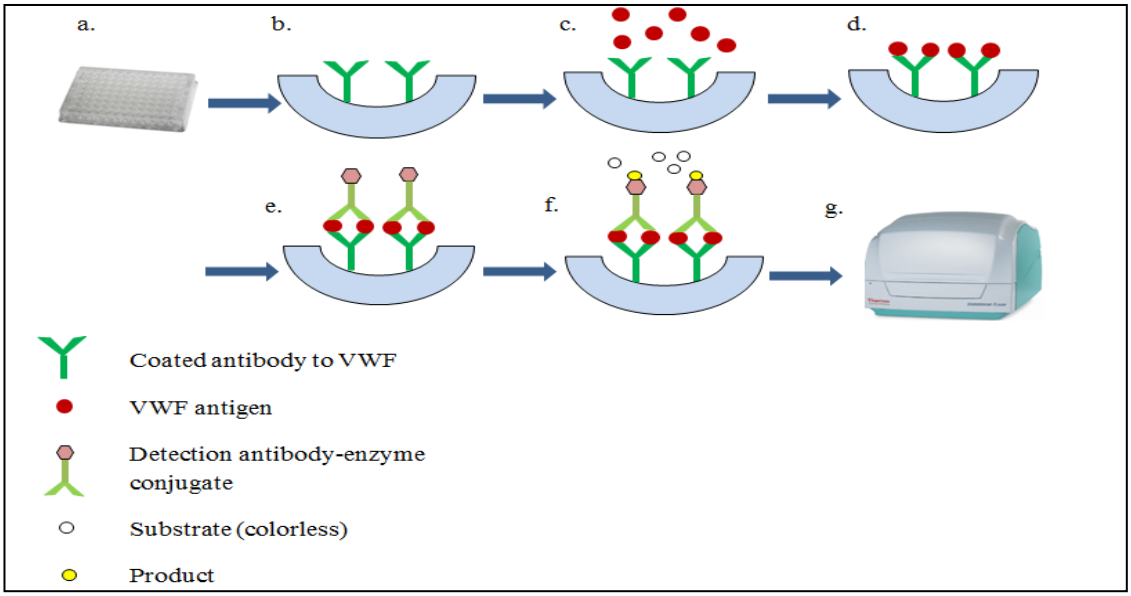

Figure 2.4 Diagram showing the principle of the ELISA technique. **A)** A 96 well micro-plate was used in ELISA method. **B)** Purified capture antibody to VWF was bound to the well and the remaining binding sites on the wells were blocked using bovine serum albumin. **C)** The plate was washed, and then supernatants, cell lysates and reference plasma samples were applied to the micro well. **D)** VWF antigen present in samples binds to coated antibodies. **E)** After washing, detecting-enzyme conjugate antibody is applied to enable forming a sandwich complex between the coating and detection antibodies. **F)** Colorless peroxidase substrate is added. After a fixed time, the colour of substrate is changed to yellow in proportion to the concentration of VWF antigen**. G)** The plate is read using plate reader at an optical density of 490 nm.

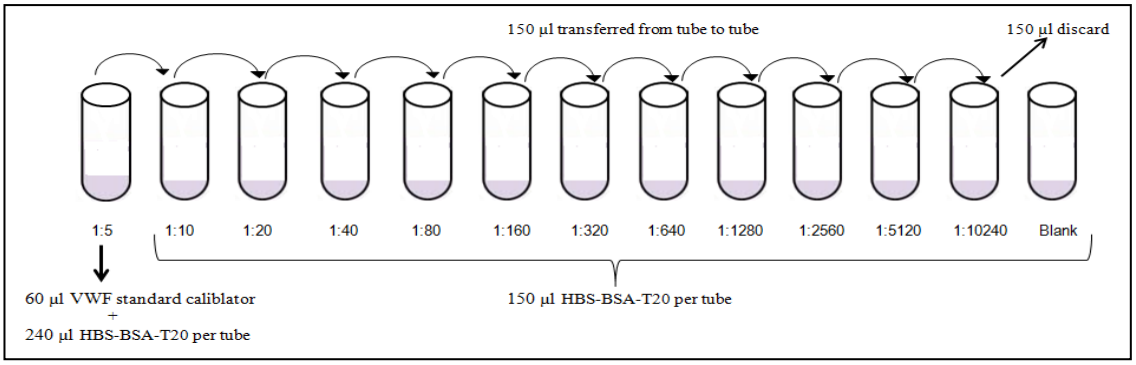

Figure 2.5 Summary of double serial dilution to create a series of solutions starting from 1:5 down to 1:10240 using VWF standard calibrator to produce a standard curve. Firstly, a 1:5 dilution was prepared by adding 60 µl of stock reference plasma into 240 µl HBS-BSA-T20 sample diluent. Sample was mixed thoroughly then 150 µl of 1:5 dilution was transferred into the second tube to produce 1:10 dilution. This process was repeated until a dilution of 1:10240 was reached. Blank contains sample diluent only.

2.2.14.3. ELISA data analysis

All results from the plate reader appeared as an optical density (OD). In order to calculate the level of expressed VWF:Ag from transfected HEK293T cells, a standard curve was produced using a standard control pooled plasma containing VWF with known concentration. The concentration of VWF in cell lysates and supernatants was calculated using the standard curve plotted between the known concentrations of each diluted reference plasma against its corresponding OD. The concentration of expressed VWF:Ag was measured and converted to international units per decilitre (IU/dL). Also, the expression level of transfection data was normalised to correct for transfection efficiency of the cells using Renilla expression. The VWF concentration was divided by Renilla expression to give a ratio, from which mutants were then compared to wild type expression. The mean values and standard deviation of wild-type, homozygous and heterozygous mutations including supernatants and lysates were calculated for all three experiments. Finally, the levels of VWF either homozygous or heterozygous were expressed as a percentage compared to the expressed level of wild-type.

2.2.15. Statistical analysis

Data including mean values, standard deviation and bar chart were analysed and prepared using Microsoft Excel 2010 (Microsoft Software, USA) and GraphPad Prism version 5 (GraphPad Software, San Diego, CA). Comparison of mean values was carried out using One-way ANOVA. Results were considered statistically significant at $P < 0.05$.

2.2.16. Multimer analysis

Multimer analysis of wild-type-VWF and VWF mutants expressed *in vitro* was performed by Prof. Ulrich Budde (Hamburg, Germany). VWF multimer analysis was undertaken on cell supernatants and size separated on medium resolution 1.6% sodium dodecyl sulphate (SDS) agarose gel (Budde et al., 2008b).

2.2.17. Immunofluorescence analysis

Wild-type and mutant *VWF* constructs were transiently transfected into HEK293 cells in order to determine the intracellular storage of VWF within pseudo WPB. Transfected cells were seeded in 6 well plates on glass coverslips at a cell density of 150,000 cells/ well in 2 ml of DMEM with10% FBS 24 hr prior to transfection. Transfection was undertaken using a plasmid concentration of 2.5 µg/ml in total. On the day of transfection, 2.5 µg of wild-type and mutant plasmids were diluted in 2 ml of DMEM reduced serum media in wild-type, homozygous and heterozygous states. 10 µl of Lipofectamine LTX was added to the mixture. Following 30 min incubation at room temperature, 2 ml of the mixture was added drop-wise into each well. The plate was incubated at 37 °C/5% CO_2 for 48 hr to allow VWF expression.

2.2.17.1. Immunofluorescence staining

Forty eight hr post transfection, transfected cells were stained with immunofluorescent antibodies. Cell media was aspirated from each well followed by three wash steps with 1 ml PBS for 5 min each to ensure removal of all remaining media. After washing, 1 ml of BD cytofix solution buffer (Biosciences, San Diego, USA) was added and incubated for 20 min to fix cells into coverslip. After 3 washes with 1 ml of PBS, 1 ml of PBS/1%TritonX-100 was added to each well in order to permeabilise the cells followed by incubation for 10 min and washing 3 times with PBS. In order to block non-specific sites, one ml of 1% bovine serum albumen BSA-PBS solution was added followed by incubation for 20 min. After 3 washes with 1 ml PBS, 1.5 ml of 1:500 primary antibodies was added to each well. Primary antibody solution was prepared by diluting 3 µl of anti-VWF rabbit primary antibody (DakoCytomation, Glostrup, Denmark) and 3µl of mouse anti-α-tubulin primary antibody (Sigma-Aldrich, UK) to 1.5 ml of 1% BSA-PBS. Cells were incubated in a wet box at 4 °C overnight. After incubation, primary antibodies were aspirated followed by washing 3 times with 1 ml of PBS for 15 min each. This was followed by adding 1.5 ml of 1:500 secondary antibody solutions which was prepared by diluting 3 µl of anti-rabbit Alexa Fluor 488 VWF green secondary antibody and 3µl of anti-mouse Alexa Fluor 555 of α-tubulin red secondary antibody (Invitrogen, USA) to 1.5 ml of 1% BSA-PBS. After one hr incubation in the dark, the secondary antibody solution was aspirated followed by 3 washes for 15 min each with 1 ml PBS and two washes with 1 ml dH_2O

for 5 min each. dH_2O was aspirated and coverslips were left to air-dry for 10 min. Coverslips were removed from the well and placed over 25 µl of mounting media on a microscope slide. After 15 min incubation at RT in the dark, the edges of the coverslips were sealed with nail varnish to prevent drying out of the cell sample. The cells were analysed on Zeiss LSM 510 Meta confocal laser microscope using Apochromat 40X/ 1.2 water UV-VIS-NIP objective.

Also, to determine the localisation of VWF within WPB-like organelles, a similar protocol was undertaken using VWF and the ER marker protein disulfide-isomerase (PDI). In this experiment, mouse anti-PDI primary antibody (Abcam, UK) was used to stain cells instead of mouse anti-α-tubulin primary antibody in addition to anti-VWF rabbit primary antibody. Cells were analysed on Zeiss LSM 510 Meta confocal laser microscope using Apochromat 63X/ 1.4 oil Ph3 UV-VIS-NIP objective using transmitted light with phase contrast.

Chapter 3

Sequence re-analysis of *VWF* in the EU-MCMDM-1VWD study

3. Sequence re-analysis of VWF in the EU-MCMDM-1VWD study

3.1. Introduction

The EU study (MCMDM-1VWD) carried out mutational analysis on a group of IC who were historically diagnosed with type 1 VWD. This study successfully identified mutations in almost 70% of IC using various techniques with variable sensitivity. However this cohort analysis failed to determine the genetic variants associated with VWD in the remaining 30% of cases (Goodeve et al., 2007). The failure of this study to identify the genetic cause in these IC may be due to several reasons. The mutational analysis of *VWF* was performed using various techniques including CSGE, SSCP, DHPLC and direct sequencing which had variable sensitivity ranging between 75% and 100% and may have caused mutations to be missed. Also, mutations may have also been missed due to human error. Moreover, it is known that *VWF* is a highly polymorphic gene, and the presence of SNP within primer annealing sites can lead to mono allelic amplification that could mask a heterozygous genetic variant and this could cause a mutation to be missed (Thomas et al., 2006a, Hampshire et al., 2010). This part of the study aimed to re-analyse and re-sequence all 52 exons of *VWF* in IC where point mutations were likely to have been missed either due to there being a SNP within primer binding sites or due to insensitivity of the mutation analysis previously undertaken.

The EU study failed to detect mutations in 42 IC who had normal multimers. The median level of VWF:Ag in these IC was 49 IU/dL and the IC presented with an average BS of 8. Blood group O accounted for almost 76% of IC and complete co-segregation of *VWF* with VWD was observed in only 19% of this group. Hence the recruitment criteria was based on a historical diagnosis of VWD, possibly not phenotypic, VWF:Ag was used over RCo activity because of the SNP polymorphism that can have a severe effect on activity if present and hence interfere with the assay and skew any results.

IC selected for the current study either had no mutation detected or had a *VWF* mutation detected that was not sufficient to explain the patient's phenotype. Eighteen IC diagnosed with type 1 VWD who had no mutation identified or in whom a mutation was found but did not explain the disease phenotype, had a low level of VWF:Ag less than the lower end of the normal range or presented with bleeding, and showed co-segregation between VWD and *VWF* within the EU study were selected (Figure 3.1). Out of 18 IC included in this study, two families had been excluded from the original study due to a markedly low levels of VWF (P9F18) and insufficient DNA sample (P10F5) (Goodeve et al., 2007). The selection criteria involved IC with VWF:Ag levels less than 50 IU/dL or with BS > 3. Out of 18 IC, 5 (28%) already had a previously identified mutation(s) with a low level of VWF:Ag and the remaining cases showed

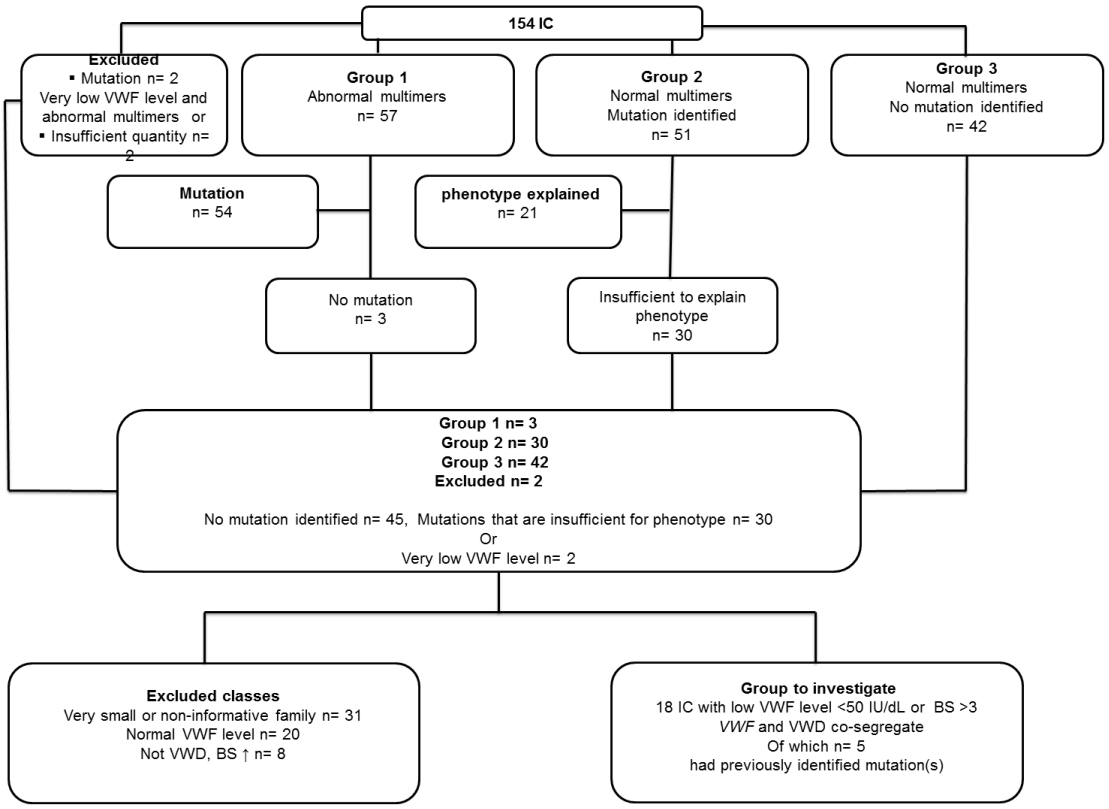

Figure 3.1 Flow chart shows the selection criteria for the VWD IC recruited in this study

Table 3.1: Phenotypic data for 18 ICs

Index Case	Bleeding score	VWF:Ag IU/dL	VWF:RCo IU/dL	FVIII:C IU/dL	VWF:FVIIIB	pp/Ag	VWF:CB IU/dL	RCo/Ag	Multimer structure	ABO blood group genotype	Previously identified mutation
P1F2II:1	19	43	38	57	Normal	1.1	58	0.88	Normal	O/O	
P2F13I:3	6	27	29	66	Normal	2.9	34	1.07	Normal	O/O	
P4F5I:1	13	16	15	25	Normal	7.0	11	0.94	Normal	O/O	
P4F7II:1	9	51	57	45	Normal	1.4	68	1.12	Normal	O/O	
P5F1II:3	2	37	32	28	Het	1.8	43	0.86	Normal	O/A	p.R854Q
P6F4II:1	10	57	35	74	Normal	0.9	33	0.61	Normal	O/O	
P6F9II:1	15	44	42	44	Normal	2.0	74	0.95	Normal	O/O	
P7F8I:2	3	38	39	107	Normal	2.2	46	1.03	Normal	O/O	
P8F2II:2	6	26	40	75	Normal	2.4	43	1.54	Normal	O/A2	p.Q2544X
P8F3I:2	8	61	50	125	Normal	1.4	25	0.82	Normal	®NA	
P8F5II:1	4	49	56	78	Normal	1.5	50	1.14	Normal	O/O	
P9F14II:2	18	3	3	7	Normal	8.5	1	1	Abnormal	O/A	p.[R924Q;C1927R] c.1533+1G>T
P9F18I:1	9	3	3	3	*NI	0.0	0.7	1	Abnormal	O/O	p.S539fs
P10F5II:2	4	48	41	84	Normal	0.0	63	0.85	Normal	O/O	
P10F7II:1	12	55	42	88	Normal	1.8	56	0.76	Normal	O/O	
P10F8II:1	10	49	52	14	2N	1.3	57	1.06	Normal	O/O	p.R816W
P10F9II:3	9	46	53	80	Normal	2.0	64	1.15	Normal	O/O	
P12F5II:1	13	39	42	57	Normal	1.7	58	1.08	Normal	O/O	
Normal range	-3-3	48-167	47-194	57-198	Normal	1-1.5	66-226	0.6-1.62	Normal	-	

*Not interpretable, ®Not available, (Ag) antigen, RCo (ristocetin cofactor), FVIII:C (factor VIII coagulant activity), pp (pro-peptide), CB (collagen binding), Het (Heterozygous), 2N (type 2N VWD)

no mutation (Table 3.1). Fourteen IC (78%) had VWF:Ag levels less than 50 IU/dL and the other four had a level slightly higher than the lower normal range (51-61 IU/dL), but had high BS ranging between 8-12 (Table 3.1). Complete co-segregation was observed in 6 (33%) IC and blood group O/O genotype was predominant and found in 14 IC (78%), two IC were O/A, one IC was O/A2 while ABO genotype was not available in one IC (Table 3.1). Therefore, amplification and re-sequencing of *VWF* in 18 IC who showed no mutation during the EU study using primers that showed no SNP within their sequences and direct DNA sequencing to sequence all *VWF* 52 exons and closely flanking intronic regions contributed in identifying mutations in several IC which were missed in the previous study.

3.2. Primer design and SNP screen

For the purpose of designing *VWF* primers and ensuring no SNP within primer sequences, an extensive in *silico* analysis was performed using tools described in section 2.2.1. Avoidance of the presence of SNP underneath the annealing site of primers was undertaken throughout this study to prevent the possibility of an amplification error that could hide the presence of heterozygous mutation(s). All 52 pairs of primers used in the EU study were screened for the presence of SNP within primer sequences. Out of these, 32 primer pairs showed no SNP and were used to amplify *VWF* in the 18 IC (Appendix Table 4), while SNP were found in 16 primers including those for exons 8, 12, 14, 15, 18, 20 and 36 (Appendix Table 10). SNP within primer sequences were identified by using the Manchester SNP Check tool (http//ngrl.manchester.ac.uk/SNPCheckv2/snpcheck.htm, last accessed November 2010) and a manual check by eye through comparison with the genomic *VWF* sequence reference (Section 2.2.1). Twenty primer pairs were re-designed to amplify the *VWF* exons and closely flanking intronic regions, out of which 12 primers were within the *VWFP* region (exons 23-34) whilst the remaining were redesigned for amplification of exons 1, 8, 12, 14, 15, 18, 20 and 36. Nine primers were redesigned due to the presence of both together SNP within the primer binding sequence and because primer nucleotides were too close to the target exon, eight primers were re-designed due to only the presence of SNP within primer sequences and three were redesigned due to either an amplification problem or a primer sequence error (Appendix 10). Primers outside of the *VWFP* region were designed using Primer3 online software (Section 2.2.1) and primers for amplification of exons with overlap to *VWFP* were designed manually with mismatch to the pseudogene. During primer design, it was ensured that the last nucleotide within the primer sequence was approximately 50 nucleotides from the target exon sequence with no SNP in the primer sequence and mismatches introduced between gene and pseudogene were included to de-stabilize binding to *VWFP* and to confer maximum specificity of *VWF* as described in section 2.2.1, but due to the constraints of the small number of possible positions to

design primers in the pseudogene region, it was not always possible to design primers following these criteria (Figure 3.2). Mismatches between gene and pseudogene were introduced into primers in the pseudogene region as seen in figure 3.2. Mismatches were introduced to reverse primers of exons 26, 33 and 34 and to both forward and reverse primers of exon 28 in order to ensure maximum *VWF* specificity and to de-stabilise binding to *VWFP*. Appendices 11 and 12 show the re-designed primers in the study including primer sequences, introduced mismatches, GC content, annealing temperature and product size.

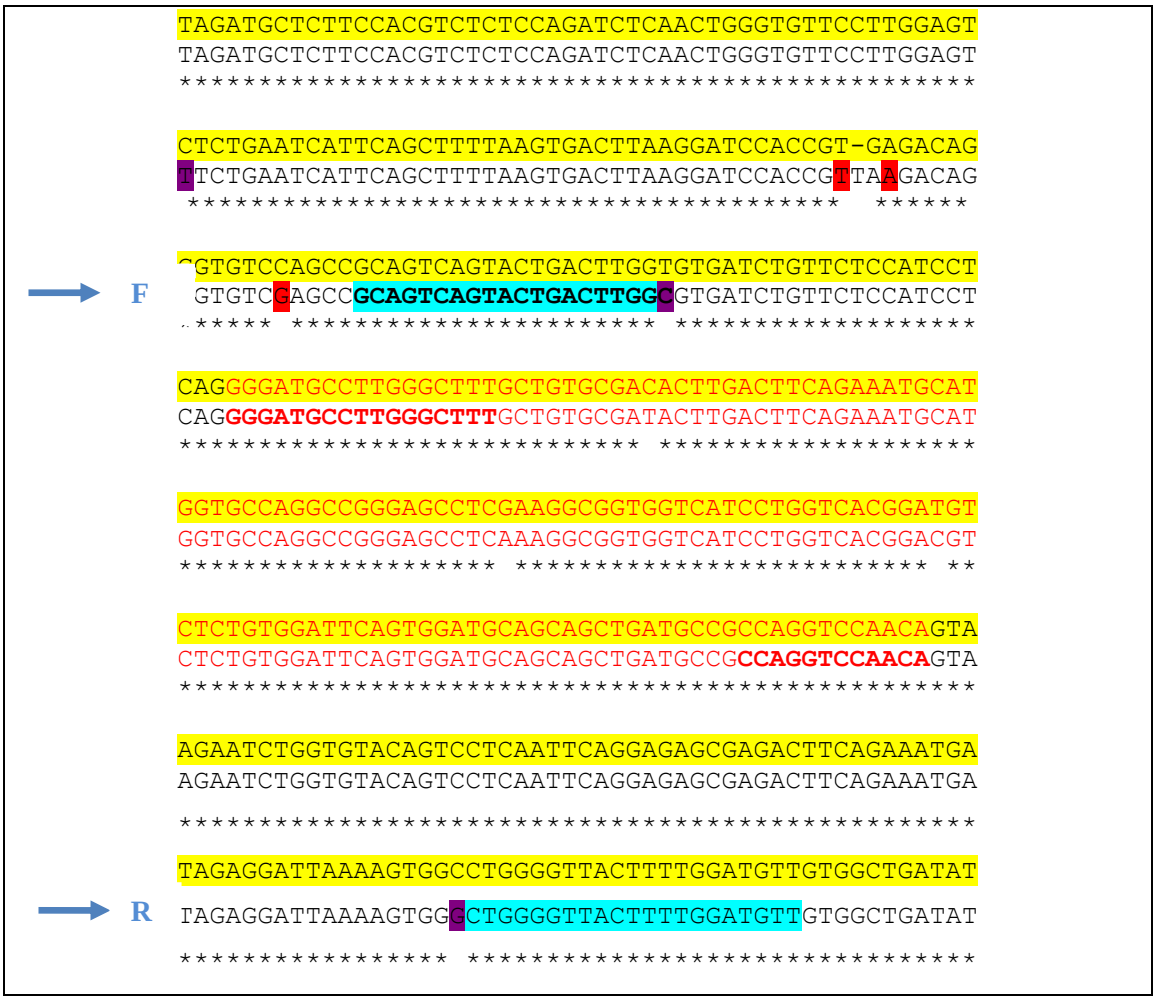

Figure 3.2 Alignments between *VWF* and *VWFP* and mismatch locations (exon 31)

This figure shows the process of designing primers by including mismatches between the gene and pseudogene. Nucleotides in bold red the exonic region. Nucleotides of the pseudogene are highlighted in yellow while black nucleotides represent true *VWF*. Presence of asterisks represents the matches between the gene and pseudogene while the absence of asterisks represents mismatches sites between them. Nucleotides highlighted in turquoise represent forward and reverse primers used to amplify exon 31, the attached nucleotide highlighted in violet represents the mismatches between *VWF* and *VWFP* within primer sequence, blue arrows refer to forward and reverse primers. Nucleotides highlighted in red represent reported SNP. The forward primer was not 50 nucleotides from the exonic region due to presence of SNP within the mismatched area.

3.3. PCR optimisation

Initially, all newly re-designed primers were used to amplify *VWF* exons using standard PCR conditions. These conditions included denaturation at 94 ℃ for one min, annealing at 60 ℃ for one min, extension at 72 ℃ for one min for 35 cycles using a 1.5 mM concentration of $MgCl_2$. The purpose of that was to minimise time required for PCR optimisation and also for the simplicity of amplification. Moreover, to save the quantity of IC DNA samples, 3 DNA control samples collected from the BTS were used to optimise the PCR reaction for the newly designed *VWF* primers.

With the initial conditions, most exons (13 exons out of 19) did not require any further optimisation and showed ideal amplification at the standard PCR conditions with the exception of primers for exons 15, 26, 27, 28, 32 and 33 which required further specific optimisation. PCR optimisation was performed by changing the annealing temperature, number of cycles or $MgCl_2$ concentration in order to alter the specificity of the reaction.

3.3.1. Specific exon optimisation

The six exons required further PCR optimisation due to either the appearance of non-specific bands or failure of amplification during initial PCR optimisation are listed in Appendix Table 11 and 12. The exon 15 reaction was optimised at annealing temperature of 55℃ for 32 cycles, the optimal amplification of exon 26 was established at annealing temperature of 60℃ and 32 cycles, the optimal amplification of exon 27 was established at annealing temperature of 60℃/1.5 mM $MgCl_2$ and 35 cycles (Figure 3.3), exon 32 was optimised at annealing temperature of 56 ℃ for 35 cycles (Figure 3.4) and the optimal amplification conditions of exon 33 was achieved at annealing temperature of 61℃ with 2.5 mM $MgCl_2$ for 35 cycles (Appendix Table 11 and 12).

3.3.1.1 Exon 28

During the MCMDM-1VWD study, exon 28 was amplified using 1 amplicons and conventional PCR to cover the entire 1.4 kb sequences followed by sequencing the entire exon 28 using 4 overlapping amplicons (Appendix 5). Although exon 28 is a large exon of 1.4 kb in size, its amplification was initially optimised using conventional PCR conditions. The calculated melting temperature was 59℃. However, when performing PCR using the calculated Tm, at initial annealing temperature (60℃) and at 64℃, the PCR reaction for exon 28 failed to amplify at these annealing temperatures. Following these failures, the annealing temperature was further lowered to 55, 53, 52 and 50℃ and combined with a range of $MgCl_2$ concentrations (1.5, 2, 2.5, 3, and 4 mM) at each temperature. However, the PCR reaction still failed to amplify. Following

persistent failure, a long PCR reaction was designed as described in Section 2.2.2.3. The calculated melting temperature for the exon 28 primers according to the Phusion polymerase manufacturer's instructions was 67°C. When performing long PCR using this calculated melting temperature, a strong and clear amplification product could be observed on the agarose gel (Figure 3.5). Therefore, the optimal amplification conditions for primers of exon 28 were achieved at 67°C/32 cycles using long range PCR conditions.

3.4. Confirmation of *VWF* amplification

As mentioned previously there is high sequence similarity (97%) between *VWF* and *VWFP*. To ensure that the amplification was for the *VWF* rather than the *VWFP*, the generated amplicons of control samples were analysed using DNA sequencing. Mismatched sites and sequence differences between *VWF* and *VWFP* were compared in the generated sequences from all amplicons of this region. As a result, all amplifications were for *VWF* and none of the amplicon sequences corresponded to the pseudogene (Figure 3.6).

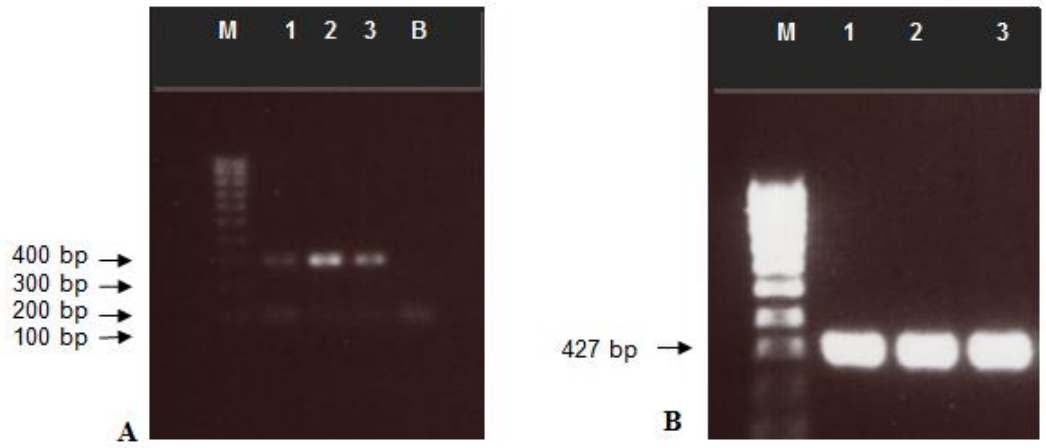

Figure 3.3 Amplification of exon 27 on a 1% agarose gel. A) amplification at 60°C and 1.5 mM $MgCl_2$ faint bands are shown, **B)** strong amplification at 62°C/2.5 mM $MgCl_2$. M; hyperladder IV, 1-3 BTS control samples; B negative control. Arrow indicates amplicons size.

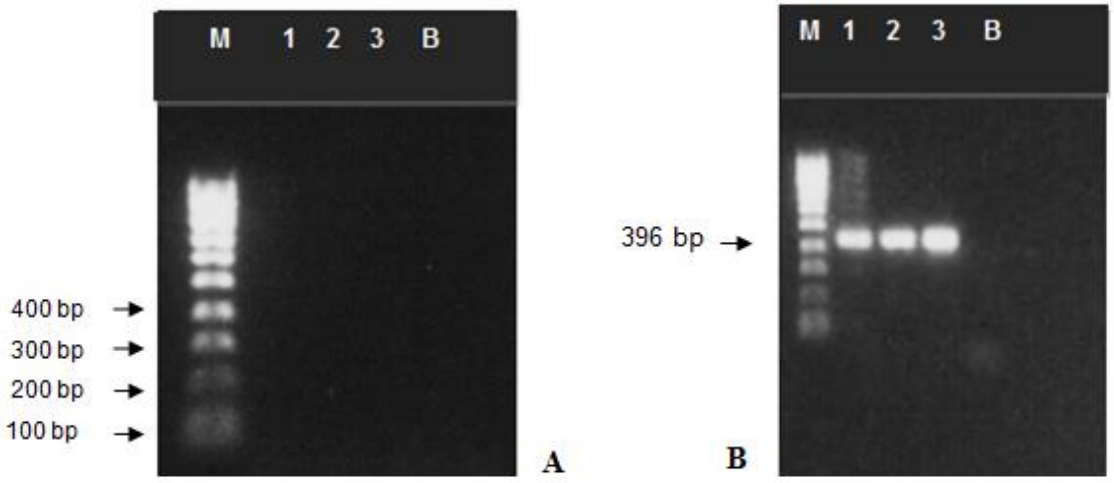

Figure 3.4 Amplification of exon 32 on a 1% agarose gel. A) Failure of amplification at 60°C, **B)** Amplification at 56°C and 1.5 mM $MgCl_2$. M; hyperladder IV, 1-3 BTS control samples; B negative control. Arrow indicates amplicons size.

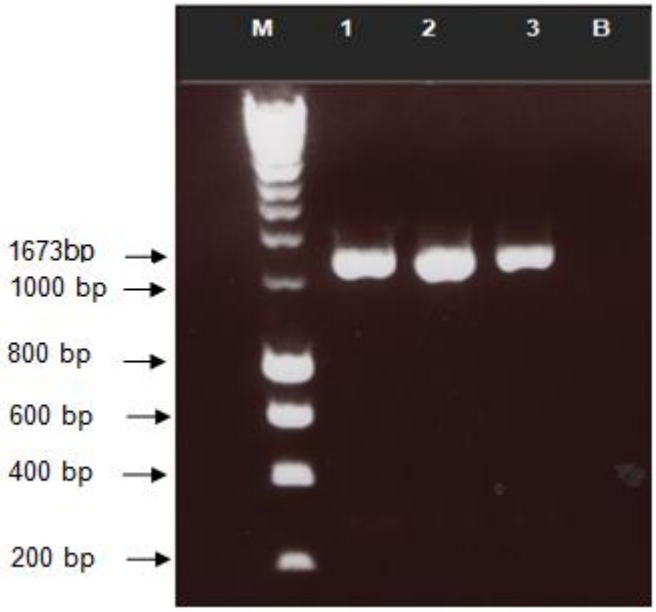

Figure 3.5 Amplification of exon 28 on a 1% agarose gel. Long range PCR amplicon at 67°C. M; hyperladder I, 1-3 BTS control samples; B negative control. Arrow indicates the size of amplicon.

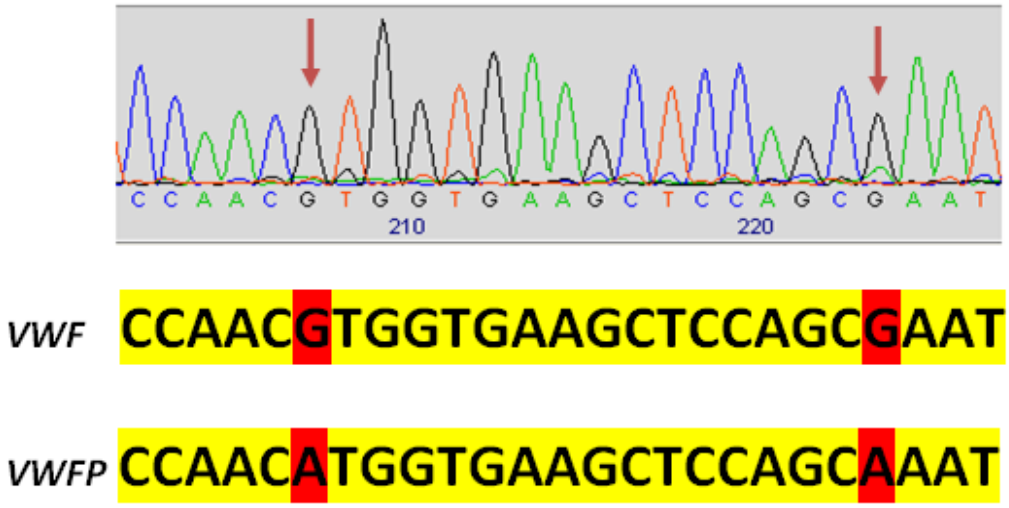

Figure 3.6 Chromatogram of part of *VWF* exon 32 indicating mismatch sites between *VWF* and *VWFP*. Nucleotides marked with red arrows represent differences between *VWF* *VWFP*. Mismatched sites are highlighted in red.

3.5. *VWF* amplification and sequencing

During the original study conducted by MCMDM-1VWD, 30% of IC showed no mutation. Out of those, 18 families were re-analysed who presented with low level of VWF, had significant bleeding and no mutation identified or a mutation did not account for phenotype. Throughout the study, the newly designed primers and previously used primers that showed no SNP underneath their annealing sites were successfully amplified and sequenced for 52 *VWF* exons covering exonic and flanking regions for all IC listed in table 3.1 to detect any possible missed candidate mutations located within the entire *VWF* exonic and flanking regions.

3.6. Identified VWF mutations and polymorphisms

Initially, only the IC from each family was screened and when a candidate mutation was identified in any IC, it was analysed in all remaining family members including affected and unaffected members in order to determine the inheritance of the mutation. Analysis of the sequencing results revealed no new SNP, but four mutations, out of which 3 novel were identified in four index cases in exons 26, 28, 39 and intron 12. Three of these IC already had a mutation previously identified that was insufficient to explain their phenotype. The newly detected candidate mutations can be categorised into three groups, missense changes were identified in exons 26 and 39, a silent change was present in exon 28 and a splice-site mutation was located in intron 12 (Table 3.2). None of these newly novel identified mutations have been

detected prior to this study. However, many previously reported polymorphisms were identified. All previously reported SNP that were identified in this study are summarised in Appendix 13.

Table 3.2 List of candidate missed and previously candidate mutations identified in this study

IC	Location	Nucleotide change	Amino acid change	Previously identified candidate mutation
P5F1II:3	Exon 39	c.6811T>G	p.W2271G	p.R854Q (2N)
P9F18I:1	Exon 26	c.3469T>C	p.C1157R	p.S539Lfs*38
P10F5II:2	Exon 28	c.4146G>T	p.L1382=	Nil
P10F8II:1	Intron 12	c.1432+1G>T	Splice change leading to exon skipping	p.R816W (2N)

3.6.1. Mutation result in family P5F1

During analysis of DNA sample of P5F1II:3 IC, 22 nucleotide changes were detected. These changes included twenty known heterozygous polymorphisms (Table 3.3), 2 of which were shown to have an effect on protein sequence (Section 1.9.3.1.2.5) and two candidate mutations. The candidate mutations included one novel missense mutation detected in exon 39 and a previously reported missense change c.2811G>A predicted to result in p.R854Q that impairs VWF binding to FVIII in one IC. The novel heterozygous point mutation was identified in the exonic region located at nucleotide position 6811 where T was replaced by G (c.6811T>G) as shown in figure 3.7. This mutation has not been reported previously and was found only in one IC (P5F1II:3). This novel missense mutation resulted in a substitution of the amino acid tryptophan located at position 2271 of the VWF protein with a glycine (p.W2271G). Tryptophan is one of the largest amino acids while glycine is the smallest of the 20 amino acids (Figure 3.8). However, tryptophan and glycine amino acids also differ in other properties. Subsequently, sequence analysis for this fragment was performed for all family members that comprised the IC, two AFM and one UFM. By using bi-directional DNA sequencing, the candidate mutation in addition to the IC was detected in both AFM (I:2 and II:2), while the UFM (II:6) showed normal sequence (Figure 3.9).

Table 3.3: List of 20 known heterozygous SNP in IC P5F1II:3

SNP reference number	Nucleotide change	Amino acid change	Effect on protein expression	SNP location Exon/Intron
rs2286608	c.1-64C>T		No	Intron 1
rs1800378	c.1451A>G	p.H484R	No	Exon 13
rs7312411	c.1548T>C	p.Y516=	No	Exon 14
rs1063856	c.2365A>G	p.T789A	Yes*	Exon 18
rs1063857	c.2385T>C	p.Y795=	Yes†	Exon 18
rs216321	c.2555A>G	p.Q852R	No	Exon 20
rs1800380	c.2880G>A	p.R960=	No	Exon 22
rs34877178	c.2968-53G>A		No	Intron 22
rs3858686	c.2968-125C>T		No	Intron 22
rs56121649	c.3109-90G>C		No	Intron 23
rs56068059	c.3109-128G>T		No	Intron 23
rs6127535	c.5049A>C	p.A1683=	No	Exon 28
rs17491334	c.6064-71C>T		No	Intron 35
rs177702	c.6799-14C>T		No	Intron 38
rs10849371	c.6846A>G	p.T2282=	No	Exon 39
rs55867239	c.6977-22C>T		No	Intron 40
rs216867	c.7239T>C	p.T2413=	No	Exon 42
rs2270239	c.7549-59A>C		No	Intron 44
rs11063962	c.7771-13C>T		No	Intron 46
rs7976955	c.8442+204C>T		No	3' untranslated region

*Associated with alteration in VWF levels and in perfect linkage disequilibrium with SNP, † associated with alteration in VWF levels in CHARGE study (Smith et al., 2010).

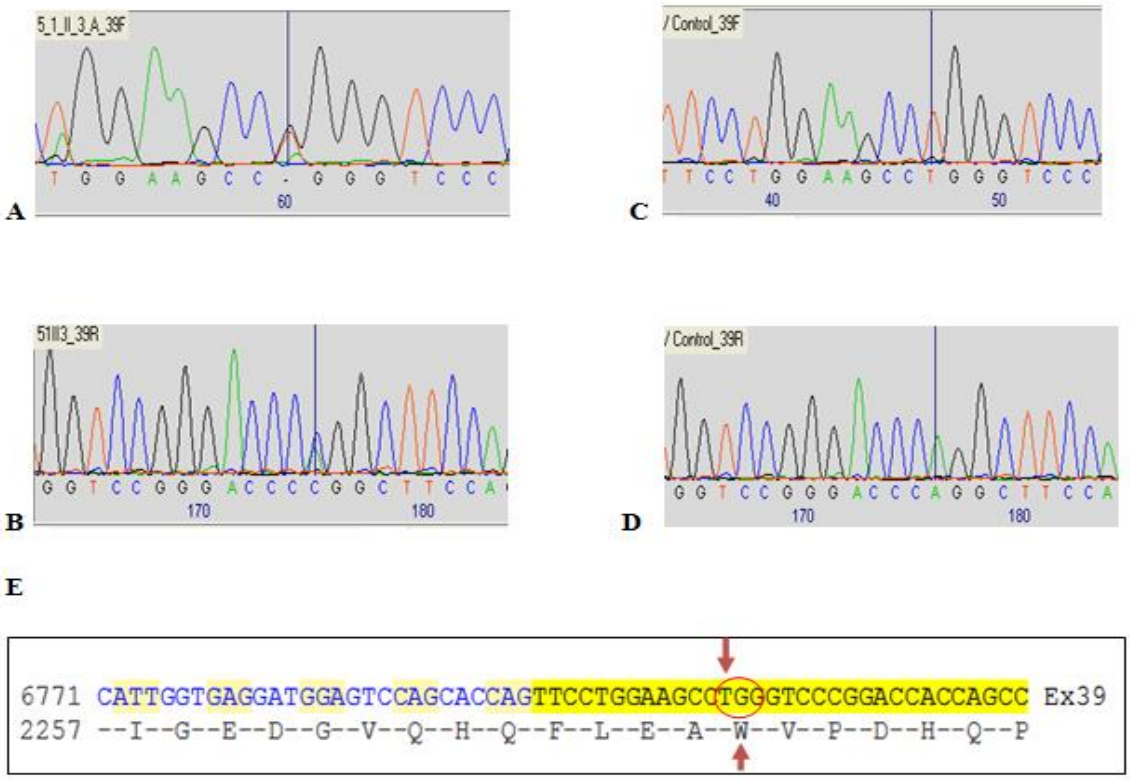

Figure 3.7 Heterozygous c.6811T>G point mutation in P5F1
A and **B** show the bidirectional sequencing of the heterozygous c.6811T>G mutation in exon 39, **C** and **D** show bidirectional sequencing of the wild type control. **E** shows the alignment of human cDNA to the exon 39 predicted amino acid sequence. The red arrows indicate the affected nucleotide (T) and amino acid (tryptophan). The TGG codon encoding tryptophan has been substituted to GGG that encodes glycine.

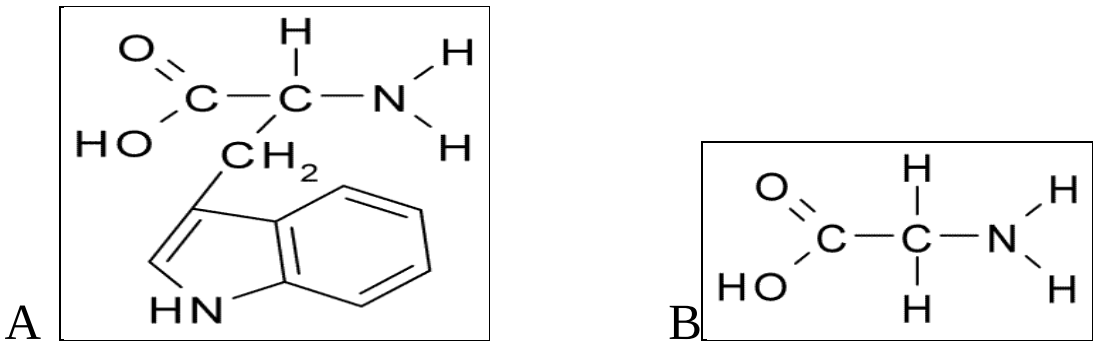

Figure 3.8 Chemical structures of amino acids A (tryptophan) and B (glycine). Source: www.wikimedia.org.

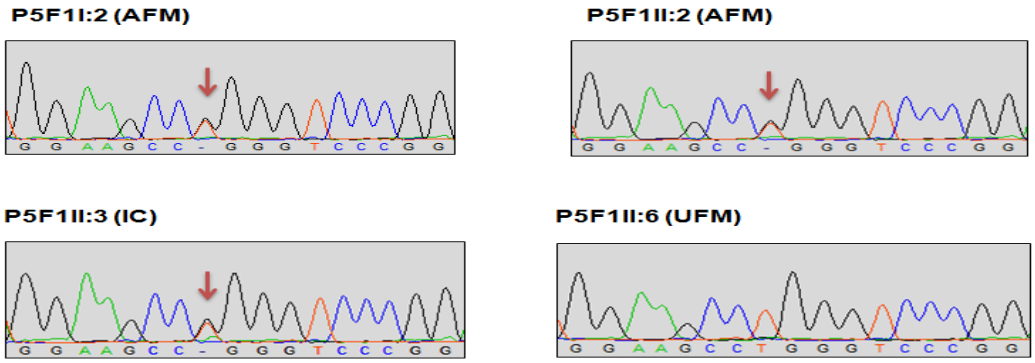

Figure 3.9 Sequence analysis results of family P5F1II:3. The candidate mutation c.6811T>G is marked by a red arrow. This mutation found in the IC and the AFM was absent from the UFM**.**

3.6.1.1. Linkage and mutation analysis in family P5F1

To assess the linkage between *VWF* and clinical and phenotypic data in recruited families, the MCMDM-1VWD study had previously performed linkage analysis (Eikenboom et al., 2006). Three different linkage analysis markers were applied to detect linkage between VWD and *VWF*. The $GT_{(n)}$ repeat marker is located within the promoter region, while the $TCTA_{(n)}$ repeat (STR III) and $TCTA_{(n)}$ repeat (STR II) both are located within intron 40 (Figure 3.10). P5F1II:3 was a small family consisting of four members, including three patients and one UFM. Therefore, it was not possible to establish definitive linkage between VWD and *VWF* in this family (Eikenboom et al., 2006). The p.R854Q mutation which affects VWF binding to FVIII was found in the two children P5F1II:3 (IC) and P5F1II:2 (AFM) and was likely to have originated in their father (Not tested). The presence of this mutation (p.R854Q) likely explains the low level of FVIII in the children who carry this mutation and the normal level of FVIII in the mother who does not carry the p.R854Q mutation (Figure 3.10). The level of VWF:Ag was markedly decreased in the IC and AFM who carried p.W2271G, ranging from 37-38 IU/dL, VWF:RCo ranging between 32-43 IU/dL , while the level of FVIII:C was reduced in the IC (28 IU/dL) and the AFM child P5F1II2 (34 IU/dL) and normal in the mother P5F1I2 (85 IU/dL) who lack the p.R854Q mutation. BS was normal in all except AFM P5F1I2 probably due to low age (Table 3.4). However, this family showed reduced phenotypic data and O/A blood group genotype. Linkage analysis results indicated that the IC and AFM (II:2) who carry p.R854Q shared a haplotype [191]-[159]-[174] (GT repeat, STRIII and STRII) indicated by the green allele which originated from the father, while the haplotype [189]-[151]-[174] (black allele) associated with p.W2271G was found in all AFM and the IC. The latter markers co-segregated with the low levels of VWF and FVIII. Briefly, although this family was small, linkage analysis showed clear co-segregation of haplotype with VWD.

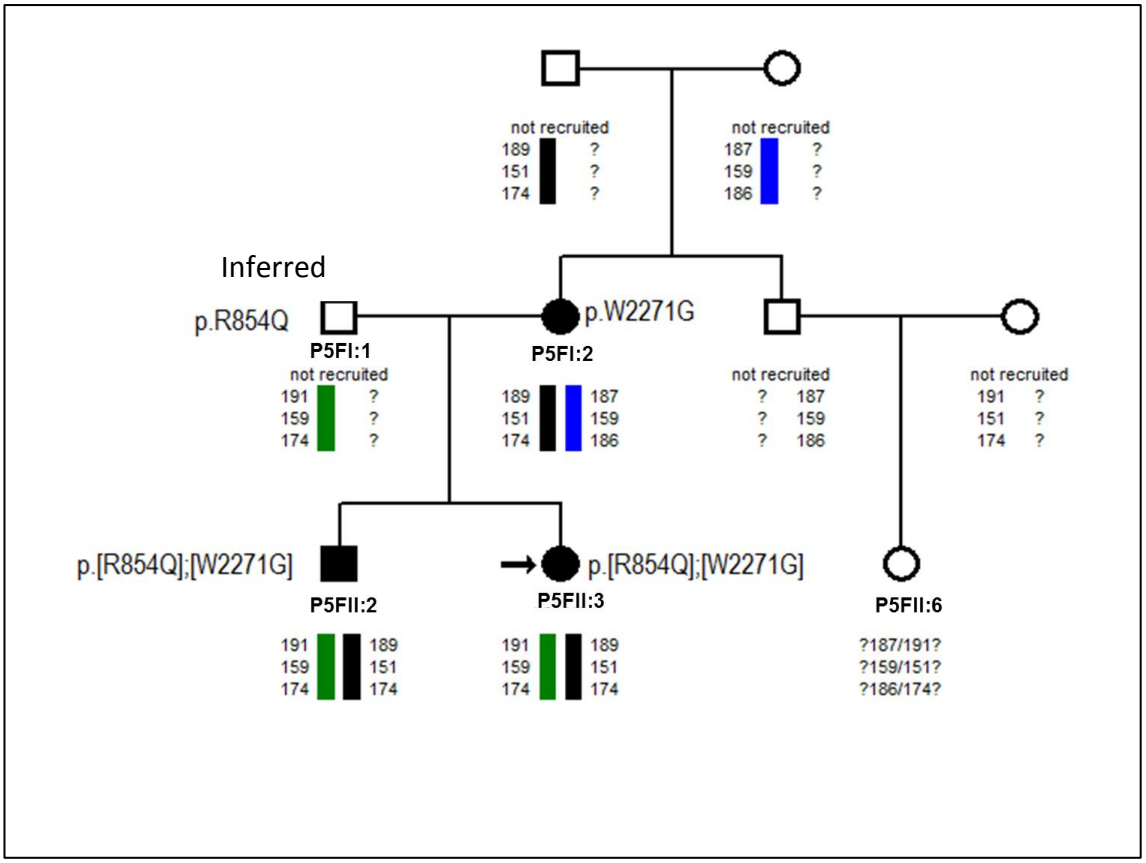

Figure 3.10 Pedigree of family P5F1 showing linkage analysis and mutation results. The linkage analysis marker order from top to bottom is: $GT_{(n)}$ promoter dinucleotide repeat (bp), $TCTA_{(n)}$ repeat (bp) (STR III) and $TCTA_{(n)}$ repeat (bp) (STR II). The linkage analysis results are shown underneath each family member. Females are indicated by circles and males by squares. Filled symbols represent AFM and the black arrow indicates the index case. Mutant allele [189]-[151]-[174] associated with p.W2271G and [191]-[159]-[174] associated with p.R854Q.

Table 3.4 Phenotypic data for family P5F1

Family member	Age* (years)	Status	BS	VWF:Ag IU/dL	VWF:RCo IU/dL	FVIII:C IU/dL	Multimer profile	ABO genotype
I:2	46	AFM	7	38	37	85	Normal	O/A
II:2	23	AFM	-1	37	43	34	Normal	O/A
II:3	21	IC	2	37	32	28	Normal	O/A
II:6	28	UFM	-2	73	59	91	Normal	O/A

*At recruitment

3.6.1.2. p.W2271G protein prediction and multiple species alignment

Three different tools were used to predict the effect of amino acid substitutions on protein function. These tools included SIFT, PolyPhen2 and Align GVGD (section 2.2.5) (Table 3.5). SIFT predicts the effects of amino acid substitutions on protein function based on sequence homology and amino acid physical properties. The score ranges from 0 to 1 where 1 is neutral and 0 is damaging. The PolyPhen2 tool predicts the potential impact of amino acid replacement on the function and structure of human protein using straightforward physical properties such as site and type of substitution. The scores range from 0 to 1 where 0.2 is less likely to be damaging and high positive scores are damaging and 0 indicates a neutral effect of amino acid replacement on human protein function (Paulin and Henikoff, 2006). The Align GVGD tool predicts the effect of missense substitutions in a target protein in a spectrum from enriched deleterious to enrich neutral. GD measures the biochemical variations such as polarity and composition of amino acids between mutant and normal amino acids while GV measures the quantity of biochemical variations in the affected position. GD <60 may not affect the structure or function of the protein while >60 is probably damaging. The effect of align GVGD is ordered from class C0 which indicates less likely to be damaging to most likely class C65 which indicates most likely damaging. The amino acid substitution of tryptophan by glycine at position 2271 in VWF was analysed by all these methods to be a damaging mutation and thereby was predicted to affect the function and structure of VWF. SIFT, PolyPhen2 and Align-GVGD tools all predicted that the p.W2271G amino acid variant was probably damaging.

Table 3.5 Prediction methods used for amino acid substitution with prediction score and range of score for each

Prediction tool	Range of possible scores	Prediction score for p.W2271G
SIFT	0-1	0 (damaging)
PolyPhen2	0 to positive number	1 (probably damaging)
Align GVGD	C0-C65	Class C65, GD 183.79 (most likely damaging) GV 0.00

In addition to the *in silico* analysis of the protein substitution, evolutionary conservation of the tryptophan located at position 2271 was undertaken through alignment with the VWF amino acid protein sequence of twelve different species using MULTALIN as described in section 2.2.8. As a result, the p.W2271 was found to be completely conserved in VWF in all aligned species (Figure 3.11). This result indicated that this conserved residue was likely to be important in VWF protein structure and/or function.

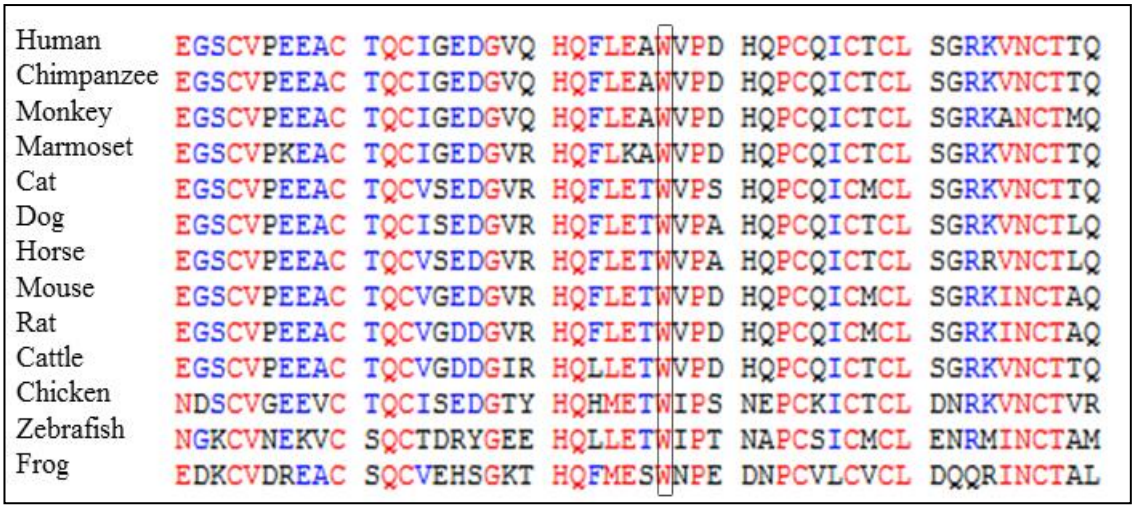

Figure 3.11: Schematic representation of the evolutionary conservation of p.W2271 across thirteen VWF orthologues which indicates complete conversation. Residue p.W2271 is highlighted by a rectangle (http://mutalin.toulouse.inra.fr/mutalin/).

3.6.2. Mutation analysis in P9F18 family

In order to find a candidate missed mutation, the entire *VWF* coding sequence and exon/intron boundaries regions of IC P9F18I:1 were analysed using PCR amplification followed by direct sequencing. Analysis of *VWF* sequences within the IC detected two heterozygous missense candidate mutations in addition to 23 previously known heterozygous polymorphisms (Table 3.6). One novel heterozygous point mutation was identified in the exonic region of exon 26, c.3469T>C predicted to result in p.C1157R as shown in figure 3.12, while the other mutation was previously known with a single nucleotide deletion located in exon 14 (c.1614del) predicted to result in the frameshift mutation p.S539Lfs*38. The novel mutation located in the D3 domain was found only in one IC (P9F18I:1). It involved substitution of cysteine which is considered an important amino acid required for disulphide bond formation in the VWF protein. Subsequently, this candidate mutation was analysed in all family members that included one AFM and three UFM. By using bi-directional DNA sequencing, the candidate mutation c.3469T>C was sought and detected in AFM I:2, but was absent from all UFM, I:3 II:1 and II:2 (Figure 3.12). The frameshift mutation c.1614del was detected in all members including IC, AFM and UFM, except for I:3. Forward and reverse primers used in the original study to amplify *VWF* exon 26 were checked for the presence of SNP underneath their annealing sites using the SNP Check tool (Section 2.2.1). As a result, four SNP were detected, three in the forward primer and one in the reverse one detected at the 3' end (Table 3.7).

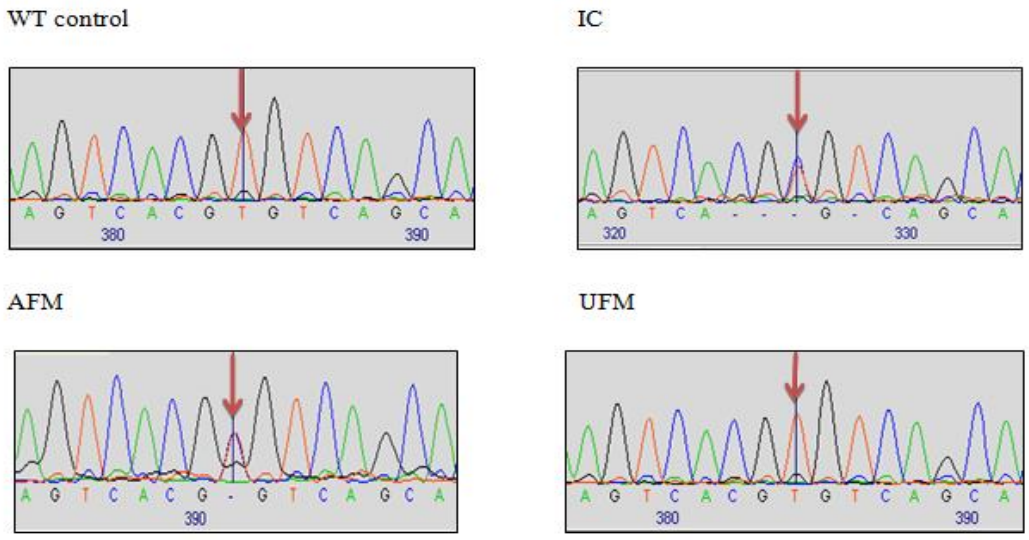

Figure 3.12 Heterozygous c.3469T>C point mutation in P9F18 family
Sequence analysis results of family P9F18 showing the heterozygous change, a T>C at nucleotide position 3469**.** The nucleotide c.3469T>C is marked by a red arrow. This mutation was found in the IC and the AFM and absent from the UFM.

Table 3.6: List of 23 known heterozygous SNP in the IC P9F18I:1

SNP reference number	Nucleotide change	Amino acid change	Effect on protein expression	SNP location Exon/Intron
rs2286608	c.1-64C>T		No	Intron 1
rs3213721	c.997+32G>A		No	Intron 8
rs55907031	c.998-27C>T		No	Intron 9
rs1800375	c.1173A>T	p.T391=	No	Exon 11
rs1800376	c.1182A>C	p.S394=	No	Exon 11
rs1800377	c.1411G>A	p.V471I	No	Exon 12
rs1800378	c.1451A>G	p.H484=	No	Exon 13
rs1063856	c.2365A>G	p.T789A	Yes*	Exon 18
rs1063857	c.2385T>C	p.Y795=	Yes†	Exon 18
rs216325	c.2546+25C>T		No	Intron 19
rs216321	c.2555A>G	p.Q852R	No	Exon 20
rs1800380	c.2880G>A	p.R960=	No	Exon 22
rs34877178	c.2968-53G>A		No	Intron 22
rs3858686	c.2968-125C>T		No	Intron 22
rs56121649	c.3109-90G>C		No	Intron 23
rs73051263	c.3222+31C>T		No	Intron 24
rs177702	c.6799-14C>T		No	Intron 38
rs216867	c.7239T>C	p.T2413=	No	Exon 42
rs216868	c.7082-7C>T		No	Intron 42
rs2286646	c.8115+66T>C		No	Intron 49
rs7962217	c.8113G>A	p.G2705R	No	Exon49
rs2270152	c.8116-20A>C		No	Intron 50
rs2362483	c.8253+32T>C		No	Intron 51

*Associated with alteration in VWF levels and in perfect linkage disequilibrium with SNP, † associated with alteration in VWF levels in CHARGE study (Smith et al., 2010).

Table 3.7 Identified SNP underlying the primer annealing sites for the *VWF* exon 26 primers

Forward primer (Exon-26)	Reverse primer (Exon-26)
CCCCAACATT**A**TCTCCAGATG**GC**	CCTATCCCATCCCACCAGCC**T**

*Nucleotides highlighted in red represent reported SNP

3.6.2.1. Linkage analysis and mutation study in family P9F18

This family included five members, two affected (IC+AFM) and three unaffected members (Figure 3.13). The IC (I:1) and the AFM (I:2) carried two mutations on two different alleles (compound heterozygous); the newly identified p.C1157R and the previously known p.S539Lfs*38 were present with very low levels of VWF:Ag, VWF:RCo and FVIII, increased BS (9-10) and abnormal multimers (Table 3.8). The presence of the previously identified heterozygous p.S539fs alone did not explain the increased values of BS and a very low levels of VWF:Ag in the IC and AFM who carry the additional mutation p.C1157R. Also, the presence of p.S539fs alone can explain the mild to moderate reduction of VWF:Ag, VWF:RCo and FVIII in the UFM who does not carry the p.C1157R mutation. The phenotypic data of the IC and AFM demonstrated undetectable levels of VWF:Ag, VWF:RCo and FVIII:C (<3 IU/dl) for each parameter in both with abnormal multimer pattern and the level of VWF:Ag, VWF:RCo and FVIII was mildly reduced ranging from 48-60, 45-69 and 41-75 IU/dL respectively in the UFM. The IC had O/O blood group genotype while the AFM had O/B (Table 3.8). It has been described that the VWF D3 domain is involved in the process of multimerization and FVIII binding and the presence of a missense mutation within this domain can potentially affect protein folding, multimerization, maturation, secretion and the transport pathway in addition to impairing binding to FVIII.

Linkage analysis results indicated that a shared haplotype [187]-[163]-[174] (GT repeat, STRIII and STRII) respectively which is associated with the frameshift mutation c.1614del is present in all members including the AFM and two of UFM, while the IC and the AFM shared an additional haplotype (black allele) [187]-[159]-[174] which completely co-segregated with the low level of VWF and FVIII:C. In summary, this family showed reduced phenotypic levels of VWF and FVIII:C, an abnormal multimer pattern and co-segregation of affected haplotypes with the disease. The candidate mutation p.C1157R located in D3 domain was classified as type 2A(IIE) and its presence in compound heterozygosity with p.S539fs was classified as type 3 VWD. However, the mutant alleles co-segregated with the disease phenotype and were inherited in an autosomal recessive manner.

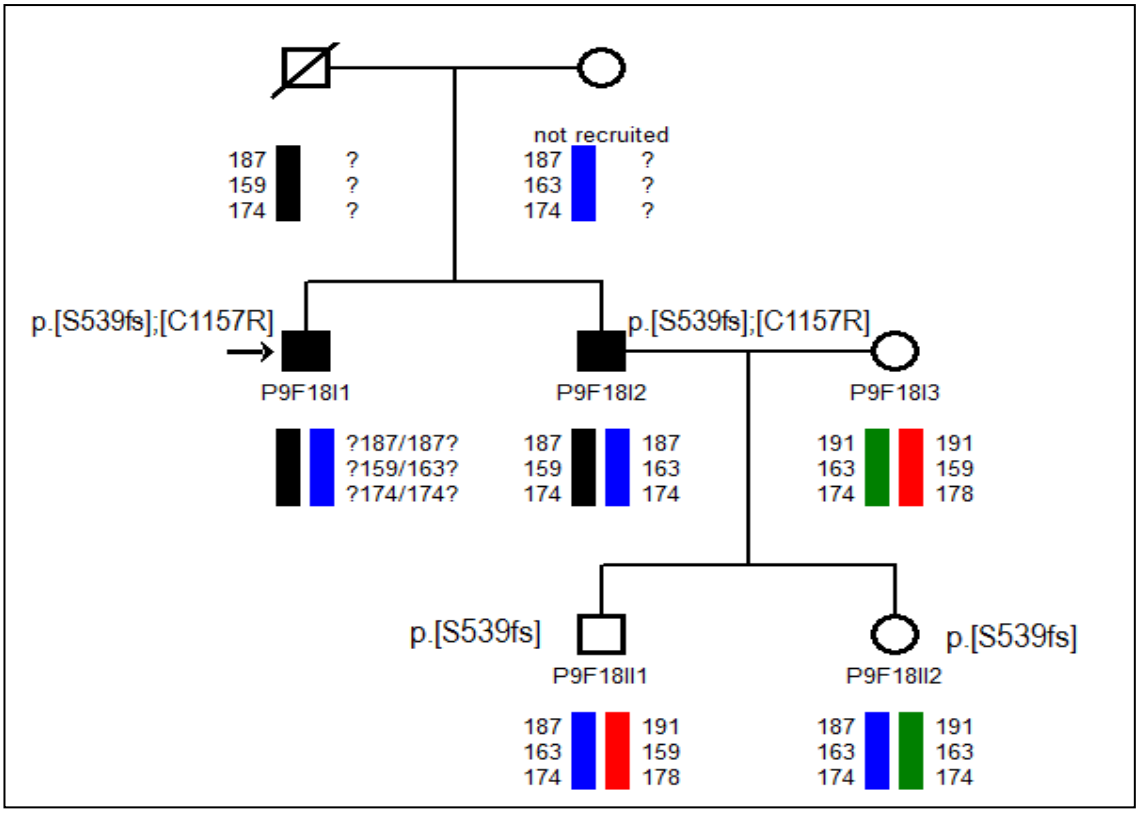

Figure 3.13 Pedigree of family P9F18 showing linkage analysis and mutation results. The linkage analysis marker order was as previously described and is shown underneath each member. Females are indicated by circles and males by squares. Filled symbols represent AFM and the black arrow indicates the index case. Both mutant alleles [187]-[159]-[174] associated with p.C1157R and [187]-[163]-[174] associated with p.S539fs are shown in the AFM while mutant allele [187]-[163]-[174] associated with p.S539fs is shown in UFM.

Table 3.8 Phenotypic data for family P9F18

Family member	Status	BS	VWF:Ag IU/dL	VWF:RCo IU/dL	FVIII:C IU/dL	VWF:FVIIIB	Multimer profile	ABO genotype
I:1	IC	9	<3	<3	<3	NI*	Abnormal	O/O
I:2	AFM	10	3	3	3	NI*	Abnormal	O/B
I:3	UFM	-2	48	45	41	NT†	Normal	O/A2
II:1	UFM	2	60	69	74	NT†	Normal	A2/B
II:2	UFM	0	53	50	75	NT†	Normal	O/B

* Not interpretable † Not tested

3.6.2.2. p.C1157 protein predictions and multiple species alignment

Three different *in silico* tools described in section 2.2.5 (SIFT, PolyPhen2 and Align GVGD (Table 3.9) were used to predict the effect of amino acid substitutions on protein function. SIFT and PolyPhen2 tools predicted that the p.C1157R amino acid variant was probably damaging with 0 and 1 scores respectively. Also the Align-GVGD tool had the same deleterious effect and suggested that the p.C1157R variant is most likely damaging.

Table 3.9 Prediction methods used for amino acid substitution with prediction score and range of scores for each tool

Prediction tool	Range of possible scores	Prediction score
SIFT	0-1	0 (damaging)
PolyPhen2	0 to positive number	1 (Probably damaging)
Align GVGD	C0-C65	Class C65, GD 179.53 (most likely damaging) GV 0.00

Evolutionary conservation of the cysteine located at position 1157 was undertaken through alignment with the VWF amino acid protein sequence of twelve different species using MULTALIN tool as described in section 2.2.8. As a result, p.C1157 was found to be completely conserved in VWF in all aligned species (Figure 3.14). This result indicated that this highly conserved residue was potentially important for VWF protein structure and function.

Figure 3.14: Schematic representation of the evolutionary conservation of p.C1157 across thirteen orthologues which indicates complete conversation. Residue p.C1157 is highlighted by a black rectangle (http://mutalin.toulouse.inra.fr/mutalin/).

3.6.3. Mutation analysis in family P10F5

During analysis and sequencing of *VWF* exon/intron boundaries in all 18 IC, twenty eight variants were detected in IC P10F5II:2. Among all, one known silent change (Hampshire et al., 2010, Corrales et al., 2012) in addition to 27 previously known heterozygous polymorphisms were detected (Table 3.10). This silent heterozygous point mutation c.4146G>T was identified in exon 28 in the IC (II:2) which was predicted to result in silent change p.L1382= (Figure 3.15). This silent mutation located in the A1 domain has been reported previously in 2 patients who had two additional mutations in the heterozygous state (Corrales et al., 2012). The identified mutation was analysed in all family members including one AFM and two UFM using bi-directional DNA sequencing. The c.4146G>T was found in the AFM (I:1) and was absent from the UFM I:2 and II:1. No other change was detected in this IC previously.

Table 3.10: List of 27 known heterozygous SNP in IC P10F5II:2

SNP reference number	Nucleotide change	Amino acid change	Effect on protein expression	SNP location Exon/Intron
rs2286608	c.1-64C>T		No	Intron 1
rs7980045	c.657+11A>C		No	Intron 6
rs1800378	c.1451A>G	p.H484R	No	Exon 13
rs7312411	c.1548T>C	p.Y516=	No	Exon 14
rs216293	c.2282-42C>A		No	Intron 17
rs1063856	c.2365A>G	p.T789A	Yes*	Exon 18
rs1063857	c.2385T>C	p.Y795=	Yes†	Exon 18
rs216325	c.2546+25C>T		No	Intron 19
rs216321	c.2555A>G	p.Q852R	No	Exon 20
rs1800380	c.2880G>A	p.R960=	No	Exon 22
rs34877178	c.2968-53G>A		No	Intron 22
rs3858686	c.2968-125C>T		No	Intron 22
rs73051263	c.3222+31C>T		No	Intron 24
rs56121649	c.3109-90G>C		No	Intron 23
rs56068059	c.3109-128G>T		No	Intron 23
rs4008538	c.3414C>T	p.N1138=	No	Exon 26
rs216312	c.3675-75A>G		No	Intron 27
rs216311	c.4141A>G	p.T1381A	No	Exon 28
rs216310	c.4641T>C	p.T1547=	No	Exon 28
rs216305	c.5665-118G>A		No	Intron 33
rs17491334	c.6064-71C>T		No	Intron 35
rs177702	c.6799-14C>T		No	Intron 38
rs10849371	c.6846A>G	p.T2282=	No	Exon 39
rs55867239	c.6977-22C>T		No	Intron 40
rs216867	c.7239T>C	p.T2413=	No	Exon 42
rs2270239	c.7549-59A>C		No	Intron 44
rs2270151	c.8155+50C>T		No	Intron 50

*Associated with alteration in VWF levels and in perfect linkage disequilibrium with SNP, † associated with alteration in VWF levels in CHARGE study (Smith et al., 2010).

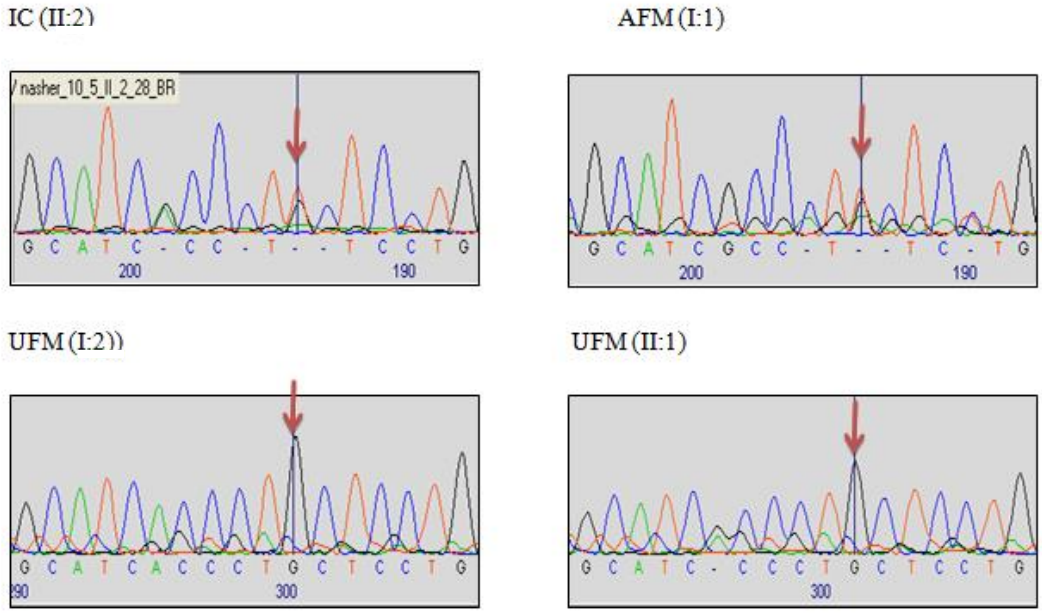

Figure 3.15 Heterozygous c.4146G>T point mutation in P10F5 family

Sequence analysis results of family P10F5**.** The nucleotide c.4146G>T is marked by a red arrow. This candidate mutation was found in the IC and the AFM and was absent from the UFM.

3.6.3.1. Linkage analysis and mutation study in family P10F5

This small family had only four members, two affected and two unaffected individuals (Figure 3.16). The phenotypic data from the IC (II:1) and AFM (I:1) who both carried the c.4146G>T mutation indicated a mild increase in BS (4-6), moderate reduction of VWF:Ag in the plasma (48 and 54 IU/dl) respectively, moderate reduction of VWF:RCo (41 and 61 IU/dl) and normal plasma level of FVIII:C values. All family members had an O/O blood group genotype (Table 3.11). The linkage study revealed a common haplotype [193]-[155]-[174] (GT repeat, STRIII and STRII) respectively to be associated with c.4146G>T which was identified in the IC and the AFM (black allele), while absent in the UFM. The mutant allele co-segregated with the low level of VWF:Ag and VWF:RCo and was in accordance with an autosomal dominant pattern of inheritance. In summary, this family showed reduced VWF levels in analysis of phenotypic data and O/O blood group genotype in the IC and AFM. Although this family is small, it showed co-segregation of affected haplotype with the disease.

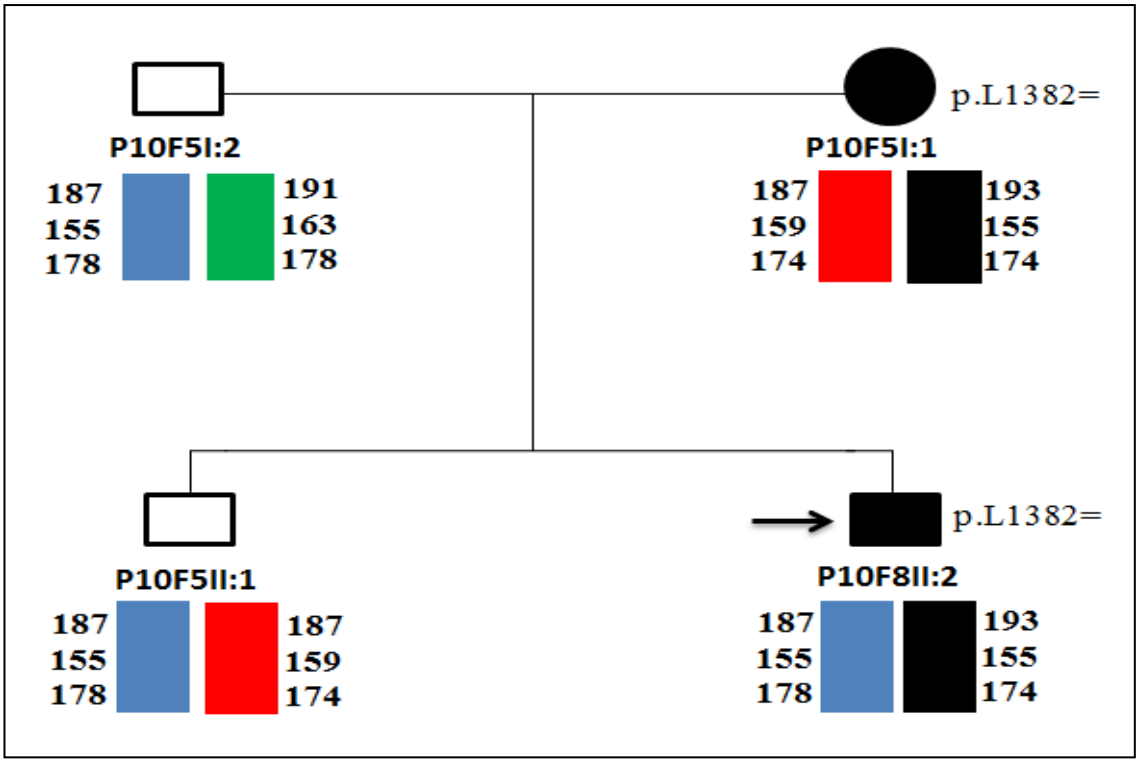

Figure 3.16 Pedigree of family P10F5 showing linkage analysis and mutation results. The linkage analysis marker order was as previously described and is shown underneath each member. Females are indicated by circles and males by squares. Filled symbols represent AFM and the black arrow indicates the IC. The mutant allele [193]-[155]-[174] was present in the IC and AFM.

Table 3.11 Phenotypic data for family P10F5

Family member	Status	BS	VWF:Ag IU/dL	VWF:RCO IU/dL	FVIII:C IU/dL	Multimer pattern	ABO genotype
I:1	AFM	6	54	61	87	Normal	O/O
I:2	UFM	-1	95	78	144	Normal	O/O
II:1	UFM	3	78	53	90	Normal	O/O
II:2	IC	4	48	41	84	Normal	O/O

3.6.3.2. *In silico* splice-site prediction

In order to predict if there was any possible influence of the c.4146 G>T variant on mRNA splicing, four online *in silico* prediction tools; MaxEntScan: scorsplice (MES), splice site prediction by neural network, human splice finder (HSF) and NetGene2 splice prediction were used (Section 2.2.6). The results were analysed after comparing the wild-type and mutant sequences and predicted no difference between wild-type and mutant and no effect on donor and acceptor splice site sequences. Moreover, splicing is known to be regulated by splice enhancer and silencer sequences which can occur within both coding and non-coding sequences. In order to predict the potential effect of the silent change (c.4146G>T) on splicing enhancer and silencer elements, three bioinformatics online *in silico* prediction tools (ESE, HSF and RESCUE-ESE) were used. As a result, these tools showed a significant difference between the wild-type and mutant sequences and identified three variations that were predicted to lead to disruption of enhancer sequences in addition to creation of three silencer sequence (Table 3.12). Therefore, the c.4146G>T change may disrupt the exonic splicing enhancer (ESE) sites and alter the splicing mechanism. Also, the graphical codon usage analyser (GCUA) tool which compares the frequency of use of two different triplet codons encoding the same amino acid was used (http://gcua.schoedl.de/) as some codons are recognised more efficiently by transfer RNA (tRNA) compare to others which can alter the efficiency and accuracy of translation (Hershberg and Petrov, 2008). GCUA compares the frequency usage between the wild-type (CTG) and mutant (CTT) codons which both encode leucine. As a result, the mutant codon generates a 68% lower frequency than the wild-type. The wild-type codon (CTG) is more frequently used than mutant codon (CTT) which may affect the rate of translation and protein folding and therefore alter the protein structure and function (Figure 3.17).

Table 3.12 *In silico* prediction of effect of c.4146G>T in splice regulatory elements

cDNA position	WT motif	Enhancer motif value (0-100) WT score	Enhancer motif value (0-100) mutant score
c.4142	ACCCTGCT	34.22	0 (site broken)
c.4147	GCTCCTGA	27.81	0 (site broken)
c.4143	CCCTGCTC	39.28	0 (site broken)

cDNA position	WT motif	Silencer motif WT sequence	Silencer motif mutant sequence
c.4144	CCCTGC		CCTTCT (new site)
c.4145	CCCTGC		CTTCTC (new site)
c.4146	CCCTGC		TTCTCC (new site)

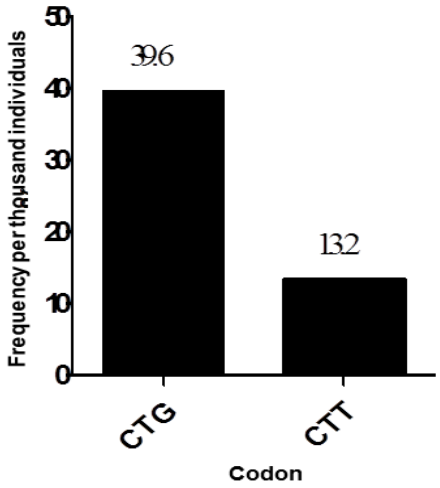

Figure 3.17 The relative frequency values of normal codon CTG and mutant codon CTT that all encode leucine in *Homo sapiens*. The frequency of CTT mutant codon used by leucine is 68% less than wild-type CTG triplet codon (Nakamura et al., 2000).

3.6.4. Splice mutation c.1432+1G>T and linkage analysis in P10F8 family

During analysis of the entire *VWF* coding sequence plus exon/intron boundaries of all 18 IC using PCR amplification followed by direct sequencing, twenty four variants were detected in P10F8II1 including 22 known heterozygous polymorphisms and two candidate mutations (Table 3.13). One novel intronic change was identified at the donor splice site of intron 12 c.1432+1G>T in the IC P10F8II:1 (Figure 3.18). This change was detected in the IC II:1 who previously had a known 2N mutation in exon 19 (c.2446C>T) which is predicted to result in p.R816W, while the AFM (II:2) showed only the intronic change c.1432+1G>T and the previously identified mutation p.R816W was not observed in the unaffected mother (I:2).

The phenotypic data in the IC and AFM confirmed a reduced level of VWF:Ag in plasma 49 and 47 IU/dl respectively (Figure 3.19). BS was increased (10) in the IC who had a reduced value of FVIII:C of 14 IU/dl (Table 3.14). However, analysis of the phenotypic and genotypic data from the P10F8 family suggested that the samples had potentially been incorrectly labelled in the original EU study. By examining the previously described marker data from linkage analysis, a non-linkage pattern was present in this family. Although the IC II:1 and the AFM II:2 had the same mutation and common haplotype, the maternal allele was absent from both children, providing further evidence for a sample error (Figure 3.19). These findings led to the exclusion of this family from a previously analysis of linkage of *VWF* to VWD (Eikenboom et al., 2006).

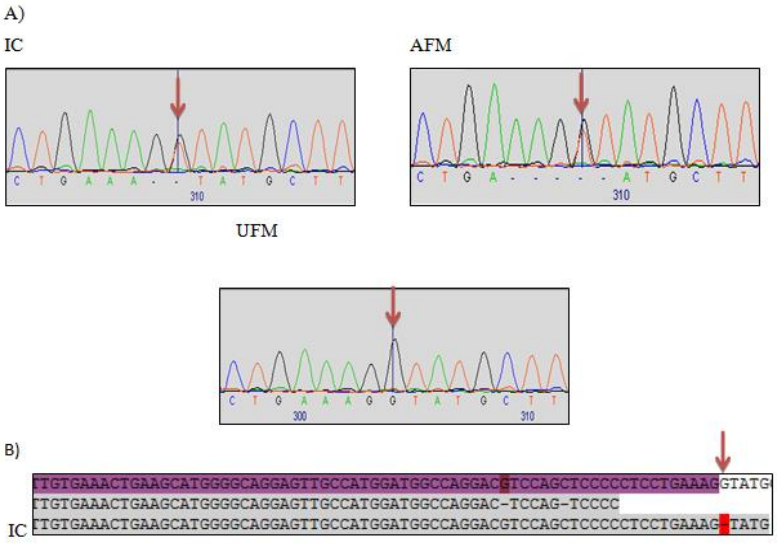

Figure 3.18 A) Sequence chromatogram analysis results of family P10F8 showing the heterozygous c.1432+1G>T substitution. This mutation was found in the IC and the AFM and absent in the UFM. **B)** Partial sequence of intron 12. The red arrow indicates the sequence alteration between the WT and IC showing the G>T change.

Table 3.13: List of 22 known heterozygous SNP in IC P10F8II:1

SNP reference number	Nucleotide change	Amino acid change	Effect on protein expression	SNP location Exon/Intron
rs2286608	c.1-64C>T		No	Intron 1
rs1800378	c.1451A>G		No	Exon 13
rs61908661	c.1945+24C>T		No	Intron 15
rs1063856	c.2365A>G	p.T789A	Yes*	Exon 18
rs1063857	c.2385T>C	p.Y795=	Yes†	Exon 18
rs216321	c.2555A>G	p.Q852R	No	Exon 20
rs1800380	c.2880G>A	p.R960=	No	Exon 22
rs34877178	c.2968-53G>A		No	Intron 22
rs3858686	c.2968-125C>T		No	Intron 22
rs56121649	c.3109-90G>C		No	Intron 23
rs73051263	c.3222+31C>T		No	Intron 24
rs177702	c.6799-14C>T		No	Intron 38
rs10849371	c.6846A>G	p.T2282=	No	Exon 39
rs55867239	c.6977-22C>T		No	Intron 40
rs216867	c.7239T>C	p.T2413=	No	Exon 42
rs216868	c.7082-7C>T		No	Intron 42
rs2286646	c.8115+66T>C		No	Intron 49
rs7962217	c.8113G>A	p.G2705R	No	Exon49
rs2270152	c.8116-20A>C		No	Intron 50
rs2270151	c.8155+50C>T		No	Intron 50
rs2362483	c.8253+32T>C		No	Intron 51
rs7976955	c.8442+204C>T		No	3' untranslated region

*Associated with alteration in VWF levels and in perfect linkage disequilibrium with SNP, † associated with alteration in VWF levels in CHARGE study (Smith et al., 2010).

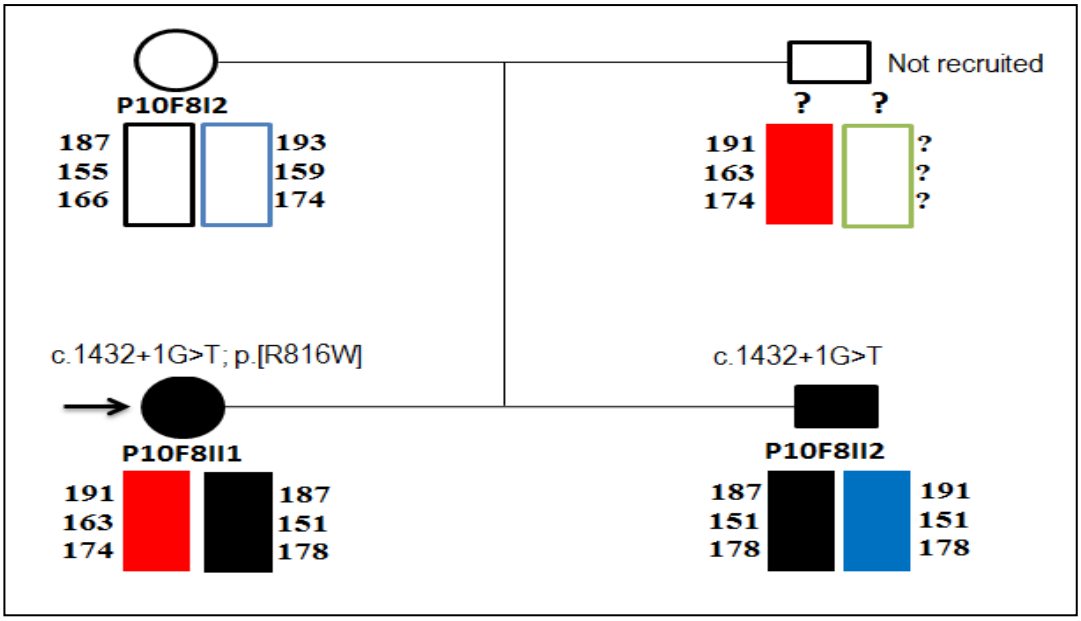

Figure 3.19 Initial pedigree of family P10F8 showing linkage analysis and mutation results. The linkage analysis marker order was as previously described and is shown underneath each member. Females are indicated by circles and males by squares. Filled symbols represent AFM and the black arrow indicates the index case. No maternal allele was present in either of the children II:1 and II:2.

Table 3.14 Initial phenotypic data for family P10F8

Family member	Status	BS	VWF:Ag IU/dl	VWF:RCo IU/dl	FVIII:C IU/dl	VWF:FVIIIB	Multimer profile	Blood group
I:2	UFM	4	145	141	120	Normal	Normal	O/A2
II:1	IC	10	49	52	14	2N	Normal	O/O
II:2	AFM	-1	47	67	113	Normal	Normal	O/O

Forward and reverse primers used in the original study to amplify *VWF* exon 12 were checked for the presence of SNP underneath their annealing sites using the SNP Check tool. As a result, two SNP were detected in the forward primer only, located in the middle and at the 3' end of the primer sequence (Table 3.15).

Table 3.15 Identified SNP underlying the primer annealing site for the *VWF* exon 12 primer

Forward primer (Exon-12)	Reverse primer (Exon-12)
TTGAGGCCTTT**C**TCTGATTA**A**	GGCCAGGGTTGAGAAGGA

***Nucleotides highlighted in red represent reported SNP**

3.6.4.1. Review of linkage analysis and mutation in P10F8 family

In order to determine the linkage of mutations within this family, 6 SNP markers were assessed to establish whether there was likely to have been a sample mix up through comparison of the mutations present within the family and also the phenotype of individuals within the family. These new SNP markers are listed in table 3.16. However, in an attempt to find the reason of the non-linkage pattern in this family, the genotypic and phenotypic data of the mother I:2 (UFM) and II:2 (AFM) were swapped. As a result of this exchange, the mother I:2 became the AFM, while the healthy son (II:2) became the UFM. After this modification, linkage study results demonstrated a common haplotype [CTGTGA] which was associated with the c.1432+1G>T change observed in the IC which apparently originated from the mother (I:2) (Figure 3.20). Also, the type 2N mutation p.R816W which affects VWF binding to FVIII was found only in the IC (daughter) and likely originated in the father who not recruited. The presence of the p.R816W mutation in the IC explains the reduction of FVIII:C level in the IC and the normal levels in the son and the mother who do not carry the p.R816W variant.

With the pedigree modifications, the IC who was compound heterozygous for two mutations revealed a high bleeding score of 10 in addition to low levels of VWF:Ag, VWF:RCo and FVIII:C in plasma, 49, 52 and 14 IU/dl respectively, while the AFM (I:2) who had only the intronic change c.1432+1G>T revealed a reduction in VWF:Ag level of 47 IU/dl and normal values of VWF:RCo and FVIII:C. Both IC and AFM had an O/O blood group genotype (Table 3.17).

In summary, with using the new SNP markers and swapping the genotypic and phenotypic data between two family members with taking into account that initial categorisation of BS in AFM and UFM was likely correct, more logical results were obtained. The affected members of this family showed a moderate reduction of phenotypic data. However, the mutant allele [CTGTGA] in the IC and AFM co-segregated with a reduced level of VWF and was accordant with a haploinsufficient allele.

Table 3.16 The new SNP markers used for linkage analysis showing SNP number and its location

Rs No	Nucleotide substitution	SNP location
rs216883	c.6799-2826C>T	Intron- 38
rs216856	c.7288-839T>C	Intron- 42
rs11063965	c.7548+170G>A	Intron- 44
rs4764478	c.7729+252T>A	Intron- 45
rs2363309	c.7887+5813G>A	Intron- 47
rs10849363	c.7888-3597A>G	Intron- 47

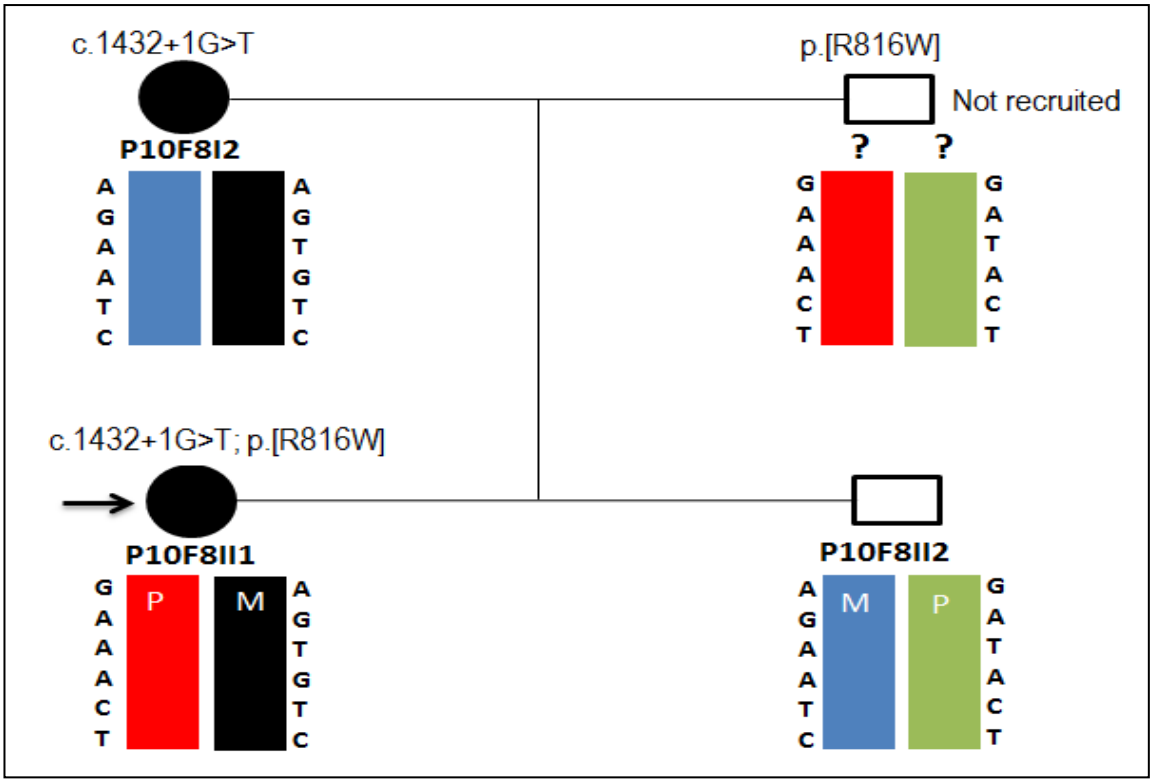

Figure 3.20 Revised pedigree of family P10F8 showing linkage analysis and mutation results using new SNP markers. The linkage analysis markers are shown underneath each member. Females are indicated by circles and males by squares. Filled symbols represent AFM and the black arrow indicates the index case. The mutant black allele [AGTGTC] associated with c.1432+1G>T was observed in the IC and AFM and mutant red allele [GAAACT] associated with p.R816W.

Table 3.17 Phenotypic data for family P10F8 after modification

Family member	Status	BS	VWF:Ag IU/dl	VWF:RCo IU/dl	FVIII:C IU/dl	VWF:FVIIIB	Multimer pattern	Blood group
I:2	AFM	4	47	67	113	Normal	Normal	O/O
II:1	IC	10	49	52	14	2N	Normal	O/O
II:2	UFM	-1	145	141	120	Normal	Normal	O/A2

3.6.4.2. *In silico* splice site prediction

In order to examine the possible influence of the variant located at *VWF* sequence c.1432+1G>T donor splice site on splicing mechanisms, several *in silico* online prediction tools were used (Section 2.2.6). The results from each prediction tool of wild type and mutant sequences were compared with each other. The results indicated that c.1432+1G>T candidate mutation most likely resulted in disruption of the splice donor-site of exon 12. Results achieved from the neural network, NetGene2 and MES predicted that this splice variant alters the consensus splice donor site sequence and likely results in the skipping for exon 12 after comparing the wild-type and mutant sequences (Table 3.18). Human Splice Finder suggested that this change may abolish the wild type exon 12 donor site but also create a new exon 12 donor site which would result in retention of 1bp of intron 12 and result in a frameshift. This splice site change could result in skipping of exon 12 which further causes loss of all 139 nucleotides of exon 12 and produces a stop codon 9 amino acids downstream of the mutation (p.C432Vfs*9). However, review of these prediction tools suggests that a consensus of at least three tools should be used to decide a likely outcome.

Table 3.18 *In silico* prediction tools to determine the effects of c.1432+1G>T

Splice site prediction tool	Donor splice site score WT allele c.1432+1G	Range of score	Donor splice site score mutant allele c.1432+1G>T
Neural network	0.96	0-1	0 (splice site loss)
NetGene2	0.95	0-1	0 (splice site loss)
MES	9.55	0-10	1.05 (splice site loss)
HSF	88.0	0-100	61.23 (possible splice site loss)

3.6.5. Confirmation of the presence of mutations previously identified

During analysis of DNA samples of all 18 IC, 4 additional nucleotide changes that were previously identified were detected in two IC. They included c.7630C>T in exon 45 in PF2II:2 family, which is predicted to result in p.Q2544*.

3.6.5.1. Mutation analysis in family P9F14

The other three changes were all found in IC P9F14III:1 and included one splice change located in the donor splice site of intron 13, c.1533+1G>T and two missense changes, c.2771G>A in exon 21 and c.5779T>C in exon 34 which are predicted to result in the p.R924Q and p.C1927R respectively. The identified mutations in the IC (II:2) were analysed in all family members including two AFM and three UFM. The c.1533+1G>T was found in the UFM (I:1) and was

absent from the AFM (I:2), (III:1) and from both UFM (II:1) and (II:3). The other two changes c.2771G>A and c.5779T>C were detected in the AFM (1:2 and III:1) in addition to the UFM (II:3) and absent from UFM (I:1) and (II:1) (Figure 3.21).

3.6.5.1. Linkage analysis and mutation study in family P9F14

This family included six members, three AFM and three UFM (Figure 3.21). The IC (II:2) carried three mutations; a splice change c.1533+1G>T, on one allele and two other mutations p.[R924Q;C1927R], on the other allele and presented with undetectable levels of VWF:Ag and VWF:RCo (<3 IU/dL), FVIII (7 IU/dL), a high BS (18), O/A genotype and absent multimers (Table 3.19). The splice change originated from the unaffected father and p.[R924Q;C1927R] on the same allele originated from the affected mother. The p.[R924Q;C1927R] were found in the two AFM (I:2 and III:1). The phenotypic data of the AFM (III:1) who had O/O blood group genotype indicated markedly reduced of VWF:Ag (19 IU/dL), VWF:RCo (18 IU/dL), FVIII:C (25 IU/dL) and abnormal multimers (smeary pattern) while the levels of VWF:Ag, VWF:RCo and FVIII:C in the AFM (I:2) who had A/A blood group genotype was moderately reduced to 57, 58 and 63 IU/dL respectively in addition to normal multimers. Also, p.[R924Q;C1927R] were found in UFM (II:3) who had a similar phenotype to AFM (1:2), abnormal multimer and blood group genotype A/B (Table 3.19). Linkage analysis results indicated that a shared haplotype (red allele) [191]-[155]-[174] (GT repeat, STRIII and STRII) respectively which was associated with the splice mutation c.1533+1G>T was present in the IC and unaffected father, while the IC (II:2) AFM (I:2), (III:1) and UFM (II:3) shared an additional haplotype (black allele) [187]-[159]-[182] which incompletely co-segregated with the level of VWF and FVIII.

In summary, this linkage study revealed a non-linkage pattern and the *VWF* mutation inheritance pattern was not completely certain in this family. Although, the IC, the AFM (I:2 and III:1) and UFM (II:3) had the same mutations and common haplotype, they presented with variable phenotypes and this may due to incomplete penetrance and age variation.

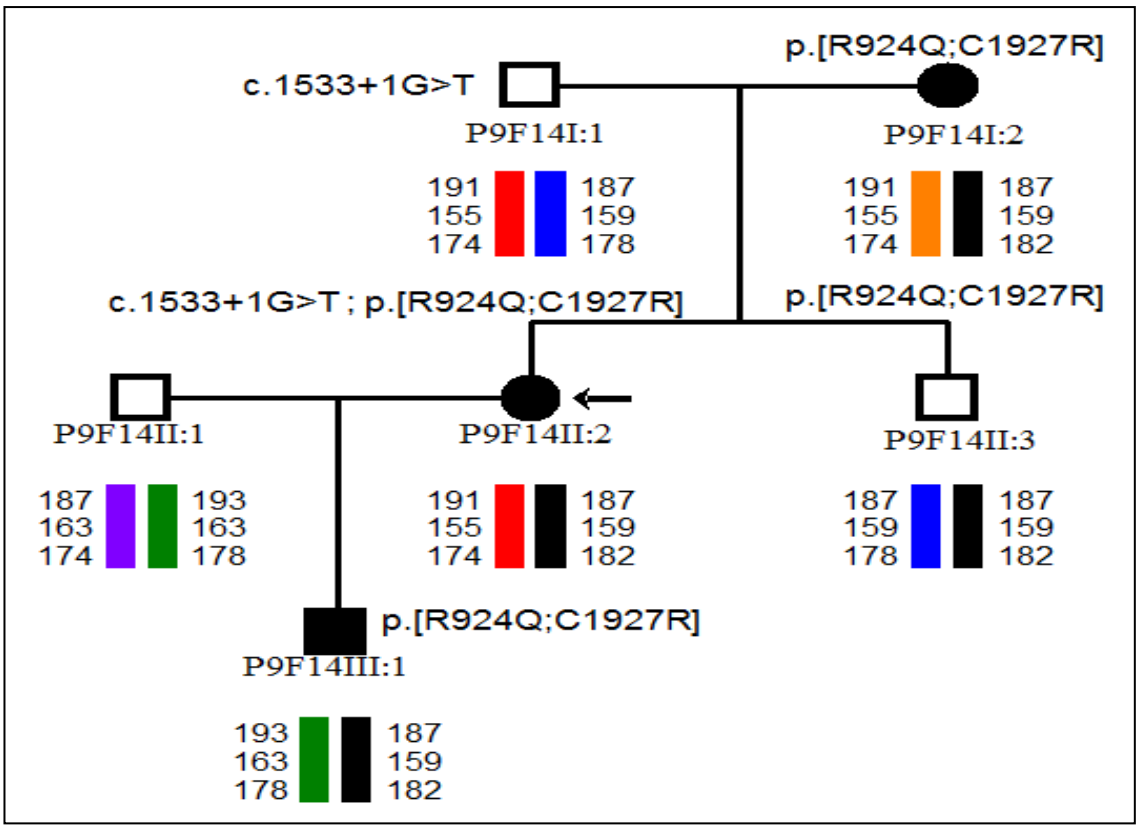

Figure 3.21 Pedigree of family P9F14 showing linkage analysis and mutation results. The linkage analysis marker order was as previously described and is shown underneath each member. Females are indicated by circles and males by squares. Filled symbols represent AFM and the black arrow indicates the index case.

Table 3.19 Phenotypic data for family P9F14

Family member	Status	BS	VWF:Ag IU/dL	VWF:RCo IU/dL	FVIII:C IU/dL	CB/Ag	Multimer pattern	ABO genotype
I:1	UFM	0	88	79	82	NT	Normal	O/O
I:2	AFM	4	57	58	63	NT	Normal	A/A
II:1	UFM	0	150	215	88	NT	Normal	O/A
II:2	IC	18	3	3	7	0.33	Abnormal	O/A
II:3	UFM	5	57	80	50	NT	Abnormal	A/B
III:1	AFM	1	19	18	25	0.63	Abnormal	O/O

3.6.5.2. *In silico* predictions

In silico tools described in section 2.2.5 (SIFT, PolyPhen2 and Align GVGD) were used to predict the effect of p.C1927R on protein function. As a result, SIFT and polyPhen2 tools predicted that the p.C1927R amino acid variant was probably damaging with 0 and 1 scores respectively. Also the Align-GVGD tool predicted the same deleterious effect and suggested that the p.C1927R variant is most likely damaging. Furthermore, the human VWF amino acid sequence was aligned to protein sequences of twelve different species using the MULTALIN tool as described in section 2.2.8. As a result, p.C1927 was shown to be a highly conserved residue and is potentially important for VWF protein structure and function (Figure 3.22).

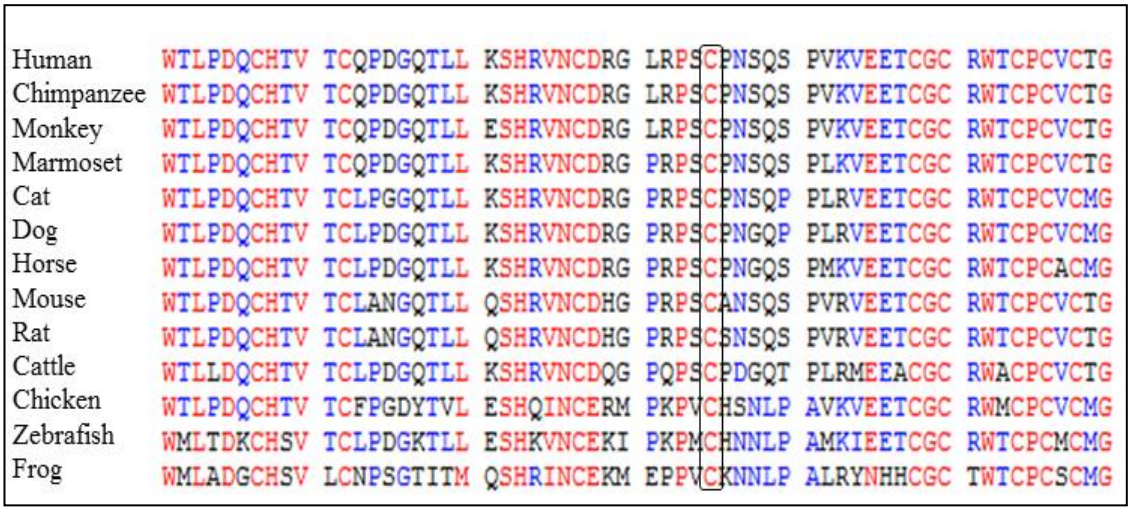

Figure 3.22: Schematic representation of the evolutionary conservation of p.C1927 across thirteen orthologues. Residue p.C1927 is highlighted by a black rectangle (http://mutalin.toulouse.inra.fr/mutalin/).

The study conducted by Hickson *et al* (2010) predicted no effect of the p.R924Q variant on VWF function or on the intron 20 acceptor/intron 21 donor splice sites (Hickson et al., 2010). Also, results obtained from the neural network, MES and HSF tools predicted that the splice variant c.1533+1G>T alters the consensus splice donor site sequence and a skip of exon 13 is very likely after comparing the wild-type and mutant sequences (Table 3.20).

Table 3.20 *In silico* prediction tools to determine the effects of c.1533+1G>T

Splice site prediction tool	Donor splice site score WT allele c.1432+1G	Range of score	Donor splice site score mutant allele c.1533+1G>T
Neural network	0.98	0-1	0 (splice site loss)
MES	10.3	0-10	1.67 (splice site loss)
HSF	90.7	0-100	63.8 (possible splice site loss)

For the remaining 14 IC, no new mutation(s) were identified, but heterozygous SNP were detected in each. The least SNP number (11) were present in IC P7F8I:2, while IC P10F5II:1 showed the highest number of SNP (27) (Appendix Table 13).

Also, 8 IC out of 18 IC were investigated for the presence of CNV and as a result, none of them showed any large deletion or insertion (Appendix Table 14) (Cartwright et al., 2013).

3.7. Discussion

This study aimed to re-analyse and re-sequence *VWF* among 18 IC historically diagnosed with type 1 VWD, where point mutations were most likely to have been missed during the original MCMDM-1VWD study. One of the hypotheses proposed that mutations in *VWF* may have been missed in a proportion of type 1 VWD patients who were analysed in the original study due to either lack of sensitivity of the detection methods used or due to presence of SNP underneath primer annealing sites (Goodeve et al., 2007). In the original study, several mutation detection methods have been used to analyse *VWF* exonic regions. These methods included SSCP, CSGE, DHPLC and direct DNA sequencing (Zhang et al., 1994, Abuzenadeh, 1998, Schneppenheim et al., 2000, Goodeve et al., 2003), but these mutation detection methods were not sufficiently sensitive to identify all point mutations that may be present in the EU cohort. These methods range in their degree of sensitivity between 75% to 100% based on the DNA size and sequence context (Markoof et al., 1998, Whittock et al., 1999, Eng et al., 2001).

3.7.1. Polymorphism screening and mono-allelic amplification

It was proposed that mutation within the 30% of IC from the MCMDM-1VWD study who showed no identified mutation could possibly have been missed due to limitations of sensitivity of mutation scanning methods that were previously used, due to presence of mono-allelic amplification or due to a large deletion or duplication that would not be detected by the methods used. In addition the presence of SNP within primer sequences especially at the 3' end of the primer annealing sites can prevent the effective annealing of the primers to the template DNA and thereby lead to reduced or absent amplification of the target fragment. To avoid mono-allelic amplification, historical PCR primers used in the MCMDM-1VWD cohort were checked and screened for the presence of SNP within primer annealing sites. Primers found to have SNP within their annealing sites were re-designed. In this study, a significant number of *VWF* primers (20 primer pairs) were redesigned according to the criteria described in section 2.2.1. They were re-designed either due to presence of SNP within the primer sequence or other reasons such as some primers were too close to the target exon, due to poor amplification or due to presence of errors in primers sequences (Appendix 10). However, in the *VWFP* region, it was not always possible to design primers following the required criteria, due to the constraint of the small number of possible positions to design primers in this region (Figure 3.2). As a result, the last nucleotide of forward primers of exon 30 and 31 and the reverse primer for exon 27 were closer to the target exon than 50 nucleotides. The reason for the constraint was that the presence of SNP within gene-pseudogene mismatched areas prevented design of primers in these regions due to the high sequence homology between the two regions. Also, in order to maximise the specificity of *VWF* amplification, to prevent the amplification of the pseudogene and to de-

stabilise binding of primer to *VWFP*, mismatches between *VWF* and *VWFP* were introduced to forward and reverse sequence of primers of several *VWF* exon (Section 3.2).
These newly optimised re-designed primers and previously used primers that showed no SNP within their sequences were used to successfully amplify and sequence all 52 *VWF* coding exons and flanking intronic regions in 18 selected IC that showed no genetic alteration in the original study (MCMDM-1VWD) or mutation that did not fully explain their VWD. Moreover, these newly designed primers were used to confirm that no further point mutation(s) had been missed because of mono-allelic amplification. In order to avoid the mono-allelic amplification during PCR, primers should regularly be checked for the presence of SNP within their annealing sites and re-designed when necessary.

3.7.2. Hypothesis 1; detection of missed mutation in MCMDM-1VWD study

Throughout this study, four mutations, three of which were novel, were identified in four families. Screening for potential missed mutations in *VWF* within 18 IC revealed two missense mutations in exon 26 and 39, one silent mutation in exon 28 and one splice mutation in intron 12 plus three previously identified mutations (Table 3.2). No new SNP were identified, but 57 different known SNP in different intronic and exonic *VWF* regions were found in all studied 18 IC (Appendix 13).

One novel heterozygous mutation was identified in the exonic region of exon 39 (c.6811T>G) in P5F1 II:3 IC predicted to result in p.W2271G . The French family consisted of four members, one IC, two AFM and one UFM. In addition to the index case, the two AFM were heterozygous for this mutation whereas the UFM was negative. Also during mutational analysis of this IC, no new SNP were identified (Appendix 13).
The p.W2271G missense mutation which is located in the D4 assembly has not been identified previously. This heterozygous mutation was likely to be responsible for the abnormal phenotype observed in the IC and AFM. The level of plasma VWF:Ag was markedly decreased in IC and AFM ranging from 37 to 38 IU/dL (normal range 48-167 IU/dL) and levels of VWF:RCo ranging between 32 to 43 IU/dL (normal range 47-194 IU/dL). Moreover, the levels of FVIII:C were significantly reduced in the IC (28 IU/dL) and AFM P5F1II2 (34 IU/dL) although their bleeding scores were normal ranging between -1 to 2, while the other AFM P5F1I:2 who had a high bleeding score of 7 showed a normal level of FVIII:C (85 IU/dL) (normal range 57-198 IU/dL). A second mutation c.2561G>A predicted to result in p.R854Q that affects the binding of FVIII to VWF was present in the two children, IC II:3 plus AFM II:2, but was absent from their mother AFM I:2. The presence of p.R854Q is sufficient to explain reduced FVIII:C levels in the children and normal levels in the mother who does not carry this mutation. Moreover, the bleeding score is affected by age due to an increased chance of haemostatic challenges

especially post-delivery, post dental and surgical procedures which can explain the higher BS in the mother and lower BS in children due to reduced exposure to bleeding challenges (Montgomery, 2005). These mutations may possibly explain the significantly low levels of plasma VWF and FVIII:C in the index case and affected members. VWF level is influenced by type of ABO blood group. Souto *et al* (2000) reported that the mean VWF levels in the normal population having blood group with one O allele were 25-30% lower than those having no O allele. Also, the average level of VWF in individuals with one O allele (AO) was 2-5% lower than the average level in individuals with no O allele, that is the (AA) genotype (Souto et al., 2000). All family members were phenotypically blood group A, but presence of one O allele (AO) with presence of mutation may contribute to slight reduction of VWF level. The multimer analysis of all family members revealed a normal pattern. The p.W2271G mutation was fully penetrant and appears sufficient to cause VWD in this family. The linkage study in this family showed an autosomal dominant inheritance pattern with a common mutant allele [189]-[151]-[174] (GT repeat, STRIII and STRII) in the IC and affected members which co-segregated with the disease phenotype (Figure 3.10).

To determine whether the p.W2271G substitution could be responsible for the reduction in VWF levels and to evaluate the mechanism underlying this mutation, *in silico* prediction was performed. Glycine is a simple amino acid and is the smallest of the 20 amino acids having only two hydrogen atoms, while tryptophan is larger and has a complex carbon ring structure. The replacement of the largest amino acid tryptophan that has a very large steric hindrance with the smallest one glycine that has very less steric hindrance at protein position 2271 is likely to cause conformational changes and thereby disturb protein expression and structure. As a result, this mutation is predicted to be probably damaging and thereby is likely to affect VWF structure or function. In type 1 VWD, mutations have been reported to increase the rate of VWF clearance, reduce secretion or slightly increase the susceptibility of VWF to ADAMTS13 and cleavage. This candidate mutation located in the D4 assembly is most likely increase the intracellular retention and thereby reduce VWF secretion as previously described (Eikenboom et al., 2009). Mutations in the D4 assembly may lead to production of mis-folded protein which subsequently binds to a chaperone protein in the ER. Chaperones cause accumulation of mis-folded mutant protein in the ER and prevent their transport to the Golgi and facilitate protein degradation by the proteosome in the cytosol (Brodsky and McCracken, 1997). The substitution of tryptophan to glycine may cause the partial quantitative deficiency of VWF due to accumulation and retention of protein subunits within the ER resulting in reduction of VWF secretion. Several mutations (p.L2207P, p.C2257S and p.R2287W) located in the D4 assembly were identified in patients with type 1 VWD. These patients presented with high BS, moderate reduction in the levels of VWF:Ag ranging between 26-47 IU/dL, moderate reduction of VWF:RCo ranging

between 19-49 IU/dL and normal multimers (Goodeve et al., 2007, Eikenboom et al., 2009) which are similar to phenotypic data observed in AFM with p.W2271G. An *in vitro* expression study of *VWF* mutations located in the D4 assembly that identified in patients with type 1 VWD were shown to impair the VWF secretion due to marked intracellular retention as the pathogenic mechanism and a normal multimer pattern (Eikenboom et al., 2009). Also, the expression of missense mutations identified in patients diagnosed with type 3 VWD located in the D4 assembly that involved cysteine changes showed reduced secretion due to intracellular retention within the cell (Solimando et al., 2012). Moreover, mutation p.S2179F located in the D4 assembly can influence VWF survival in plasma and thus increase a rate of clearance indicating additional mechanism of mutation in this assembly although this family involved in our study showed normal clearance (Haberichter et al., 2006).
Family P5F1 was originally screened and sequenced for *VWF* mutations by using manual and fluorescent CSGE methods during the EU study. Although the pre-screening method CSGE followed by DNA sequencing for mutation detection is a sensitive, rapid and reproducible method, direct DNA sequencing remains the gold standard method used for detection of mutations. Primers used in the original study to amplify *VWF* exon 39 were checked for the presence of SNP underneath their annealing sites. Although there was no SNP found in the forward and reverse primers used, it is assumed that this mutation could have been missed due to lack in the degree of sensitivity of the CSGE methods used, which is estimated around 76% (Hinks et al., 1999, Eng et al., 2001) or due to technical error.

Mutation analysis revealed a second novel heterozygous mutation which was missed during EU study. This missense mutation was located in exon 26 where c.3469T>C was predicted to result in the amino acid change p.C1157R in the IC of P9F18 family. This IC had an additional previously known mutation of one nucleotide deletion in exon 14 (c.1614del) predicted to result in the frameshift deletion p.S539fs and lead to premature termination codon (PTC). No new polymorphisms were identified in the P9F18I1 (IC).

This family included a total of five individuals, two affected members (IC+AFM) who showed undetectable levels of VWF:Ag, VWF:RCo and FVIII:C of 3 IU/dL in both and high bleeding scores of 9 and 10 respectively. The remaining members were healthy individuals who presented with normal levels of phenotypic parameters and normal bleeding scores.

To determine whether the p.C1157R substitution could be responsible for the reduction in VWF levels and to evaluate the mechanism underlying this mutation, *in silico* prediction was performed (Section 2.2.5). As a result, this mutation in the form of a substitution of cysteine which is essential for disulphide bridge formation between cysteine residues to arginine at VWF

codon 1157 is predicted to be probably damaging and thereby is likely to affect VWF structure or function.

The nucleotide changes were investigated in all family members which showed that p.C1157R was identified in the IC (I:1) and the AFM (I:2) while the frameshift mutation was detected in all AFM and in two UFM, II:1 and II:2, and UFM (I:3) did not show any nucleotide change. The IC and AFM who had the p.C1157R and p.S539fs variants showed an abnormal pattern of multimer structure and reduced HMW multimers, whilst a normal multimer pattern was observed in the UFM who had only p.S539fs. The presence of a frameshift mutation alone in the IC (I:1) and AFM (I:2) was insufficient to explain the very low level of VWF:Ag, VWF:RCo and FVIII:C and abnormal multimer pattern, but may explain the normal level of VWF level in UFM who harboured only this variant. The UFM (II:1 and II:2) who carried p.S539fs only presented with normal BS and that could be explained due to reduced number of haemostatic challenges that is affected by age or may due to a haplosufficiency mechanism where a single copy of normal gene is sufficient to contribute to normal function of VWF. The most carriers of null allele do not have bleeding symptoms (Nichols et al., 2008a, Bowman et al., 2013), but symptomatic patients who are heterozygous for frameshift mutation can be classified as type 3 carrier VWD. The frameshift mutation may contribute to the reduction of VWF level due to non-sense mediated decay (NMD) mechanism that degrades mRNA containing PTC to prevent the production of a truncated protein. These findings suggest that the presence of two mutations on different alleles were likely responsible for the very low plasma level of VWF in the affected members of this family and could be classified as type 3 VWD. The patient was subsequently classified as having VWD3 and was compound heterozygous for p.C1157R with p.S539fs. In the current classification, mutations within D3 assembly that cause intracellular retention and disturb multimer assembly are classified as type 2A(IIE) (Schneppenheim et al., 2010).

p.C1157R has not been identified previously, but a mutation at the same codon with a different substituted amino acid has been described. Hommais *et al* (2006) identified a heterozygous change c.3470G>T predicted to result in a p.C1157F mutation in a family with unclassified VWD. *In vitro* expression and transfection studies reported that the recombinant heterozygous VWF (rVWF-C1157F) was retained within the ER which resulted in a failure to form HMW multimers and reduced secretion (Hommais et al., 2006a).

The p.C1157R missense mutation which is located in the D3 assembly has not been identified previously. Cysteine residues in VWF are essential and involved in the formation of covalent disulphide bridges between the sulfhydryl (-SH) groups of pairs of cysteines within or between VWF polypeptide chains. The D3 assembly is located at the amino-terminal of the pro-VWF

dimer and is known to be essential for multimer production and assembly and the presence of cysteine loss mutation p.C1157R in this location could explain the abnormal multimers observed in AFM who had p.C1157R and normal multimers found in UFM who had the frameshift variant only. Moreover, the D3 assembly is the region responsible for the binding of VWF to FVIII and some mutations in this domain may reduce FVIII binding. The substitution of cysteine with arginine may impair the multimer formation and lead to the protein being retained and degraded within the ER and thereby reduced secretion of VWF.

Several mutations located in the D3 domain have been identified that may impair VWF multimerisation and lead to type 2A VWD. The hallmark of VWF among these patients is the reduction of HMW multimers, decreased secretion and decreased platelet function (Sadler et al., 2006). Most mutations that have been identified in D3 assembly are associated with type 2A VWD and found to impair multimerisation leading to a reduction in HMW multimers. These mutations include p.C1149Y, p.Y1146C, p.C1130F and p.C1125G, while other mutations, such as p.C2739Y and p.C2754W, cause a near absence of HMW multimers and low secretion when present in homozygous form (Tjernberg et al., 2004, Schneppenheim et al., 2010). Patients who harboured mutations clustered in D3 assembly may present with similar phenotypes that include a moderate reduction of VWF:Ag, VWF:RCo and aberrant multimer pattern classified as type 2A(IIE). The secretion defect may be due to mutations affect multimerization causes intracellular retention and results in rapid clearance (Haberichter et al., 2008, Schneppenheim et al., 2010). The common feature of VWF oligomers observed in patients with mutations in D3 assembly was the presence of abnormal triplet structure with lack of outer bands results from proteolysis of mutant VWF by ADAMTS13.

The linkage study in family P9F18 demonstrated an autosomal recessive inheritance pattern and shared a common mutant allele [187]-[159]-[174] (GT repeat, STRIII and STRII) respectively in the IC and the AFM who had an elevated BS, very low VWF:Ag and abnormal multimer associated with p.C1157R mutation and also a common mutant allele [187]-[163]-[174] in the IC, AFM (I:2), UFM (II:1 and II:2) which is associated with the frameshift mutation (Figure 3.13). All these findings co-segregated with the low level of VWF:Ag and disease phenotype.

Family P9F18 was initially screened and sequenced for *VWF* mutation by using the DHPLC method during the EU study. SNP within the primer sequence could mask a heterozygous genetic defect, and this could cause a mutation to be missed (mono-allelic amplification) (Eikenboom et al., 1994, Thomas et al., 2006b, Hampshire et al., 2010). However, it is assumed that this mutation could have been previously missed in the MCMDM-1VWD study due to presence of a SNP found underneath both of the forward and reverse primer annealing sites (Table 3.7).

In family P10F5, a silent heterozygous mutation was identified during EU study. It was identified in exon 28 and could be responsible for the phenotype present. This silent change was located in the A1 domain at nucleotide position c.4146G>T, and was predicted to result in the silent change p.L1382=. This change had been identified previously during the MCMDM-1VWD and it was found in the female AFM (I:1) and IC was not analysed due to absence of sufficient quantity of DNA sample (Hampshire et al., 2010). However, it was excluded from a previous re-analysis of MCMDM-1VWD patients due to unavailability of a sufficient quantity of DNA in family members to rule out the co-segregation of the mutation with type 1 VWD (Hampshire et al., 2010).

In the current study, it was identified in the IC (II:2) who did not have any additional pathogenic change, but in whom 27 previously known heterozygous polymorphisms were found and also identified in the AFM (I:1). It was detected currently because less DNA is now needed using direct sequencing.

In order to confirm whether this change was a SNP, it was screened in 107 healthy individuals and was absent from all but 4, with low frequency of 0.996/0.004 within the Caucasian population.

This family consisted of four members, two affected members and two healthy individuals. The IC (II:2) and the affected mother (I:1) showed a mild reduction in plasma levels of VWF:Ag, VWF:RCo and FVIII:C with bleeding scores of 4 and 6 respectively. The healthy individuals presented with normal phenotypic data and normal bleeding scores.

The identified variant c.4146G>T was examined in all family members and it was found in addition to the IC in the AFM (I:1) but was absent from the remaining individuals (Figure 3.16). All family members had a normal multimer pattern and had O/O ABO genotype which may contribute to the reduction of VWF level in the affected individuals.

Using the previously described linkage markers, the affected mother and the son (IC) who had an elevated BS and abnormal phenotype shared a mutant allele [193]-[155]-[174] (GT repeat, STRIII and STRII) respectively (Figure 3.16) which segregated with the silent change. This synonymous variant was examined for any potential creation of new splice site and *in silico* analysis predicted that the change would not create a new donor or acceptor splice site but was found to have a potential effect on splicing regulatory enhancers and silencers. Also, the wild-type triplet codon CTG was found more frequently used than mutant codon CTT which may influence translation rate and protein folding (Nakamura et al., 2000).

Primers used in the original study to amplify *VWF* exon 28 were checked for the presence of SNP underneath their annealing sites. Although there was no SNP found in the forward and reverse primers used, this mutation was not missed, but excluded from the MCMDM-1VWD study because the IC was not originally screened due to insufficient DNA and only the family members were screened first and it was identified in the AFM.

Unlike regular mutations that impair protein production when one specific amino acid is replaced by another, it was previously believed that silent changes that encode the same amino acid with different codons cannot lead to a genetic disease. Knobe *et al*, (2008) studied the effect of a silent mutation c.321G>A predicted to result in p.V107= in exon 5 of the *F9* gene in five Swedish families diagnosed with haemophilia B. The absence of other variants in the remaining exons, closely flanking introns and the promoter was confirmed. As a result, it was assumed that the silent *F9* change reduces the translation rate and thus impairs protein folding. No effect on splicing mechanisms was predicted (Knobe et al., 2008).

It has been suggested that apparently silent change may always not be neutral and may play an essential role for translation and gene function of regulatory elements including for messenger RNA (mRNA). The silent change may alter kinetics of protein translation and folding via different mechanisms. It was found that silent substitutions can be affected by codon frequency as some codons are recognised more efficiently by tRNA corresponding to this codon compared to others which can alter the efficiency and accuracy of translation (Hershberg and Petrov, 2008, Zhang et al., 2010). Following transcription, mRNA moves through ribosome forming rRNA-protein complex followed by transferring the amino acids by different transfer RNA (tRNA) at variable speed to link the amino acid to the growing polypeptide chain. However, the triplet code alteration resulting in a silent change may affect the mutant codon translation rate, translation efficiency, protein folding and expression due to variable speed of tRNA transportation of the replacement mutant codon (Sorensen and Pedersen, 1991, Lavner and Kotlar, 2005). Also, the synonymous codon exchange impairs the translation rate which subsequently alters ribosome movement on mRNA. The acceleration or delay of nearby multiple ribosomes movement affects mutant codon folding and can terminate translation due to mis-folding (Komar et al., 1999, Nackley et al., 2006).

Experimental studies showed that silent mutations can impair mRNA folding, stability of secondary structure of mRNA and the rate of translation and thereby impair gene function (Sharp et al., 1995, Chamary et al., 2006, Shabalina et al., 2006). As a result of this codon bias, silent mutations can change mRNA shape, impair its normal translocation with the ribosome and delay its translation rate and protein production.

It was believed that mRNA acts as a carrier of genetic code and transmitting of genetic information from genes to functional protein only, but recent studies have shown that mRNA plays an essential role of controlling and regulating numerous nucleotide signals that are required for protein production and function (Sauna and Kimchi-Sarfaty, 2011, Shabalina et al., 2013).

The rate of protein expression is influenced by the position of the affected nucleotide within the triplet codon. Shah *et al* (2008) reported a reduction in the rate of expression when the nucleotide change is present at the third position of a silent codon which impairs transport of the codon by tRNA (Shah et al., 2008).

Hurust (2011) reported that a silent mutation in *IRGM* gene encoding (immunity-related GTPase family, M) found in patients with Crohn's disease can be highly deleterious. The nucleotide change leading to a silent change may form a small section of mRNA which has a sequence complementary to micro RNA (miRNA) forming a double stranded RNA which is destroyed or prevented from translation (Hurst, 2011).

Furthermore, it was suggested that the silent mutations may affects mRNA splicing by destroying or creating splicing site sequences including exonic splicing enhancer (ESE) or exonic splicing silencer (ESS) sites resulting in abnormal splicing mechanism and causes exon skipping and NMD which could contribute to VWD pathogenicity (Blencowe, 2000, Pan et al., 2008). However, the presence of the silent change in the affected members of the EU family may impair splicing mechanism contributing to the reduction of the VWF level due to NMD.

From these findings, silent mutation alters the translation rate, protein mis-folding or disrupts splicing mechanism can be considered as the possible mechanisms in this family.

Family P10F8 were shown to have a novel heterozygous intronic change at the donor splice site of intron 12 c.1432+1G>T in IC II:1 in addition to previously identified p.R816W (type 2N). This small family consisted of three members, one IC, one AFM and one UFM. In addition to the IC, the AFM was heterozygous for this mutation whereas the UFM was negative for the substitution.

This substitution was located within the donor splice site of intron 12 and had not been identified previously. This heterozygous mutation was likely to be responsible for the abnormal phenotype observed in the IC (daughter) and AFM (son) who showed a reduction in the level of VWF:Ag. Initially, this family was excluded from the original EU study due to absence of a maternal allele in the offspring and also this family was non informative for linkage between *VWF* and type 1 VWD. The non-linkage between family members was re-assessed by using

new SNP markers and swapping the genotypic and phenotypic data of the mother I:2 and the son II:2. As a result of these modifications and according to revised linkage analysis and family pedigree, it was suggested that two mutant alleles were inherited by the daughter (IC). They include the mutant allele [CTGTGA] that was associated with the c.1432+1G>T change which seems to have originated from the mother I:2 and the mutant allele [TCAAAG] which was associated with the type 2N (p.R816W) mutation which affects VWF binding to FVIII found only in the IC (daughter) and was likely to have originated in the father who was not recruited.

In this family, the IC (II:1) who was compound heterozygous for c.1432+1G>T and p.R816W and had high BS, mild reduction of VWF:Ag (49 IU/dL) and VWF:RCo (52 IU/dL) levels, a significant reduction of FVIII:C level (14 IU/dL) resulting from presence of p.R816W that affects binding of FVIII to VWF but not multimer profile. The mother (I:2) was heterozygous for c.1432+1G>T only and exhibited a normal BS, mild reduction of VWF:Ag (47 IU/dL) and normal VWF:RCo and FVIII:C levels. The AFM who had the c.1432+1G>T mutation bleeds and this may be due to haploinsufficiency where produced VWF was reduced in all AFM. Both mutant alleles were absent from the son (UFM) who exhibited normal phenotypic data. The presence of the c.1432+1G>T mutation that leads to a null allele may possibly explain the mild reduction of plasma VWF levels in the IC and in the AFM. Moreover, the presence of splice donor and the p.R816W mutations in the IC in addition to blood group O (O/O) may explain the reduced level of FVIII:C in the IC and the normal levels in the son and mother who did not carry this variant.

The splice donor site mutation was incompletely penetrant and this was explained by mild reduction of plasma phenotypes in the IC and this may be more deleterious when second defect on the other *VWF* allele is co-inherited.

Several splice-site mutations have been identified in VWD patients (James et al., 2004, Gadisseur et al., 2007). *In vitro* study of donor splice-site variant c.3538+1G>A found in *VWF* intron 26 identified in type 2A/IIE VWD patient was found to cause exclusion of exon 26 (James et al., 2004). Nesbitt *et al* (1999) reported the presence of a donor splice site mutation in intron 25 which results in a null allele in two unrelated patients who had two different type 2N mutations; p.R854Q and p.T791M respectively on their second alleles. A third patient was found to have type 2N p.T791M co-inherited with a stop codon p.Q1707*. These patients were phenotypically diagnosed as type 1 VWD and were found to have a mild reduction of VWF:Ag and VWF:RCo levels with very low levels of FVIII:C and absent binding of FVIII to VWF. Initially, the presence of type 2N mutations was not enough to explain the observed phenotype in the IC especially markedly reduced levels of FVIII. The phenotype was consistent with the compound heterozygosity (Nesbitt et al., 1999). Also, type 2N mutation p.G785E was identified

in combination with a stop codon variant in a patient diagnosed with type 1 VWD who showed mild reduction in VWF:Ag and severe reduction of FVIII:C (Gu et al., 1997). The presence of a donor splice site mutation in one allele causes a mild effect in VWF level and this may be due to haploinsufficiency.

The linkage study in this family showed an autosomal dominant inheritance pattern with a common mutant allele [CTGTGA] in the IC and affected members associated with c.1432+1G>T which co-segregated with the disease phenotype (Figure 3.20). To determine whether the c.1432+1G>T substitution could be responsible for the reduction in VWF levels and to evaluate the mechanism underlying this mutation, *in silico* prediction was performed. The results achieved from splice prediction tools indicated that the c.1432+1G>T candidate mutation was most likely to be deleterious and resulted in disruption of the splice donor-site sequence and skipping of exon 12. This may abolish the wild-type exon 12 donor site and would result in retention of intron 12 sequence and it is predicted to result in a frameshift p.C432Vfs*9. The donor splice site c.1432+1G>T likely causes a null allele and results in reduction of VWF level in the AFM due to NMD mechanism that degrades mRNA containing PTC.

SNP within the primer sequence were sought and it was therefore assumed that this mutation could have been previously missed in the MCMDM-1VWD study due to presence of SNP found underneath the forward primer annealing site (Table 3.15).

This study was able to confirm the presence and detect mutations that were previously identified by the EU study. Three mutations were detected in the study in one IC and also detected in this study included c.1533+1G>T; p.[R924Q;C1927R]. The splice prediction tools indicated that the c.1533+1G>T candidate mutation was most likely to be deleterious and resulted in disruption of the splice donor-site sequence and a skip of exon 13. This may abolish the wild-type exon 13 donor site and would result in retention of intron 13 sequence, skipping of exon 13 sequence and loss of 101 amino acid. It was predicted to result in a frameshift p.G478Cfs*138 which creates a stop codon 138 amino acids, downstream of the mutation. It was predicted to produce a null allele due to NMD. Also, the p.C1927R was predicted to be damaging to VWF and p.R924Q predicted to have no effect on VWF expression.

The level of plasma VWF is influenced by multiple factors either genetic, environmental or both. For the remaining index cases listed in table 3.1 who showed no mutation neither in the original study nor in this study despite the reduction of VWF level, may due to presence of a large deletions or duplications that could not be detected by the standard sequencing methods and require an advanced mutation detection method. Cartwright *et al* (2013) identified large deletions of exon 4-5 in three of these IC in addition to deletions of exon 3, exons 32-34 and 33-

34 in one IC each (total of 6 large deletions) within this cohort where no *VWF* mutation had been identified in the original EU study (Cartwright et al., 2013). Eight out of 18 IC were investigated for the presence of CNV, but none of them showed any large deletions or duplications.

Mutations may also be missed due to deep intronic or transcriptional changes in regions of *VWF* not analysed. Mutations in these regions may alter the normal splice sites or may impair the initiation of normal translation process. Mutations in deep intronic regions can impair normal splicing due to creation of an aberrant pseudoexon within intronic regions that impair mRNA synthesis (Khelifi et al., 2011). Also, it has been found that mutations in deep intronic regions can create new cryptic splice site that disrupt mRNA normal synthesis (Corrales et al., 2011, Pezeshkpoor et al., 2013).

Furthermore, mutation may be missed due to the presence of a genetic defect in another gene outside of *VWF* such as *STXBP5*, *STX2*, *STAB2*, *CLEC4M* and *SCARA5* which have been shown to correlate with VWF:Ag levels (Smith et al., 2010, Rydz et al., 2013).

Of the 14 IC with no *VWF* mutation after further screening, 10 patients had VWF:Ag levels less than 50 IU/dL and the remaining 4 less than 62 IU/dL (between 51-61 IU/dL). The bleeding score in these IC was significant (>3) ranging between 3 and 19 (Table 3.1). The multimer pattern was normal in all remaining IC except one IC (P9F14II:2) who showed abnormal multimers. The level of VWF is decreased significantly in the normal population with blood group O rather than other blood groups (Gill et al., 1987, Shima et al., 1995). The *ABO* genotype for all 14 IC was O/O except for two IC P8F2II:2 (O/A2) and P8F3I:2 where *ABO* genotype was not determined. These findings may support the effect of different gene loci on the level of VWF. None of the remaining 14 IC had large deletion or insertion (Appendix 14).

In conclusion, this research was able to identify four mutations, three of which were novel in exons 26, 39, intron 12 in addition to silent change in exon 28 in four families. These mutations were missed in the previous MCMDM-1VWD study due to limitations in the sensitivity of the methods used, due to technical error or due to the presence of SNP within PCR primer annealing sites leading to mono-allelic amplification. These findings confirmed that direct DNA sequencing is a sensitive method for mutation detection and the presence of SNP within primer sequences may hide heterozygous mutations. The presence of other genetic alterations in *VWF* such as heterozygous deletions or duplications or the presence of genetic defects elsewhere in *VWF* or in other genes may affect the level of VWF and thus the extent of bleeding. Further investigations are required in order to explain the molecular pathogenesis behind mucocutaneous bleeding and reduced VWF levels in these cases with a historic diagnosis of type 1 VWD.

Chapter 4

In vitro expression of type 1 VWD candidate mutations

4. *In vitro* expression of type 1 VWD candidate mutations

4.1. Introduction

Type 1 VWD is characterized by a partial quantitative deficiency of plasma VWF, variable penetrance and expressivity. VWF is synthesised in endothelial cells and megakaryocytes. Pre-pro VWF dimerisation and folding take place in ER via formation of disulfide bonds between adjacent VWF monomers through their c-terminal regions (Katsumi et al., 2000). VWF that is successfully dimerised and folded in the ER moves to the Golgi apparatus where multimerisation occurs via disulfide bonds between adjacent D3 assemblies to produce HMW multimers (Section 1.4) (Mayadas and Wagner, 1992). VWF that shows improper folding is retained in the ER which is rapidly degraded causing reduced secretion (Lodish, 1988, Hurtley and Helenius, 1989).

The European Union study (MCMDM-1VWD) successfully identified candidate mutations throughout *VWF* in approximately 70% of type 1 VWD IC and these are mostly made up of missense mutations. The remaining IC showed no candidate mutations (Goodeve et al., 2007, Hickson et al., 2010). The current study was able to identify additional novel mutations that were missed in the previous analysis (Section 3.6). Eighteen out of 42 IC who showed no previously identified mutations or mutations that were identified, but were insufficient to explain the patient's phenotype were screened using direct sequencing for the presence of missed mutations. As a result, four mutations were identified in four index cases, two novel missense changes; c.3469T>C (p.C1157R) and c.6811T>G (p.W2271G) in exons 26 and 39 respectively, one silent change; c.4146G>T (p.L1382=) in exon 28 and one novel splice change; c.1432+1G>T in intron 12. *In silico* analysis of the newly identified mutations suggested that the two missense mutations were probably damaging, the silent mutation was predicted to disrupt several exonic splicing enhancer (ESE) sites and alter the splicing mechanism and the splice change was predicted to result in a frameshift due to retention of intron 12. The purpose of *in vitro* expression is to try and determine how each mutation has an effect within the cells and to understand the main mechanisms that lead to disease pathogenicity. These mechanisms need to be found in order to understand the function of the mutations and to try and replicate the phenotype of the patients using *in vitro* expression. For the particular mutations, in the heterozygous form type 1 VWD phenotype is examined and in the homozygous form a potential type 3 VWD phenotype is examined.

Previous studies have investigated the mechanism of several novel mutations that resulted in VWD by *in vitro* expression. Eikenboom *et al* (2009) performed *in vitro* expression on 14 candidate missense mutations identified within the MCMDM-1VWD cohort. Mutant constructs

were generated by undertaking site-directed mutagenesis on pcDNA3.1 plasmid containing VWF cDNA expressed in COS-7 cells. The expressed mutations were located in a number of VWF domains and some involved cysteine residues. As a result, intracellular retention and impaired secretion of VWF were recognised as the main mechanisms behind the pathogenicity for some of the mutations (Eikenboom et al., 2009). Also, a cluster of mutations in the VWF D3 assembly identified in patients with type 2A(IIE) VWD were expressed. Most of these mutations involved cysteine residues and were expressed using the 293-EBNA cell line (Schneppenheim et al., 2010). This study showed that most of these D3 assembly mutations lead to intracellular retention as the main mechanism of pathogenicity in addition to abnormal multimers.

Since patients' blood was not available and hence BOEC cells could not have been prepared, a heterologous expression system was used whereby transient transfection of the desired mutant plasmid into cell lines to measure an outcome was used. Many expression studies for VWF have used various mammalian cell lines including HEK293T, Aat20 and COS-7 (Eikenboom et al., 2009, Schneppenheim et al., 2010). However, HEK293T cells have a number of advantages over COS-7 cells for analysis of VWF mutants. The HEK293T cells were first described in 1977 (Graham et al., 1977). They are a specific cell line originally obtained from human embryonic kidney obtained from a foetus that was legally aborted and the 293 comes from the product of his 293rd experiment. These cells are widely used for expression of various genes and contain the simian vacuolating virus 40 (SV40) origin of replication that enables transformation of many cell types. HEK293T cells contain the SV40 large T-antigen required for plasmid replication and result in a high level of transient expression of gene products.

HEK293T cells were selected particularly to be used for transient transfection for wild-type and mutant *VWF* in this study. HEK293T cells do not express endogenous VWF hence only VWF that is transiently transfected will be expressed. Also, these cells make WPB-like organelles for storage of VWF. The formation of WPB-like organelles requires VWF to be present. The cell line is very easy to culture, to transfect and very hardy, making them a good and readily transfectable cell line to use. They are characterized by fast growth reaching 70-90% confluency within 48 hr of splitting.

Transfection using Lipofectamine was undertaken to introduce plasmid DNA containing the full length VWF cDNA into HEK293T cells. Lipofectamine LTX transfection reagent was the selected method used to mediate and deliver the plasmid containing the full length VWF cDNA into HEK293T cells. Compared to other transfection methods, Lipofectamine LTX has low toxicity. Also, there is no need to change the media after 4-6 hr unlike other more toxic reagents. Moreover, Lipofectamine LTX reagent is highly efficient at transfecting cells and

hence a large proportion of cells may be transfected. Lipofectamine was used to transiently introduce full length wild-type and mutant plasmid DNA into HEK293T cell lines (Section 2.2.13.5).

The presence of a candidate mutation in *VWF* resulting in a missense change does not conclusively confirm that this mutation is the main cause of the VWD phenotype in the patient. One of the main aims of this study was to transfect the mutagenized plasmid bearing mutant cDNA (recombinant VWF-r*VWF*) into HEK293T mammalian cells and to perform *in vitro* expression of selected VWF mutations during this study in order to determine the effect of candidate mutations on VWF structure and function. Also, this study was aimed to analyse the multimer structure of secreted VWF in addition to confocal microscopy to evaluate the effect of mutants in VWF storage following transfection.

In each transfection experiment, the efficiency of transfection was evaluated using Renilla plasmid as a control in transfections via measuring the luciferase activity. Renilla was used in order to correct for transfection efficiencies and to confirm that the quantities of expressed protein detected by ELISA was a true reflection of what was happening in the cells.

Six mutations detected in the EU study were subjected to further study in order to determine the mechanisms by which the mutations identified affect VWF synthesis and secretion. Three candidate missense mutations identified in two IC were expressed in this study. First, c.6811T>G predicted to result in the p.W2271G mutation located in D4 assembly that was identified in family P5F1 with type 1 VWD in addition to a second mutation p.R854Q known to impair VWF binding to FVIII (Section 3.6.1). The affected members having this novel mutation presented with moderate bleeding symptoms and were found to have reduced levels of VWF:Ag, VWF:RCo and a marked reduction in FVIII level in individuals who had both mutations (Section 3.6.1.1). Secondly, two missense mutations, c.2771G>A in exon 21 and c.5779T>C in exon 34 which were predicted to result in p.R924Q (D3 assembly) and p.C1927R (D4 assembly) respectively were identified in family P9F14 on the same allele (Section 3.6.5). The affected members harbouring these two changes presented with moderate reductions in their phenotypic data.

Since the p.W2271G and p.C1927R are located in the D4 assembly and appeared to be responsible for type 1 VWD, their effect on VWF level and structure were analysed using *in vitro* expression. *In vitro* expression studies of various mutations located in the same assembly showed a secretion defect of VWF due to intracellular retentions in type 1 and type 3 VWD patients. The transient transfection using COS-7 cells undertaken on four mutations; p.L2207P, p.C2257S and p.R2287W located in the D4 assembly showed a significant reduction of secreted VWF accompanied by intracellular retention and abnormal HMW multimers when present in

homozygous form (Eikenboom et al., 2009). Also, the expression of p.L2207P and p.C2257S in the heterozygous form results in a significant secretion defect due to intracellular retention and normal HMW multimers. The other mutations not involve cysteine residues; p.R2287W showed a mild secretion defect while p.P2063S revealed normal VWF expression (Eikenboom et al., 2009, Hampshire and Goodeve, 2013).

The heterozygous transfection of cysteine loss mutations p.C2184S and p.C2212R located in the D4 assembly identified in type 3 VWD showed a moderate reduction of secreted VWF and normal multimers while homozygous forms of both mutations illustrated a severe reduction, intracellular retention and abnormal multimers (Solimando et al., 2012).

In an attempt to investigate whether these candidate mutations were the major cause for the observed phenotype correlated with type 1 VWD in affected patients, *in vitro* expression of mutant rVWF was carried out using transient transfection. In order to create a specific mismatch, QuikChange® lightning site-directed mutagenesis was used.

The transfection experiments of mutant and wild-type constructs were conducted in triplicate and repeated three times and the level of intra and extracellular VWF was measured using the ELISA method. The initial set up and optimisation of the ELISA and transfection methods was previously performed within the group.

4.2. Results

4.2.1. Confirmation of wild type VWF cDNA sequence

The pcDNA3.1/Hygro (-) expression plasmid containing the full-length wild type human *VWF* cDNA was kindly provided by Prof. Reinhard Schneppenheim, Germany. The full length *VWF* cDNA originated from the *VWF*-PMT2 plasmid which was transferred to a pcDNA3.1/Hygro (-) expression plasmid. The *VWF* cDNA was introduced into the plasmid using two restriction enzymes, *Eco*RI and *Not*I, producing a 14kb pcDNA3.1VWF plasmid.

The wild-type *VWF* cDNA3.1 was isolated from *E.coli* NM554 cells. The entire VWF cDNA plasmid was sent for sequencing and the received data was aligned to the VWF reference sequence (Gene ID: ENSG00000110799; Accessed May 2011) (Section 2.2.12.5.1). As a result, the two sequences aligned except for the presence of five variant sites (Table 4.1). All detected variants were reported in the ISTH VWF mutation database and none of them would be expected to impair VWF function or structure (www.ragtimedesign.com/vwf/polymorphism, Accessed May 2011) (Section 2.2.12.5.1).

Table 4.1 List of SNP identified in full length *VWF* cDNA

Nucleotide change	Location Exon/intron	Minor allele frequency % (1000 genomes)	Amino acid change	Effect on protein expression
c.2555A>G	Exon 20	10.3	p.R852Q	No effect
c.4141A>G	Exon 28	27	p.T1381A	No effect
c.4414G>C	Exon 28	15	p.D1472H	No effect
c.4641T>C	Exon 28	30	p.T1547=	Silent
c.7239T>C	Exon 42	14.3	p.T2413=	Silent

4.2.2. Efficiency of site-directed mutagenesis and transformation

A series of different quantities of DNA plasmid template of 10, 25, 50 and 100 ng were added to separate mutagenesis reactions in order to optimise the number of colony following transformation. Mutagenesis was then performed on each template with primers designed to introduce the identified mutations into the plasmid VWF cDNA. As a result, the best colony number was achieved when using a template quantity of 100 ng. At this DNA quantity, more than 5 colonies grew on transformed agar. The number of colonies was less when using 50ng and no colonies were observed when using 10 and 25ng.

Also, the efficiency of mutagenesis and transformation was evaluated using pWhitescript 4.5 kb and pUC18 control plasmids respectively (Section 2.2.12.4). The pWhitescript control plasmid contains a TAA stop codon instead of the CAA codon that encodes glutamine at amino acid position 9 that appears normally in the ß-galactosidase gene. The oligonucleotide control primers used for mutagenesis of the control plasmid produce a point mutation on the pWhitescript plasmid where T in the stop codon replaced by C enables creation of the glutamine found in the wild-type sequence. However, following transformation of control plasmid in XL10-Gold ultracompetent cells on agar plates containing IPTG and X-gal, the colonies of pWhitescript plasmid that contains a stop codon appear white due to inactivity of ß-galactosidase gene, while the control plasmid that contains the normal sequence of ß-galactosidase gene due to mutagenesis shows blue coloured colonies due to metabolisation of glutamine.

The efficiency of mutagenesis of the pWhitescript control plasmid and of transformation of the pUC18 control plasmid were evaluated by calculating the percentage of blue colonies from the transformation of pWhitescript and pUC18 control plasmids on agar plates containing IPTG and

X-gal. As a result, the mutagenesis and transformation were highly efficient with values of 96.2 and 98.7% respectively.

4.2.3. Mutagenesis

Initially the plasmid DNA was sent for sequencing following mini-prep to confirm the presence of the desired mutation only. As a result, the sequencing data successfully showed the presence of the desired change in the plasmid DNA for all examined variants listed in appendix 8. The T>G transition at nucleotide 6811 for the rVWF-G2271, predicted to result in amino acid exchange of tryptophan by glycine, c.2771G>A for the rVWF-Q924 predicted to result in exchange of arginine by glutamine and c.5779T>C predicted to result in exchange of cysteine by arginine were successfully introduced into the full length VWF recombinant plasmid (Figure 4.1). Also, both mutations p.[R924Q;C1927R] were successfully introduced into the full length rVWF on the same allele to mimic the allelic state. Mutagenesis was undertaken using pcDNA3.1 plasmid template in order to express the novel candidate mutations p.W2271G, p.R924Q. p.C1927R and p.[R924Q;C1927R] respectively (Figure 4.1). Additional sequencing of the entire VWF cDNA for each revealed no further mutations following the maxi-prep.

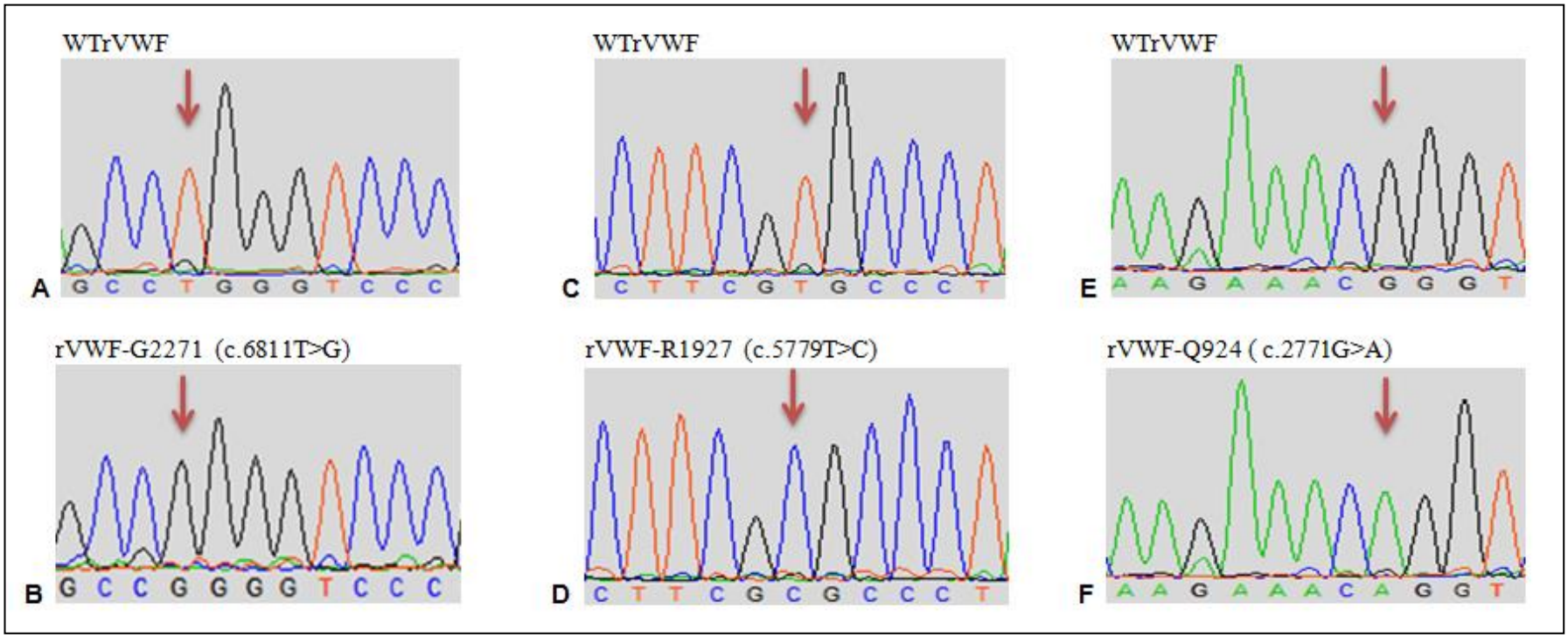

Figure 4.1 Sequence chromatographs to show introduction of novel variants into the cDNA VWF plasmid. A, C and **E** show the wild type VWF cDNA sequence**. B)** Shows the p.W2271G change (c.6811T>G); **D)** shows the p.C1927R change (c.5779T>C); **F)** shows the p.R924Q change (c.2771G>A.

4.2.4. *In vitro* expression of recombinant VWF containing the candidate mutations

The rVWF plasmid harbouring each candidate mutation was transiently transfected into HEK293T cells in parallel with rVWF-WT plasmid using Lipofectamine to evaluate the effect of the candidate mutation on VWF expression. In order to mimic the *in vivo* state and to replicate the phenotypic pattern of patients with each mutation, co-transfection of mutations was carried out using three different conditions. The first experiment was conducted to mimic the wild-type state using 100% (6µg) wild-type plasmid while in the second condition; the same quantity of mutant plasmid was transfected in order to mimic the mutant homozygous state. In the third condition, a mixture of 50% wild-type (3µg) and 50% of recombinant mutant plasmid (3µg) was transfected making a final quantity of 6 µg in order to mimic the heterozygous state of the mutation (Section 2.2.13.5). For each condition, transfection was undertaken in triplicate and repeated three times. The tissue culture supernatant and harvested cell lysate were collected 48 hr post transfection (Section 2.2.13.6). Following co-transfection, the level of VWF:Ag secreted from HEK293T cells into the growth medium and that retained within the HEK293T cells resulting from expression of transfected plasmids bearing wild-type and mutant sequences was analysed using ELISA (Section 2.2.14.2). The expression level of transfection data was normalized to correct for transfection efficiency of the cells using Renilla.

The expression data of wild-type, homozygous and heterozygous plasmids in the medium and cell lysates was calculated using the standard curve plotted between the known concentrations of each diluted reference plasma against its corresponding optical density (OD) (Figure 4.2).

The VWF concentration was divided by Renilla expression to give a ratio, from which mutants were then compared to wild type expression. Mean values of VWF either homozygous or heterozygous mutant were expressed as a percentage with respect to the expressed level of wild-type. Statistical analysis including mean values, standard deviation (SD), one way test and "analysis of variance (ANOVA)" to compare mean values of wild-type, homozygous and heterozygous VWF with each other were calculated.

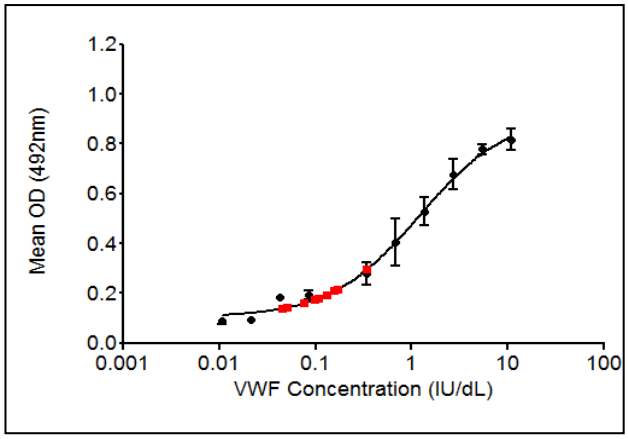

Figure 4.2 VWF standard ELISA curve plotted between reference VWF plasma with known concentration (x) against its corresponding OD (y). The red dots represent the VWF antigen level expressed by transfected HEK293T cells with mutant plasmid after 48 hr. The expression data of wild-type, homozygous and heterozygous in the medium and cell lysates was calculated against the readings of VWF level in the reference plasma calibrator.

4.2.5. Quantitative analysis of supernatant and cell lysates following transfection of HEK293T cells with rVWF-WT and mutant plasmid (rVWF-G2271)

Analysed mean values of secreted VWF obtained by expression of wild-type plasmid alone, mutant plasmid alone (homozygous) and mutant plasmid co-expressed with WT (heterozygous) are shown in table 4.2. The observed mean values of secreted VWF:Ag of mutant heterozygous and homozygous rVWF-G2271 into growth medium were significantly decreased to 23% and 3.5% respectively compared to 100% of rVWF-WT (Figure 4.3). The difference in the secreted VWF level for heterozygous and homozygous states compared to wild-type was statistically significant with *P* values of <0.0001 (ANOVA) (Figure 4.3). In the HEK293T cell lysate, data showed mildly increased mean values of retained VWF of heterozygous rVWF-G2271 in the cells compared with the corresponding values of 100% wild-type with values of 109.5% (*P*>0.05) and intracellular mean values of VWF:Ag of homozygous rVWF-G2271 was significantly increased to 130.6% (*P*<0.05) compared to the wild-type (Table 4.3) (Figure 4.3).

In summary, the p.W2271G change lead to a significant difference in the level of secreted VWF:Ag in both heterozygous (77%) and homozygous (96.5%) states compared to 100% of wild-type and these values attained statistical significance indicating that p.W2271G results in VWF secretion defect due to intracellular retention. Also, the expression data from HEK293T cell lysates indicated an increase in the level of retained VWF within the cells, although this increase was not significant in the heterozygous state, but was significant for the homozygous mutant.

Table 4.2 The mean values and standard deviation of secreted VWF:Ag levels post-transfection for WT and mutant plasmids (rVWF-G2271) in HEK293T cells

VWF (supernatant)	Mean (%)	*SD
rVWF-WT (homozygous)	100.0	21.0
WT:Mut (50:50) (heterozygous)	23.0	8.8
rVWF-W2271G (homozygous)	3.5	2.5

*SD= standard deviation

Table 4.3 The mean values and standard deviation of retained VWF:Ag levels harvested post-transfection for WT and mutant plasmids (rVWF-G2271) in HEK293T cells

VWF (Cell lysate)	Mean (%)	*SD
rVWF-WT (homozygous)	100.0	20.0
WT:Mut (50:50) (heterozygous)	109.5	18.5
rVWF-W2271G (homozygous)	130.6	29.5

*SD= standard deviation

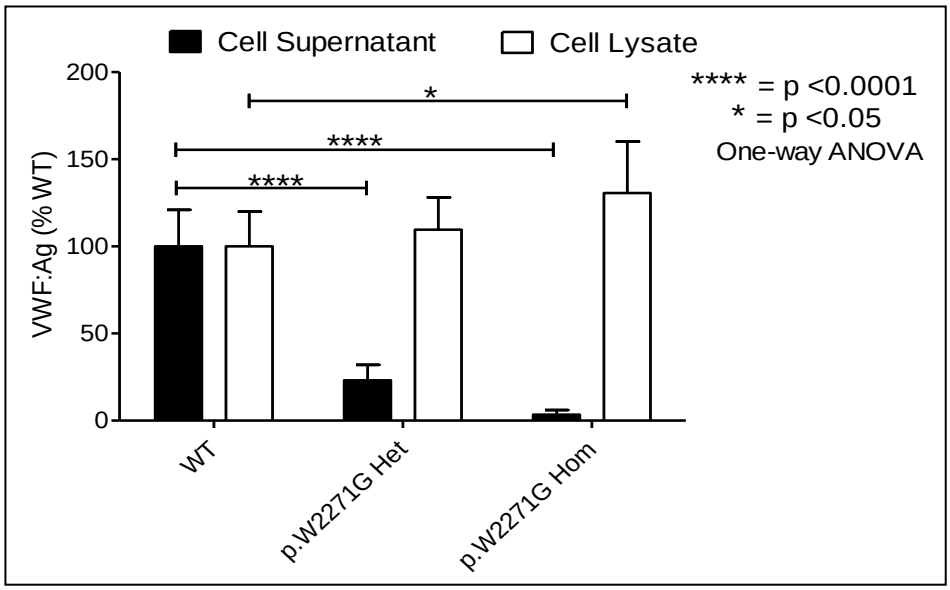

Figure 4.3 Mean levels of VWF:Ag in both supernatant and cell lysates of HEK293T cells transfected with WT and mutant expression plasmids showing the effect of the p.W2271G mutation on *VWF* expression. Results are expressed as a percentage in comparison with wild-type. The horizontal black bars represent the extent of difference between mean values of VWF:Ag between wild-type and mutant VWF. The vertical black bars indicate the standard deviation. Statistical test used was one-way ANOVA.

4.2.5.1. Multimer analysis of expressed mutation

The multimeric composition of VWF secreted from the transfected HEK293T cells into the growth medium was evaluated using medium resolution 1.6% sodium dodecyl sulphate (SDS) in agarose gel electrophoresis (Section 2.2.16). A full array of multimer bands was observed in the normal VWF in plasma composed of high, intermediate and low molecular weights multimers. Each multimer band consists of triplet bands that include a central band located between two faint satellite proteolytic bands. For each mutation, multimers were analysed for transfections of rVWF-wild-type, mutant-rVWF and co-transfection of wild-type with mutant (hybrid) secreted from HEK293T cells (media). All obtained multimer analysis results in the current study were kindly provided by Prof. Ulrich Budde on medium resolution 1.6% SDS gels at 1:3 or 1:5 dilutions (Hamburg, Germany).

4.2.5.1.1. Multimer analysis for the p.W2271G VWF protein secreted from HEK293T cells

The secreted rVWF results from transfection of wild-type plasmid, rVWF-G2271 plasmid and co-transfection of mutant/wild-type were analysed for multimer pattern using 1.6% medium resolution SDS agarose gel. As a result of multimer analysis, a significant defect in multimerisation with a complete loss of high-molecular weight VWF (HMW-VWF) multimers was observed in the homozygous state. The multimeric composition of rVWF secreted from HEK293T cells in the heterozygous state showed the presence of a full set of multimers with relative reduction of large multimers in comparison to wild-type multimers (Figure 4.4).

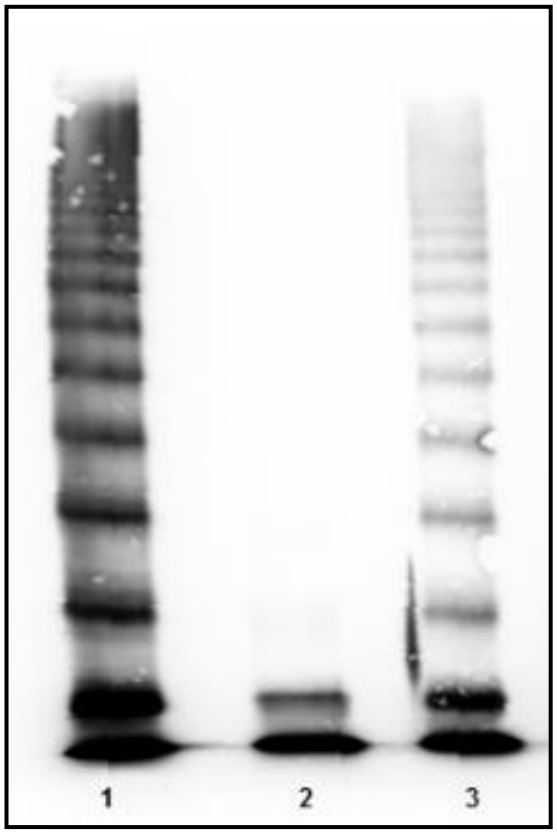

Figure 4.4 Multimer analysis of secreted rVWF from HEK293T cells transfected with p.W2271G. Multimer pattern of wild-type (lane 1), homozygous rVWF-G2271 (lane 2) and heterozygous rVWF (lane 3) mutants electrophoresed on 1.6% medium resolution SDS gel at 1:5 dilution. VWF multimers of homozygous mutant rVWF-G2271 (lane 2) showed a totally absence of HMW-VWF multimers with presence of only dimers in comparison to wild-type (lane 1). The multimeric composition of rVWF resulting from the heterozygous state post *in vitro* expression (lane 3) demonstrated a relative reduction of large multimers in comparison to wild-type multimers.

4.2.5.2. Immunofluorescence staining and confocal microscopy imaging of expressed mutations

Following *in vitro* expression of mutants in HEK293 cells, transfected cells were stained and examined using a confocal microscope in order to determine the intracellular storage. For each mutation, confocal microscopy was undertaken in the homozygous and heterozygous forms and compared to wild-type. The shape of WPB-like structure, size and frequency of each form was compared to those of wild-type. To determine intracellular storage of VWF, cells were stained with two markers to visualise VWF and the cell membrane using two pairs of antibodies; anti-VWF rabbit primary antibody and an anti- rabbit Alexa Fluor 488 green secondary antibody to visualise intracellular VWF, the second pair of antibodies was the mouse anti α-tubulin primary antibody and an anti-mouse Alexa Fluor 555 red secondary antibody as a cell membrane marker.

The confocal microscopy images of each mutation to determine intracellular storage were presented in 3x3 rows, first horizontal row represents VWF (green) for wild-type, homozygous and heterozygous forms respectively. The middle horizontal row represents the cell membrane marker α-tubulin (red) and the lower horizontal row shows a merge of VWF and α-tubulin staining for all forms within HEK293 cell line.

Also, to determine the localisation of VWF within cells, cells were stained with anti-VWF rabbit and mouse anti-ER PDI primary antibodies using transmitted light with phase contrast. Alexa Fluor 488 green and Alexa Fluor 555 red secondary antibodies were used respectively.

The confocal images of each mutation to detect VWF localisation were presented in 4x3 rows, first vertical row represents VWF (green) for wild-type, homozygous and heterozygous forms respectively. The second vertical row represents the ER-PDI marker (red) and the third vertical row represents a merge of VWF and PDI staining for all forms within HEK293 cell line. The last vertical row shows images of cells by phase contrast.

4.2.5.2.1. Confocal microscopy of p.W2271G

The effect of p.W2271G on VWF storage within HEK293 heterologous cell lines was evaluated using confocal microscopy. *In vitro* expression of the p.W2271G revealed a secretion defect resulting from intracellular retention. In the wild-type form, small rounded punctate WB-like vesicles were formed throughout the cells (Figure 4.5 A and C). In the homozygous form of p.W2271G mutant, WPB-like vesicles were present, but appeared larger in size and this may be due to stacking of WPB-like organelles on top of each other, also WPB were more in number and localised VWF diffuse staining patterns were observed in comparison to the wild-type (indicated with a white arrow, Figure 4.5 D). Similarly to homozygous, in the heterozygous form of p.W2271G mutant, WPB-like organelles were formed, but smaller than those in the homozygous state with presence of diffuse staining pattern (indicate with white arrow) (Figure 4.5 G). The presence of the diffuse staining pattern may be due to VWF WPB-like structures accumulated over each other in cross-section analysis caused by intracellular retention. These findings suggested that p.W2271G has an influence in WPB storage. Also, confocal microscopy confirms *in vitro* findings of increased intracellular retention.

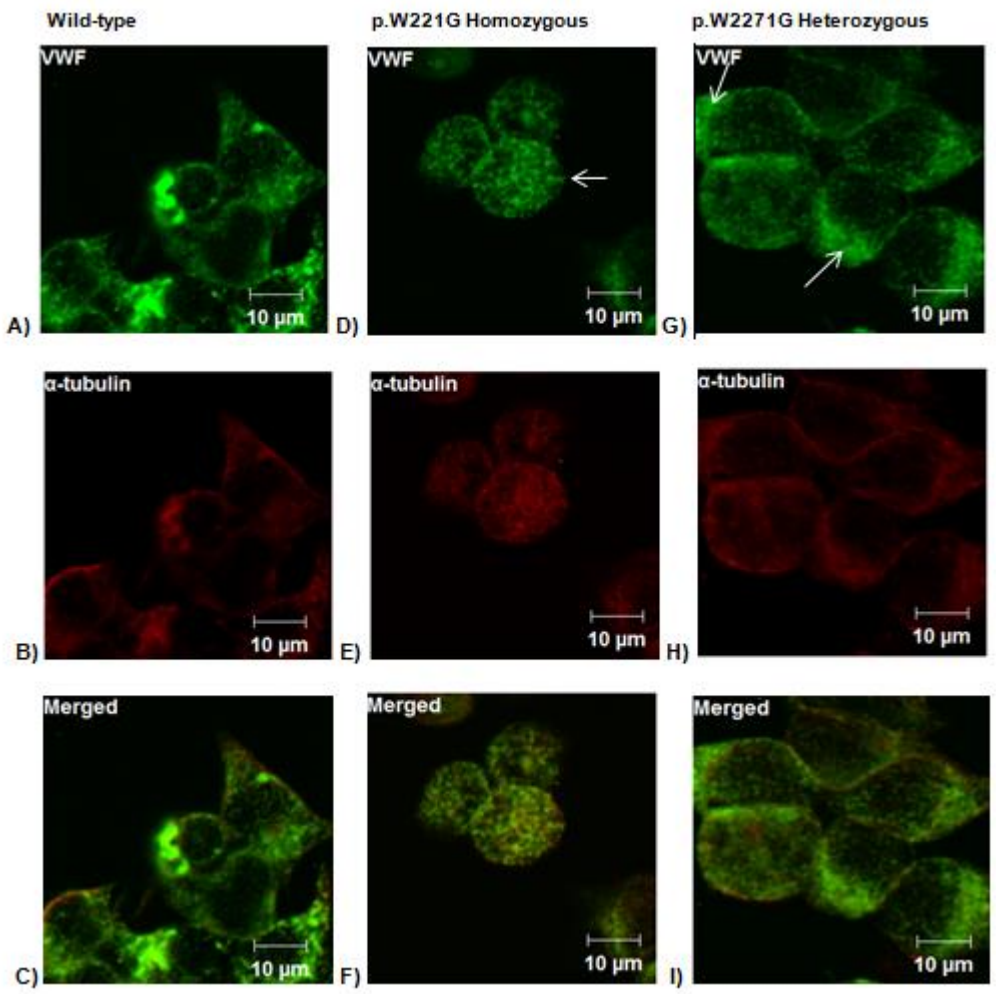

Figure 4.5 Intracellular storage of rWT and rVWF-G2271 mutant in HEK293 cells by confocal microscopy. A, D and G) Represent VWF (green) after transfection of wild-type, homozygous and heterozygous plasmids respectively into HEK293 cells. White arrows indicate regions where there was diffuse staining of VWF within the cell. **B, E and H)** Represent the cell membrane marker α-tubulin (red) after transfection of wild-type, homozygous and heterozygous respectively into HEK293 cells. **C, F and I)** Represent merged images of VWF and α-tubulin staining for wild-type, homozygous and heterozygous respectively transfected into HEK293 cells. Cells of the upper horizontal row **(A, D and G)** were stained with rabbit anti-VWF primary and anti-rabbit Alexa Fluor 488 for VWF (green), while cells of the middle horizontal row (**B, E and H)** were stained with mouse anti-α-tubulin and anti-mouse Alexa Fluor 555 for the cell membrane α-tubulin marker (red). The lower horizontal row **(C, F and I)** shows a merge of VWF and α-tubulin staining.

4.2.5.2.2. Confocal microscopy of p.W2271G to determine retention of VWF in the ER

Confocal microscopy showed the formation of small rounded punctate WB-like organelles in the wild-type form (Figure 4.6 A and C). As shown by the co-localisation of VWF and PDI marker, the homozygous form of p.W2271G showed the presence of rounded punctuate pseudo WPB-like organelles and led to significant retention of VWF in the ER compared to wild-type (Figure 4.6 E and G). The retention of VWF in ER was observed but appeared reduced when p.W2271G expressed in the heterozygous form (Figure 4.6 I and K). These findings postulated that p.W2271G led to reduce VWF secretion due to retention of VWF in the ER.

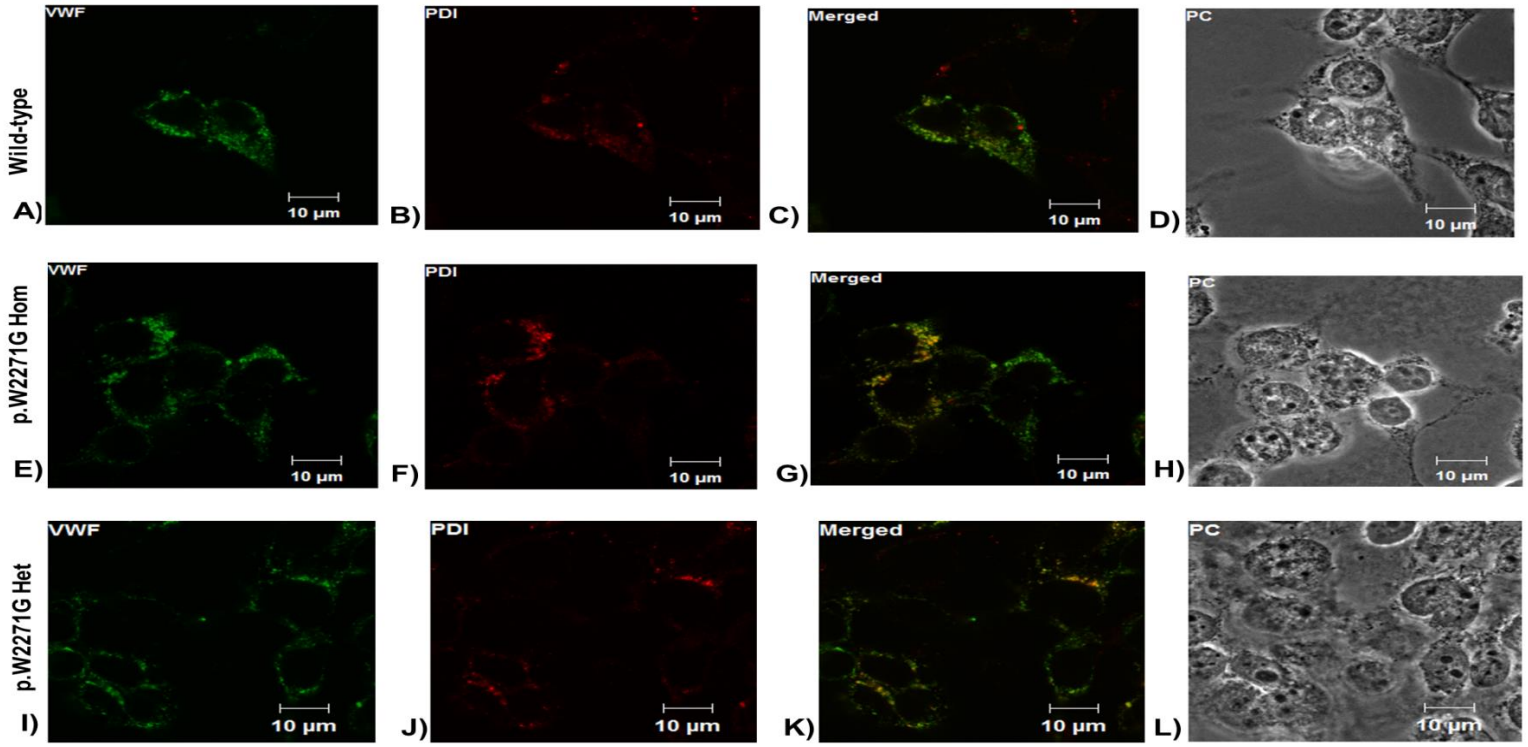

Figure 4.6 Intracellular localisation of VWF in rWT and rVWF-G2271 mutant in HEK293 cells. A, E and I) Represent VWF (green) after transient transfection of wild-type, homozygous and heterozygous plasmids respectively into HEK293 cells. **B, F and J**) Represent the ER marker PDI (red) after transfection of wild-type, homozygous and heterozygous respectively into HEK293 cells. **C, G and K**) Represent merged images of VWF and PDI staining for wild-type, homozygous and heterozygous respectively transfected into HEK293 cells**. D, H and L**) Represent phase contrast (PC) image for wild-type, homozygous and heterozygous respectively transfected into HEK293 cells. Cells of the column (**A, E and I)** were stained with rabbit anti-VWF primary and anti-rabbit Alexa Fluor 488 for VWF (green), while cells of the second column (**B, F and J**) were stained with mouse anti-PDI and anti-mouse Alexa Fluor 555 for the ER marker (red). The Third column (**C, G and K**) shows a merge of VWF and PDI.

4.2.6. *In vitro* expression of recombinant VWF containing the candidate mutations p.R924Q and p.C1927R

The variants c.2771G>A predicted to result in p.R924Q and c.5779T>C predicted to result in p.C1927R were previously identified in one family (P9F14) in IC (III:1) and AFM within the EU study. These two variants were found on the same allele (Section 3.6.5). Each mutation was successfully introduced alone into the full length VWF recombinant plasmid in order to express the candidate mutations p.R924Q and p.C1927R. Also, both mutations were successfully introduced into the full length rVWF on the same allele to mimic the allelic state.

Three separate experimental conditions were performed including; transfection of rVWF-Q924 alone, transfection of rVWF-R1927 alone and transfection of both mutants rVWF [R1927;Q924] on the same allele. Transfection for each mutant was undertaken as previously described (Section 2.2.13.5).

4.2.6.1. Quantitative analysis of supernatant and cell lysates following transfection of HEK293T cells with rVWF-WT and mutant plasmid (rVWF-Q924)

The measured values of VWF in cell supernatant and cell lysates are shown in tables 4.4 and 4.5. *In vitro* expression of rVWF-Q924 showed that the rVWF values measured in growth medium of mutant heterozygous and homozygous was reduced to 97% and 91.5% respectively with no significant change compared to 100% rVWF-WT (Figure 4.7).

Analysis of the intracellular VWF showed no significant change in mean values of VWF in the heterozygous and homozygous state with values of approximately 87% and 88% respectively compared to 100% of rVWF-WT (Figure 4.7).

In summary, *in vitro* expression of rVWF-Q924 suggested that this candidate mutation (p.R924Q) had no effect on VWF secretion and does not lead to intracellular accumulation of VWF within cells. The secretion of homozygous p.R924Q was not significantly reduced compared to wild-type VWF.

Table 4.4 The mean values and standard deviation of secreted VWF:Ag levels post-transfection for WT and mutant plasmids (rVWF-Q924) in HEK293T cells

VWF (Supernatant)	Mean (%)	*SD
rVWF-WT (homozygous)	100.0	16.0
WT:Mut (50:50) (heterozygous)	97.0	21.7
rVWF-R924Q (homozygous)	91.5	9.6

*SD= standard deviation

Table 4.5 The mean values and standard deviation of retained VWF:Ag levels harvested post-transfection for WT and mutant plasmids (rVWF-Q924) in HEK293T cells

VWF (Cell lysate)	Mean (%)	*SD
rVWF-WT (homozygous)	100.0	19.0
WT:Mut (50:50) (heterozygous)	87.0	17.0
rVWF-R924Q (homozygous)	88.0	15.0

*SD= standard deviation

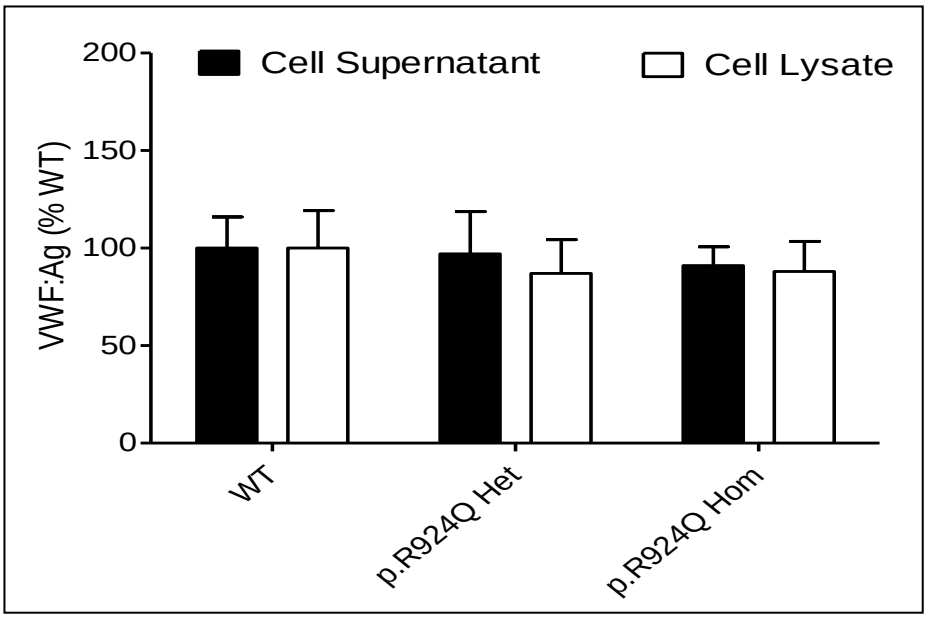

Figure 4.7 Mean levels of VWF:Ag in both supernatant and cell lysates of HEK293T cells transfected with WT and mutant expression plasmids showing the effect of the p.R924Q mutation on *VWF* expression. Results are expressed as a percentage in comparison with wild-type. The vertical black bars indicate the standard deviation. Statistical test used is one-way ANOVA.

4.2.6.1.1. Multimer analysis for the p.R924Q VWF protein secreted from HEK293T cells

The multimer analysis of rVWF of p.R924Q mutation collected following *in vitro* expression showed that both the heterozygous and homozygous state produced normal VWF multimers containing high, intermediate and low molecular weight bands similar to the multimeric pattern observed in the wild-type (Figure 4.8). The obtained results after *in vitro* expression reflected the p.R924Q has no effect on VWF multimer formation although it's located in D3 domain.

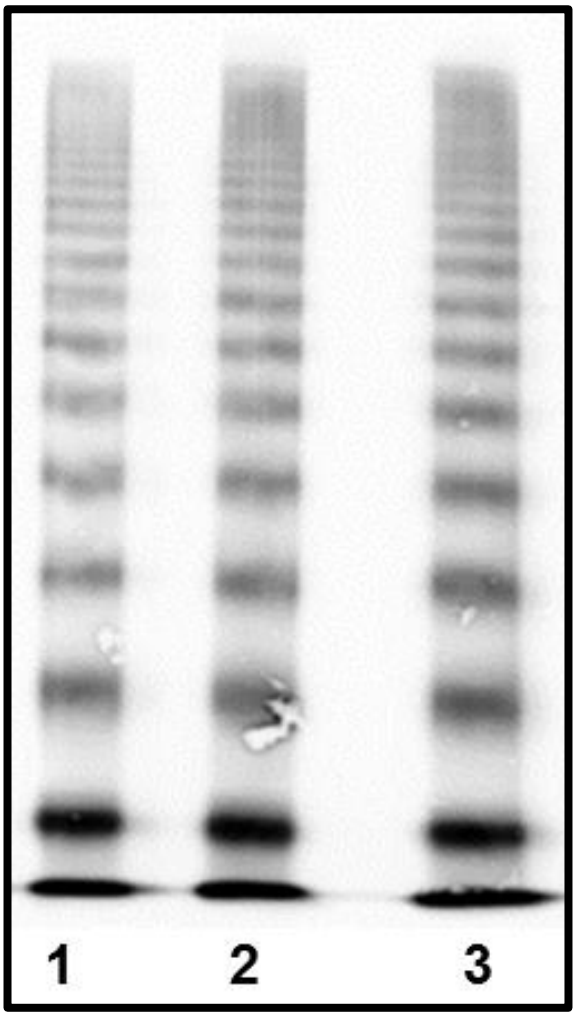

Figure 4.8 Multimer analysis of rVWF p.R924Q secreted from HEK293T cells Multimer pattern of wild-type rVWF (lane 1), mutant homozygous rVWF-Q924 (lane 2) and heterozygous rVWF (lane 3) electrophoresed on 1.6% medium resolution SDS gel at 1:5 dilution are shown. The multimeric composition of rVWF resulting from transfecting cells with mutant and hybrid showed normal VWF multimer patterns similar to the multimeric pattern of wild-type.

4.2.6.1.2. Confocal microscopy of p.R924Q

In vitro expression of p.R924Q located in D3 assembly showed no significant effect in VWF expression or multimerisation. Intracellular imaging of wild-type showed the formation of WPB-like structures with presence of punctuated rounded organelles throughout the cell (Figure 4.9 A and C). Similarly to the wild-type pattern, both homozygous and heterozygous patterns showed the presence of WPB-like organelles that appeared similar in shape and size to ones observed in wild-type (Figure 4.9 D, F, G and I). Confocal microscopy suggested that p.R924Q does not affect VWF synthesis or storage when present alone or in the presence of wild-type.

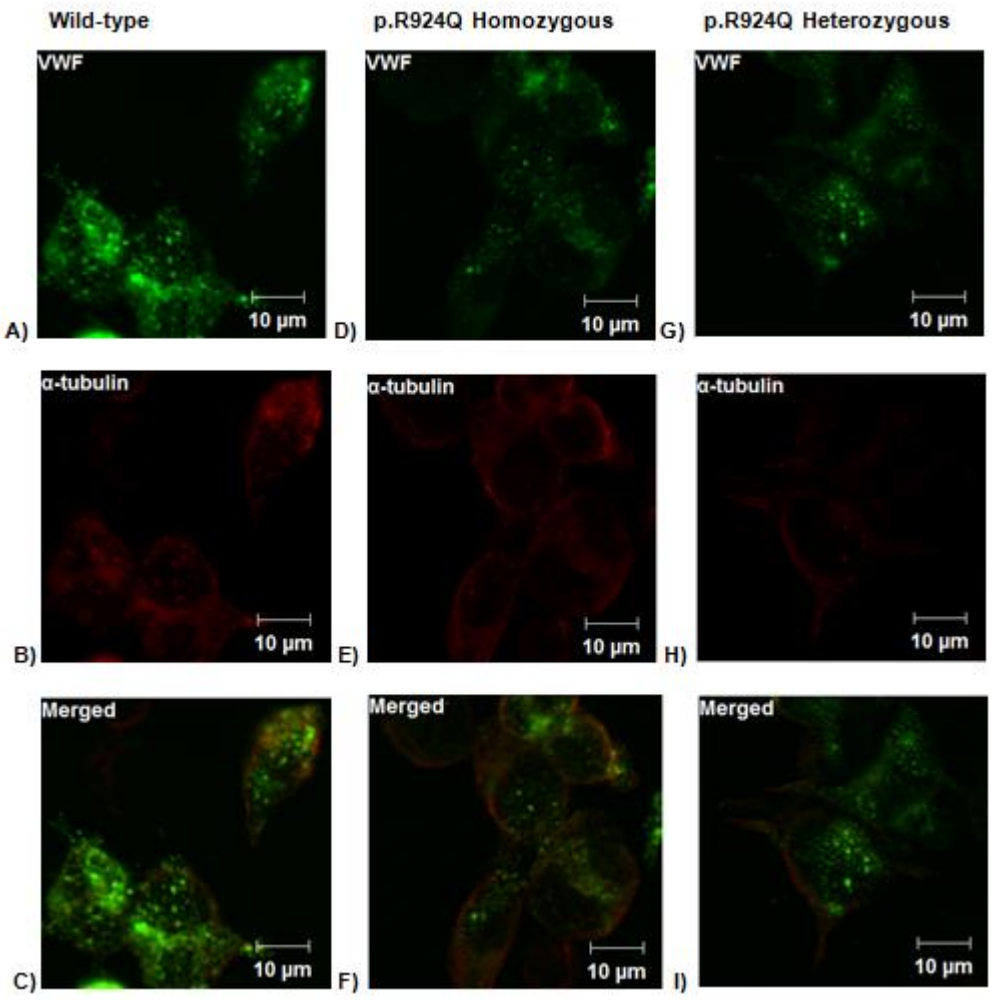

Figure 4.9 Intracellular storage of rWT and rVWF-Q924 mutant in HEK293 cells by confocal microscopy. A, D and G) Represent VWF (green) after transfection of wild-type, homozygous and heterozygous respectively into HEK293 cells. **B, E and H)** Represent the cell membrane marker α-tubulin (red) after transfection of wild-type, homozygous and heterozygous respectively into HEK293 cells. **C, F and I)** Represent merged images of VWF and α-tubulin staining for wild-type, homozygous and heterozygous respectively transfected into HEK293 cells. Cells were stained as described in figure 4.5.

4.2.6.2. Quantitative analysis of supernatant and cell lysates following transfection of HEK293T cells with rVWF-WT and mutant plasmid (rVWF-R1927)

The mean values of secreted VWF obtained by expression of wild-type plasmid alone, mutant plasmid alone (homozygous) and mutant plasmid co-expressed with wild-type (heterozygous) are shown in table 4.6. *In vitro* expression indicated that the observed mean values of secreted VWF of mutant heterozygous and homozygous rVWF-R1927 into growth medium were significantly decreased. In the homozygous form of p.C1927R there was a significant 89% reduction in the secreted VWF, while the heterozygous form resulted in a 81% reduction compared to 100% of rVWF-wild-type (Figure 4.10). The difference in the secreted VWF:Ag level for heterozygous and homozygous states compared to wild-type was statistically significant with *P* values of $p<0.0001$.

In the HEK293T cell lysate, data for secreted VWF (Table 4.7) interestingly showed that intracellular mean values of VWF:Ag of homozygous rVWF-R1927 was significantly increased to 145% ($P<0.0001$) compared to the wild-type (Figure 4.10) and decreased mean values of retained VWF:Ag of heterozygous rVWF-R1927 in the cells compared with the corresponding values of 100% wild-type with values of 78% ($p<0.05$).

In summary, the p.C1927R leads to a significant reduction in the level of secreted VWF in both heterozygous and homozygous states. Also, the expression data from HEK293T cell lysates indicated a significant increase in the level of retained VWF within cells in the homozygous state that could lead to intracellular retention.

Table 4.6 The mean values and standard deviation of secreted VWF:Ag levels post-transfection for WT and mutant plasmids (rVWF-R1927) in HEK293T cells

VWF (Supernatant)	Mean (%)	*SD
rVWF-WT (homozygous)	100.0	15.0
WT:Mut (50:50) (heterozygous)	19.2	2.5
rVWF-C1927R (homozygous)	10.8	1.4

*SD= standard deviation

Table 4.7 The mean values and standard deviation of retained VWF:Ag levels harvested post-transfection for WT and mutant plasmids (rVWF-R1927) in HEK293T cells

VWF (Cell lysate)	Mean (%)	*SD
rVWF-WT (homozygous)	100.0	6.0
WT:Mut (50:50) (heterozygous)	78.0	14.8
rVWF-C1927R (homozygous)	145.0	23.0

*SD= standard deviation

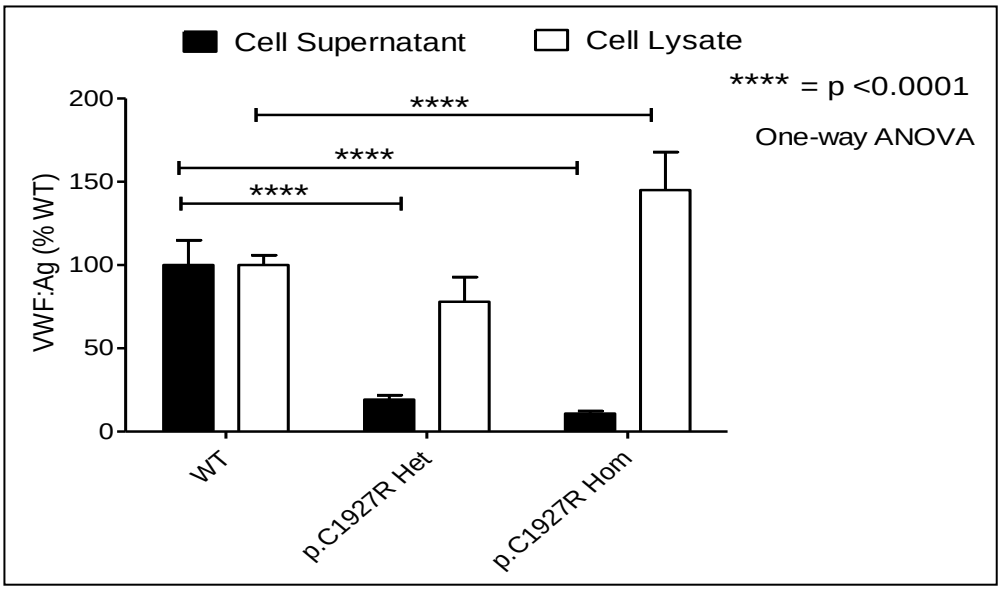

Figure 4.10 Mean levels of VWF:Ag in both supernatant and cell lysates of HEK293T cells transfected with WT and mutant expression plasmids showing the effect of the p.C1927R mutation on *VWF* expression. Results are expressed as a percentage in comparison with wild-type. The horizontal black bars represent the extent of difference between mean values of VWF:Ag between wild-type and mutant VWF. The vertical black bars indicate the standard deviation. Statistical test used is one-way ANOVA.

4.2.6.3. Quantitative analysis of supernatant and cell lysates following transfection of HK293T cells with rVWF-WT and mutant plasmid rVWF [R1927;Q924]

Mutation p.C1927R in combination with p.R924Q located on the same allele were expressed to replicate the allelic mutations found in the patient. The measured values of VWF in cell media and cell lysates are shown in tables 4.8 and 4.9. *In vitro* expression of rVWF [R1927;Q924] showed that the rVWF values measured in growth medium of mutant heterozygous and homozygous were reduced to 32% and 11% respectively with a significant reduction ($p<0.0001$) compared to 100% of rVWF-WT (Figure 4.11).

The VWF level from HEK293T cell lysate of transfected cells obtained from three different experiments of homozygous rVWF-R1927+Q924 was significantly increased to 150% ($P<0.001$) compared to the 100% wild-type (Figure 4.11) and decreased mean values of retained VWF:Ag of heterozygous rVWF-R1927+Q924 in the cell lysates compared with the corresponding values of 100% wild-type with values of 80% ($p>0.05$).

In summary, the p.[C1927R;R924Q] lead to a significant reduction in the level of secreted VWF in both heterozygous and homozygous states. Also, the expression data from HEK293T cell lysates indicated a significant increase in the level of retained VWF within the cells in the homozygous state resulted from intracellular retention. Also, comparing the mean values of released and retained VWF of mutant plasmid rVWF-R1927 alone to mean values of mutant plasmid rVWF [R1927;Q924] showed no significant differences between the two sets of experiments which indicated the lack of effect of p.R924Q on VWF expression. However, the levels of VWF obtained from *in vitro* expression of p.[C1927R;R924Q] was comparable to the expressed VWF levels of p.C1927R alone.

Table 4.8 The mean values and standard deviation of secreted VWF:Ag levels post-transfection for WT and mutant plasmids (rVWF-R1927+R924Q) in HEK293T cells

VWF (Supernatant)	Mean (%)	*SD
rVWF-WT (homozygous)	100.0	6.0
WT:Mut (50:50) (heterozygous)	32.0	8.0
rVWF-C1927R+R924Q (homozygous)	11.0	2.7

*SD= standard deviation

Table 4.9 The mean values and standard deviation of retained VWF:Ag levels harvested post-transfection for WT and mutant plasmids (rVWF-R1927+R924Q) in HEK293T cells

VWF (cell lysate)	Mean (%)	*SD
rVWF-WT (homozygous)	100.0	7.0
WT:Mut (50:50) (heterozygous)	80.0	11.5
rVWF-C1927R+R924Q (homozygous)	150.0	32.0

*SD= standard deviation

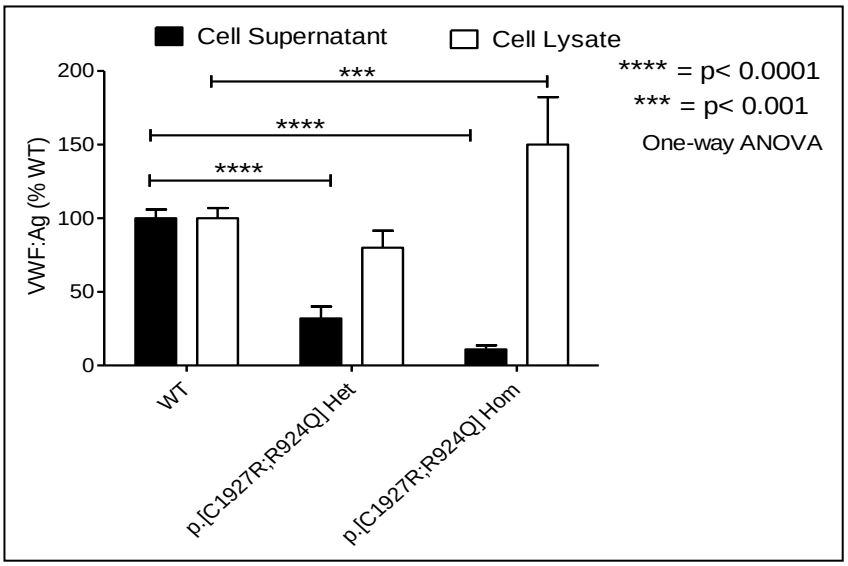

Figure 4.11 Mean levels of VWF:Ag in both supernatant and cell lysates of HEK293T cells transfected with WT and mutant expression plasmids showing the effect of p[.C1927R;R924Q] mutation on VWF expression. Results are expressed as a percentage in comparison with wild-type. Black line represent the significant difference of mean value of VWF:Ag between wild-type and mutant VWF. Upper bar indicated the standard deviation. Statistical test used is one-way ANOVA.

4.2.6.3.1. Multimer analysis for the rVWF-R1927 and rVWF [R1927;Q924] rVWF protein secreted from HEK293T cells

Multimer analysis of VWF secreted from HEK2293T cells into the growth medium from transfection of wild-type plasmid, rVWF-R1927 plasmid and co-transfection of mutant/wild-type in addition to similar experiments for rVWF-R1927+Q924 was analysed using 1.6% medium resolution SDS agarose gel. As a result, the HMW-VWF multimers observed in the homozygous form of the p.C1927R alone showed the presence of some HMW and dimers indicating that p.R924Q may acts as a modifier of phenotype (Figure 4.12A2). The multimer analysis for the p.[C1927R;R924Q] mutations revealed a complete absence of HMW-VWF multimers in the homozygous form with presence of only dimers in comparison to wild-type multimers (Figure 4.12B2). The analysis of heterozygous form multimer showed normal multimers in p.C1927R when expressed alone and a relatively decrease of HMW-VWF in comparison to wild-type multimers in p.[C1927R;R924Q] mutant (Figure 4.11 A3&B3).

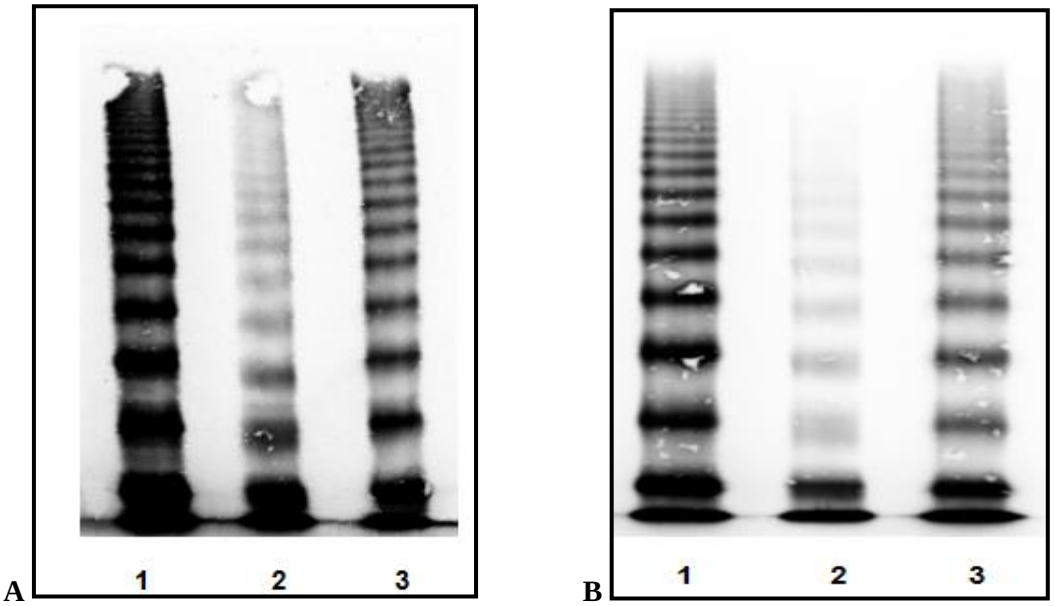

Figure 4.12 Multimer analysis of secreted rVWF from HEK293T cells transfected with p.C1927R (A) and p.[C1927R;R924Q] (B) mutants. Multimer analysis of wild-type (lane 1), mutant rVWF (lane 2) and hybrid rVWF (lane 3) electrophoresed on 1.6% medium resolution SDS gel at 1:5 dilutions respectively are shown. The multimeric composition of rVWF-R1927 (A) and rVWF-R1927+Q924 (B) resulting from transfecting cells in the heterozygous forms (lanes A3 & B3) showed a reduced proportion of HMW but not loss of HMW multimers in comparison to wild-type multimers in p.[C1927R;R924Q] and normal multimers in p.C1927R alone. The homozygous form of the p.[C1927R;R924Q] revealed a totally loss of HMW-VWF multimers but there are some of HMW-VWF present in p.C1927R alone (lanes A2 & B2).

4.2.6.3.2. Confocal microscopy of p.C1927R and p.[C1927R;R924Q]

In vitro expression of the p.C1927R revealed a secretion defect resulting from intracellular retention. In the wild-type form, small rounded punctate WPB-like organelles were present (Figure 4.13 A and C). Confocal analysis of the p.C1927R mutant in the homozygous form showed the presence of punctuated rounded WPB-like vesicles, but localised VWF diffuse staining patterns were also observed in the analysed cross-section (indicated with white arrow, Figure 4.13 D) in comparison to the wild-type (Figure 4.13 D and F). This diffuse pattern may be explained due to stacking of WPB-like organelles on top of each other. Unlike the homozygous form, the heterozygous forms of p.C1927R showed the presence of punctuate rounded WPB-like organelles similar to those observed in wild type (Figure 4.13 G and I). These findings suggested that p.C1927R does influence in WPB storage. The pattern of localised diffuse pattern observed in the homozygous form supports the *in vitro* findings of increased intracellular retention.

Similarly to p.C1927R, the confocal imaging of p.[C1927R;R924Q] showed the presence of WPB-like organelles with presence of diffuse staining patterns similar to WPB and patterns shown in p.C1927R in homozygous form. These diffuse patterns represent accumulation of VWF over each other (indicate with white arrow, Figure 4.14 D and F). These organelles appeared relatively larger in size compare to those present in wild-type. In the heterozygous form of p.[C1927R;R924Q], WPB-like organelles are visualised and appeared punctuate and round similar to those seen in wild type (Figure 4.14 G and I). Confocal analysis indicated that p.[C1927R;R924Q] influences WPB storage.

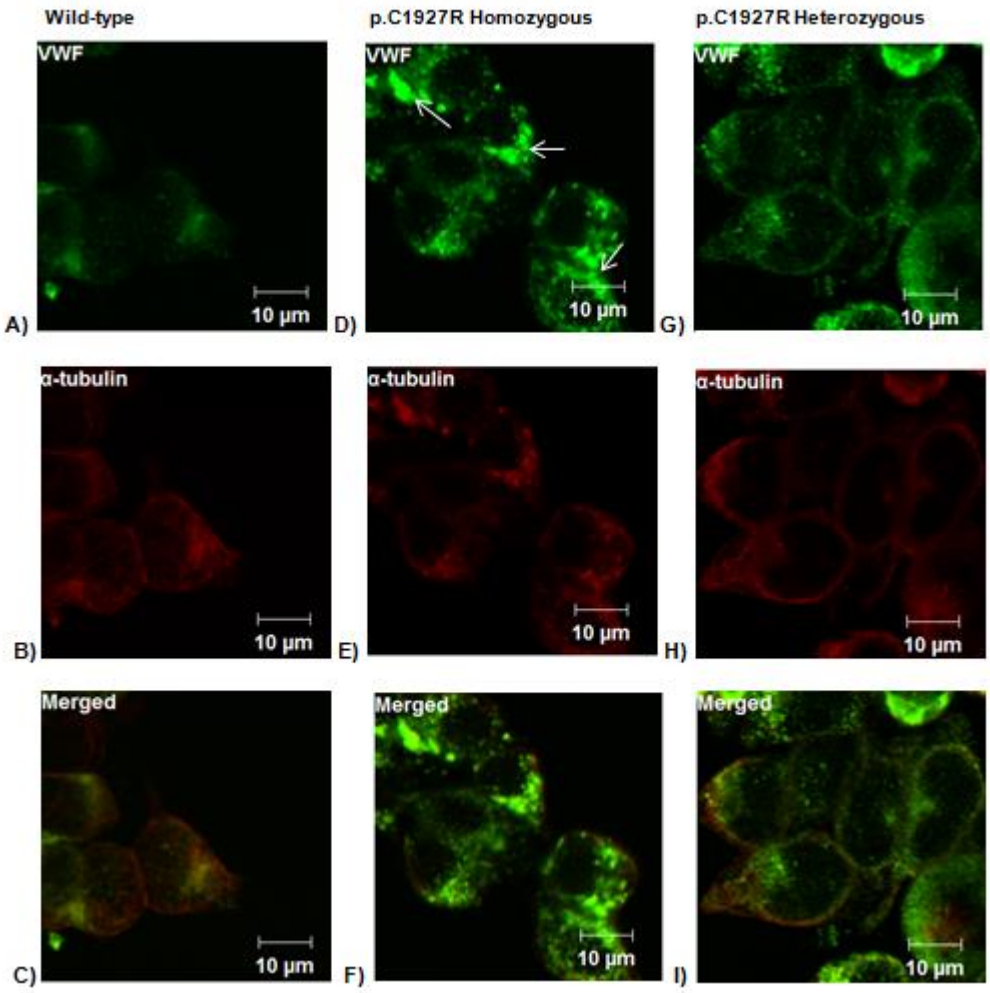

Figure 4.13 Intracellular storage of rWT and rVWF-R1927 mutant in HEK293 cells by confocal microscopy. A, D and G) Represent VWF (green) after transfection of wild-type, homozygous and heterozygous plasmids respectively into HEK293 cells. White arrows indicate regions where there was diffuse staining of VWF within the cell. **B, E and H)** Represent the cell membrane marker α-tubulin (red) after transfection of wild-type, homozygous and heterozygous respectively into HEK293 cells. **C, F and I)** Represent merged images of VWF and α-tubulin staining for wild-type, homozygous and heterozygous respectively transfected into HEK293 cells. Cells were stained as described in figure 4.5.

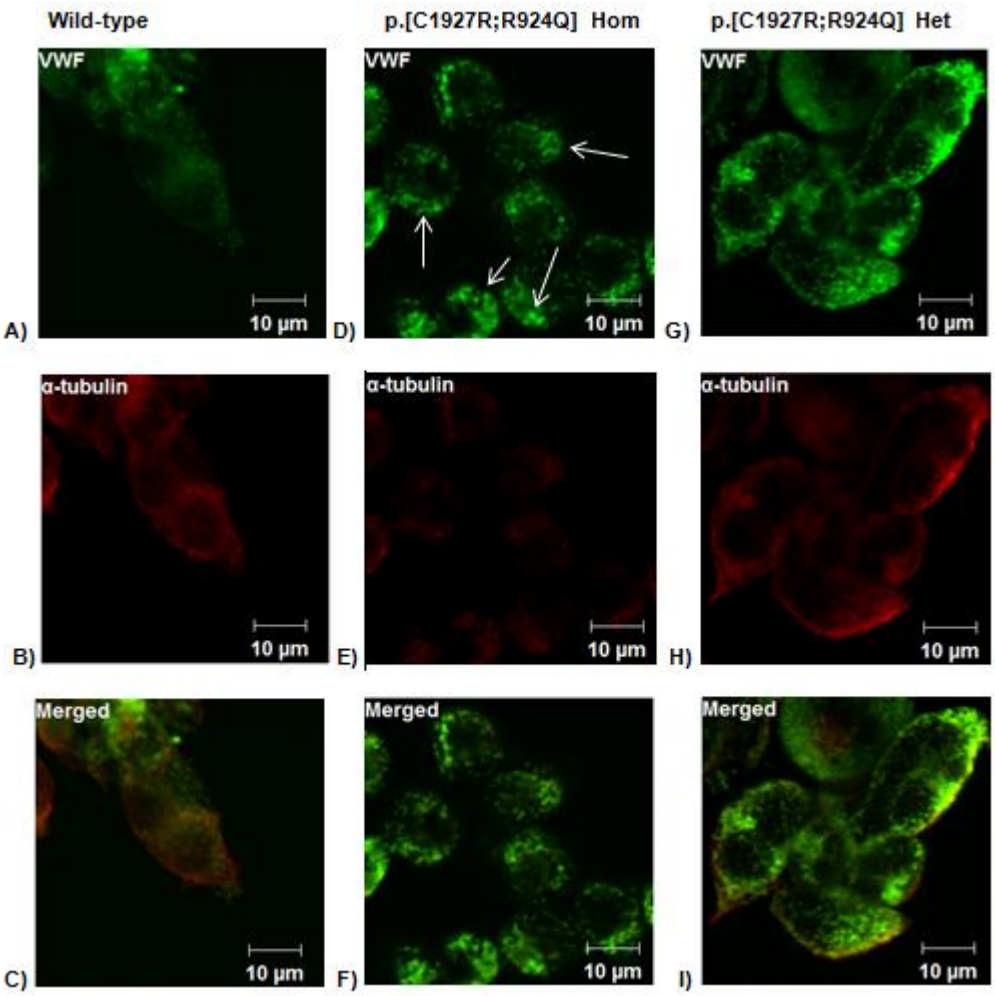

Figure 4.14 Intracellular storage of rWT and rVWF-R1927+Q924 mutant in HEK293 cells by confocal microscopy. A, D and G) Represent VWF (green) after transfection of wild-type, homozygous and heterozygous plasmids respectively into HEK293 cells. White arrows indicate regions where there was diffuse staining of VWF within the cell. **B, E and H)** Represent the cell membrane marker α-tubulin (red) after transfection of wild-type, homozygous and heterozygous respectively into HEK293 cells. **C, F and I)** Represent merged images of VWF and α-tubulin staining for wild-type, homozygous and heterozygous respectively transfected into HEK293 cells. Cells were stained as described in figure 4.5.

.

4.2.6.3.3. Confocal microscopy of p.C1927R and p.[C1927R:R924Q] to determine retention of VWF in the ER

Confocal analysis using VWF and PDI markers revealed the formation of rounded punctate WB-like organelles in the wild-type as observed in figure 4.15 A and C. In comparison to the WPB-like organelles observed in the wild-type images, similar rounded punctuate organelles were seen accompanied by accumulation of VWF in the ER when p. C1927R expressed in the homozygous form (Figure 4.15 E and G). In the heterozygous form of p.C1927R, similar size of pseudo WPB organelles were observed with also presence of VWF significantly retained in the ER (Figure 4.15 I and K). These findings indicated that VWF appeared to be retained in the ER.

The confocal images of p.[C1927R;R924Q] were also analysed using co-staining of VWF and PDI-ER markers. The obtained findings were similar to those observed when p.C1927R expressed alone. In the homozygous form of p.[C1927R;R924Q], the rounded punctuate pseudo WPB organelles were found (Figure 4.16 A and C) and considerable retention of VWF in the ER was observed (Figure 4.16 E and G). The retention of VWF in the ER also was observed when p.[C1927R;R924Q] was co-transfected with wild-type. The retention was less pronounced than that seen in the homozygous form (Figure 4.16 I and K). These results indicated that both p.C1927R and p.[C1927R;R924Q] variants caused marked retention of VWF in the ER.

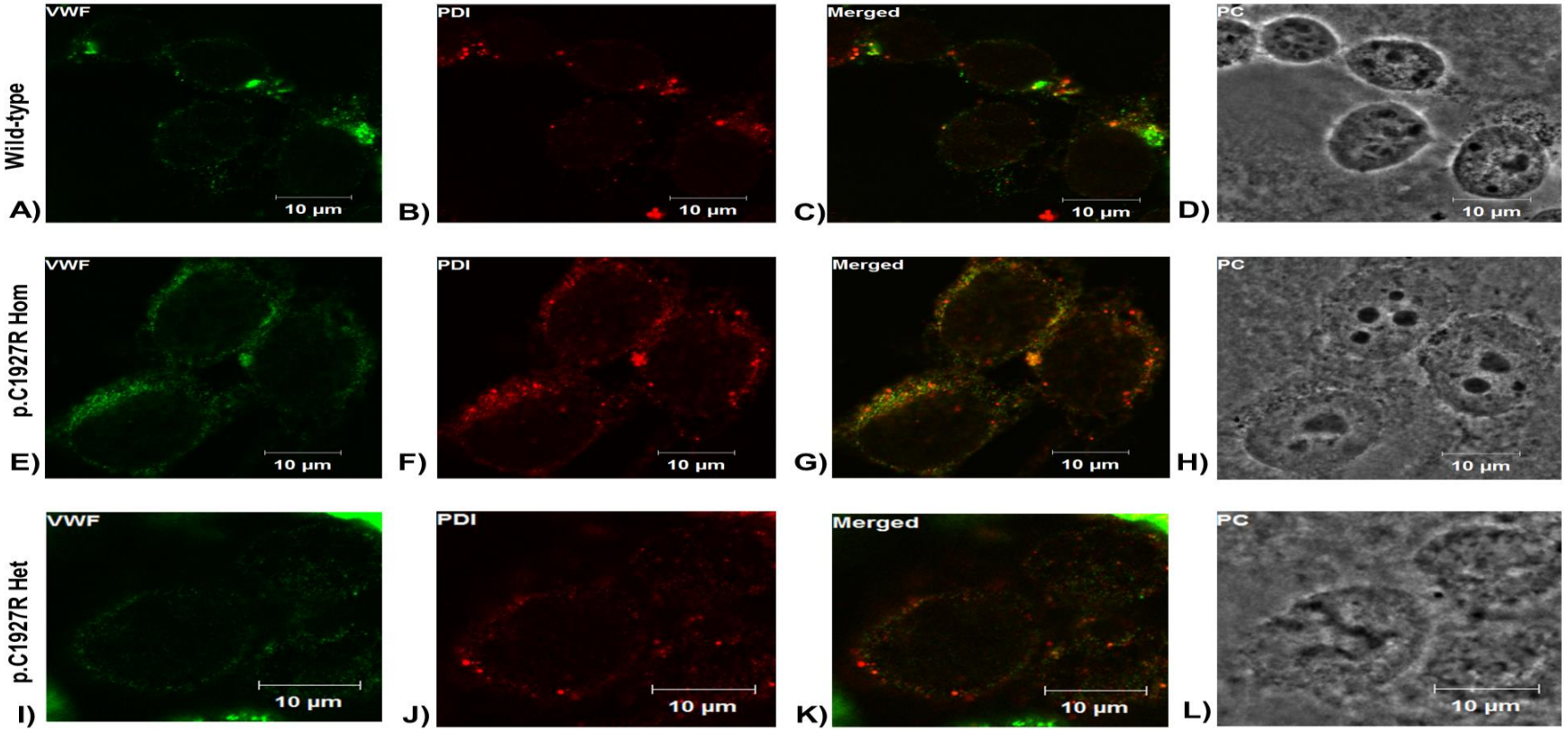

Figure 4.15 Intracellular localisation of VWF in rWT and rVWF-R19271 mutant in HEK293 cells. A, E and I) Represent VWF (green) after transient transfection of wild-type, homozygous and heterozygous plasmids respectively into HEK293 cells. **B, F and J**) Represent the ER marker PDI (red) after transfection of wild-type, homozygous and heterozygous respectively into HEK293 cells. **C, G and K**) Represent merged changes of VWF and PDI staining for wild-type, homozygous and heterozygous respectively transfected into HEK293 cells**. D, H and L**) Represent phase contrast (PC) image for wild-type, homozygous and heterozygous respectively transfected into HEK293 cells. Cells were stained as previously described.

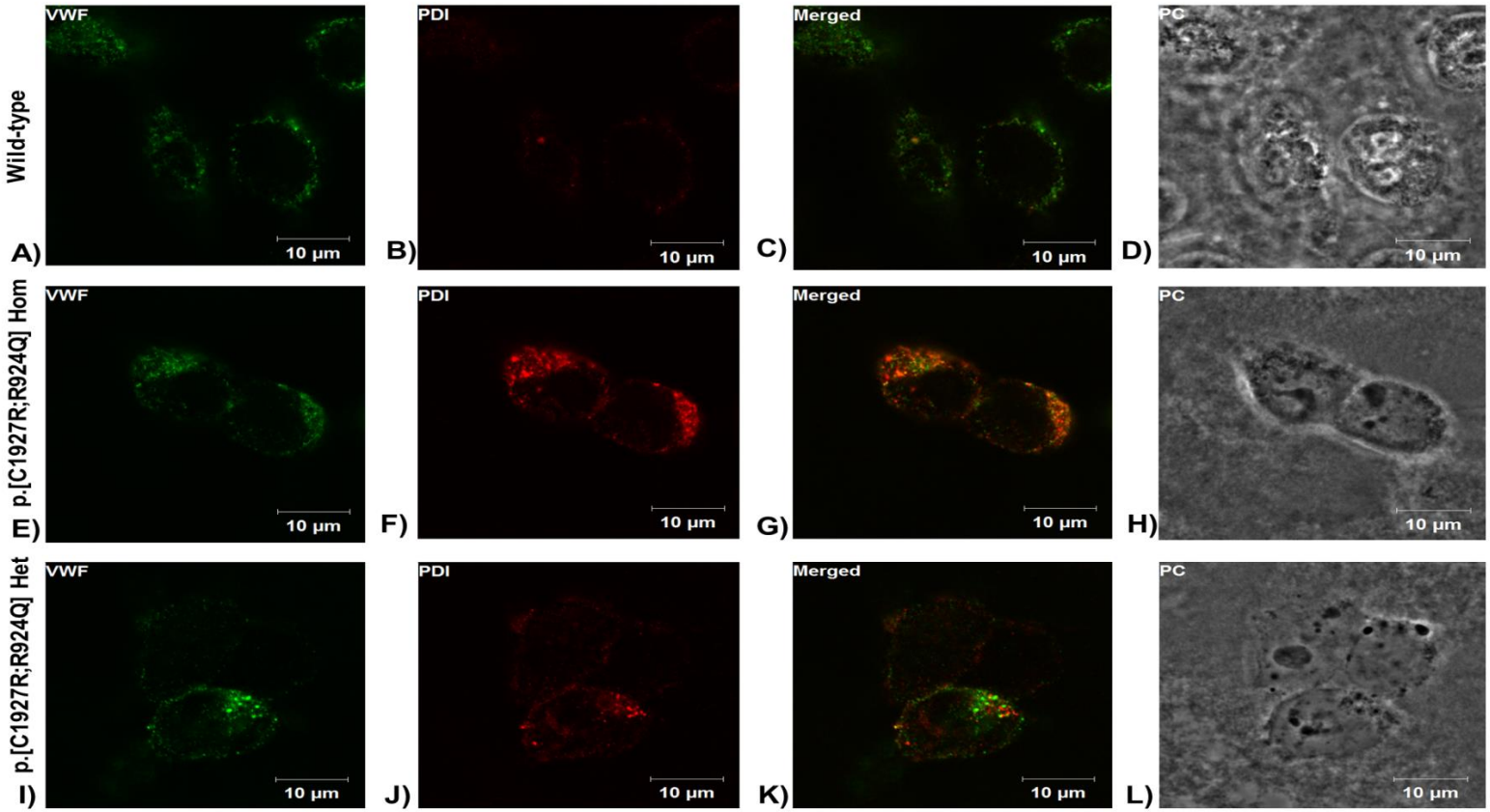

Figure 4.16 Intracellular localisation of VWF in rWT and rVWF-R1927+Q924 mutant in HEK293 cells. A, E and I) Represent VWF (green) after transient transfection of wild-type, homozygous and heterozygous plasmids respectively into HEK293 cells. **B, F and J**) Represent the ER marker PDI (red) after transfection of wild-type, homozygous and heterozygous respectively into HEK293 cells. **C, G and K**) Represent merged changes of VWF and PDI staining for wild-type, homozygous and heterozygous respectively transfected into HEK293 cells**. D, H and L**) Represent phase contrast (PC) image for wild-type, homozygous and heterozygous respectively transfected into HEK293 cells. Cells were stained as previously described.

4.3. Discussion

In this chapter, *in vitro* expression studies of 4 candidate missense heterozygous mutations identified in patients historically diagnosed with type 1 VWD was performed. These experiments have been designed to examine whether the mutations identified might be responsible for the disease phenotype and considered as causative for the observed partial quantitative deficiency of VWF in the investigated patients. Another aim of these expression studies was to define the possible mechanisms associated with each genetic change. The expressed missense mutations included; one novel missense mutation found in one family p.W2271G (Section 3.6.1), where the other two missense mutations were detected previously during the EU study; p.R924Q identified in several families and p.C1927R found in combination with p.R924Q (Section 3.6.5) in addition to expression of both mutation p.[C1927R;R924Q] that were found on the same allele in one family (Section 3.6.5.1).

4.3.1. *In vitro* expression of p.W2271G

When mutant plasmid rVWF-G2271was transfected in a homozygous form, the obtained levels of secreted VWF:Ag showed a significant reduction of VWF:Ag ($p<0.0001$). The reduced secretion of VWF was accompanied by a significant increase in the retained VWF ($p<0.05$) compared to the corresponding levels of wild type. The homozygous form of rVWF-G2271 mutant indicated complete loss of HMW-VWF multimers.

When the mutated plasmid rVWF-G2271 was co-transfected with the recombinant wild type to mimic the heterozygous state, the levels of VWF:Ag secreted were significantly lower than levels of wild type ($p<0.05$) with no significant change of retained VWF:Ag in cell lysates ($p>0.05$) compared to wild type. The level of retained VWF:Ag was significantly increased when both mutated plasmids were co-transfected compared to co-transfection of mutant plasmid with wild-type. However, p.W2271G resulted in a reduction of VWF secretion into the growth medium.

Multimer analysis of secreted mutant VWF produced from transfection of rVWF-G2271 plasmid in the heterozygous form showed nearly normal multimers with a relative reduction which is similar to those observed in patients and AFM plasma. The mild differences between normal multimer patterns observed in patient plasma who harbour p.W2271G in the heterozygous form and the multimers obtained from *in vitro* expression can be explained due to variation between cell lines used *in vitro* from *in vivo* (Figure 4.4).

Similar to multimerisation, the missense mutation p.W2271G located in D4 assembly has an effect in VWF storage. It was able to produce WPB-like granules, but pseudo WPB-organelles were stacked over each other and retained in the ER compared to those present in wild-type.

Confocal microscopy suggested the occurrence of intracellular retention of VWF in the ER. This mutant was able to synthesise VWF although it impairs multimerisation and storage.

Therefore, the homozygous form of p.W2271G resulted in reduced secretion, abnormal multimers and VWF storage but the heterozygous form affected only VWF secretion and storage.

However, the achieved results from transfection studies indicated that p.W2271G resulted in a significant reduction (77%) of secreted rVWF from mutant heterozygous compared to wild-type indicating a dominant negative nature of this mutation. These findings are similar to VWF level *in vivo* and similar to the phenotypic data found in the affected members (Section 3.6.1.1). The affected members who were heterozygous for the mutation p.W2271G presented with mild bleeding symptoms (BS: 2-7) and demonstrated a moderate reduction of phenotype data and blood group genotype of O/A (Section 3.6.1.1). The levels of VWF:Ag and VWF:RCo in the IC who harboured this mutation in the heterozygous state was decreased to 37 and 32 IU/dL respectively with normal plasma multimers (Appendix 15).

Therefore, *in vitro* expression of the p.W2271G mutation into HEK293T cells indicated that secretion of mutated rVWF-G2271 was significantly reduced due to intracellular retention that is impaired due to the effect of the mutation on intracellular transport. The significant defect resulting from p.W2271G can be possibly explained due to a dominant negative mechanism when mutant protein impairs the activity of wild-type usually by dimerizing with it.

In silico predictions indicated that this mutation is probably damaging and *in vitro* expression confirmed these predictions.

An essential aim of expression studies is to investigate the disease causing mechanism. The presence of a mutation within *VWF* can alter the VWF processing including assembly, secretion and expression and reduced secretion can thus be explained. Some mutated protein is characterized by mis-folding and poor assembly in the ER. In mammals, there are proteins found in the ER called chaperones that act as a checkpoint for the presence of any mis-folded, incompletely assembled proteins. When mis-folded or mutated protein is recognised by chaperones in the ER, they bind the mutated protein and rather than pass protein to the Golgi apparatus, chaperones support a reversed transport of mutated protein from ER to the cytosol, where they are retained and then degraded by the proteasome complex (Brodsky and McCracken, 1997). These chaperones include calnexin (CNX) and calreticulin (CRT) (Ellgaard et al., 1999). However, the novel p.W2271G mutation appear to cause intracellular retention and accumulation of VWF in the ER that may impair the intracellular transport resulting in reduced secretion into the growth media when mutant plasmid was transfected in HEK293T cells. These

findings suggested that p.W2271G is likely to act through a dominant-negative mechanism as the level of secreted VWF in the heterozygous state is less than 50% (23%). A dominant-negative effect occurs when the mutant allele impairs the activity of the wild-type allele.

Intracellular retention has been observed previously in different mutations located in D4 assembly associated with partial quantitative deficiencies of VWF in patients with type 1 and type 3 VWD. Eikenboom *et al* (2009) expressed 14 *VWF* mutations identified in patients with type 1 VWD from the MCMDM-1VWD study. All patients were heterozygous for these mutations that were transfected in COS-7 cells. Out of 14, four candidate mutations were located in the D4 assembly including; p.L2207P, p.C2257S, p.R2287W and p.P2063S. The transient transfection of rVWF-P2207 and rVWF-S2257 in COS-7 cells showed significant intracellular retention, highly reduced secretion and formation of HMW multimers with an altered anodic band migration the VWF compared with wild type. Moreover, the co-transfection of rVWF-P2207 and rVWF-S2257 with rVWF-WT indicated reduced VWF secretion accompanied by intracellular retention and normal multimers (Eikenboom et al., 2009). The expression of the other two mutations p.[R2287W;P2063S] located on the same allele in the D4 assembly that do not involve cysteine residues indicated mild reduction of secretion of p.R2287W while p.P2063S was considered as a non-pathogenic (Eikenboom et al., 2009, Hampshire and Goodeve, 2013). Also, the transfection of two missense mutations located in the D4 assembly identified in type 3 patients, p.C2184S and p.C2212R that both involved cysteine changes in COS-7 cells indicated a severe reduction in secretion of 83% and 79% respectively due to intracellular retention within the cell and abnormal multimers, while the co-transfection performed to confirm the recessive nature of these mutations showed reduced secretion of 45% and 11% respectively in comparison to wild-type and normal multimers (Solimando et al., 2012). However, the cells used in these studies, COS-7 cells do not form WPB-like structures and hence are not fully representative of the VWF expression pathway.

Type 1 VWD is mostly inherited as an autosomal dominant trait and patients usually present with mild to moderate reduction in VWF:Ag, VWF:RCo and FVIII:C with normal multimers that is characterized by a partial quantitative deficiency of VWF (Keeney and Cumming, 2001). The achieved results obtained by expression studies of p.W2271G demonstrated that this mutation resulted in reduced secretion due to intracellular retention of VWF which further causes partial quantitative deficiency of plasma VWF and suggests the dominant negative nature of this variant. On the basis of impaired secretion and intracellular retention, p.W2271G is considered as the cause of type 1 VWD phenotype. Therefore, these findings confirmed that this mutation is responsible for the patient phenotype and is classified as type 1 VWD.

4.3.2. *In vitro* expression of p.C1927R

In vitro expression of rVWF-R1927 indicated that this mutation significantly reduced the level of secreted VWF:Ag ($p<0.0001$) in both homozygous and heterozygous states and this reduction was accompanied by a significant increase in the retained VWF:Ag ($p<0.0001$) compared to wild type when transfected in a homozygous form only. The multimer analysis of rVWF in the homozygous form showed a loss of HMW-VWF, but some HMW-VWF multimers were present while a normal HMW multimers were observed in the heterozygous form. These findings are similar to the multimers found in the AFM (I:2) plasma who also carries this mutation in addition to p.R924Q.

However, *in vitro* expression of p.C1927R suggested that this mutation impaired VWF secretion from the HEK293T cells into the growth medium due to the intracellular retention in the cell. p.C1927R resulted in a significant VWF secretion defect potentially through a dominant negative mechanism where the mutant VWF alters the function of wild-type. Although p.C1927R impairs VWF secretion, it does not affect VWF synthesis and was able to produce WPB organelles, but could impair VWF storage.

These findings suggested that p.C1927R appeared to reduce VWF secretion, impair multimerisation and VWF storage when expressed in the homozygous form, but the heterozygous form of p.C1927R appeared to influence VWF secretion and storage significantly. Confocal analysis suggested that this variant leads to secretion defect due to retention of VWF in the ER.

In silico predictions using several prediction tools showed that the loss of cysteine in this mutation is probably damaging which is consistent with the *in vitro* expression findings (Section 3.6.5.2). The substitution of cysteine which is required for interchain disulphide bond formation between cysteine amino acids by arginine is likely to impair multimer formation and lead to retained and degraded mis-folded mutant protein within the ER thereby reducing secretion of VWF. The disulphide bonds between adjacent cysteine are important for proper protein folding, packaging and release. The presence of any mutation causing cysteine loss may impair protein folding and multimerization, thereby resulting in retention of VWF in ER and reducing secretion due to degradation of mutant protein in the ER. p.C1927R is located in the linker between the A3 and D4 domains according to the original domain structure (Figure 1.1). This region between A3 and D4 domains is rich with cysteine and was re-annotated and named as D4N as a part of D4 assembly (Figure 1.1) (Zhou et al., 2012). The D4N region has a large number of cysteines (8) and losses of cysteine results in unpaired cysteines which can affect protein folding and tertiary structure and thereby is likely to create abnormal multimer formation and retention of VWF within cells.

The results obtained by expression studies of p.C1927R are consistent with phenotypic data found in affected members who have this mutation in combination with p.R924Q as p.R924Q had no significant effect on VWF expression. Levels of VWF and FVIII:C were reduced in plasma in patients who harboured p.R924Q in combination with other change (Hickson et al., 2010). The two AFM who had the p.C1927R and p.R924Q only on the same allele presented with moderate reductions in the level of VWF:Ag ranging between 19-57 IU/dL and moderate reduction in the levels of VWF:RCo ranging between 18-58 IU/dL and this variations may be due to variable penetrant pattern and age in the AFM. One AFM had normal multimers and the other one had abnormal multimers (Appendix 16). The achieved results from heterozygous transfection of rVWF-R1927 and rVWF-Q924 together on the same allele showed a 68% reduction of secreted rVWF compared to wild-type. The phenotypic data found in AFM (I:2) and UFM (II:3) who harboured both mutations is almost different to the VWF expressed in this study and this may due to in-complete penetrance or due to different ages (Appendix 16). Also, the IC who has both mutations in addition to an intronic donor splice site mutation c.1533+1G>T in intron 13 presented with a high BS (18), severe reduction of VWF:Ag, VWF:RCo (3 IU/dL) and FVIII:C (7) in addition to an absence of multimers (Section 3.6.5.1) as the donor splice site variant was likely to contribute to the abnormal phenotype observed in the IC due to NMD which prevents protein formation in addition to the effect of other mutations. However, the missense p.C1927R mutation can be considered as the major contributor to the partial quantitative deficiency of VWF in the two AFM and the UFM who harboured these two variant.

Several mutations involving the loss of cysteine residues located in the D4 assembly have been reported. The expression of p.C2257S located in the D4 assembly identified in a type 1 VWD patient in COS-7 showed a very similar effect of reduced secretion and intracellular retention similar to our findings (Eikenboom et al., 2009). Moreover, the transfection of two missense mutations located in the D4 assembly identified in type 3 patients, p.C2184S and p.C2212R into COS-7 cells indicated a severe reduction, intracellular retention within the cell and abnormal multimers in homozygous form as previously described (Solimando et al., 2012).

The achieved results obtained from expression studies showed that p.C1927R is responsible for the moderate reductions of VWF levels and appears to act through dominant negative mechanism and could indicates the dominant negative nature of this variant.

4.3.3. *In vitro* expression of p.R924Q

The p.R924Q mutation appeared to have no significant effect on the level of VWF compared to expressed wild type when transfected in both heterozygous and heterozygous states. Although

p.R924Q is located within D3 assembly which is essential for the normal multimerization process, a full array of normal multimers, normal synthesis and normal storage were observed in both homozygous and heterozygous forms. Therefore, *in vitro* expression studies have indicated that p.R924Q does not affect VWF synthesis, storage or multimerisation significantly when present either in homozygous or heterozygous form.

In silico predictions showed that this mutation had no significant effect either on VWF expression or on splice sites which is compatible with earlier expression findings using COS7 cells (Hickson et al., 2010). The level of VWF:Ag and VWF:RCo in AFM who have the p.R924Q in combination with p.C1927R show a moderate reduction of VWF:Ag and VWF:RCo levels. When reviewing EU cases, the AFM (P8F1I:1) who had only p.R924Q presented with high BS (13), normal to a mild reduction of VWF levels and normal multimers, while the IC P6F5II:1 who had p.R924Q in combination with p.R1205H that is known to increases VWF clearance showed markedly decreased levels of VWF:Ag, VWF:RCo and FVIII at 11, 7 and 18 respectively with a high BS at 18, but the UFM (II:3) who had only p.R924Q presented with normal BS (-1) and normal phenotypic levels, with all 3 parameters above 50 IU/dL (Appendix 17). Within the EU study, a number of IC who harbour only p.R1205H presented with high BS with mean value of 12 ranging between 6-18, VWF:Ag mean value of 9 ranging between 3-21 IU/dL), VWF:RCo mean value of 8 ranging between 3-25 IU/dL and FVIII:C with mean value of 16 ranging between 3-32 IU/dL indicated the mild effect of p.R924Q on VWF level. Also, the P7F3II:1 IC who had p.R924Q co-inherited with p.R854Q that impairs binding to FVIII showed a reduction of VWF:Ag, VWF:RCo and FVIII at 25, 38 and 15 IU/dL respectively, but their AFM (I:2) who had only p.R924Q presented with high BS (8) and normal phenotypic data (Goodeve et al., 2007, Hickson et al., 2010). It has been observed the presence of high BS in patient with p.R924Q although normal levels of VWF and this may be explained due to presence of other factors that cause bleeding without affecting VWF levels.

The MCMDM-1VWD study has reported the presence of p.R924Q mutation in 6 IC, one was heterozygous and the remaining five had this mutation in combination with other variants. The identified p.R924Q in association with second mutation include: 1) p.[R924Q;R1351L] on the same allele; 2) p.[R1205H];[R924Q] in 2 different alleles; 3) c.3675-14G>A + p.R924Q in 2 different alleles; 4) p.[R854Q];[R924Q] in two different alleles and 5) p.[C1927R;R924Q] on the same allele (Goodeve et al., 2007). It was observed that the presence of p.R924Q alone is insufficient to influence VWF, but when combined with other mutation may affect disease phenotype (Goodeve et al., 2007). Moreover, it was reported that the IC who was heterozygous for *de novo* p.R1205H in combination with p.R924Q that inherited from his mother presented

with moderate to severe bleeding symptoms, unlike the mother who showed mild bleeding symptoms due to presence of p.R924Q mutation alone and blood group O (Woods et al., 2013).

This variant was identified in 3.6% of IC diagnosed with type 1 VWD in EU study and was found almost in 1.4% of healthy Caucasian alleles (Goodeve et al., 2007, Hickson et al., 2010). All three multicentre type 1 VWD cohort studies have reported the presence of the c.2271G>A variant in IC. It was documented as the second most frequent variant in the Canadian study and was considered as a benign change in the UK study (Cumming et al., 2006, Goodeve et al., 2007, James et al., 2007). Also, Casais *et al* (2006) have reported the presence of heterozygous c.2771G>A variant in three symptomatic patients who had normal levels of VWF:Ag and reduced levels of FVIII (Casais et al., 2006).

Although many studies had examined p.R924Q, there was inconsistency in the behaviour and characteristics of this genetic variant (Table 4.10). The p.R924Q variant was first described as a polymorphism in a type 2N VWD patient who was compound heterozygous with p.C1060R on the other allele and had moderately reduced FVIII binding capacity. *In vitro* expression of rVWF-Q924 showed normal binding to FVIII (Hilbert et al., 2003). Casais *et al* (2006) linked the presence of this mutation with mild bleeding symptoms and decreased FVIII/VWF:Ag ratios while Lester *et al* (2008) suggested that this variant in some cases may behave as a null allele (Lester et al., 2008). Many experimental expression studies have investigated the effect of p.R924Q on VWF expression, FVIII and its binding to VWF in order to define the exact effect on VWF and the pathogenic significance but none of them had defined the exact mechanism. *In vitro* expression of rVWF-Q924 in COS-7 and AtT-20 cells indicated that p.R924Q has no significant effect on VWF expression, synthesis, storage or intracellular trafficking (Berber et al., 2009). Also, following immunofluorescence antibody staining the WPB granules from patient's BOEC line appeared larger in size WPB and diffuse cytosolic pattern in comparison to normal WPB size and type observed in cells from normal individual (Berber et al., 2009). Moreover, Berber et al (2009) suggested that not all alleles harbour p.R924Q are identical and the probability of the presence of an additional defect on the same allele carries p.R924Q may explain the variation of BOEC morphology between patients and healthy individuals. p.R924Q was found in a compound heterozygous patient with an additional type 2N mutation (p.R816W), low levels of FVIII and reduced FVIII binding capacity (VWF:FVIIIB). Hickson *et al* (2010) demonstrated that rVWF-Q924 had a benign effect on VWF expression, normal levels of FVIII:C and VWF, normal multimers, normal binding capacity and normal clearance (Hickson et al., 2010). However, these findings suggested that the p.R924Q alone has a minor influence on VWF expression unless co-inherited with a second mutation. In some individuals, however p.R924Q behaves differently and this may due to the presence of a further un-identified second sequence variant on the same allele change. Moreover, Hickson *et al* (2010) observed that

individuals with blood group O in combination with p.R924Q had reduced levels of VWF:Ag and FVIII compared to individuals with this variant who had non-O blood groups. The levels of VWF:Ag and FVIII:C in heterozygotes for c.2771G>A in combination with blood group O was 35% lower compared to those with non-O blood groups who were homozygous for c.2771G (Hickson et al., 2010). These findings suggested that the presence of p.R924Q alone is insufficient to influence VWF, but co-inheritance with a second *VWF* mutation may contribute to disease phenotype (Berber et al., 2009, Hickson et al., 2010). The achieved results in this study showed a mild effect of p.R924Q on VWF expression which is compatible with previous findings.

Table 4.10 List of publications relevant to p.R924Q variant

Author	Year	Findings
Hilbert *et al*	2003	Described as a polymorphism in type 2N VWD patient
Casais *et al*	2006	Causes mild bleeding and decreases FVIII:C/VWF:Ag ratios
Lester *et al*	2008	Behaves as a null allele
Berber *et al*	2009	Expression study showed no significant effect on VWF expression, synthesis or storage. Low level of FVIII when co-inherited with type 2N VWD mutation. Abnormal large WPB and diffuse staining pattern were observed in patient BOEC line
Hickson *et al*	2010	Had no significant effect on VWF expression, normal clearance and normal binding to FVIII
Woods *et al*	2013	Presence of p.R924Q alone insufficient to influence VWF expression unless co-inherited with other variant.

4.3.4. *In vitro* expression of p.[R924Q;C1927R]

Expression studies of recombinant mutant VWF (rVWF-R1927 and rVWF-Q924) showed significantly reduced secretion in the levels of VWF:Ag in the heterozygous and homozygous state ($p<0.0001$) compared to rVWF-WT with significantly increased intracellular retention when transfected in homozygous form ($p<0.05$). A relatively reduction of VWF multimers was observed in the heterozygous form and a complete loss of HMW-VWF multimers in the homozygous form indicating that p.R924Q may acts as a modifier of phenotype. Also, this variant appeared to affect storage function in both forms as WPB-like organelles were retained in the ER through confocal microscopy. These results appeared to be similar to the expression findings of p.C1927R when expressed alone, but mild effect was observed in VWF multimeric and synthesis indicating the that p.R924Q acts as a modifier of phenotype.

These findings were similar to expression data obtained when p.C1927R was transfected alone and no significant differences between the two sets of expression data were observed. However,

in vitro expression studies confirmed that p.R924Q had no significant effect on VWF expression unlike multimerisation. These findings suggested that a significant effect has been observed when this variant p.R924Q is co-inherited with a second mutation or with blood group O (Berber et al., 2009, Hickson et al., 2010). Therefore, the presence of both mutations p.[R924Q;C1927R] on the same allele resulted in a significant secretory defect of VWF due to intracellular retention and abnormal multimerisation. These findings are nearly similar to phenotypic data observed in patients who had these mutations on the same allele (Section 3.6.5.1).

4.3.5. Conclusion

In conclusion, the transient expression system using HEK293T cells conducted in this study is expected to result in better reflection of *in vivo* VWF expression level of rVWF as the cells have WPB-like storage structure compared to other cell lines such as COS-7 and Aat20cells that do not store VWF. Also, *in vitro* expression studies demonstrated that mutations located in the D4 assembly resulted in reduced VWF secretion due to intracellular retention of VWF as previously described for other *VWF* mutations in this region (Eikenboom et al., 2009).

Heterozygosity for the p.W2271G and p.C1927R mutations resulted in a VWF secretory defect which can result in partial quantitative deficiency of VWF in patient plasma and contributes to type 1 VWD and expression findings were similar to phenotypic data obtained in affected members. Moreover, p.R924Q seems to have a mild effect on VWF expression and thereby causes mild form VWD phenotype as observed in IC, but a more significant effect is observed when co-inherited with a second mutation and/or blood group O genotype. p.R924Q is considered as a phenotypic modifier of VWF level rather than as a pathogenic variant.

Chapter 5

In vitro expression of non-type 1 VWD mutations

5. *In vitro* expression of non-type 1 VWD

5.1. Introduction

Currently, VWD is classified into three main types; quantitative deficiencies which can be partial quantitative deficiency (type 1) and complete quantitative deficiency (type 3) and type 2 which is characterized by abnormal function of VWF due to presence of mutation within *VWF*. Type 3 VWD is inherited as an autosomal recessive trait and patients with homozygous or compound heterozygous mutations are usually present with severe bleeding symptoms accompanied by undetectable VWF in plasma (Federici, 2004). It has been reported that 20% of type 3 VWD mutations are missense located within D1 and D2, D4 and CK domains while null allele mutations comprise 80% of all mutation throughout *VWF* (Baronciani et al., 2003, Bowman et al., 2013).

Type 2 VWD is subdivided into four subtypes: 2A, 2B, 2M and 2N (Section 1.9.2). Type 2A is the commonest subtype caused by mutations that affect the normal binding of VWF to platelets due to an absence or reduction in HMW-VWF multimers. These mutations can be within the CK domain and disrupt dimerization process, within D2 and D3 domains which can impair multimerization process and can be within the A1 or A2 domains resulting in degradation of VWF due to either poor multimerisation or increased sensitivity to ADAMTS13. Type 2A can be further divided into subtypes. Type 2A(IIC) is inherited as autosomal recessive and characterised by severely reduced HMW multimers and increased dimers due to presence of mutations located in the D2 domain that impair multimerisation and further reaction with platelets (Meyer et al., 1997). The type 2A(IID) dominantly inherited subtype is characterised by the presence of mutations in the CK domain that impair pro VWF dimerisation and lead to secretion of small multimers with an aberrant triplet structure due to chain termination (Schneppenheim et al., 1996). The 2A(IIE) subtype is inherited as autosomal dominant and characterized by the lack of HMW VWF multimers and absence of outer bands within the triplet structure indicating reduced ADAMTS13 proteolytic cleavage. Type 2A(IIE) occurs due to presence of mutations primarily in the D3 domain that can disrupt multimerization and multimer assembly (Zimmerman et al., 1986, Schneppenheim et al., 2010) (Section 1.9.2.1). Patients with this subtype present with mild to moderate bleeding symptoms and abnormal functional assays with decreased VWF:RCo activity due to lack of VWF multimers (Enayat et al., 2001, Schneppenheim et al., 2001a, Schneppenheim et al., 2010).

The pre-pro and mature VWF consist of various domains which are responsible for the major functions needed during vascular injury (Figure 1.1A). Also, these domains play an essential role in catalysing VWF intramolecular dimerization and multimerization via disulfide bonding.

Dimerization is achieved in the ER by forming disulfide bonds between two adjacent monomers via their carboxyl termini and multimerization of dimers takes place in the Golgi apparatus by forming disulfide bonds between two adjacent D3 assemblies. The D3 assembly of VWF is essential for the multimerization process and is also required for VWF binding to FVIII. Expression studies of a cluster of mutations in the D3 assembly of *VWF* in a group of patients classified as VWD type 2A(IIE) showed reduced secretion, intracellular retention and lack of HMW multimers (Zimmerman et al., 1986, Hommais et al., 2006a, Schneppenheim et al., 2010).

During analysis of 18 EU IC who showed no previously identified mutations or had mutations that not fully explain disease phenotype, four mutations were identified in four IC, three of which were novel (Section 3.6). Out of them, one novel missense heterozygous mutation was identified in exon 26, in the D3 domain, c.3469T>C predicted to result in p.C1157R in one IC, from family P9F18, who had previously a single nucleotide deletion c.1614del in exon 14 (D2 domain) predicted to result in the frameshift mutation p.S539Lfs*38.

Initially, the P9F18 family was part of the EU study and historically diagnosed as type 1 VWD. The IC and family members samples were analysed for VWF:Ag, VWF:RCo, FVIII:C and multimers. Due to absence of multimers and undetectable levels of VWF in the IC and AFM, this family was considered as type 3 phenotype rather than type 1 and excluded from the main study (Goodeve et al., 2007). The frameshift mutation p.S539Lfs*38 was identified in the IC, AFM and two of the UFM (Appendix 18) and its presence alone was not sufficient to explain the undetectable level of plasma VWF, abnormal multimers and high BS in the AFM. The identification of the newly identified mutation p.C1157R in addition to the previously identified frameshift change could explain the very low level of phenotypic data in addition to abnormal multimers in the IC and AFM. p.C1157R which is located in the D3 domain may be able to be classified as type 2A(IIE) when inherited in the heterozygous form according to previously expressed mutations in the same domain (Schneppenheim et al., 2010). *In silico* prediction of the newly identified mutation p.C1157R suggested that this missense change was probably damaging, while the frameshift variant p.S539Lfs*38 is likely to impair the secretion of VWF due to NMD.

One of the main aims of this study was to investigate whether these mutations were the major cause for the observed phenotype correlated with VWD types in affected patients, to determine the effect of these mutations on VWF structure and function and also to understand the mode of pathogenicity of mutations identified through *in vitro* expression. The mutagenized plasmid carrying mutant cDNA (*rVWF*) was transiently transfected into HEK293T cells using the Lipofectamine transfection method as previously described in chapter 2.

5.2. Results

5.2.1. Mutagenesis

The pcDNA3.1/Hygro (-) expression plasmid containing the full-length wild-type human *VWF* cDNA was used to introduce the desired change and for transfection to investigate the effect of candidate mutations on the level and structure of VWF. PCR based site-directed mutagenesis was performed on the recombinant vector that contained the wild-type human *VWF* cDNA to introduce a specific mismatch for p.C1157R (c.3469T>C) and p.S539Lfs*38 (c.1614del) variants to be expressed in HEK293T cells. As a result, the sequencing data successfully showed the presence of the desired change in the plasmid DNA examined for variants following mini-prep. The sequencing data obtained for rVWF-R1157 and rVWF-L539fs mutations containing the desired variant are shown in figure 5.1.

In order to confirm that the examined plasmid contained only the desired mutation and no additional changes were present in the plasmid that could possibly disrupt VWF expression, the plasmid DNA was isolated using QIAGEN maxi-prep. The entire *VWF* cDNA was sent for sequencing and the obtained result successfully revealed no further mutations following the maxi-prep.

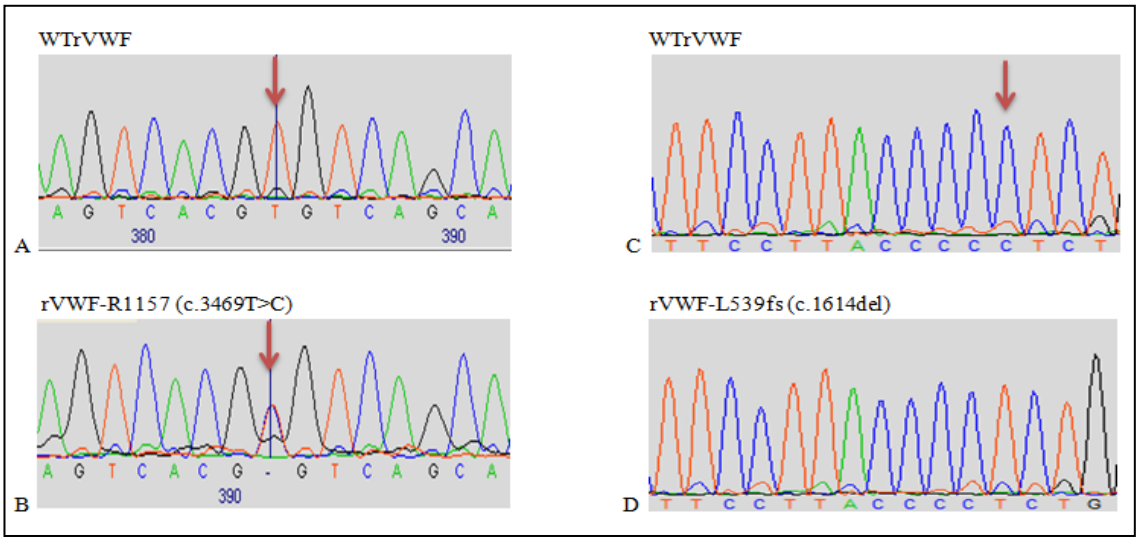

Figure 5.1 Sequence chromatographs to show introduction of novel variants into the cDNA VWF plasmid. A and **C** show the wild-type *VWF* cDNA sequence. **B)** Shows the p.C1157R change (c.3469T>C); D) shows the p.S539Lfs*38 change (c.1614del).

5.2.2. *In vitro* expression of recombinant VWF containing the candidate mutations p.C1157R and p.S539Lfs*38

The variants c.3469T>C predicted to result in p.C1157R and c.1614del predicted to result in p.S539Lfs*38 were previously identified in one family (P9F18) within the EU study. The IC (I:1) and AFM (1:2) carried both mutations on two different alleles while the UFM II:1 and II:2 carried only the frameshift variant p.S539fs (Section 3.6.2).

Three separate experimental conditions were used in order to replicate the phenotypic pattern of patients with each mutation including; transfection of rVWF-R1157 alone, transfection of rVWF-L539fs alone and co-transfection of both mutants rVWF [R1157];[L539fs] found on two different alleles to mimic the compound heterozygous state using 50% of each variant p.C1157R and p.S539fs in parallel with rVWF-wild-type.

The rVWF-R1157 and rVWF-L539fs plasmids were transiently transfected into HEK293T cells in parallel with rVWF-wild-type plasmid using Lipofectamine to evaluate the effect of these mutations on VWF expression using the protocol described in chapter 2 (Section 2.2.13.5).

5.2.3. Quantitative analysis of supernatant and cell lysates following transfection of HEK293T cells with rVWF-wild-type and mutant plasmid (rVWF-R1157)

The mean values of secreted VWF obtained by expression of wild-type plasmid alone, mutant plasmid alone (homozygous) and mutant plasmid co-expressed with wild-type (heterozygous) are shown in table 5.1. *In vitro* expression indicated that the observed mean values of secreted VWF of heterozygous and homozygous rVWF-R1157 into growth medium was decreased to 45% and 2% respectively compared to 100% of rVWF-wild-type (Figure 5.2). The difference in the secreted VWF level for heterozygous and homozygous states compared to wild-type were statistically significant with *P* values of $p<0.0001$.

In the HEK293T cell lysate, data for secreted VWF (Table 5.2) interestingly showed that intracellular mean values of VWF of both heterozygous and homozygous rVWF-R1157 was significantly increased to 147% ($p<0.001$) and 290% ($P<0.0001$) respectively compared to the corresponding values of 100% wild-type (Figure 5.2).

In summary, the measured mean values of VWF suggested that this mutation p.C1157R with loss of a cysteine residue located in D3 domain lead to a significant reduction in the level of secreted VWF in both heterozygous and homozygous states. Also, the expression data from HEK293T cell lysates indicated a significant increase in the level of retained VWF within cells in the homozygous and heterozygous states that lead to intracellular retention.

Table 5.1 The mean values and standard deviation of secreted VWF:Ag levels post-transfection for wild-type and mutant plasmids (rVWF-R1157) in HEK293T cells

VWF (Supernatant)	Mean (%)	*SD
rVWF-WT (homozygous)	100.0	15.0
WT:Mut (50:50) (heterozygous)	45.0	10.0
rVWF-C1157R (homozygous)	1.8	0.5

*SD= standard deviation

Table 5.2 The mean values and standard deviation of retained VWF:Ag levels harvested post-transfection for wild-type and mutant plasmids (rVWF-R1157) in HEK293T cells

VWF (Cell lysate)	Mean (%)	*SD
rVWF-WT (homozygous)	100.0	14.0
WT:Mut (50:50) (heterozygous)	147.0	26.0
rVWF-C1157R (homozygous)	291.0	50.0

*SD= standard deviation

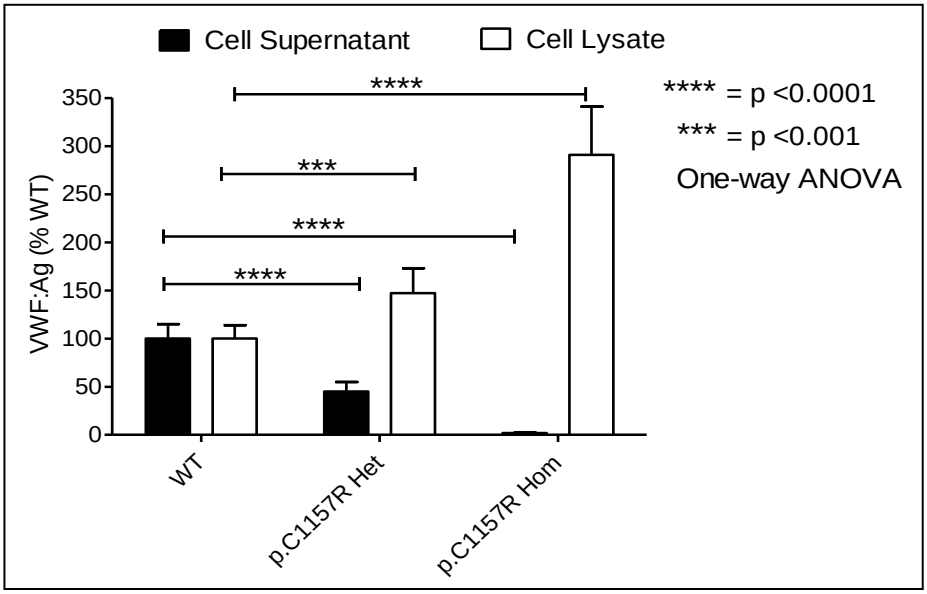

Figure 5.2 Mean levels of VWF:Ag in both supernatant and cell lysates of HEK293T cells transfected with wild-type and mutant expression plasmids showing the effect of the p.C1157R mutation on *VWF* expression. Results are expressed as a percentage compared to wild-type. The horizontal black bars represent the extent of difference between mean values of VWF:Ag between wild-type and mutant VWF. The vertical black bars indicate the standard deviation. Statistical test used is one-way ANOVA.

5.2.3.1. Multimer analysis for the p.C1157R VWF protein secreted from HEK293T cells

The secreted rVWF results from transfection of wild-type plasmid, rVWF-R1157 plasmid and co-transfection of mutant/wild-type were analysed for multimer pattern using a 1.6% medium resolution SDS agarose gel. As a result, the multimeric composition of rVWF secreted from HEK293T cells showed the presence of a full set of multimers in wild-type and a relative reduction of HMW multimers when expressed in heterozygous state. The transfection of the p.C1157R multimers showed that in the homozygous state there was a complete absence of high-molecular weight VWF (HMW-VWF) multimers with presence of only dimers indicating the importance of the D3 domain in VWF multimerisation (Figure 5.3).

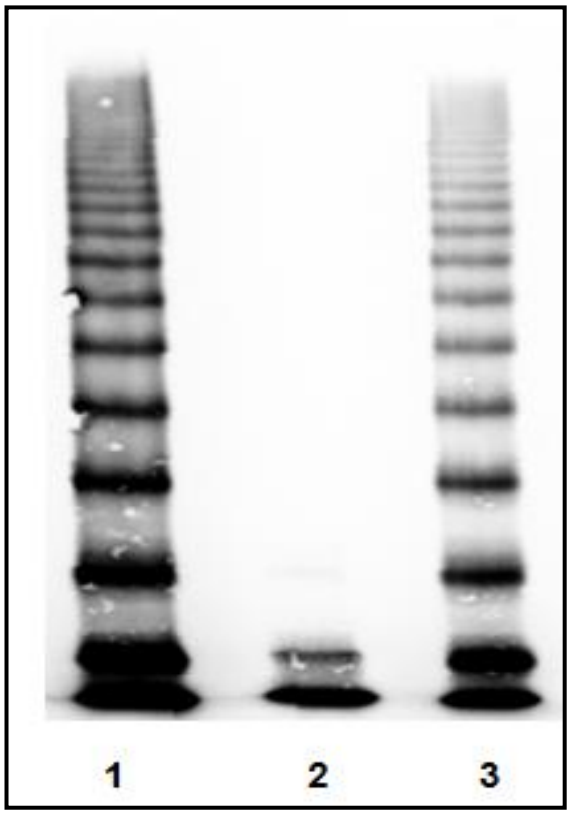

Figure 5.3 Multimer analysis of secreted rVWF from HEK293T cells transfected with p.C1157R in comparison to wild-type. Multimer pattern of wild-type (lane 1), homozygous rVWF-R1157 (lane 2) and heterozygous rVWF (lane 3) mutants electrophoresed on 1.6% medium resolution SDS gel at 1:5 dilution are shown. VWF multimers of homozygous rVWF-R1157 mutant (lane 2) showed complete loss of HMW-VWF forms with formation of only dimers in comparison to wild-type (lane 1). The multimeric composition of rVWF resulting from transfecting cells with heterozygous mutant (lane 3) showed a relative reduction of HMW multimers in comparison to wild-type.

5.2.3.2. Confocal imaging of p.C1157R

Confocal microscopy was undertaken to evaluate the effect of p.C1157R on VWF storage within the HEK293 heterologous cell line. *In vitro* expression of the p.C1157R revealed a secretion defect resulting from intracellular retention. In the wild-type form, WB-like vesicles were present and appeared rounded and punctate (Figure 5.4 A and C). In the homozygous form, localised VWF diffuse staining patterns were observed (indicated with a white arrow, Figure 5.4 D) in one cross section through the cell (Figure 5.4 D and F). The diffuse pattern may be due to VWF WPB-like structures stacking on top of each other in cross-section analysis caused by intracellular retention. In the heterozygous form, WPB-like organelles were formed with a diffuse staining pattern similar to homozygous but to a lesser degree (indicated with a white arrow) (Figure 5.4 G and I). p.C1157R does not appear to affect WPB synthesis, but confocal confirms *in vitro* findings of increased intracellular retention.

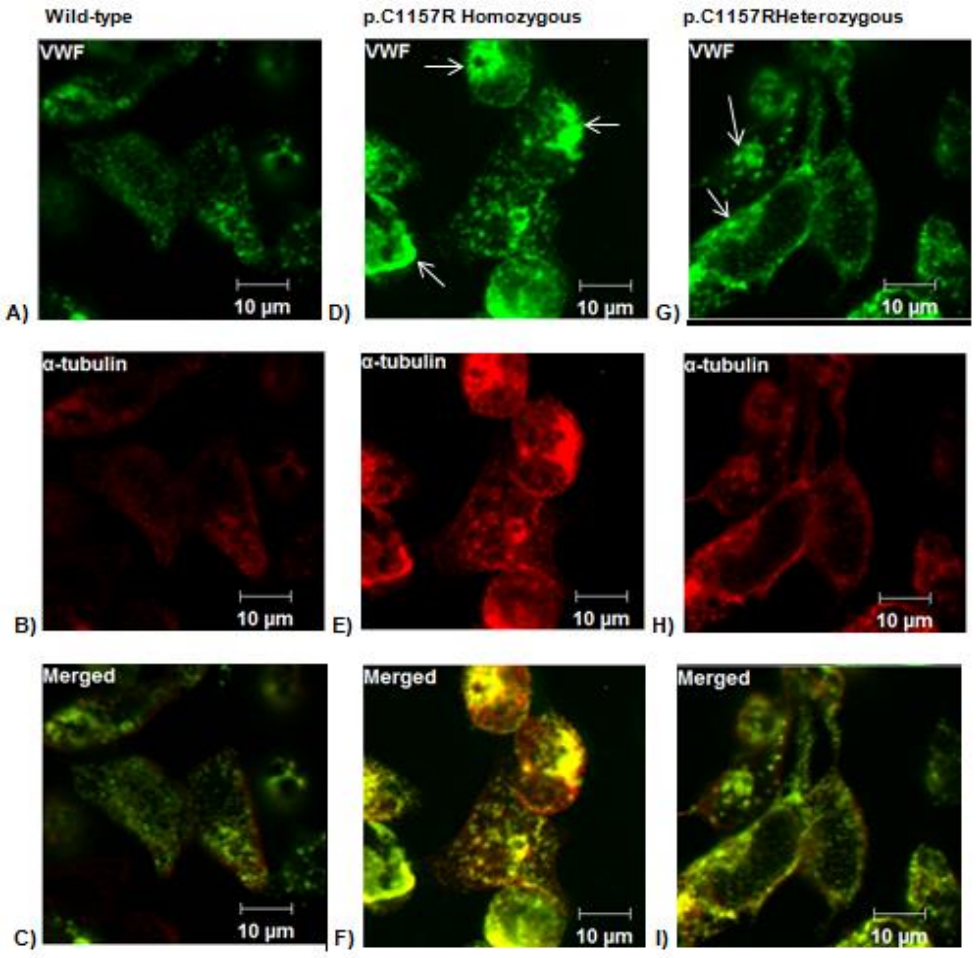

Figure 5.4 Intracellular storage of rWT and rVWF-R1157 mutant in HEK293 cells by confocal microscopy. A) Represents VWF (green) after transfection of wild-type into HEK293 cells. **B)** Represents the cell membrane marker α-tubulin (red) after transfection of wild-type into HEK293 cells. **C)** Represents merged images of VWF and α-tubulin staining for wild-type transfected into HEK293 cells. **D)** VWF (green) after transfection of homozygous p.C1157R into HEK293 cells. White arrows indicate regions where there was diffuse staining of VWF within the cell. **E)** VWF (red) after transfection of homozygous p.C1157R into HEK293 cells. **F)** Merged changes of VWF and α-tubulin staining for homozygous p.C1157R transfected into HEK293 cells. **G)** VWF (green) after transfection of heterozygous p.C1157R into HEK293 cells. White arrows indicate regions where there was diffuse staining of VWF within the cell. **H)** VWF (red) after transfection of heterozygous p.C1157R into HEK293 cells. **I)** Merged changes of VWF and α-tubulin staining for heterozygous p.C1157R transfected into HEK293 cells. Cells of the upper horizontal row **(A, D and G)** were stained with rabbit anti-VWF primary and anti-rabbit Alexa Fluor 488 for VWF (green), while cells of the middle horizontal row (**B, E and H)** were stained with mouse anti-α-tubulin and anti-mouse Alexa Fluor 555 for the cell membrane α-tubulin marker (red). The lower horizontal row **(C, F and I)** shows a merge of VWF and α-tubulin staining.

5.2.3.2.1. Confocal microscopy of p.C1157R to determine retention of VWF in the ER

In vitro expression of the p.C1157R showed a significant defect in VWF secretion resulting from intracellular retention. Confocal microscopy confirmed the retention of VWF within the ER using co-staining of VWF and PDI, ER markers. The pseudo-WPB organelles within the transfected HEK293 cells appeared rounded and punctuate in the wild-type (Figure 5.5A and C). The WPB-like organelles formed by homozygous mutant p.C1157R were also rounded and punctuate but appeared smaller in size when compared to wild-type. Confocal imaging illustrated that most of the synthesised VWF was retained within the ER when expressed in the homozygous form (orange organelles) as observed in figure 5.5 E and G. The retention of produced VWF was also observed when cells were co-transfected with wild-type but was less pronounced than that seen in the homozygous form (Figure 5.5 I and K). These confocal imaging using VWF and ER markers suggested that p.C1157R impaired VWF storage and secretion due to retention of VWF within the ER.

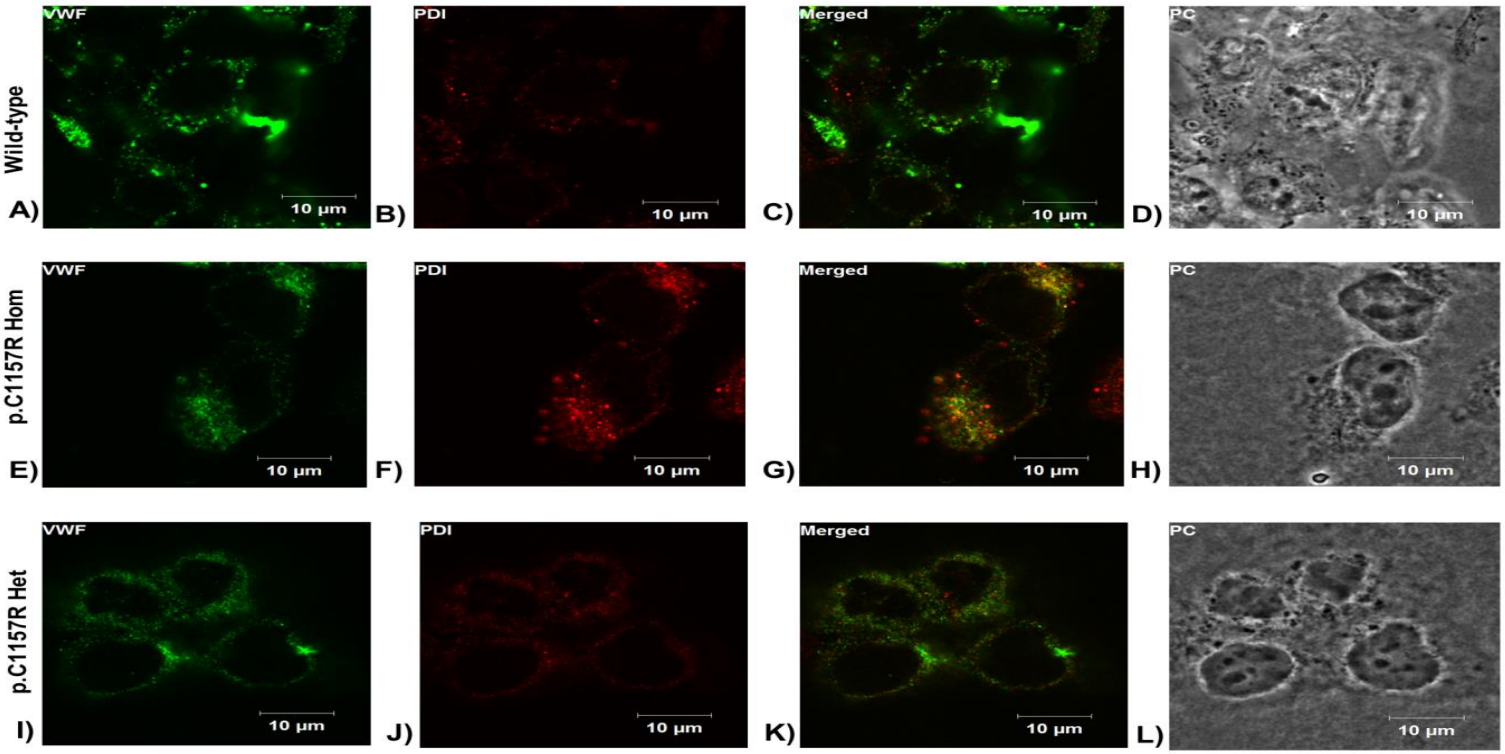

Figure 5.5 Intracellular localisation of VWF in rWT and rVWF-R1157 mutant in HEK293 cells. **A, E and I**) Represent VWF (green) after transient transfection of wild-type, homozygous and heterozygous plasmids respectively into HEK293 cells. **B, F and J**) Represent the ER marker PDI (red) after transfection of wild-type, homozygous and heterozygous respectively into HEK293 cells. C, G and K) Represent merged changes of VWF and PDI staining for wild-type, homozygous and heterozygous respectively transfected into HEK293 cells. **D, H and L**) Represent phase contrast (PC) images for wild-type, homozygous and heterozygous respectively transfected into HEK293 cells. Cells of the column (**A, E and I**) were stained with rabbit anti-VWF primary and anti-rabbit Alexa Fluor 488 for VWF (green), while cells of the second column **(B, F and J)** were stained with mouse anti-PDI and anti-mouse Alexa Fluor 555 for the ER marker (red). The Third column **(C, G and K)** shows a merge of VWF and PDI.

5.2.4. Quantitative analysis of supernatant and cell lysates following transfection of HEK293T cells with rVWF-wild-type and mutant plasmid (rVWF-L539fs)

In an attempt to investigate the effect of c.1614del on the level, structure and function of VWF, transient transfection was conducted using HEK293T cells. The analysed values of VWF in cell supernatant and cell lysates are shown in tables 5.3 and 5.4. *In vitro* expression of rVWF-L539fs showed that the rVWF mean values measured in growth medium of homozygous mutant was reduced by 99.6% with a significant change compared to 100% rVWF-wild-type (*P*<0.0001*)* and the mean values obtained by co-transfecting wild-type and mutant was also significantly reduced by 40% compared with the corresponding values of 100% wild- type VWF (*p*<0.0001) (Figure 5.6).

Also, the mean values of VWF retained within cells of heterozygous and homozygous states showed significant reductions with values of approximately 81% (*p*<0.01) and 5.7% (*p*<0.0001) respectively compared to 100% of rVWF-wild-type (Figure 5.6).

In summary, these results indicated that the secretion of homozygous and heterozygous rVWF-L539fs was significantly reduced. *In vitro* expression of rVWF-L539fs suggested that this frameshift mutation (p.S539fs) had impaired VWF secretion resulting from reduced production of VWF protein and did not lead to intracellular accumulation of VWF within the cells in both states.

Table 5.3 The mean values and standard deviation of secreted VWF:Ag levels post-transfection for wild-type and mutant plasmids (rVWF-L539fs) in HEK293T cells

VWF (Supernatant)	Mean (%)	*SD
rVWF-WT (homozygous)	100.0	14.0
WT:Mut (50:50) (heterozygous)	60.0	12.0
rVWF-S539fs (homozygous)	0.4	0.3

*SD= standard deviation

Table 5.4 The mean values and standard deviation of retained VWF:Ag levels harvested post-transfection for wild-type and mutant plasmids (rVWF-L539fs) in HEK293T cells

VWF (Cell lysate)	Mean (%)	*SD
rVWF-WT (homozygous)	100.0	14.0
WT:Mut (50:50) (heterozygous)	81.0	11.4
rVWF- S539fs (homozygous)	5.7	2.0

*SD= standard deviation

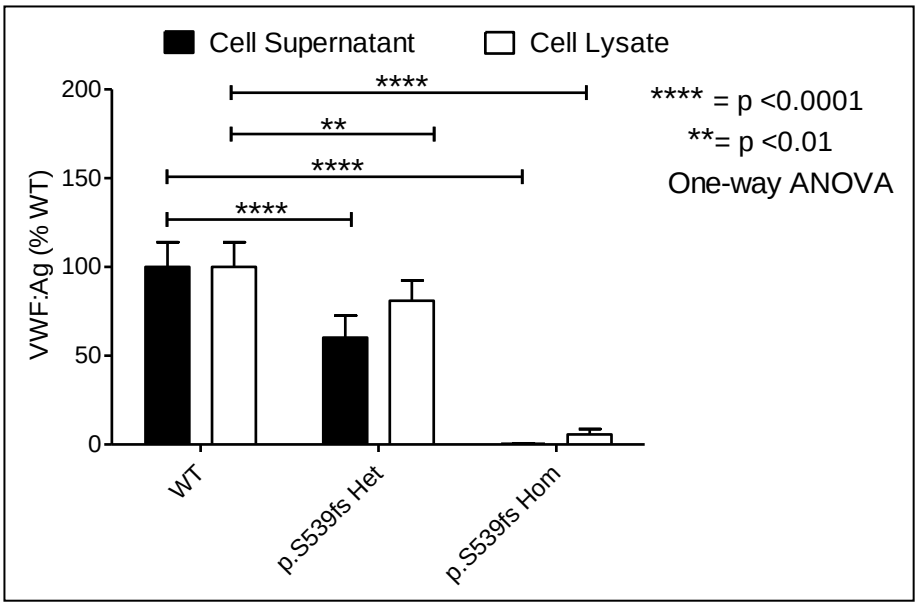

Figure 5.6 Mean levels of VWF:Ag in both supernatant and cell lysates of HEK293T cells transfected with wild-type and mutant expression plasmids showing the effect of the p.S539Lfs*38 mutation on *VWF* expression. Results are expressed as a percentage in comparison with wild-type. The horizontal black bars represent the extent of difference between mean values of VWF:Ag between wild-type and mutant VWF. The vertical black bars indicate the standard deviation. Statistical test used is one-way ANOVA.

Also, in an attempt to investigate whether the low VWF expression for the p.S539fs resulted from proteosomal degradation of mutant protein or possibly due to NMD, *in vitro* expression using standard transfection and with proteosome inhibitor was undertaken (Section 2.2.13.5.1). Transfected cells were treated with proteosome inhibitor three hours prior to harvesting to inhibit proteosome activity. Analysis of secreted VWF between uninhibited (61%) and inhibited (50%) cells in the heterozygous state showed no significant change (Figure 5.7 A). Also, no significant change was observed between uninhibited (68) and inhibited (51) on analysis of lysate VWF in the heterozygous form (Table 5.5). Analysis of secreted and lysate VWF also showed no significant differences when comparing uninhibited and inhibited values in the homozygous form (Figure 5.7 B). In the homozygous form, very low levels of VWF were expressed in both conditions (Table 5.5). Assuming that the low VWF level resulted from proteosome degradation, treatment with proteosome inhibitor would lead to an increase in the VWF level in the lysate. Therefore, the consistency of results in both experiments and absence of significant differences between uninhibited and inhibited experiments suggested that VWF protein in the cell was not degraded by a proteosomal mechanism and other mechanism potentially resulted in the low protein expression for the p.S539fs mutant.

Table 5.5 The expression mean values of secreted and retained VWF using proteosome inhibitor in the heterozygous and homozygous states

State	Uninhibited mean (%)	Inhibited mean (%)
Heterozygous supernatant	61.0	50.0
Heterozygous lysate	68.0	51.0
Homozygous supernatant	2.4	1.6
Homozygous lysate	3.3	5.0

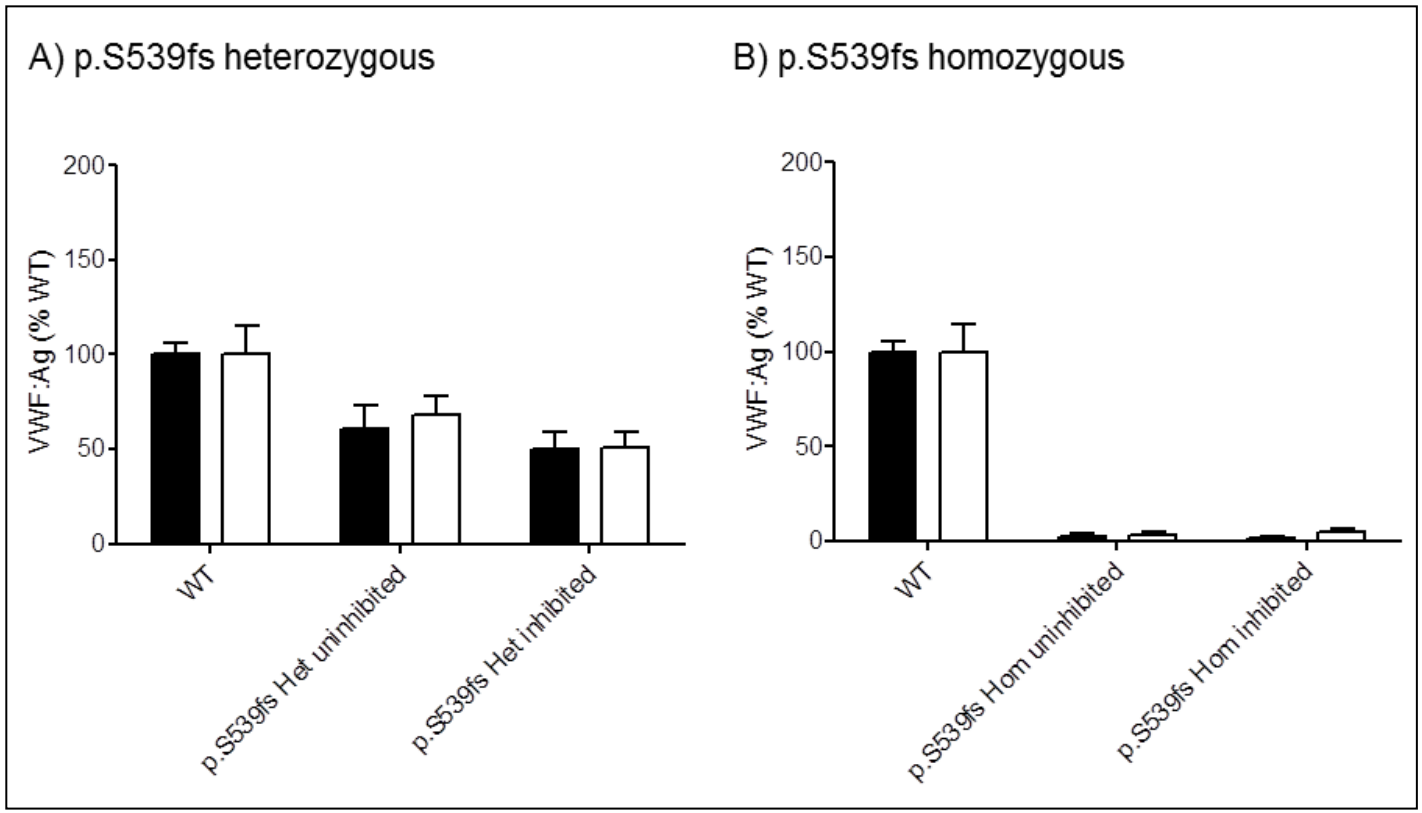

Figure 5.7 ***In vitro*** **expression of p.S539fs using a proteosome inhibitor. A)** Represents the expression of inhibited and uninhibited cells in the heterozygous form. **B)** Represents the expression of inhibited and uninhibited cells in the homozygous form. Both states showed no significant differences between VWF levels with and without proteasome inhibitor treatment for supernatant and lysate VWF. Black bars represent cell supernatant and white bars represent cell lysate.

5.2.4.1. Multimer gel analysis for the p.S539fs VWF protein secreted from HEK293T cells

The secreted rVWF from transfection of wild-type plasmid, rVWF- plasmid and co-transfection of mutant/wild-type were analysed for multimer pattern using a 1.6% medium resolution SDS agarose gel. As a result, the multimeric composition of rVWF secreted from HEK293T cells showed complete absence of HMW-VWF multimers when homozygous multimers were analysed. The multimer analysis of the heterozygous p.S539fs mutation was comparable with wild-type multimers showing the presence of a full array of multimer bands (Figure 5.8).

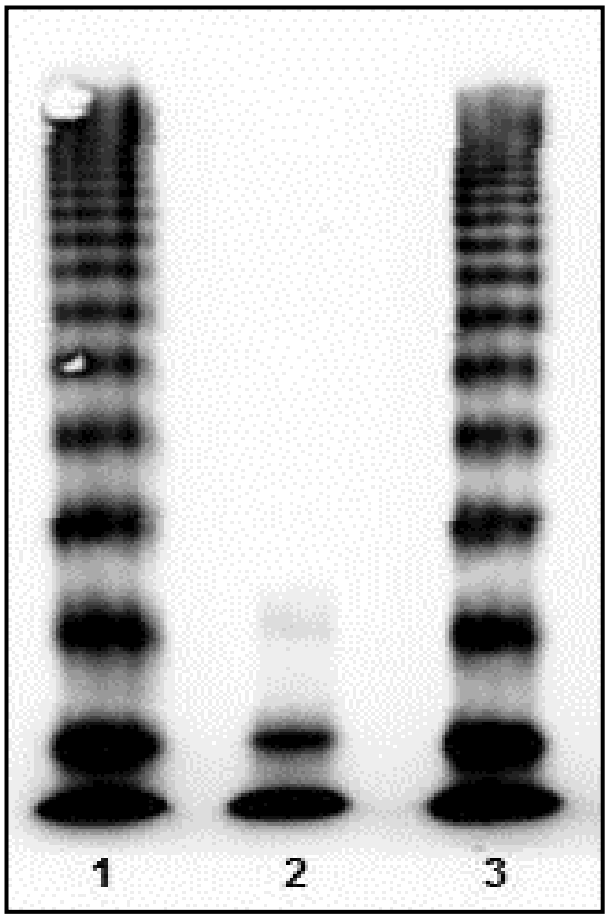

Figure 5.8 Multimer analysis of secreted rVWF from HEK293T cells transfected with p.S539Lfs in comparison to wild-type. Multimer pattern of wild-type (lane 1), homozygous rVWF-S539fs (lane 2) and heterozygous rVWF (lane 3) mutants electrophoresed on a 1.6% medium resolution SDS gel at 1:5 dilution are shown. The multimeric composition of rVWF resulting from the heterozygous state post *in vitro* expression (lane 3) showed a full array of multimers similar to those observed in wild type. VWF multimers of homozygous mutant rVWF-S539fs (lane 2) showed a total absence of HMW-VWF multimers with the presence of only the lowest molecular weight forms.

5.2.4.2. Confocal imaging of p.S539fs

The effect of p.S539fs on VWF storage was evaluated using confocal microscopy. *In vitro* expression of the p.S539fs revealed a defect in secretion accompanied by some VWF present in cell lysates when the mutant was expressed alone. Confocal imaging confirmed this finding in the homozygous form when a very small quantity of VWF were present with only diffuse intracellular staining (Figure 5.9 D and F) in comparison to rounded punctate WPB-like organelles observed in the wild-type (Figure 5.9 A and C). Unlike the homozygous form, WPB-like organelles were seen that appeared to be round and punctate but were more in number and smaller in size when compared to wild-type (Figure 5.9 G and I). Confocal imaging suggested that the p.S539fs when present with wild-type partially rescued storage ability. Also, the small amount of VWF retained in cell in the homozygous form could be due to different mRNA transcripts being produced, some of which lead to an aberrant protein being made.

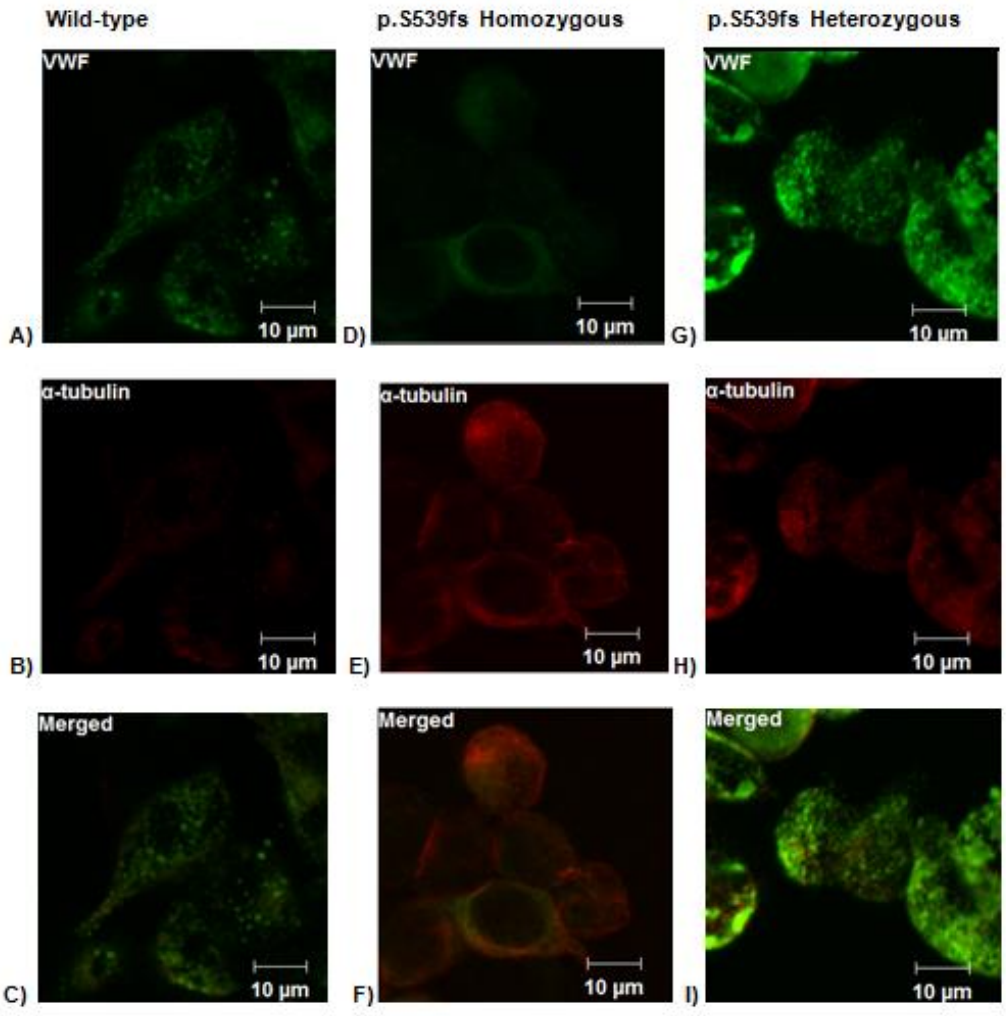

Figure 5.9 Intracellular storage of rWT and rVWF-L539fs mutant in HEK293 cells by confocal microscopy. A, D and G) Represent VWF (green) after transfection of wild-type, homozygous and heterozygous plasmids respectively into HEK293 cells. **B, E and H)** Represent the cell membrane marker α-tubulin (red) after transfection of wild-type, homozygous and heterozygous respectively into HEK293 cells. **C, F and I)** Represent merged image of VWF and α-tubulin staining for wild-type, homozygous and heterozygous respectively transfected into HEK293 cells. Cells of the upper horizontal row **(A, D and G)** were stained with rabbit anti-VWF primary and anti-rabbit Alexa Fluor 488 for VWF (green), while cells of the middle horizontal row (**B, E and H)** were stained with mouse anti-α-tubulin and anti-mouse Alexa Fluor 555 for the cell membrane α-tubulin marker (red). The lower horizontal row **(C, F and I)** shows a merge of VWF and α-tubulin staining.

5.2.5. Quantitative analysis of supernatant and cell lysates following transfection of HEK293T cells with rVWF-wild-type and mutant plasmids rVWF [R1157];[L539fs]

In order to investigate whether the presence of these two mutations p.[C1157R];[S539Lfs] on two different alleles was responsible for the observed phenotype associated with bleeding symptoms in patients carrying both variants, *in vitro* co-expression of both mutations in parallel with rVWF-wild-type plasmid was conducted using a transient transfection method. Analysed data of secreted and retained VWF obtained by co-transfection are shown in tables 5.6 and 5.7. The mean values of secreted and retained VWF were significantly reduced by 99.4%% and 64.0% respectively in comparison with the corresponding value of 100% wild-type VWF (p<0.0001) (Figure 5.10).

In summary, the measured mean values of VWF following co-transfection of rVWF-R1157 and rVWF-L539fs on two different alleles suggested a significant reduction of secreted VWF into the supernatant and those retained within the cells compared to rVWF-wild-type. These values attained statistical significance.

Table 5.6 The mean values and standard deviation of secreted VWF:Ag levels post co-transfection for wild-type and mutant plasmids (rVWF-R1157 and L539fs) in HEK293T cells

VWF (Supernatant)	Mean (%)	*SD
rVWF-WT (homozygous)	100.0	4.0
Mut:Mut (50:50) (Compound heterozygous)	0.6	0.3

*SD= standard deviation

Table 5.7 The mean values and standard deviation of retained VWF:Ag levels harvested post co-transfection for both mutant plasmids (rVWF-R1157 and L539fs) in HEK293T cells

VWF (Cell lysate)	Mean (%)	*SD
rVWF-WT (homozygous)	100.0	6.0
Mut:Mut (50:50) (Compound heterozygous)	36.0	6.0

*SD= standard deviation

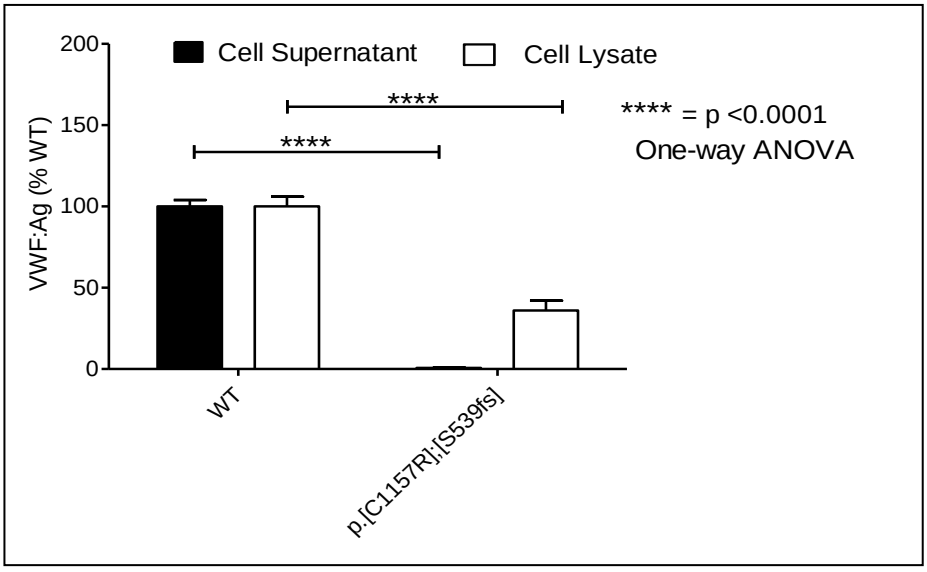

Figure 5.10 Mean levels of VWF:Ag in both supernatant and cell lysates of HEK293T cells transfected with wild-type and mutant expression plasmids showing the effect of the p.[C1157R];[S539Lfs*38] mutations on *VWF* expression. Results are expressed as a percentage in comparison with the corresponding wild-type. The horizontal black bars represent the extent of difference between mean values of VWF:Ag between wild-type and mutant VWF. The vertical black bars indicate the standard deviation. Statistical test used is one-way ANOVA.

5.2.5.1. Multimer analysis for the rVWF [R1157];[L593fs] protein secreted from HEK293T cells

Multimer analysis for the rVWF[R1157];[L593fs] compound heterozygous state secreted from HEK293T cells revealed a complete absence of HMW-VWF multimers and only the lowest molecular weight forms were visible in comparison to wild-type multimers (Figure 5.11).

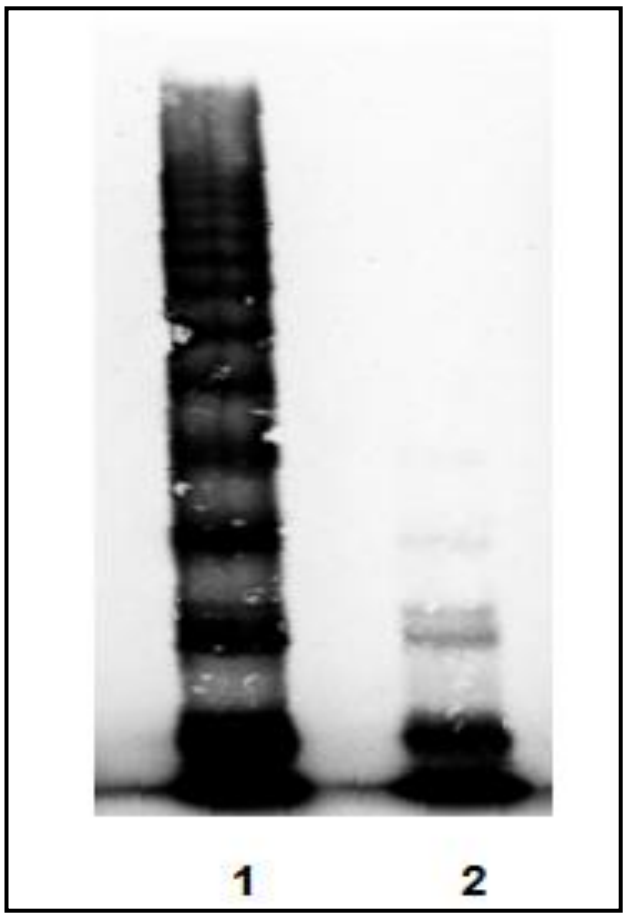

Figure 5.11 Multimer analysis of secreted rVWF from HEK293T cells co-transfected with rVWF-R1157 /rVWF-L539fs in comparison to wild-type. The multimer pattern of wild-type (lane 1) and compound heterozygous rVWF-R1157/rVWF-L539fs mutant (lane 2) electrophoresed on 1.6% medium resolution SDS gel at 1:5 dilution are shown. The multimeric composition of rVWF resulting from transfecting cells with rVWF-R1157/rVWF-L539fs mutants (lane 2) resulted in a complete loss of HMW-VWF forms and only the lowest MW and faint tetramers were observed in comparison to wild-type that showed a full set of multimers.

5.2.5.2. Confocal imaging of p.[S539fs];[C1157R]

Confocal microscopy to evaluate the effect of compound heterozygous mutations p.[S539fs];[C1157R] on VWF storage within HEK293 cell lines was undertaken. *In vitro* expression of the p.[S539fs];[C1157R] on two different alleles showed that severe secretion defect and abnormal intracellular VWF resulting from two independent mechanism that likely include NMD and intracellular retention. The confocal imaging of wild-type showed the presence of round punctate WPB-like organelles throughout the cell (Figure 5.12 A and C). Similarly to the wild-type image, the compound heterozygous mutants p.[S539fs];[C1157R] image showed punctate WPB-like organelles throughout the cell but appeared smaller than those observed in wild-type (Figure 5.12 D and F). These findings suggest that the allele carrying p.C1157R showed a mild effect in WPB storage but was still able to produce WPB-like structures retained within transfected cells. The *in vitro* expression analysis of p.[S539fs];[C1157R] mutants showed that 36% of VWF was retained in cell and this was also observed when the WPB-like organelles were visualised using confocal analysis.

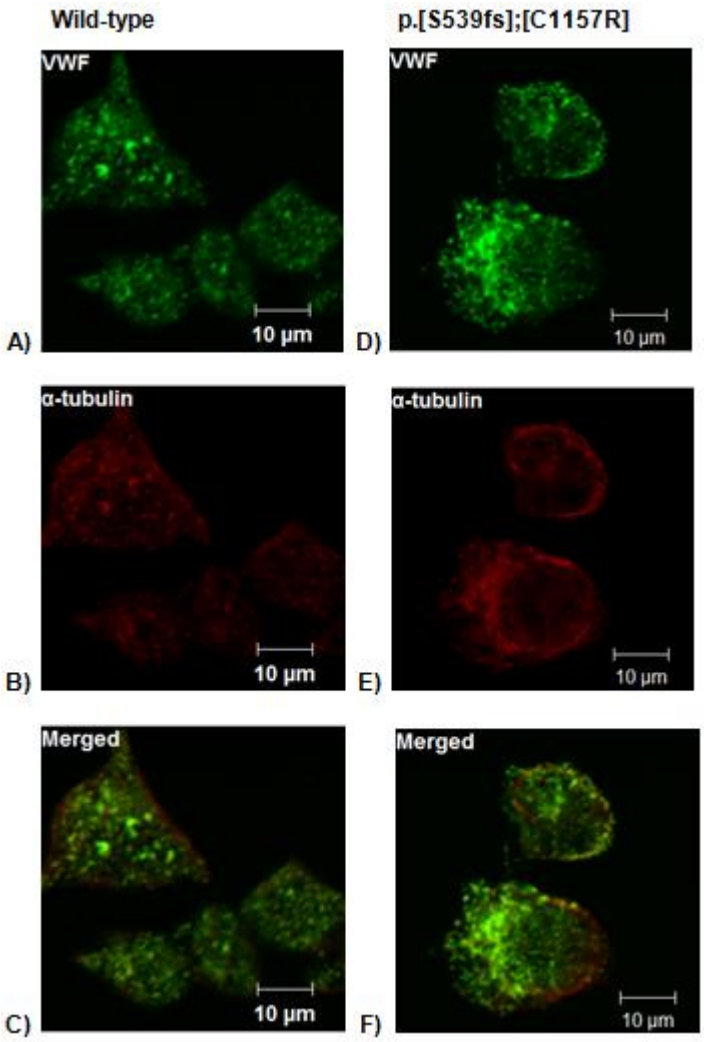

Figure 5.12 Intracellular storage of rWT and rVWF-L539fs + R1157 mutants in HEK293 cells by confocal microscopy. A and D) Represent VWF (green) after transfection of wild-type and compound heterozygous plasmids respectively into HEK293 cells. **B and E)** Represent the cell membrane marker α-tubulin (red) after transfection of wild-type and compound heterozygous respectively into HEK293 cells. **C and F)** Represent merged images of VWF and α-tubulin staining for wild-type and compound heterozygous respectively transfected into HEK293 cells. Cells of the upper horizontal row **(A and D)** were stained with rabbit anti-VWF primary and anti-rabbit Alexa Fluor 488 for VWF (green), while cells of the middle horizontal row (**B and E)** were stained with mouse anti-α-tubulin and anti-mouse Alexa Fluor 555 for the cell membrane α-tubulin marker (red). The lower horizontal row **(C and F)** shows a merge of VWF and α-tubulin staining.

5.3. Discussion

In this chapter, *in vitro* expression studies of two mutations detected in a family historically diagnosed with type 1 VWD was conducted. These mutations included one missense mutation p.C1157R and one frameshift variant p.S539Lfs*38 that were found together in affected members on two different alleles (Section 3.6.2). The affected members who were compound heterozygous for these two mutations had severe bleeding symptoms and demonstrated undetectable levels of VWF with absence of multimers (Appendix 18). Initially, due to the presence of the frameshift variant only and the AFM presenting with an undetectable level of VWF:Ag, abnormal VWF:RCo, absence of multimers and high BS, this family was classified as type 3 VWD and excluded from the study (Goodeve et al., 2007). Further identification of the novel missense mutation in the D3 domain in addition to the previously identified frameshift change could explain the observed undetectable levels of VWF and abnormal multimers in the investigated members and led to review the classification for each identified mutation alone and when both were present in the same individual. Three separate experimental expression studies were designed in order to determine the effect of each mutation on the level and structure of VWF. They included; expression of rVWF-R1157 alone, expression of rVWF-L539fs alone and co-expression of both mutants (rVWF-L539fs and rVWF-R1157) on two different alleles. The purpose of co-expression of both mutations was to mimic the compound heterozygous state and to determine whether the presence of both mutations was responsible for the complete deficiency of VWF, abnormal multimers and bleeding symptoms in the investigated patients. The recombinant plasmids carried full length *VWF* cDNA and mutated plasmids were transiently transfected into HEK293T cells using Lipofectamine method.

5.3.1. *In vitro* expression of p.C1157R

In vitro studies indicated that p.C1157R causes a secretion defect when mutant plasmid was transfected in a homozygous form, it showed a significant defect in secretion of VWF (98% lower; $P<0.0001$) compared to the wild-type VWF and higher levels of the mutant VWF by (190% higher; $P<0.0001$) were retained within cells than levels of wild-type. Also, co-transfection of mutant and wild-type plasmid showed a significant reduction of secreted VWF (55%) accompanied by a significant increase in the amount retained in the cells (47% higher; $P<0.001$). These findings suggested that this novel mutation may impair VWF secretion due to intracellular retention in the ER and possible degradation of VWF in the ER as previously described (Section 4.3.1).

Furthermore, the analysis of VWF multimers following transient transfection from media indicated the complete absence of HMW-VWF multimers in the homozygous form resulting from mutant plasmid while the hybrid plasmid in the heterozygous form clearly showed

multimers comparable to wild-type although they still showed a relative reduction of HMW multimers compared to wild-type. The presence of dimeric VWF with complete loss of HMW-VWF multimers in the homozygous form indicated the importance of D3 assembly in the VWF multimerisation process which is essential for VWF normal function and folding. Unlike multimerisation, the cysteine mutation p.C1157R located in D3 assembly had no effect on VWF synthesis and was able to form WPB similar to those present in wild-type in both homozygous and heterozygous forms, but confocal microscopy confirmed the accumulation of VWF within the cell resulting in intracellular retention.

The D3 assembly of VWF is located at the amino-terminal region of VWF and is known to be involved in the multimerization process including multimer assembly via formation of intra-disulfide and inter-disulfide bonds between adjacent D3 assemblies involving cysteine residues. Also, the D3 assembly contributes to binding of VWF to FVIII. The binding of secreted rVWF to FVIII (VWF:FVIIIB) was not tested. The location of this mutation in the D3 domain and its effect on a cysteine residue suggests the underlying mechanism. The replacement of a cysteine residue that is required for disulfide bond synthesis by a basic arginine at the N-terminal will affect normal pairing with the other cysteine in the same domain or the formation of disulfide bridges between adjacent D3 assemblies and could impair multimerization. The increased intracellular accumulation of mutant VWF may be due to protein mis-folding which may cause retention of VWF in the ER and prevent it reaching the Golgi apparatus which would result to degradation of mutant protein by the proteasome complex and secretion of only a small quantity of VWF. Furthermore, the presence of this substitution in the D3 assembly in addition to impairing production of VWF appears to explain the observed abnormal multimers found in patient's plasma. One of the major aims of this study was to identify and investigate the disease causing mechanism. The results obtained from expression studies showed that p.C1157R in the heterozygous form can cause a moderate reduction of VWF secretion and a severe reduction when found in the homozygous state due to the intracellular retention observed. Moreover, due to the presence of p.C1157R in the D3 assembly involving a cysteine residue that is known to play an essential role of VWF disulfide bonding, this mutation affects the VWF multimerisation process.

The affected members who harboured the p.C1157R mutation also co-inherited the frameshift variant p.S539Lfs*38 and none of them carried only p.C1157R (Appendix 18). Therefore, it was not possible to compare the results from transfection studies to the phenotypic data observed in affected p.C1157R heterozygous patients. Expression of p.C1157R alone was conducted in order to identify the disease causing mechanism. The affected members who were compound heterozygous for p.C1157R and p.S539Lfs*38 presented with severe bleeding symptoms, had high BS and had markedly low phenotypic data (Section 3.6.2). The levels of

VWF:Ag, VWF:RCo and FVIII:C in the IC and AFM who carried both variants was undetectable (< 3 IU/dL) with absence of HMW multimers and O/O and O/B blood group genotypes respectively. Moreover, the IC and AFM showed uninterpretable binding of VWF to FVIII. From the *in vitro* expression studies, p.C1157R had a significant effect on VWF secretion and impaired multimer assembly similar to the observed phenotype found in the AFM as p.S539Lfs*38 had no significant influence on the multimerization process when present in the heterozygous form. The observed finding showed that p.C1157R contributes to the absence of HMW multimers in the AFM when inherited in the homozygous form or in the compound heterozygous form with the second change. *In vitro* expression showed that p.C1157R can influence the level and structure of VWF and these findings are compatible with *in silico* predictions that suggested this mutation was probably damaging.

Several mutations were identified in the D3 assembly of *VWF* in patients diagnosed with VWD. Schneppenheim *et al* expressed 22 mutations correlated with the VWD 2A(IIE) phenotype located in the D3 assembly in HEK293T cells (Schneppenheim et al., 2010). Twelve of them showed loss of a cysteine, three gain of a cysteine and nine were located in exon 26. The results showed that most mutations lead to intracellular retention, reduced secretion and abnormal multimers. The hallmark of multimers observed in the expressed VWF protein was the presence of abnormal multimers in both homozygous and heterozygous forms. Many mutations in the D3 assembly involving cysteine residues were investigated previously and were also reported to cause intracellular retention, secretion defects and abnormal multimers. The co-transfection of p.C1130F and p.C1149R with wild-type *VWF* indicated reduced secretion accompanied by intracellular retention and lack of HMW multimers (Eikenboom et al., 1996, Bodo et al., 2001b, Schneppenheim et al., 2010). Also, the expression of mutations p.C1225G and p.C1227R also involving cysteine residues indicated the presence of a relative decrease of large multimers in addition to abnormal binding to FVIII and defects in secretion (Dong et al., 1994, Allen et al., 2000a, Schneppenheim et al., 2010). The mutation p.Y1146C that leads to a cysteine gain and p.T1156M that does not involve cysteines indicated the same findings as others including intracellular retention and impaired multimerization (Lethagen et al., 2002b, Schneppenheim et al., 2010). Moreover, Hommais *et al* (2006) expressed two mutations involving cysteine in COS-7 cell, one of them located at the same position p.C1157 but encoding a different amino acid p.C1157F. These mutations p.C1157F and p.C1234W were referred as ″unclassified″ and type 2A respectively. The results obtained by expression studies of p.C1157F and p.C1234W illustrated that these variants exhibited reduced secretion due to intracellular retention and had abnormal multimers and a defect in binding to FVIII. The retained VWF value of p.C1157F was 300% compared to 100% wild-type and this high value may be explained because there was no correction for transfection efficiency in the experiment and also COS-7 cells do not make

WPB-like organelles that store VWF (Hommais et al., 2006a). However, the expression of p.C1157R showed that this mutation also impaired secretion of VWF associated with intracellular retention, lack of HMW multimers but showed normal synthesis and pseudo-WPB formation using confocal microscopy. All of these findings highlight similar findings of VWF secretion, intracellular retention and abnormal multimers in this study. According to the current VWD classification, mutations located in D3 assembly that disturb multimerization can be classified as type 2A(IIE) rather than type 1 VWD (Sadler et al., 2006, Schneppenheim et al., 2010). The missense mutation p.C1157R located in the D3 assembly can be considered as the major contributor to the abnormal multimers observed in patients and could contribute to the low levels of VWF and be classified as likely to result in VWD type 2A(IIE) when inherited in the heterozygous form rather than type 1 or type 3 VWD.

5.3.2. *In vitro* expression of c.1614del; p.S539Lfs*38

In this study, the effect of the previously identified candidate frameshift deletion c.1614del located in exon 14, (D2 assembly) on VWF was investigated. Analysis of transfection and co-transfection experiments indicated a highly reduced level of secreted and retained VWF (p<0.0001) when transiently transfected in the homozygous state. The co-transfection of mutant plasmid with wild-type to replicate the heterozygous state showed a moderate and significant reduction of secreted VWF (40% lower) compared to expressed wild-type (p<0.0001) in addition to a significant reduction (p<0.01) of VWF level retained within cells. The effect of proteosome degradation on the low VWF level observed was excluded and that was confirmed by expression studies that have used proteosome inhibitor which illustrated similar findings to standard expression of p.S539fs without using the proteosome inhibitor. However, these findings indicated the significant effect of the frameshift mutation p.S539fs in VWF secretion likely resulting from NMD mechanism (Shahbazi et al., 2012).

The VWF multimers secreted into the media following transient transfection showed the presence of a full set of multimers including HMW-VWF multimers in the heterozygous form, but these was a complete loss of HMW and intermediate MW-VWF multimers resulting from mutant plasmid in the homozygous form. These analyses showed that the heterozygous frameshift mutation p.S539fs had no effect on VWF multimerisation. Furthermore, the homozygous frame-shift mutation p.S539fs that impairs multimerisation significantly altered intracellular storage of VWF with a complete absence of punctate pseudo-WPB organelles, while the heterozygous form of this mutation illustrated no significant effect on VWF storage as pseudo-WPB were formed similar to those present in wild-type. The presence of the wild-type allele with the frame-shift deletion explains the normal storage function of VWF and this can

occur through a haplosufficiency mechanism. Haplosufficiency occurs when the normal allele is sufficient to produce enough protein when the mutant allele is degraded.

The c.1614del (p.S539Lfs*38) was predicted to create a stop codon, 38 amino acids downstream of the mutation of exon 14. *In silico* prediction showed that this candidate variant may result in a null allele and this is likely to be due to a NMD mechanism. The aims of this study were to examine the effect of the identified frameshift candidate mutation on VWF expression using transient transfection experiments in HEK293T cells and also to determine the pathogenesis of this mutation in the affected members of the P9F18 family.

The results from expression studies and *in silico* prediction may be able to explain the disease mechanism. The single nucleotide deletion in *VWF* exon 14 interrupts the protein reading frame and creates a PTC. The presence of a PTC within the mRNA transcript results in synthesis of a shortened protein that is subsequently degraded by NMD. The mRNA surveillance machinery is responsible and results in a null allele (Lykke-Andersen et al., 2000, Cartegni et al., 2002). NMD is mainly observed in mutated mRNA that includes a PTC and stop codons due to insertion, deletion or mutations cause splicing errors. NMD mainly is a pathway that aims to diminish the production of potential truncated proteins during expression via removal of aberrant mRNA harboring premature termination (nonsense) codons. If translated, these mRNAs can produce truncated proteins with dominant-negative or deleterious gain-of-function activities. Exon-junction complex (EJC) are formed following mRNA splicing and found upstream of normal stop codon which are thus removed by ribosome nuclear protein (RNP) before NMD factors UPf1 is recruited. In the presence of premature termination codon, EJC are deposited downstream of the PTC which cannot be removed by RNP, allowing EJC to interact with NMD factors UPF1 which trigger mRNA decay (Chang et al., 2007). The null allele's disease mechanism can explain the moderate level of secreted VWF following co-transfection and near absence of VWF secretion following transfection of the mutant plasmid alone.

Many experimental studies investigated the effect of nonsense, small deletion, small insertion and splice site mutations that lead to PTC in open reading frames on VWF. Most mutations associated with *VWF* null alleles were identified in type 3 VWD and several were detected in type 1 VWD (Baronciani et al., 2003, Goodeve et al., 2007, Hampshire and Goodeve, 2011, Jokela et al., 2013). Also more mutations found in ISTH VWF database http://www.vwf.group.shef.ac.uk/ accessed February, 2012. Shahbazi *et al* (2012) examined the effect of the c.7674_7675insC mutation present in type 3 VWD on the expressed *VWF* mRNA. The level of mRNA was measured using real time-PCR and was found to be significantly decreased in the patient's platelets with a mean ratio (patient/wild-type) of 0.03 compared to that

in normal relatives, but the level of mRNA from a heterozygous carrier was insignificantly reduced with a mean ratio of 0.6 compared to wild-type VWF mRNA level (Shahbazi et al., 2012). These findings suggested degradation of mRNA by NMD-causing null alleles. The study conducted by Corrales *et al* (2011) used RNA isolated from patients' leucocytes and platelets and *in silico* prediction studies to investigate the effect of several splice site mutations on *VWF* mRNA transcripts. Most of these changes such as c.533-2A>G, c.8155+3G>C, c.7082-2A>G resulted in exon skipping, creation of PTC and degradation of *VWF* mRNA due to NMD and compatible effects were predicted using various prediction tools (Corrales et al., 2011). The results from these studies in terms of reduced secretion due to NMD were consistent with our findings and showed a similar effect of p.S539fs on VWF.

The P9F18 family had two AFM and three UFM (Appendix 18); the frameshift mutation p.S539Lfs*38 was present in both AFM who were compound heterozygous with p.C1157R and was present alone in two UFM. The AFM who had the p.C1157R in addition to p.S539fs variant showed a very low VWF level and abnormal multimer structure (Section 3.6.2). Therefore, it was not possible to compare the expression findings with the phenotype observed in the affected members due to presence of two mutations in each affected member. Two UFM were heterozygous for only the p.S539fs variant and presented with normal VWF level and normal multimer pattern and were asymptomatic and considered as carriers of type 3 VWD. The levels of VWF:Ag, VWF:RCo and FVIII were 53-60, 50-69 and 74-75 IU/dL respectively in the UFM carrying the p.S539fs only (Table 3.8). VWF:Ag levels from *in vitro* expression were compatible at 60% of wild-type. The presence of p.S539fs alone in UFM with absence of bleeding symptoms (BS 0-2) suggested haplosufficiency as the disease mechanism as a single copy of wild-type VWF was sufficient to maintain normal function of VWF.

Also, the obtained results from transfection studies and *in silico* predictions illustrated that this frameshift variant was likely to impair the secretion of VWF due to NMD that leads to null alleles which further causes mild quantitative deficiency of plasma VWF observed in VWD patients. These findings confirm that p.S539fs was responsible for the mild deficiency of VWF observed in UFM who carry this change and it had no effect on multimer structure when present in the heterozygous form. Type 3 VWD is mostly inherited as an autosomal recessive trait and heterozygous individuals present with a mild to moderate reduction in VWF level and normal multimers that may be characterized by a mild deficiency of VWF. According to the current classification, the presence of p.S539fsL*38 in the heterozygous form is considered as type 3 VWD carrier and may be consistent with type 3 VWD when inherited in homozygous form (Sadler et al., 2006). These findings indicated that p.S539fs is a recessive mutation and may cause bleeding only when inherited in the homozygous state or in the compound heterozygous form with an additional variant. The presence of p.S539fs in the heterozygous form in

asymptomatic members suggested them to be carriers of type 3 VWD. However, other studies have indicated that type 3 VWD carriers can be symptomatic and reported that 15-50% of type 3 VWD carriers may experience some bleeding symptoms (Nichols et al., 2008b, Bowman et al., 2013). So, not all mutations are pure recessive changes and some may be inherited as co-dominant rather than recessive.

5.3.3. *In vitro* co-expression of p.[S539fs];[C1157R]

The purpose of this experiment was to replicate the inheritance pattern found in affected members who harbour these mutations on two different alleles and also to define the possible pathogenesis leading to complete deficiency of VWF in affected patients. The results obtained from co-transfection of both mutations in parallel with wild-type indicated a very low level of secreted VWF (0.6%) into the growth medium from HEK293T cells accompanied by a significant reduction of VWF (36%) present intracellularly in comparison to wild-type. Also, multimer analysis of compound heterozygous rVWF mutants showed complete absence of HMW-VWF multimers in addition to a mild effect in VWF storage. However, the expression results of the current study showed that the compound heterozygous mutations p.[S539fs];[C1157R] located on two different alleles resulted in a severe VWF secretion defect and complete loss of HMW multimers. The nearly normal storage of compound heterozygous mutants may be due to accumulation of VWF throughout cells produced from the allele carrying p.C1157R.

The IC (I:1) and his affected brother (I:2) (Appendix 18) were compound heterozygous for the missense mutation p.C1157R in the D3 assembly and frameshift mutation p.S539fs in the D2 assembly previously reported to be associated with type 3 VWD due to the observed phenotype and absence of multimers. The presence of both mutations in affected members resulted in severe bleeding symptoms and undetectable levels of documented as VWF:Ag, VWF:RCo and FVIII:C 3 IU/dL for each parameter and absence of multimers. The very small amounts of mutated rVWF and absence of multimers resulting from co-expression of rVWF L539fs and R1157 reflected the situation in patients and was similar to the phenotypic data observed in affected members. Also, the obtained results showed a good correlation between genotype and phenotype parameters. Based on these findings, we assume that *in vivo* compound heterozygous mutations p.S539fs and p.C1157R together are likely to contribute to the poor synthesis of VWF based on two independent mechanisms: firstly, p.C1157R reduced VWF synthesis due to intracellular degradation of retained mutated VWF in ER. Also, as this mutation leads to loss of cysteine, it causes misfolding of mutant VWF and impairs normal multimerization and produces abnormal multimers. The presence of undetectable levels of VWF:Ag in patient plasma cannot be explained by intracellular retention of VWF within ER due to missense mutation located in

D3 assembly alone. However, the affected members were compound heterozygous for the frameshift mutation, p.S539fs that creates a PTC and likely leads to degradation of mRNA transcripts by the NMD mechanism and p.C1157R reduces secretion due to intracellular retention which can explain the undetectable level of plasma VWF:Ag and abnormal multimers.

These findings confirmed that compound heterozygous expression of both mutations replicated the situation in the IC and AFM via different mechanisms and the affected patients were correctly classified as type 3 VWD.

The expression study of candidate mutation p.T1156M located in the D3 domain showed intracellular retention; reduced synthesis and lacking of multimers when expressed in the homozygous form, but reduced secretion and normal multimers was observed in the heterozygous form. The IC who had p.T1156M mutation had a stop mutation p.Q2470* on the other allele and presented with severe bleeding symptoms, a very low VWF level (5-9 IU/dL) and lack of HMW multimers (Lethagen et al., 2002a). Also, an ″unclassified″ VWD patient who had p.C1157F was compound heterozygous for p.K1362T located in exon 28, A1 domain and exhibited severe bleeding symptoms, markedly decreased phenotype data and loss of multimers (Hommais et al., 2006a). The presence of both mutations p.[C1157F];[K1362T] on two alleles contributed to the reduced levels of VWF:Ag to 15 IU/dL, VWF:RCo to 11 IU/dl and FVIII:C to 21 IU/dL in addition to impaired multimerisation (Matsushita et al., 2000, Hommais et al., 2006a). The family who had p.[C1157F];[K1362T] was considered as unclassified rather than other types due to the presence of two mutations each acting through a different mechanism. Moreover, the co-expression of missense mutations p.D141Y and p.C275S both located in the D1 assembly illustrated that both impaired secretion due to intracellular retention and lead to presence of dimers only (Baronciani et al., 2008). p.D141Y was found in the compound heterozygous form with the null allele c.2016_2019del in one patient and the patient with p.C275S was compound heterozygous for nonsense mutation p.W222* (Baronciani et al., 2003). Both patients were classified as type 3 VWD and presented with severe bleeding symptoms and very low levels of VWF, abnormal function of VWF:RCo and abnormal multimers. The results from this study indicated that the effect of p.[S539fs];[C1157R] on VWF expression was consistent with other findings.

In conclusion, *in vitro* expression studies in HEK293T cells confirmed the pathogenic nature of p.S539fs and p.C1157R identified in the affected family. Based on expression studies, the presence of the single mutation p.C1157R alone located in the D3 assembly causes intracellular retention and loss of HMW multimers in patients' plasma and should be classified as type 2A(IIE). The presence of p.S539fs alone in the heterozygous state leads tol normal lev of VWF and individuals should be classified as carriers of a null *VWF* allele that could also contribute to

to other recessive form of VWD. The presence of both mutations p.[S539fs];[C1157R] in affected members is disease related and can explain the low levels of VWF and observed phenotypes. The accuracy of classification plays an important role for treatment decision and genetic counselling (Sadler et al., 2000, Sadler et al., 2006). Therefore, the presence of both changes in compound heterozygous state contributes to the complexity of classification.

Chapter 6

In vitro characterisation of silent mutation associated with type 1 VWD

6. *In vitro* characterisation of silent mutation associated with type 1 VWD

6.1. Introduction

The EU study (MCMDM-1VWD) successfully detected candidate mutations throughout *VWF* in almost 70% of type 1 VWD IC, but failed to identify mutations in the remaining IC (Goodeve et al., 2007). Eighteen IC of 77 that showed no previously identified mutations were re-sequenced using a sensitive technique and primers free of SNP within primer binding sites. As a result, four mutations were identified in four IC (Section 3.6), and one of them was a silent heterozygous mutation. This silent mutation was identified in exon 28 in the A1 domain (c.4146T>G), located at the third position of codon 1382 and was predicted to result in p.L1382= in one IC who showed no other mutation in the previous study. This change was found in the IC and AFM who had mild reductions of VWF:Ag levels and normal multimers (Appendix 19).

In silent or synonymous mutations, the nucleotide change alters the triplet codon structure but encodes the same amino acid. It was historically believed that apparent silent mutations had no effect on gene expression. However, several studies indicated that silent mutations within a gene may contribute to disease phenotype through a number of mechanisms (Duan et al., 2003, Nielsen et al., 2007). In mammals, silent changes can alter protein synthesis and may contribute to disrupting normal mRNA translation rate during gene expression through several mechanisms (Table 6.1). They include splice regulation, mRNA translation rate, ribosome trafficking and miRNA binding.

Table 6.1 List of the possible mechanisms that could be involved in silent mutations

Molecule	Level of impact	Mode of action
Splice site	Pre-mRNA	Introduces new donor or acceptor splice sites leading to partial exon skipping (Daidone et al., 2011)
ESE and ESS	Pre-mRNA splicing (Nucleus)	Exonic mutation can lead to loss of ESE or gain of ESS that causes complete or partial exon skipping (Nielsen et al., 2007)
tRNA	mRNA translation	Codon usage bias Reduces translation rate and can result in misfolded protein (Duan et al., 2003)
Ribosome	mRNA translation	Impairs movements of multiple ribosomes causing collisions that reduce translation rate leading to misfolded protein (Mitarai et al., 2008)
miRNA	mRNA translation	Leads to formation of small mRNA region complementary to miRNA sequence forming dsRNA. dsRNA is degraded (Hurst, 2011)

6.1.1. Effect of synonymous mutation on normal splicing pathway

The stored genetic information in DNA is transcribed into pre-mRNA in the nucleus which is subsequently translated into protein. The pre-mRNA contains both protein coding and non-coding regions and the removal of non-coding pre-mRNA sequences (introns) from the mRNA transcript (mRNA splicing) before translation is an important process required for the production of mature mRNA and protein synthesis. Several factors that participate in this process include exon, intron, donor and acceptor splice-sites, exonic splice enhancer (ESE), exonic splice silencer (ESS), intronic splicing enhancer (ISE) and the spliceosome. The donor splice-site located at the 5' end of the intron and acceptor splice-site at the 3' end of intron form junctions between exons and introns. The splicing process occurs in a number of steps. The splicing mechanism is mediated by small protein-RNA complexes including the spliceosome complexes, and ESE, ESS and ISE elements. The spliceosome is a protein molecule assembled from small ribonuclear proteins (snRNPs) forming the splicing machinery (Hastings and Krainer, 2001, Hurst, 2011). ESE, ESS and ISE are short RNA conserved sequences usually found in genes with long introns to facilitate handling the splicing tools during splicing found in both exons and introns that act as regulators of the splicing mechanism (Fairbrother et al., 2002). The spliceosome cleaves the pre-mRNA at the junction between exon and intron (splice-site), beginning at the 5' end of the intron (GU-sequence-donor splice-site) forming a lariat loop and then cleaves the 3' end of intron (AG-sequence-acceptor splice-site) releasing the lariat loop, joining exons together in order to produce mature mRNA containing exon coding regions only (Figure 6.1A). This process is successfully achieved with help of ESE and ESS (Berget, 1995, Chen and Manley, 2009).

In silico analysis predicted that the silent change c.4146G>T had no effect on donor and acceptor splice site sequences and therefore would not impair mRNA splicing. However, additional prediction of ESE and ESS sequences indicated that the silent change had a potential effect on both ESE and ESS sequences (Section 3.6.3.2). There are several consensus sequences present in the exonic and intronic sites that represent splice enhancer and splice silencer sequences essential for normal splicing to occur. Mutations in such sequences may destroy or create splice-site regulatory sequences and can be pathogenic leading to either splicing defects or complete exon skipping.

Several experimental studies have demonstrated that silent changes had a pathogenic effect on protein synthesis and may contribute to hampering normal mRNA translation rate through splicing changes during gene expression (Lorson and Androphy, 2000, Nielsen et al., 2007). Some exonic changes have been suggested to alter the pre-mRNA splicing either by leading to loss of the main donor/acceptor site sequences or by altering splicing regulatory sequences such

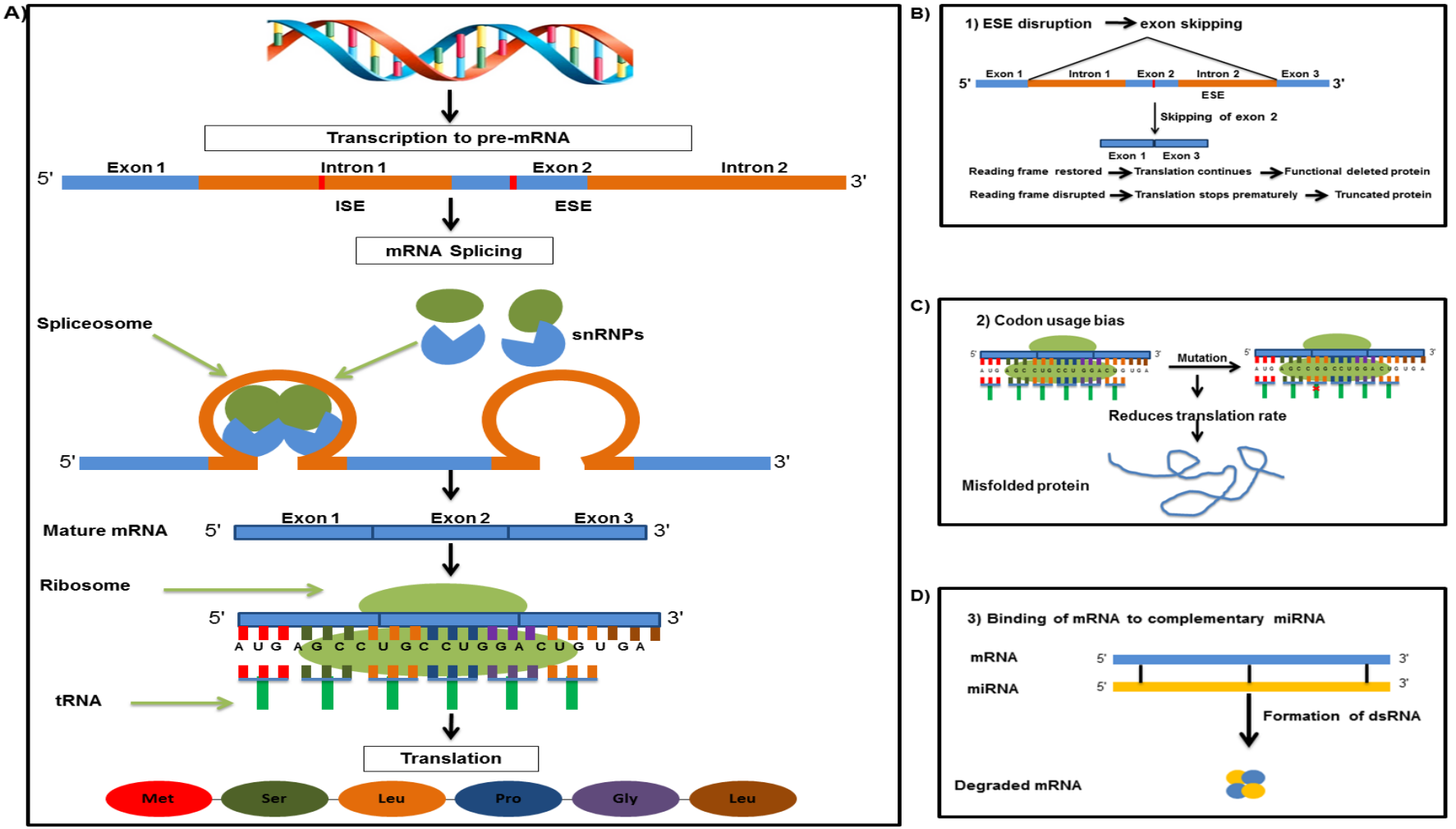

Figure 6.1 Schematic representations of normal and defective DNA transcription and translation. A) represents normal DNA transcription, splicing and translation. **B, C and D)** represent possible mechanisms acting on VWF expression associated with c.4146G>T.

as ESE and ISE and may contribute to the pathogenicity of type 1 VWD (Figure 6.1B). The presence of exonic or intronic silent changes can generate a new donor splice site causing exon skipping. The synonymous mutation c.7056C>T; p.G2352= located within *VWF* exon 41 was predicted to create a new donor splice site leading to deletion of 26 exonic nucleotides and the entire intron 41. *In vitro* expression study using a vector lacking nucleotides between 7055 and 7081 demonstrated the absence of secreted VWF when *VWF* cDNA lacked 26 nucleotides expressed in the homozygous form and 50% of VWF was secreted in heterozygous form (Daidone et al., 2011). These findings suggested that this synonymous mutation could cause the mutant allele to be missed. Pagliari et al (2013) have also studied the effect of synonymous mutation c.3390C>T;p.C1130= located in *VWF* exon 26 in three type 2A/IIE VWD patients through mRNA analysis and *in vitro* expression using transient transfection in HEK293. These patients presented with high BS, moderate reduction of plasma VWF ranging between 13-27 IU/dL and normal multimers. The analysed mRNA isolated from healthy individuals and patient platelets using RT-PCR showed that the wild-type allele is more abundant than the mutant one. *In silico* splicing analysis predicted the effect of c.3390C>T on splicing enhancers and silencers that may cause exon 26 exclusion. Transient transfection using a plasmid lacking exon 26 revealed a 55% reduction of secreted VWF accompanied by a 176% increase of VWF in the cell lysate when expressed in the homozygous form and a 32% reduction in the heterozygous form accompanied by 132% increase of VWF in cell lysate compared to 100% wild-type (Pagliari et al., 2013).

The impact of exonic silent changes on the splicing pathway is not limited only to complete exon exclusion, but it can also lead to partial exclusion causing mild to moderate splicing defects (Tournier et al., 2008). Alteration in the conserved nucleotides present in splice-sites or ESE in exon can result in abnormal splicing and causes exon skipping and NMD or alters the efficiency of splicing (Nielsen et al., 2007, Tournier et al., 2008). Truncated proteins are produced when exon skipping disrupts the reading frame producing PTC, but translation will continue if the reading frame is restored and produces functional mutant protein. Nielsen *et al* (2007) reported exon skipping of the aberrant mRNA resulting from a silent exonic mutation that impairs a putative ESE binding site in the medium-chain acyl-CoA dehydrogenase (*MCAD*) gene. Also, two exonic mutations; c.793C>T and c.794G>A identified in exon 10 of the mutL homolog 1 (*MLH1)* gene were investigated for their effect on splicing regulatory elements using a mini-gene assay and found to cause partial exon 10 skipping (Tournier et al., 2008). Not all exon skipping leads to NMD as Cartwright (2013) found that expression of type 1 VWD in-frame heterozygous exon deletions leads to a dominant-negative reduction in VWF secretion from transiently transfected HEK293T cells. The dominant negative mechanism suggests that there is no NMD but a shorter functional protein is produced (Cartwright et al., 2013).

6.1.2. Effect of synonymous mutation on translation rate and protein folding

Following splicing, the mature mRNA moves to the cytoplasm across the rough ER outer membrane where translation and protein synthesis takes place. Several molecules including mature mRNA, ribosomes, tRNA and release factor are used to achieve translation. The mature mRNA contains only exon coding regions and has a methylated cap at its 5' end and poly-A tail at the 3' end. The small subunit of the ribosome binds to the cap site of mRNA at the 5' end initiating the translation process. The tRNA molecule that contains the anti-codon complementary to the first mRNA codon binds to the AUG codon encoding methionine, followed by binding of the large subunit of ribosome forming the mRNA-ribosome complex. The second tRNA which is complementary to the second mRNA codon binds mRNA and joins the next amino acid to methionine. The elongation stage in terms of the growing polypeptide continues until the stop codon. The stop codon activates release factor that terminates translation (Figure 6.1A). Release factor is a protein that recognises the stop codon in an mRNA and contributes to termination of translation. At the end, the ribosome subunit dissociates from mRNA and the newly formed protein enters the ER to mediate its shape and conformation (Chapeville et al., 1962, Karp, 2008).

It has been found that silent changes can impair the rate of translation and protein folding during *in vivo and in vitro* translation via various mechanisms. Protein folding is a co-translational process to which mRNA, ribosome and chaperone proteins contribute. Various experimental studies have illustrated that synonymous changes can influence mRNA and protein shape, structure, folding and stability (Sharp et al., 1995, Chamary et al., 2006, Shabalina et al., 2006).

Codon usage frequency has been found to influence translation rate and efficiency, which further affects polypeptide folding (Figure 6.1C). Codons that are used more frequently are translated faster than rare codons because each codon has a particular tRNA and its relative abundance affects translation rate (Mitarai et al., 2008). A reduction in the rate of protein translation has been reported when a synonymous nucleotide change is present in the third position of the triplet codon. These variants result in disturbing the interaction between mRNA codon and the tRNA anti-codon and affect the efficient translation rate and protein folding (Shah et al., 2008).

mRNA is the carrier of genetic code and encodes amino acid sequences using the triplet code. It was reported that the less frequent codons are found at the 5' of the mRNA sequence more than in the 3' sequence and this may be attributed to either prevent ribosome traffic congestion through controlling the high translation rate or due to the need for weak mRNA secondary structure in this area to allow translation to start (Kudla et al., 2009, Klumpp et al., 2012).

Synonymous codon exchange can impair the translation rate through influencing multiple ribosome movements and causing ribosomes collisions. Frequent codons are translated faster than rare ones, preventing ribosome collisions and increasing ribosome movements (Mitarai and Pedersen, 2013).

The presence of synonymous mutations in patients with Crohn's disease results in the formation of small regions of mRNA which are complementary to miRNA, forming dsRNA (Figure 6.1D). The formed aberrant dsRNA is degraded and terminated which leads to formation of null allele (Hurst, 2011).

6.1.3. Hypothesis and aims

We hypothesised that silent mutations may have a deleterious effect on protein synthesis and structure through several mechanisms. It has been reported that silent changes can affect protein synthesis via disturbing the translation rate and protein folding which can affect the level of protein secreted. The presence of c.4146G>T in the affected family could be responsible for the phenotypes observed and could contribute to type 1 VWD. This study aimed to investigate the effect of the silent change c.4146G>T plus c.4146G>A and c.4146G>C that alter the same codon on VWF level, multimers and storage through *in vitro* expression and also aimed to understand the pathogenicity and disease causing mechanism of this change. The plasmid vectors carrying the wild-type and mutant *VWF* cDNA were transiently transfected into HEK293T cells in the heterozygous and homozygous states and VWF in supernatants and lysates VWF were quantified using ELISA.

In addition to effect of the silent change on the mRNA translation rate, it could impair normal splicing leading to either exon skipping or reducing splicing efficiency. This study aimed to investigate the effect of c.4146G>T silent mutation on splicing efficiency through mini-gene analysis.

6.2. Results

6.2.1. Graphical codon usage

Codon usage indicates the differences in codon frequency between several triplet codons that each encode the same amino acid. The graphical codon usage analyser (GCUA) (Section 2.2.10) was used to compare the frequency of the four triplet codons encoding leucine including the wild-type codon CTG, mutant codon CTT and two hypothetical triplet mutant codons CTA and CTC that differ only at the third position of the codon. The hypothetical mutant codon CTA was predicted to be the least frequently used with a 82% difference compared to the wild-type CTG codon. Also, there was a 68% and 51% difference in codon frequency between the wild-type codon and the CTT and CTC codons respectively (Figure 6.2). These findings suggested that the observed and hypothetical mutant codons are less frequently used than the wild-type codon to varying degrees and could impair protein folding and the rate of protein translation. Additional codons TTG and TTA that also encode leucine were also analysed and compared to wild-type (Figure 6.2).

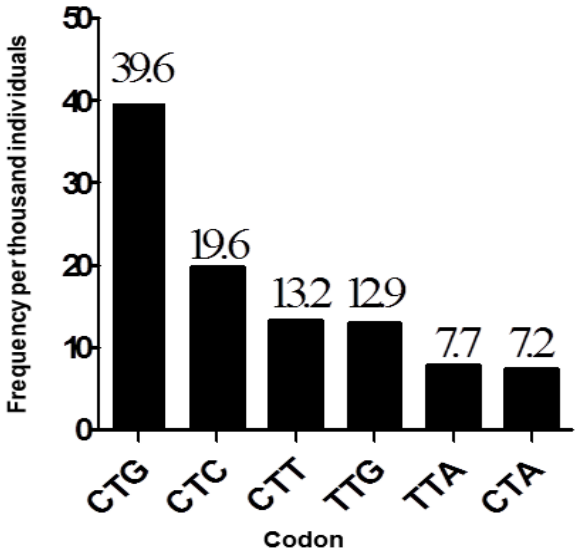

Figure 6.2 Frequencies of triplet codon usage that encode leucine at position c.4146 in *VWF* using GCUA analyser in *Homo sapiens*. CTG represents the wild-type codon at nucleotide position c.4146 of *VWF*, CTT represents the mutant codon while CTA, CTC, TTG and TTA represent the other possible codons that encode leucine. The hypothetical mutant codon CTA was 82% lower in frequency compared to wild-type, while mutant codons CTT and CTC were 68% and 51% lower in frequency respectively (Nakamura et al., 2000).

6.2.2. Location of p.L1382= in VWF

The VWF A1 domain is the site where VWF interacts with platelet GpIbα receptor and the presence of mutations within this domain may alter this interaction. The analysed crystal structure (Section 2.2.9) showed that the silent mutation p.L1382= is located within a beta sheet (Figure 6.3A) and found to be away from the α-helix site of binding with platelets (Figure 6.3B) suggesting that this silent variant is unlikely to disturb the interaction of VWF with platelet GpIbα receptor. However, whilst this variant is located away from the site of GpIbα interaction, if the protein translation rate is affected, this may modify the correct interaction between the VWF A1 domain and GpIbα receptor.

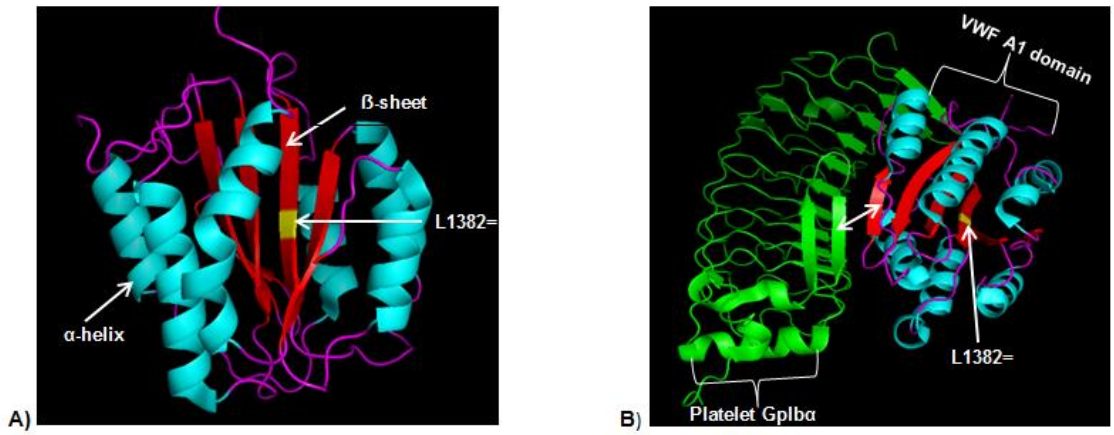

Figure 6.3 Pymol model of the 3D structural location of p.L1382= in the VWF A1 domain and area of interaction between VWF and platelet GpIbα receptor. A) Represents the site of the silent change p.L1382 (yellow) within the VWF A1 domain beta sheet (red). **B)** Represents the area of interaction between the VWF A1 domain and platelet GpIbα receptor. White two sided arrow represents the interaction between VWF and platelet (A1-GpIb binding site). The structure of the VWF A1 domain and platelet GpIbα receptor was obtained from the Protein Data Bank (PDB) (Dumas et al., 2004).

6.2.3. Mutagenesis

The expression plasmid pcDNA3.1 Hygro (-) harbouring wild-type *VWF* cDNA was used to insert the desired nucleotide change and was followed by transfection to examine the potential effect of c.4146G>T and other hypothetical changes at the same codon on the level and the structure of VWF. c.4146G>T was predicted to result in silent change p.L1382=. Also, mutagenesis was performed to introduce other possible hypothetical p.L1382= mutants c.4146G>A and c.4146G>C at the same codon which still result in leucine. The purpose of introducing the other possible mutants was to perform *in vitro* expression for all mutants and compare findings to the predicted rate of codon usage between the four possible nucleotides at position c.4146. Following mutagenesis and sequence analysis of the VWF plasmid, c.4146G>T and both hypothetical mutants c.4146G>A and c.4146G>C were successfully introduced to the *VWF* cDNA sequence with no additional nucleotide changes observed (Figure 6.4).

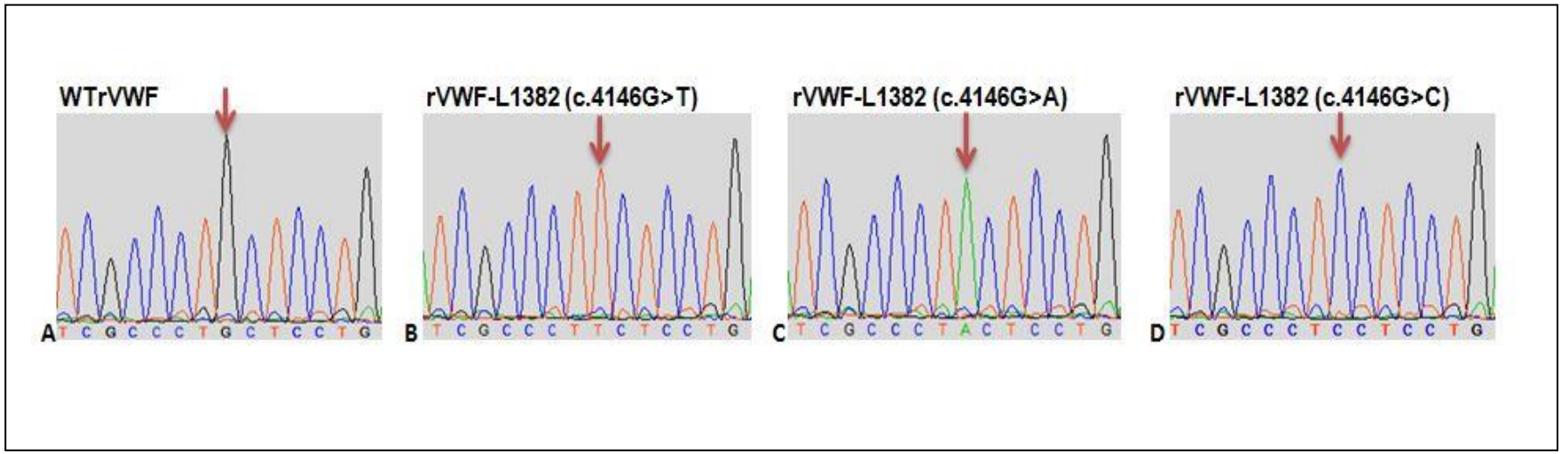

Figure 6.4 Sequence chromatographs to show introduction of silent variants into the cDNA VWF plasmid. **A)** shows the wild type VWF cDNA sequence. **B)** shows c.4146G>T; **C)** shows c.4146G>A; **D)** shows c.4146G>C.

6.2.4. *In vitro* expression of *rVWF* harbouring the candidate mutation p.L1382=

These expression experiments were aimed to evaluate whether the p.L1382= silent change has a potential effect on VWF expression. Each of the 4 possible nucleotides at c.4146, *rVWF* cDNA plasmid of wild-type, mutant c.4146G>T and hypothetical mutants c.4146G>A and c.4146G>C were expressed in HEK293T cells using the same expression system previously described (Section 2.2.13.5) and used in Chapter 4.

The transfection experiments for the mutant c.4146G>T were performed in triplicate and repeated three times for wild-type, mutant homozygous and mutant heterozygous states, while the other hypothetical mutants c.4146G>A and c.4146G>C were expressed similarly but undertaken in triplicate twice.

6.2.4.1. Quantitative analysis of the expressed rVWF-WT and mutant plasmid (c.4146G>T; rVWF-L1382) transfected into HEK293T cells

The measured mean values of secreted and intracellular rVWF are shown in tables 6.2 and 6.3. *In vitro* expression of rVWF-L1382 (c.4146G>T) interestingly demonstrated that the secreted rVWF heterozygous and homozygous mutant was significantly reduced to 60% and 76% respectively (p<0.0001 and <0.001, one way ANOVA) compared to 100% wild-type (Figure 6.5).

The level of secreted homozygous mutant VWF was 15% higher than the level of heterozygous mutant and the differences between the secreted VWF level of heterozygous and the homozygous states attained statistical significance with a p value of <0.05. To confirm these findings, a further independent clone of the plasmid harbouring the c.4146G>T change was expressed and the obtained results were similar with no significant difference with these findings (Figure 6.5).

The mean values of intracellular rVWF obtained by expression of the heterozygous c.4146G>T were significantly decreased to 77% with p values of less than 0.001. In the homozygous form, the mean levels of intracellular VWF were 103% with no significant difference when compared to 100% wild-type.

In summary, the measured mean values of VWF suggested that p.L1382= resulted in reduced VWF secretion from HEK293T cells following transfection compared to rVWF wild-type. This silent change p.L1382= led to a significant reduction in the level of secreted VWF in both homozygous and heterozygous states in addition to a significant reduction in the level of intracellular VWF when expressed in the heterozygous state. These findings suggest a significant effect of p.L1382= on VWF expression.

Table 6.2 The mean values and standard deviation of secreted VWF:Ag levels post-transfection for WT and mutant plasmids (rVWF-c.4146G>T) in HEK293T cells

VWF (Supernatant)	Mean (%)	*SD
rVWF-WT (homozygous)	100.0	6.0
WT:Mut (50:50) (heterozygous)	61.0	14.0
rVWF-L1382= (homozygous)	76.5	16.0

*SD= standard deviation

Table 6.3 The mean values and standard deviation of retained VWF:Ag levels harvested post-transfection for WT and mutant plasmids (rVWF-c.4146G>T) in HEK293T cells

VWF (Cell lysate)	Mean (%)	*SD
rVWF-WT (homozygous)	100.0	10.0
WT:Mut (50:50) (heterozygous)	77.0	15.0
rVWF-L1382= (homozygous)	103.0	18.0

*SD= standard deviation

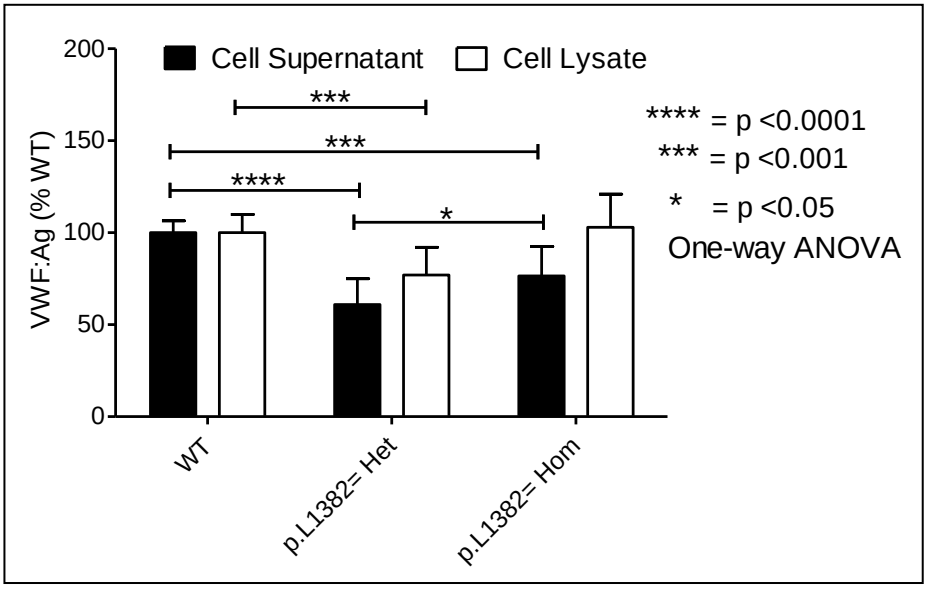

Figure 6.5 Mean levels of VWF:Ag in both supernatant and cell lysates of HEK293T cells transfected with WT and mutant expression plasmids showing the effect of the p.L1382= (c.4146G>T) mutation on *VWF* expression. Results are expressed as a percentage in comparison with wild-type. The horizontal black bars represent the extent of difference between mean values of VWF:Ag between wild-type and mutant VWF. The vertical black bars indicate the standard deviation. Statistical test used is one-way ANOVA.

6.2.4.2. Multimer analysis of wild-type and c.4146G>T; p.L1382= VWF secreted from HEK293T cells

The multimeric composition of VWF secreted from the transfected HEK293T cells into the growth medium of wild-type plasmid, mutant plasmid and co-transfection of mutant/wild-type plasmids was evaluated using medium resolution 1.6% sodium dodecyl sulphate agarose (SDS) gel electrophoresis at 1:3 dilution. As a result, the multimeric composition of rVWF secreted from HEK293T cells showed a normal multimer pattern in both homozygous and heterozygous states compared to wild-type (Figure 6.6). A full array of multimer bands composed of high, intermediate and low molecular weight multimers were observed in the wild-type VWF and in both homozygous and heterozygous forms.

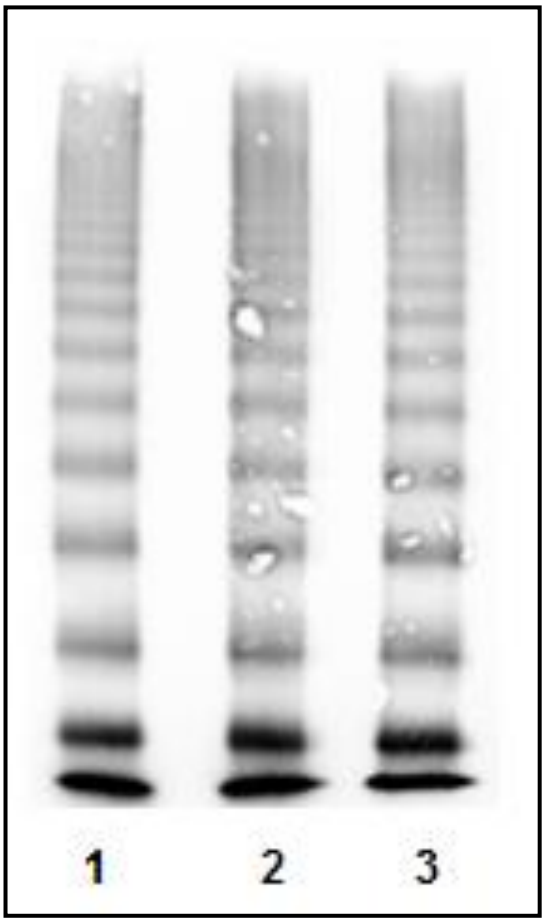

Figure 6.6 Multimer analysis of secreted rVWF c.4146G>T; p.L1382= from HEK293T cells. Multimer patterns of wild-type rVWF (lane 1), mutant rVWF-L1382 (lane 2) and hybrid rVWF (lane 3) on 1.6% medium resolution gel at 1:3 dilution are shown. The multimeric composition of rVWF resulting from transfecting cells with mutant and hybrid showed normal VWF multimer patterns with the presence of a full array of multimer bands.

6.2.4.3. Confocal microscopy imaging of c.4146

Following *in vitro* expression of mutants in HEK293 cells, transfected cells were stained and examined using a confocal microscope in order to determine the intracellular storage of VWF. For all possible nucleotide changes at c.4146, confocal microscopy was undertaken in the homozygous and heterozygous forms and compared to wild-type. The shape of WPB-like structures, size and frequency of each form was compared to those of wild-type. Cells were stained as previously described in chapter 4 (Section 4.2.5.2).

6.2.4.3.1. Confocal microscopy of c.4146G>T; p.L1382=

In vitro expression of the c.4146G>T revealed a significant VWF defect in secretion in both homozygous and heterozygous forms. Also, intracellular VWF of the heterozygous form of this variant showed a reduction compared to wild-type. Confocal imaging of wild-type showed the presence of punctate rounded WPB-like organelles throughout the cell (Figure 6.7 A and C). The visualised WPB-like structures in the homozygous form appeared similar in shape and size to those present in the wild-type (Figure 6.7 D and F). In the heterozygous form of c.4146G>T; p.L1382= silent change, punctate WPB-like structures were seen throughout the cell, but appeared relatively fewer in number in comparison to those present in the wild-type (Figure 6.7 G and I). This variant appears to affect VWF storage when present in the heterozygous form. Overall, in this mutant, the heterozygous form of the mutation results in a more severe phenotype *in vitro* than in the homozygous form. This may be due to differences between the homozygous and heterozygous mutations during protein synthesis and processing (as discussed in section 6.3.

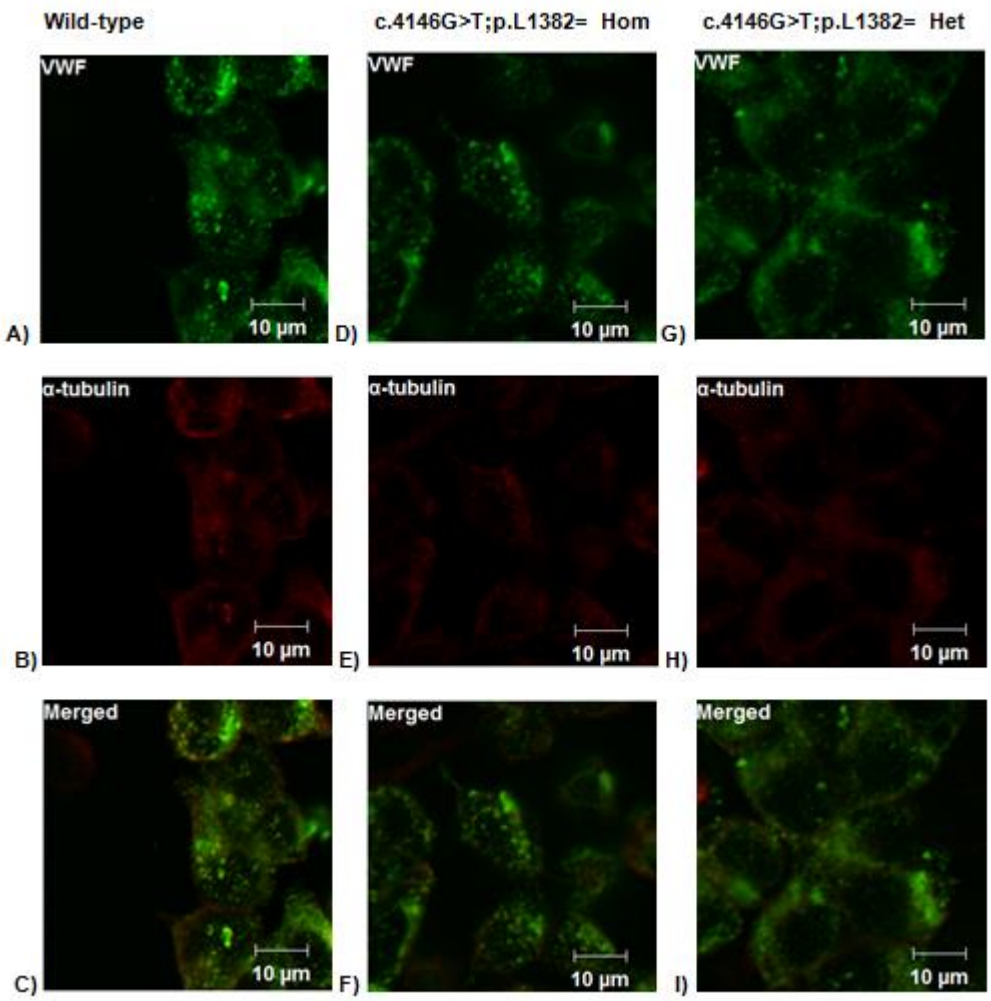

Figure 6.7 Intracellular storage of rWT and rVWF-L1382 mutant in HEK293 cells by confocal microscopy. A, D and G) Represent VWF (green) after transfection of wild-type, homozygous and heterozygous plasmids respectively into HEK293 cells. **B, E and H)** Represent the cell membrane marker α-tubulin (red) after transfection of wild-type, homozygous and heterozygous respectively into HEK293 cells. **C, F and I)** Represent merged images of VWF and α-tubulin staining for wild-type, homozygous and heterozygous respectively transfected into HEK293 cells. Cells of the upper horizontal row **(A, D and G)** were stained with rabbit anti-VWF primary and anti-rabbit Alexa Fluor 488 for VWF (green), while cells of the middle horizontal row (**B, E and H)** were stained with mouse anti-α-tubulin and anti-mouse Alexa Fluor 555 for the cell membrane α-tubulin marker (red). The lower horizontal row **(C, F and I)** shows a merge of VWF and α-tubulin staining.

6.2.5. Quantitative analysis of the expressed rVWF-WT and hypothetical mutant plasmid (rVWF-c.4146G>A; p.L1382=) transfected into HEK293T cells

The obtained results revealed a significant reduction in secretion of VWF from both heterozygous and homozygous forms of 76% ($p<0.0001$) and 65% ($p<0.001$) respectively in comparison to 100% wild-type (Table 6.4). Also, the difference between the heterozygous and homozygous forms of c.4146G>A; p.L1382= was statistically analysed and found to be significant with a p value of <0.01 (Figure 6.8).

Moreover, analysis of the intracellular VWF within cells showed that in the heterozygous form of this silent mutation, a significant 68% ($p<0.001$) reduction was observed, while a 53% ($p<0.001$) significant reduction was observed when expressed in the homozygous form in comparison to 100% wild-type (Table 6.5). The differences between cell lysate VWF levels of heterozygous and homozygous forms of this variant was statistically significant ($p<0.01$, one way ANOVA) (Figure 6.8).

Table 6.4 The mean values and standard deviation of secreted VWF:Ag levels post-transfection for WT and mutant plasmids (rVWF-c.4146G>A) in HEK293T cells

VWF (Supernatant)	Mean (%)	*SD
rVWF-WT (homozygous)	100.0	7.0
WT:Mut (50:50) (heterozygous)	24.0	3.0
rVWF-L1382= (homozygous)	35.0	2.5

*SD= standard deviation

Table 6.5 The mean values and standard deviation of retained VWF:Ag levels harvested post-transfection for WT and mutant plasmids (rVWF-c.4146G>A) in HEK293T cells

VWF (Cell lysate)	Mean (%)	*SD
rVWF-WT (homozygous)	100.0	10.0
WT:Mut (50:50) (heterozygous)	32.0	1.5
rVWF-L1382= (homozygous)	47.0	3.0

*SD= standard deviation

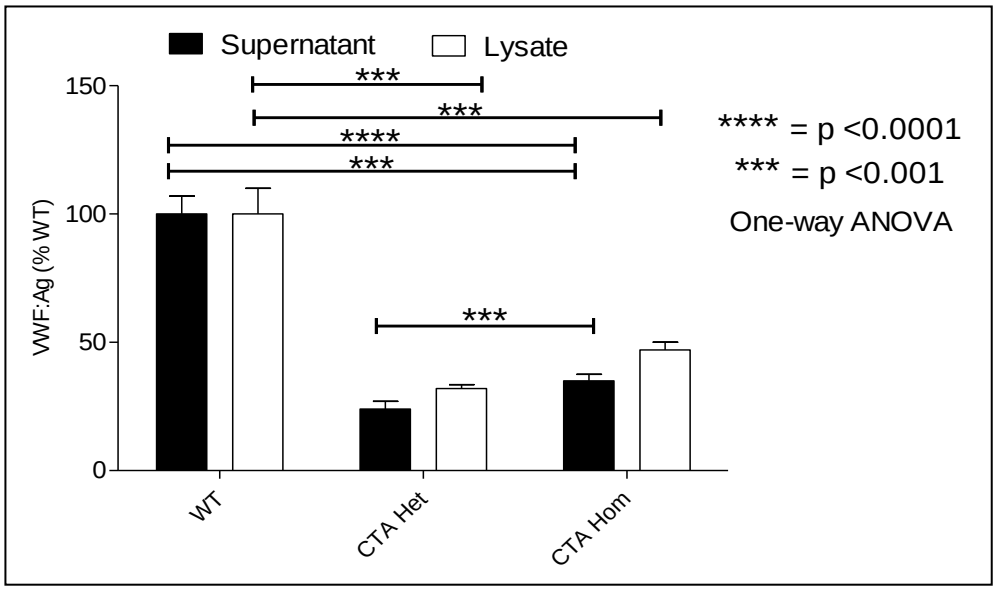

Figure 6.8 Mean levels of VWF:Ag in both supernatant and cell lysates of HEK293T cells transfected with WT and mutant expression plasmids showing the effect of the p.L1382= (c.4146G>A) mutation on *VWF* expression. Results are expressed as a percentage in comparison with wild-type. The horizontal black bars represent the extent of difference between mean values of VWF:Ag between wild-type and mutant VWF. The vertical black bars indicate the standard deviation. Statistical test used is one-way ANOVA.

6.2.5.1. Multimer analysis of wild-type and c.4146G>A; p.L1382= rVWF protein secreted from HEK293T cells

Multimer analysis of the c.4146G>A; p.L1382= revealed the presence of all multimer bands including high, intermediate and low molecular weight multimers in both homozygous and heterozygous forms similar to multimer patterns observed in the wild-type (Figure 6.9).

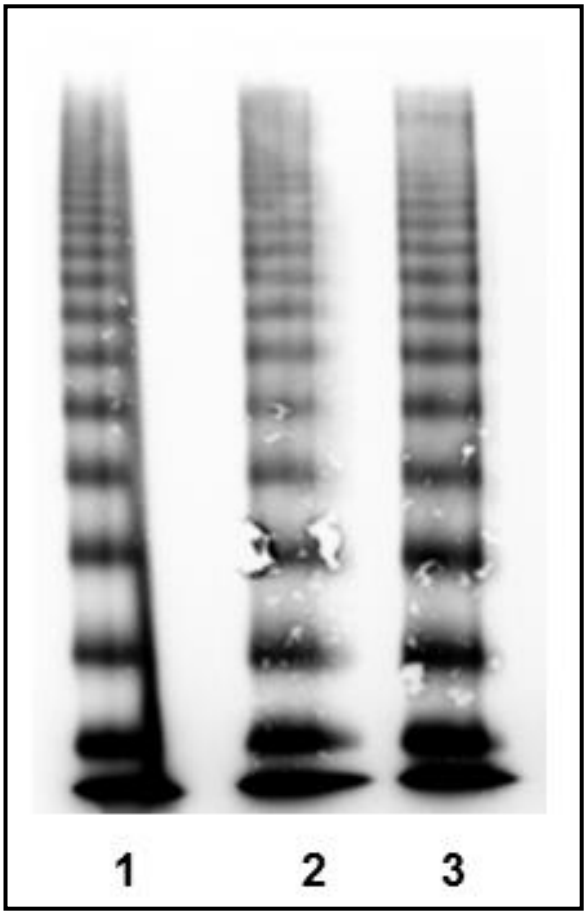

Figure 6.9 Multimer analysis of secreted rVWF c.4146G>A; p.L1382= from HEK293T cells. Multimer patterns of wild-type rVWF (lane 1), mutant rVWF-L1382 (lane 2) and hybrid rVWF (lane 3) on 1.6% medium resolution gel at 1:3 dilution are shown**.** The multimeric composition of rVWF resulting from both homozygous and heterozygous forms showed normal VWF multimer patterns with the presence of a full array of multimer bands similar to wild-type multimers.

6.2.5.2. Confocal microscopy of c.4146G>A; p.L1382=

In vitro expression of the c.4146G>A; p.L1382= revealed a significant reduction in supernatant and lysate VWF in both homozygous and heterozygous forms compared to wild-type. The punctuate round shaped WPB like organelles were visualised throughout the cell in confocal imaging of the wild-type (Figure 6.10 A and C). In the homozygous mutant form, the visualised WPB-like structures present appeared similar in shape and size to those present in the wild-type but less frequent throughout the cell (Figure 6.10 D and F). The punctate WPB-like structures found in the heterozygous form of the c.4146G>A variant were formed throughout the cell and appeared similar in size and shape to those visualised in the wild-type but with less proportion (Figure 6.10 G and I). Confocal imaging suggested that c.4146G>A has an effect on VWF storage.

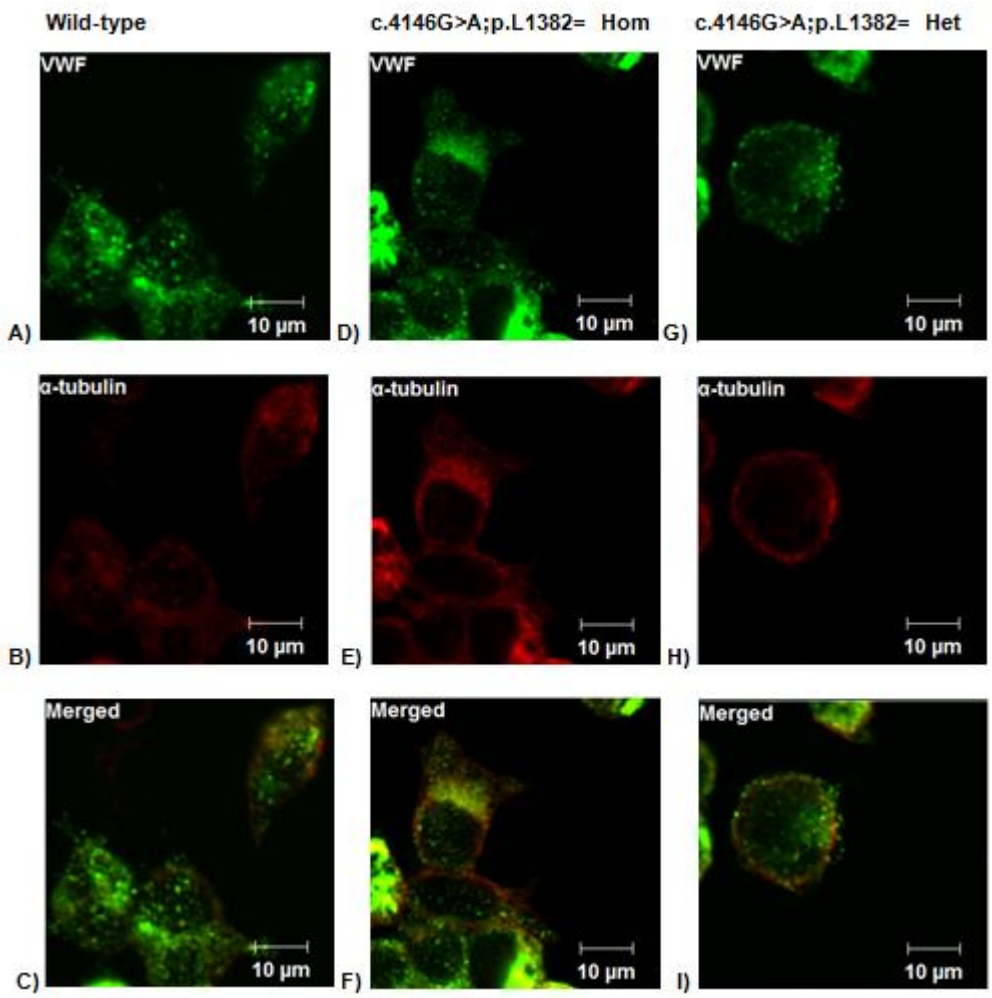

Figure 6.10 Intracellular storage of rWT and c.4146G>A;rVWF-L1382 mutant in HEK293 cells by confocal microscopy. A, D and G) Represent VWF (green) after transfection of wild-type, homozygous and heterozygous plasmids respectively into HEK293 cells. **B, E and H)** Represent the cell membrane marker α-tubulin (red) after transfection of wild-type, homozygous and heterozygous respectively into HEK293 cells. **C, F and I)** Represent merged images of VWF and α-tubulin staining for wild-type, homozygous and heterozygous respectively transfected into HEK293 cells. Cells were stained as described in figure 6.6.

6.2.6. Quantitative analysis of the expressed rVWF-WT and mutant plasmid (rVWF-c.4146G>C; p.L1382=) transfected into HEK293T cells

Analysis of secreted VWF level of hypothetical mutant c.4146G>C revealed a significant reduction in both heterozygous and homozygous forms (Table 6.6). In the heterozygous form c.4146G>C; rVWF-L1382, resulted in a significant reduction of 68% of secreted VWF when compared to 100% wild-type ($p<0.001$). The homozygous form of this mutation also revealed a significant reduction of 50% in comparison to wild-type ($p<0.001$). Furthermore, a significant difference between the secreted mean values of both heterozygous and homozygous was observed with p value of <0.05 (Figure 6.11).

Analysis of the mean values of intracellular rVWF obtained by expression of homozygous form was significantly increased to 111% with p value of <0.01. Also, in the heterozygous form of intracellular VWF a significant reduction of 40% was observed when compared to wild-type ($p<0.01$) (Table 6.7).

Table 6.6 The mean values and standard deviation of secreted VWF:Ag levels post-transfection for WT and mutant plasmids (rVWF-c.4146G>C) in HEK293T cells

VWF (Supernatant)	Mean (%)	*SD
rVWF-WT (homozygous)	100.0	7.0
WT:Mut (50:50) (heterozygous)	32.0	6.0
rVWF-L1382= (homozygous)	50.0	1.5

*SD= standard deviation

Table 6.7 The mean values and standard deviation of retained VWF:Ag levels harvested post-transfection for WT and mutant plasmids (rVWF-c.4146G>C) in HEK293T cells

VWF (Cell lysate)	Mean (%)	*SD
rVWF-WT (homozygous)	100.0	10.0
WT:Mut (50:50) (heterozygous)	60.0	2.5
rVWF-L1382= (homozygous)	111.0	13.0

*SD= standard deviation

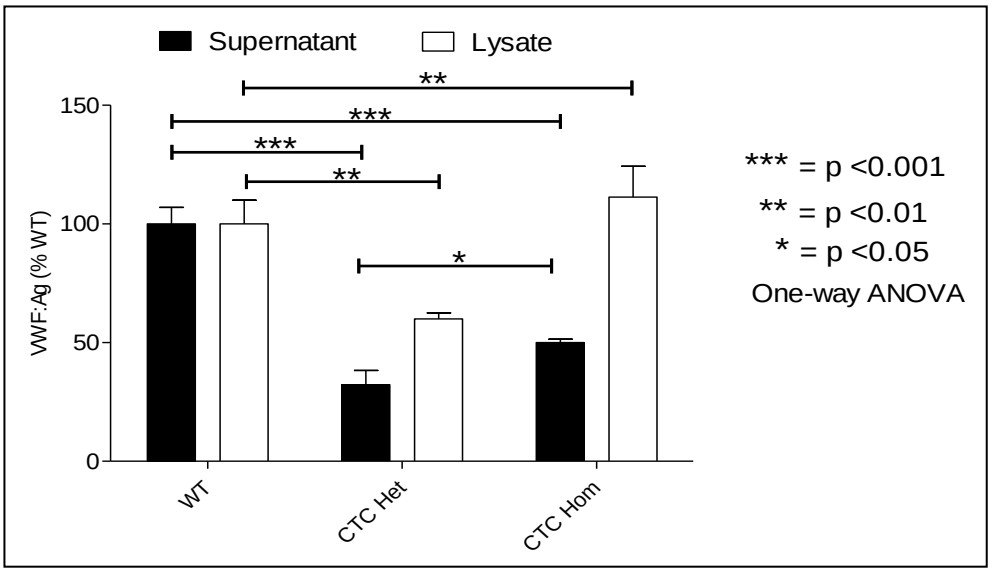

Figure 6.11 Mean levels of VWF:Ag in both supernatant and cell lysates of HEK293T cells transfected with WT and mutant expression plasmids showing the effect of the p.L1382= (c.4146G>C) mutation on *VWF* expression. Results are expressed as a percentage in comparison with wild-type. The horizontal black bars represent the extent of difference between mean values of VWF:Ag between wild-type and mutant VWF. The vertical black bars indicate the standard deviation. Statistical test used is one-way ANOVA.

6.2.6.1. Multimer analysis of wild-type and c.4146G>C; p.L1382= rVWF protein secreted from HEK293T cells

Analysis of the p.L1382=; c.4146G>C multimers revealed multimeric composition of rVWF secreted from HEK293T cells was normal in both homozygous and heterozygous states compared to wild-type multimers (Figure 6.12). A full array of multimer bands composed of high, intermediate and low molecular weight multimers was observed in the wild-type VWF and in both homozygous and heterozygous forms. However, quantity of VWF in the homozygous and heterozygous bands appeared reduced in comparison with wild-type.

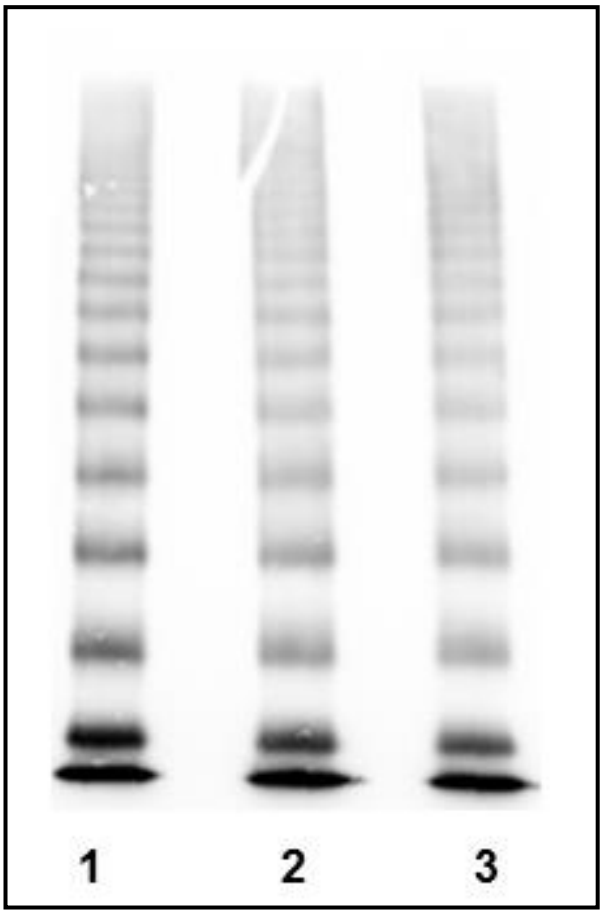

Figure 6.12 Multimer analysis of secreted rVWF c.4146G>C; p.L1382= from HEK293T cells. Multimer patterns of wild-type rVWF (lane 1), mutant rVWF-L1382 (lane 2) and hybrid rVWF (lane 3) on 1.6% medium resolution gel at 1:3 dilution are shown. The multimeric composition of rVWF resulting from both homozygous and heterozygous forms showed normal VWF multimer patterns with presence of a full array of multimer bands similar to wild-type multimers.

6.2.6.2. Confocal microscopy of c.4146G>C; p.L1382=

Similarly to the c.4146G>T variant, confocal analysis of the homozygous state showed the presence of punctate round WPB-like organelles throughout the cell comparable to those visualised in wild-type in shape and size (Figure 6.13 D and F). In the heterozygous form of this variant, punctuate round WPB-like structures were visualised throughout the cell and showed similar size and shape organelles, but appeared relatively smaller in size compared to those present in the wild-type (Figure 6.13 G and I). Confocal imaging indicated that c.4146G>A does affect VWF storage.

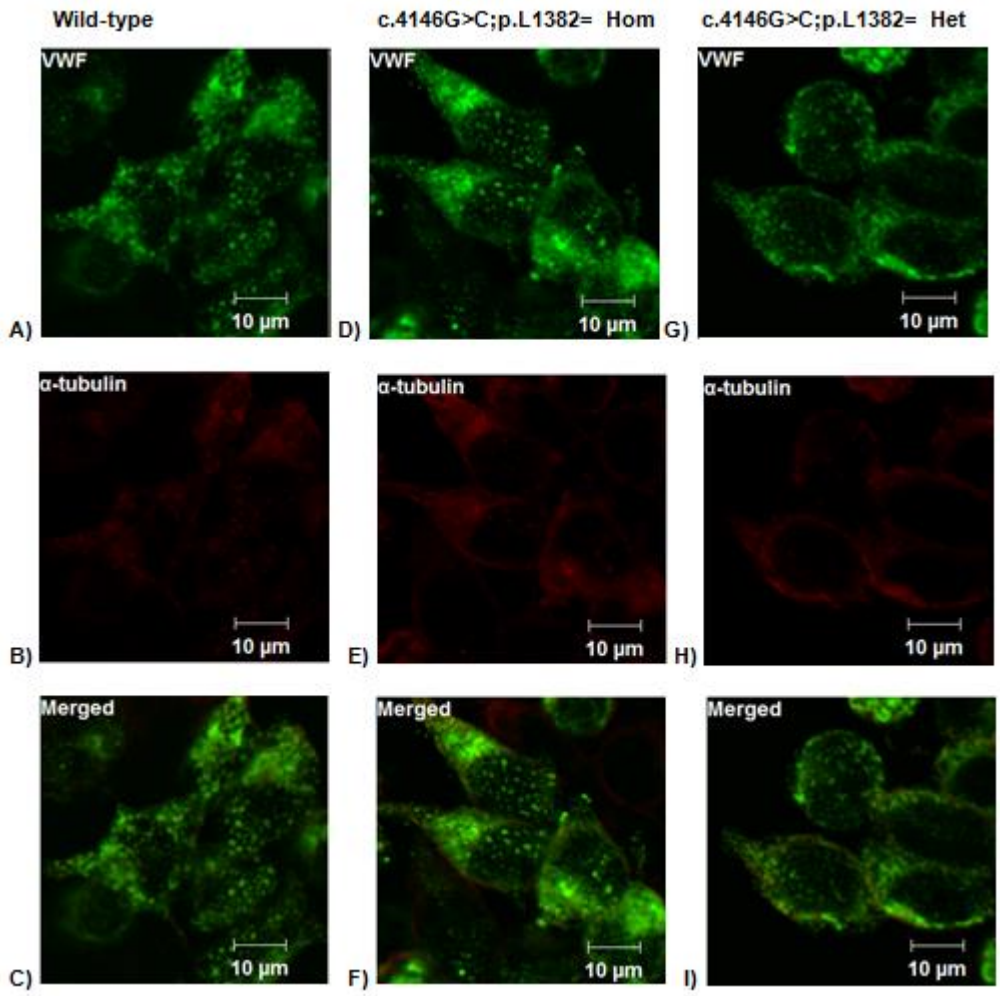

Figure 6.13 Intracellular storage of rWT and c.4146G>C;rVWF-L1382 mutant in HEK293 cells by confocal microscopy. A, D and G) Represent VWF (green) after transfection of wild-type, homozygous and heterozygous plasmids respectively into HEK293 cells. **B, E and H)** Represent the cell membrane marker α-tubulin (red) after transfection of wild-type, homozygous and heterozygous respectively into HEK293 cells. **C, F and I)** Represent merged images of VWF and α-tubulin staining for wild-type, homozygous and heterozygous respectively transfected into HEK293 cells. Cells were stained as described in figure 6.6.

6.3. Discussion

Unlike regular pathogenic mutations that are deleterious and cause genetic disease, it was historically believed that silent mutations were all benign. Recently, however it has been suggested that apparently synonymous sequence changes are not always benign and can impair splicing mechanism and disturb mRNA translation and protein folding (Mitarai et al., 2008, Daidone et al., 2011). This study aimed to investigate whether c.4146G>T;p.L1382= identified in type 1 VWD was responsible for the phenotype observed in the patient through *in vitro* expression. Also, it was aimed to identify the disease causing mechanism associated with this silent mutation as well as the two hypothetical silent changes c.4146G>A;p.L1382= and c.4146G>C;p.L1382= that encode the same amino acid and to compare findings with codon usage analysis. This mutation was identified previously (Corrales et al., 2012) and also identified in one IC in the EU study and has not been expressed previously (Goodeve et al., 2007, Hampshire et al., 2010).

p.L1382= is located in a β sheet in the A1 domain and was found to be away from the area of binding with platelets suggesting that it is unlikely to directly affect the interaction of VWF with platelet GpIbα receptor. It has been reported previously that silent mutations may affect protein folding which could alter protein conformation (Duan et al., 2003, Mitarai et al., 2008).

6.3.1. *In vitro* expression of c.4146G>T;p.L1382=

Results from *in vitro* expression indicated that this mutation results in a significant secretion defect of VWF in both heterozygous and homozygous states. Expression data from the c.4146G>T mutant showed that secreted VWF in the heterozygous and the homozygous states was significantly decreased by 39% and 23% respectively compared to wild-type. Interestingly unlike the earlier findings, these data indicated that the secreted amount of VWF released from the heterozygous mutant was significantly less than VWF released from the homozygous mutant. This experiment was repeated using an independent clone of the plasmid harbouring the c.4146 variant and similar findings were observed (Figure 6.5). To explain these findings, we hypothesised that the presence of normal and mutant alleles with reduced translation rate efficiency in the heterozygous state could cause the mutant allele to interfere with the wild-type unlike identical mutant alleles in the homozygous form. Also, *in vitro* expression is an artificial system not exactly reflecting the real *in vivo* expression system. In VWD, the expression of *VWF* silent mutants has never been reported previously. Moreover, the c.4146G>T variant resulted in a normal multimer pattern observed in both heterozygous and homozygous forms. Furthermore, pseudo WPB vesicles formed in both states indicated that p.L1382= does affect VWF formation and storage.

6.3.2. *In vitro* expression of c.4146G>A and c.4146G>C mutants

Similarly to c.4146G>T expression, expression data from hypothetical mutants; c.4146G>A and c.4146G>C also showed a significant reduction of secreted VWF in both mutants in both homozygous and heterozygous states. The expression data from c.4146G>A resulted in a significant reduction of secreted VWF to 24% and 35% in heterozygous and homozygous states respectively compared to 100% wild-type. Also, this variant caused a significant reduction of intracellular VWF to 32% and 47% in both heterozygous and homozygous respectively. The expression data of c.4146G>C showed also a significant 68% reduction in the heterozygous form. However, in the homozygous form of c.4146G>C, a significant 50% defect in VWF secretion was accompanied by a significant increase in the VWF level (111%) indicating intracellular retention. These experiments also showed that the released amount of VWF from the homozygous form was consistently higher than those from heterozygous. Both variants resulted in the formation of normal multimer patterns and pseudo-WPB organelles suggested that these variants had no effect on VWF multimerisation, but storage appeared to be reduced compared to wild-type in the heterozygous form.

During translation, each codon is recognised efficiently by a specific tRNA corresponding to this codon. Although there are 61 codons that encode 20 amino acids, the number of tRNAs is fewer at around 31 in humans which reflects the ability of one tRNA to bind with more than one codon (Ronneberg et al., 2000). According to the Wobble hypothesis, the interaction between mRNA codon and its anticodon is achieved when the first two bases of mRNA are compatible with the tRNA anticodon as the anticodon bases inosine (or pseudouridine) in all tRNA at 3rd position that can pair with any base of mRNA either C, A, G or U (Crick, 1966, Matsuyama et al., 1998). Inosine is a nucleotide commonly present in tRNA derived from inosine monophosphate that can pair with all natural nucleotides. The Wobble hypothesis showed that each nucleotide has two possible anticodons or tRNAs (Table 6.8).

Table 6.8 Wobble hypothesis

Anticodon (tRNA)	Codon (mRNA)
C	G
U	A,G
G	U,C
I	U,C,A

C: cysteine, U: uracil, G: guanine, I: inosine

It has been found that some amino acids prefer specific codons more than others that encode the same amino acid to achieve efficient and accurate translation. So, efficient translation is achieved when tRNA with higher abundance complementary to mRNA codon are used (codon

usage bias) (Akashi, 1994). Therefore, each codon is recognised efficiently by a specific tRNA corresponding to this codon and the presence of a nucleotide change leads to a synonymous change that could alter translation rate through codon usage bias. Frequencies of codon usage data were compiled from 257,468 gene coding sequences from 8792 different organisms. These data were obtained from GenBank DNA sequence database (Nakamura et al., 2000). Codon usage analysis can predict the frequency difference between high and low abundance codons which can alter mRNA structure, the translation rate and protein folding. The wild-type codon CTG showed the highest codon usage frequency and mutant triplet codon CTT showed a 68% lower frequency (Nakamura et al., 2000). *In vitro* expression of silent mutants confirmed the deleterious effect of p.L1382= on VWF production. Codon usage data illustrated that CTC is a more abundant codon more than CTA and this is compatible with *in vitro* expression findings. This data also, demonstrated that CTC is more frequently used than mutant codon CTT, which was not reflected in the *in vitro* expression data. *In vitro* expression is an artificial system not fully sensitive enough to mimic or represents the *in vivo* expression system and this could explain the differences between expression and codon usage data. Also, there may be differences in tRNA abundance between overall codon usage data and HEK293T cells and this may explain result variability.

The mutant VWF produced following transfection displayed a defect in VWF secretion confirming the effect of silent change p.L1382= on VWF expression was likely due to codon usage. From these findings, we hypothesised that p.L1382= does influence the production of VWF and speculate that the mechanism is due to an alteration of the translation rate and producing mis-folded protein. However, we demonstrated that the synonymous change c.4146G>T contributes to a partial deficiency of VWF leading to bleeding symptoms observed in type 1 VWD patients.

The impact of the silent mutation p.L1382= on VWF expression was documented through *in vitro* expression and codon usage bias. The levels of VWF:Ag measured in plasma of the IC and the AFM who harboured c.4146G>T was around 50 IU/dL (Appendix 19) and the *in silico* splicing prediction tools indicated a significant difference between wild-type and mutant sequences indicating that the exonic nucleotide change may also affect regulatory splicing elements through loss or gain of exonic regulatory elements and impair the splicing mechanism, but did not generate new donor or acceptor splice sites. Therefore, we assume that it is also possible for the exonic nucleotide change c.4146G>T identified in P10F5 family to impair splicing enhancers or silencers causing skipping of exon 28 (Figure 6.1B). The skipping of exon 28 was predicted to result in a stop codon p.C1225* at the end of exon 27. This skipping of exon 28 would then further produce a PTC causing degradation of the mutant allele due to NMD, this may affect all or only some of the mRNA produced from the mutant allele. The

second hypothesis was derived from the *in silico* prediction that indicated the possibility of c.4146G>T to reduce the efficiency of splicing via disrupting essential ESE and ESS elements. These predictions need to be confirmed. Further work may help to confirm the contribution of various mechanisms on pathogenicity and to define the exact disease causing mechanism of these silent mutations (Future work, section 7.1).

Previous studies have been undertaken in different conditions to investigate the pathogenicity of silent mutations linked to different diseases. In a study of haemophilia B patients who presented with mild bleeding symptoms and a moderate reduction of FIX levels (15-20 IU/dL) (Knobe et al., 2008), the isolated mRNA from a haemophilia patient who harboured a c.321G>A;p.V107= synonymous mutation and from a healthy individual were reverse transcribed and then subsequently amplified using PCR to produce cDNA. The analysed cDNA from the patient and control individual were similar lengths indicating the absence of exon skipping and intron retention. Therefore, the hypothesis of the effect of this silent variant on splicing was excluded as a pathological mechanism and other mechanisms could contribute to the phenotype observed in the haemophilia B patients. *In vitro* expression of a plasmid containing the *F9* cDNA c.321G>A;p.V107= mutation in HEK293T cells showed normal coagulant activity of produced FIX protein indicating the subtle effect of this silent change on *F9* expression, but it was hypothesised that it may alter the translation rate and protein folding *in vivo* (Knobe et al., 2008, Hamasaki-Katagiri et al., 2012). A reduced FIX level following *in vitro* analysis of mRNA from patients with p.V107= was observed when independent study was undertaken and these findings were compatible with *in silico* analysis confirming the adverse impact of p.V107= on *F9* mRNA stability, codon usage and structure (Kimchi-Sarfaty et al., 2011). Moreover, work on the effect of a silent change on translation efficiency by Shah et al (2008) was undertaken in a patient who was homozygous for hyperinsulinism. *In vitro* expression of a vector containing c.570C>T; p.A190= in *KCNJ11* followed by Western blot analysis showed the absence of bands when expressed in the homozygous form in comparison to strong bands observed in wild-type indicating the impact of the silent variant on the translation rate and protein production (Shah et al., 2008).

It has been reported that the level of cognate tRNA and strong codon bias is directly proportional to frequency of codon usage and the presence of that replacement of a synonymous codon may affect the protein shape, structure, efficiency of protein translation and folding (Shabalina et al., 2006, Mitarai et al., 2008). In order to investigate the effect of silent changes on ribosome movement and protein folding, Komar et al (1999) replaced 16 rare codons present in the chloramphenicol acetyltransferase (*CAT*) gene in *E.coli* by more frequent ones using *in vitro* mutagenesis and measuring the activity of released wild-type and mutant mRNA. The results showed that the replaced mutant codons affected ribosome traffic, ribosome movements

and impaired protein translation and folding (Komar et al., 1999). Moreover, Fung et al (2009) suggested that the silent nucleotide change and the frequency of codon usage could cause ribosome stalling or delaying (Sunohara et al., 2004) that further impairs protein folding and leads to abnormal structure and function of *MDR1* mRNA that encodes a membrane-bound transporter (Fung and Gottesman, 2009). Furthermore, the wild-type and mutant mRNA carrying a silent mutation in human dopamine receptor D2 (*DRD2*) was investigated by Duan et al (2003). The results suggested that the synonymous c.957C>T found in *DRD2* expressed less DRD2 protein than wild-type and this was caused by abnormal mRNA folding that result from reduction in the stability of the mRNA and protein translation (Duan et al., 2003).

Also, many experimental studies have studied the effect of exonic mutations in splicing regulatory elements. Analysis of mRNA extracted from patients with spinal muscular atrophy revealed that exonic nucleotide changes can create or destroy the ESE or ESS which mediates exon skipping and results in a truncated protein (Lorson and Androphy, 2000). Also, similar results were obtained by Gaildrat et al (2012) who investigated the effect of mutation located in exon 7 of the breast and ovarian cancer gene (*BRCA2*) on the splicing pathway using a minigene assay. The extracted mRNA following transient transfection of mutant and wild-type constructs into HeLa cells was reverse transcribed. The cDNA of mutant and wild-type was amplified and electrophoresed on an agarose gel. As a result, the shortness of mRNA length in mutant compared to wild-type indicated that the exonic mutation disturbed splicing regulatory elements which caused skipping of an exon and produced truncated protein. These findings highlight the adverse impact of exonic nucleotide changes on splicing mechanism (Gaildrat et al., 2012).

In conclusion, this study provided experimental evidence using *in vitro* expression and codon usage bias that c.4146G>T is likely to be the major cause of the phenotype observed in the affected members who harbour this mutation and was able to highlight the adverse impact of this silent variant on protein expression likely through altering mRNA translation rate and protein folding. It was suggested that this variant may cause subtle effects on protein folding or efficiency of the splicing mechanism. Although we were able to demonstrate that this silent mutation c.4146G>T has an effect on protein expression, we were unable to determine exactly how the c.4146G>T results in VWD. Moreover, this work has not excluded any effect of c.4146G>T on ESE or ESS elements. Therefore, additional experiments are required in order to confirm the disease causing mechanisms. This study aimed to investigate the effect of c.4146G>T silent mutation on splicing efficiency through analysis of the predicted loss of ESE in the splicing pathway through mini-gene analysis but this experiment was discontinued (Future work). Ideally this analysis would use either extracted mRNA from a VWD patient carrying this silent change, mRNA extracted from transfected cells or mRNA analysis following

a splicing minigene assay to assess the splicing regulatory elements of mutant and wild-type sequence segments (Future work, section 7.1).

Chapter 7

Discussion

7. Discussion

VWD type 1, the most common variant of all VWD types, is characterised by partial quantitative deficiency of VWF which results in mild to moderate mucocutaneous bleeding symptoms. The previous MCMDM-1VWD study previously investigated the molecular genetic basis of type 1VWD and undertook mutation scanning and sequencing of the *VWF* gene in 150 IC (Goodeve et al., 2007). Mutations were identified in 70% of IC and most were missense mutations while other variants such as splice, transcriptional and nonsense mutations in addition to small deletions and insertions were detected in lower proportions. Several mutation detection techniques were used for mutational analysis in this cohort study including SSCP, CSGE, DHPLC and direct DNA sequencing. These methods have variable degrees of sensitivity ranging between 75-100% (Markoof et al., 1998, Whittock et al., 1999, Eng et al., 2001).

Although the EU study provided valuable details about the clinical and molecular basis of type 1 VWD, it failed to detect mutations in the remaining IC. Reasons for this failure may include SNP within primer annealing sites leading to lack of mutant allele amplification or insensitivity of mutation analysis methods. Also, a number of patients who were negative for mutations may bleed due to other bleeding disorders and may have been falsely positive diagnosed as having type 1 VWD. Moreover, mutations were missed in the initial study due to presence of large heterozygous deletions which cannot be detected using standard methods (Cartwright et al., 2013). The presence of large heterozygous deletions could prevent binding of a primer to the template when using standard PCR causing only the normal allele to be amplified and sequenced. Standard PCR and sequencing would not be able to detect large deletions or duplications due to the presence of the wild-type allele.

The aims of this project were to re-analyse all primers used in the initial MCMDM-1VWD cohort for the presence of SNP underneath primer binding sites to avoid mono-allelic amplification as the primers used in the historical EU study were designed prior to the availability of complete *VWF* sequence with little knowledge of SNP, and to reanalyse all *VWF* exons and closely flanking intronic regions using direct DNA sequencing in IC where the clinical phenotype suggested that mutations may have been missed. A further aim was to determine the mechanisms by which mutations identified affect VWF synthesis, secretion and storage.

The hypothesis that mutations were missed in the previous EU study due to the presence of SNP within primer binding sites or lack of sensitivity of mutation scanning methods used was

initially investigated. Previously missed mutations were detected in type 1 and type 2 VWD patients who were initially negative for mutations following screening of primers for the presence of SNP (Thomas et al., 2006b, Hampshire et al., 2010). *In silico* analysis was performed to screen all previously used PCR primers for presence of SNP within primer binding sites and when necessary new primers were designed. However, for the current project, all newly designed primers and primers free of SNP underneath their binding sites were successfully used for amplification and sequencing of *VWF* exons and closely flanking regions.

Eighteen IC (5 where a previously identified heterozygous mutation did not fully explain phenotype and 13 with no mutation identified) having low VWF levels and significant bleeding were investigated. Mutations were missed in the historical MCMDM-1VWD study due to limitations in sensitivity of previous analyses (p.W2271G) and SNP within primer annealing sites (p.C1157R and c.1432+1G>T) while the IC with p.L1382= was excluded from the study previously due to an insufficient quantity of DNA sample. As the quantity of DNA used is now lower, it was possible to include this individual.

Of the 18 IC analysed for the presence of mutations, heterozygous mutations were identified in four families (22%); novel missense mutations p.W2271G (in compound heterozygosity with p.R854Q), novel missense p.C1157R (in compound heterozygosity with p.S539Lfs*38), silent mutation p.L1382= and the novel splice mutation c.1432+1G>T (in compound heterozygosity with p.R816W). p.W2271G and p.C1157R, predicted to be damaging by *in silico* analysis, affect fully conserved residues.

Unlike p.R854Q and p.R816W, p.W2271G and c.1432+1G>T segregated with disease phenotype and their presence alone or in compound heterozygosity with p.R854Q (VWF:Ag 37-38 IU/dL, VWF:RCo 32-43 IU/dL, FVIII:C (p.[W2271G];[R854Q]) 28-34 IU/dL, FVIII:C (p.W2271G) 85 IU/dL) and p.R816W (VWF:Ag 47-49 IU/dL, VWF:RCo 52-67 IU/dL, FVIII:C (c.1432+1G>T;p.R816W) 14 IU/dL, FVIII:C (c.1432+1G>T) 113 IU/dL) explain phenotype differences in the affected families.

The presence of p.W2271G, p.L1382= and c.1432+1G>T appeared to explain the partial quantitative deficiency of VWF and bleeding symptoms observed in IC and AFM historically diagnosed with type 1 VWD. Also, the presence of p.C1157R along with p.S539fs was the main cause for the severe reduction of VWF in the AFM. Therefore, these identified mutations contribute to the pathogenesis of VWD in these patients. The detection of missed mutations within *VWF* in the patients who had reductions in their VWF level can explain the disease

phenotype observed in the IC who showed no mutation or insufficient mutations in the previous study.

In addition to p.W2271G, p.C1157R and p.L1382=, *in vitro* expression studies of recombinant mutant VWF was undertaken for p.C1927R, p.R924Q and p.S539fs. Moreover, expression study was conducted for the two hypothetical mutations c.4146G>A and c.4146G>C that both resulted to the silent mutation p.L1382=.

Previous *in vitro* expression investigations of missense mutations indicated that mutations located within the D3 and D4 domains can lead to intracellular retention and reduced VWF secretion as previously described (Hommais et al., 2006a, Eikenboom et al., 2009). In the homozygous state of the previous expressed missense mutation in D3 and D4 assemblies, VWF secretion was reduced accompanied by intracellular retention in addition to defects in multimerisation, while the heterozygous form resulted in reduced secretion and a relative reduction in HMW multimers. Furthermore, some mutations in the D3 assembly of VWF affected VWF:FVIIIB and resulted in abnormal binding of VWF to FVIII (Hommais et al., 2006a).

Expression studies of recombinant mutant VWF (rVWF-G2271, rVWF-R1927 and rVWF-R1157) showed significantly reduced VWF secretion levels in the homozygous state compared to rVWF-wild-type with significantly increased intracellular retention. In the heterozygous state, all variants also resulted in significantly reduced secretion while intracellular retention was observed only in rVWF-R1157. Furthermore, a complete absence of HMW multimers was observed when expressed in the homozygous form, whereas in the heterozygous form, multimers ranged between normal and relatively reduced HMW. p.C1157R when inherited alone can be classified as type 2A(IIE) due to similarities with a number of mutations in the D3 assembly that have been classified as type 2A(IIE) (Schneppenheim et al., 2010).

In vitro expression analysis indicated that p.W2271G and p.C1927R resulted in a defect in VWF secretion possibly through a dominant negative mechanism. Although p.R924Q is located in the D3 assembly, which is important for VWF multimerisation, expression study showed that it acts as a modifier of VWF level and appears to have had no significant effect on VWF synthesis or secretion.

The historical studies previously undertaken on *VWF* mutations such as nonsense, small deletions or insertions that lead to PTC in the open reading frame in type 1 and type 3 VWD found significant VWF reduction in the homozygous and heterozygous forms. The level of

expressed mRNA measured using RT-PCR showed a significant reduction of secreted VWF compared to wild-type that indicated mRNA degradation through NMD (Shahbazi et al., 2012). The extracted mRNA from VWD patients with splice site changes that lead to the creation of PTC was measured and showed significant reduction in comparison to healthy individuals (Corrales et al., 2011). The c.1614del mutation located in exon 14 of a single nucleotide deletion that leads to PTC creation resulted in a significant reduction in VWF secretion probably through NMD when expressed in the homozygous form was accompanied by loss of multimers and WPB-like organelles. Only a mild reduction in secreted VWF was observed when c.1614del was expressed in the heterozygous form through haplosufficiency mechanism. However, c.1614del is a recessive mutation (type 3 VWD) and may cause bleeding only when inherited in the homozygous form or in the compound heterozygous with an additional mutation. Up to 50% of type 3 carriers symptoms may bleed dependant on their *VWF* mutation, ABO blood group or other genetic factors (Bowman et al., 2013).

Interestingly, the expression analysis highlights the adverse impact of silent mutations p.L1382= on VWF expression. It has been reported previously that silent changes may impair protein expression through several mechanisms. The presence of exonic silent changes can generate new splice sites causing partial exonic deletions that produce either functional protein or truncated protein (Daidone et al., 2011). Also, it has been reported that silent change can destroy or create splicing regulatory elements which affect splicing efficiency (Nielsen et al., 2007). Furthermore, the efficiency of mRNA translation rate and ribosome movements has been reported to result from silent mutation (Duan et al., 2003, Mitarai and Pedersen, 2013). Additionally, silent change may lead to small mRNA binding with miRNA producing dsRNA which is eliminated (Hurst, 2011). It seems likely that p.L1382= contributes to VWF deficiency due to its effect on translation rate or on splicing regulatory elements. It would be of interest to undertake further investigations to evaluate the effect of p.L1382= on splicing regulatory elements and translation rate.

Overall, this research has deciphered further genetic and molecular understanding of type 1 VWD through identification of additional missense and splice site mutations that were previously missed in the original MCMDM-1VWD mutational screening. *In vitro* expression of missense mutations appeared to correlate with affected individuals clinical phenotype. Of significance, expression of the p.L1382= silent mutation has shown that this synonymous mutation may play a role in type 1 VWD pathogenesis and provides novel insight into VWD disease mechanisms. A number of synonymous variants have been reported in the EU study that were previously considered to be silent. Therefore, *in silico* analysis and *in vitro* expression of p.L1382= has provided insight into a new research field and that should encourage further

investigations to study the association between these synonymous changes and phenotypes observed in type 1 VWD patients. *In vitro* characterisation of silent variants is not always sufficient and may remain inconclusive to identify the disease pathogenicity. This research also highlighted that the p.R924Q mutation located in D3 domain, when inherited on its own, does not contribute to disease pathogenesis, but a deleterious effect is observed when co-inherited with another variant. This research has provided further insight on the effect of heterozygous mutations on the pathogenesis of type 1 VWD.

7.1. Future work

Among the remaining IC who did not show any mutation neither in the original EU-cohort nor in this study, although they had reduced VWF level, the cause of VWD may arise from the presence of large heterozygous deletions or duplications of single or multiple exons of *VWF* that were previously unable to be detected by standard sequencing methods. A large exon 4-5 homozygous deletion was identified in type 3 VWD and exon 4-5 heterozygous deletion was identified as the aetiology of type 1 VWD in the UK patients and could likely contributes to bleeding symptoms in type 1 VWD patients (Sutherland et al., 2009a).

Recently, 104 of the 150 IC from the historical MCMDM-1VWD cohort were screened for exon copy number variation utilising MLPA analysis. In total 6 deletions were identified involving the heterozygous deletion of exon 3, exons 32-34 and exons 33-34 with the previously reported exons 4-5 deletion being identified in the remaining 3 IC. Heterozygous deletion breakpoints were also identified, allowing for the design of a multiplex PCR assay to identify deletions in other investigations. However, the study stated that MLPA looked at exons only, does not aid in identification of the intronic areas deleted in *VWF* and hence further investigations of mutation negative IC could be undertaken using the next approach array comparative genomic hybridisation (aCGH) to identify intronic copy number variations.

Whilst no additional mutations were found in the remaining 14 IC, additional mutations could be present in deep intronic and regulatory regions of *VWF*, which cannot realistically be analysed through the methods utilised in this project. The three multi-centre type 1 VWD studies conducted in EU, UK and Canada only searched for mutations in exons 2-52 (coding region), in small areas around the non-coding regions, approximately 50 bp into each end of each intron and in small parts (2kb) of the promoter. The presence of mutations within large regions of introns and the *VWF* promoter in addition to exon 1 may lead to alterations in the quantity of VWF. In other genes, it has been reported that mutations within intronic regions could disrupt the splicing mechanism and alter mRNA production (Khelifi et al., 2011,

Pezeshkpoor et al., 2013). Analysis of the Duchenne muscular dystrophy gene (*DMD*) which encodes several transcripts has shown that mutations in this gene cause dystrophinopathies. It has been reported that the presence of deep intronic deletions lead to pseudoexon (PE) activation and may impair the splicing mechanism of the PE and contribute to the pathogenesis of muscular dystrophy (Khelifi et al., 2011). PE are sequences similar to exonic sequence present within intronic regions created due to intronic alteration flanked by abnormal splice site consensus which are not normally seen in wild-type mRNA. Also, it has been reported that one or more deep intronic variants can create new cryptic splice sites that result in the insertion of intronic sequences into the mRNA and a premature stop codon in haemophilia A patients (Bagnall et al., 1999, Pezeshkpoor et al., 2013). Therefore, using aCGH analysis and next generation DNA sequencing of *VWF* to search for non-protein coding region variants in these individuals with no mutation identified is suggested as the next step.

aCGH and next generation sequencing can sequence the large *VWF* intronic regions and promoter to search for variants that cannot be detected by the standard DNA sequencing method. aCGH is a method of detection of CNV either large deletions or duplications within DNA. In this method, the patient DNA is labelled with one coloured dye and control DNA samples pooled from a healthy individual including males and females is labelled with a different colour. Subsequently, these labelled DNAs are combined and hybridised to a microarray which consists of thousands of oligonucleotide probes specific to the investigated regions. This approach can be used therefore to analyse the entire *VWF* for CNV which may include large deletions and duplications in exonic, intronic and regulatory regions. This method would detect CNV that were missed in the MCMDM-1VWD study due to only investigating exonic regions with MLPA.

Also, analysis of mRNA isolated from VWD patients who had VWF levels <35 IU/dL is an effective method to identify deep *VWF* intronic mutations. The isolated RNA is reverse transcribed into cDNA using RT-PCR followed by amplification the cDNA which is then electrophoresed to measure its size in comparison with that of a healthy individual and also fully sequenced to determine its changes. mRNA samples were not available from the historical study.

Mutations in the upstream promoter region may lead to the pathogenesis of type 1 VWD. Mutations within the promoter region could alter transcription factor binding sites in the affected allele, thereby leading to a reduction in RNA transcription. A study reported in 2010, identified a 13 bp deletion (c.-1522_-1510del13) within the proximal promoter region that impairs binding of the transcription factor protein Ets to the *VWF* promoter and markedly

reduces gene expression thus contributing to type 1 VWD (Othman et al., 2010). Also, the 3 type 1 VWD studies identified a number of variants located within the 3kb of the proximal promoter region, but some of these variants were also found in healthy control individuals and were most likely SNP rather than mutations (Cumming et al., 2006, Goodeve et al., 2007, James et al., 2007). Moreover, a study conducted by Schwachtgen *et al*, 1997 showed that a deletion of a small section of the *VWF* promoter reduces transcription because it decreases Ets transcription factor binding (Schwachtgen et al., 1997). However, searching for mutations in the deep regulatory regions using next generation sequencing or aCGH could contribute to defining the pathogenesis of type 1 VWD in the EU-cohort who still showed no mutation although they have a bleeding history.

Intronic regions of genes can contain miRNA binding sites and can also encode miRNA sequences. The 3'-UTR (un-translated region) and other regions of mRNA may contain binding sites for microRNA (miRNA) that regulate mRNA translation. These regulatory elements affect mRNA polyadenylation and stability, translation efficiency and codon termination and mutations within 3'-UTR region can influence the termination codon, secondary structure or polyadenylation signal and can thus cause disease. Also, the presence of mutations in polyadenylation signals can impair transcriptional termination, for example α-thalassemia (Harteveld et al., 1994, Prior et al., 2007). Therefore, further genetic analysis of these regions using LR-PCR and sequencing may enhance our understanding of possible genetic changes that may alter *VWF* in type 1 VWD.

In the IC investigated where no mutations have still been identified, it is possible that there are still mutations present that have been missed due to the limitations of the PCR methodology undertaken, as discussed previously. However, it is possible in these IC that the historical diagnosis of type 1 VWD was incorrect and there was a misdiagnosis of VWD as the causative bleeding disorder. This has been shown in the P9F18 family, who were initially categorised as having type 1 VWD but were reclassified as having type 3 VWD (which formed the basis of chapter 5 *in vitro* analysis). The EU investigation recruited patients with a historical diagnosis of type 1 VWD and even after phenotypic analysis, did not exclude patients who had 'atypical' VWD (abnormal multimers). This was to try and minimise the potential for mutations to be missed in *VWF*.

Additionally, the variability of VWF levels within the general population can be explained due to both environmental and genetic factors including epigenetic modifications. Epigenetics is defined as heritable changes that alter gene expression and activity but do not alter the DNA nucleotide sequence (Goldberg et al., 2007). These non-genetic changes that affect chromatin

are regulated by two modifications: DNA methylation and histone modification that package the genome into the nucleus via binding with histone proteins forming nucleosome complexes (Bernstein et al., 2007). Histone modification includes histone acetylation, methylation and ubiqutination. Methylation and heterochromatin hide DNA making it inaccessible to transcriptional factors and thereby inactivate DNA transcription and activity. In contrast, heritable changes alter DNA methylation such as loss of methylation sites (hypomethylation) or cause chromatin to be less condensed making DNA more accessible and result in increased DNA transcription and activity. It has been shown that levels of VWF increase with increasing age which contributes to VWF variability among the normal population (Nossent et al., 2006). This variation may be due to decreases in DNA methylation or histone modification that occurs with age that make DNA more accessible. Decreased methylation would activate DNA transcription and expression (De Smet and Loriot, 2013). It would be of interest to determine whether the methylation or histone patterns of the *VWF* promoter alter with age and could be investigated in the MCMDM-1VWD control cohort. These further analyses may enhance our understanding and knowledge of type 1 VWD pathogenesis especially in individuals with borderline VWF levels. Several approaches have been used to evaluate the DNA methylation state but bisulphite modification and sequencing have been considered as the gold standard test. This analysis of bisulphite treatment is based on variable sensitivity of cytosine and methylcytosine (5-MeC) to bisulphite that causes DNA deamination. Bisulphite treatment converts unmethylated cytosine to uracil while methylcytosine remains resistant (Clark et al., 2006, Darst et al., 2010). DNA amplification and sequencing using specific primers could determine the level of DNA methylation. This test could help to explain the effect of epigenetic modification on VWF expression among VWD patients and the normal population. Also, next generation sequencing can be used to evaluate the level of methylation among VWD patients. Also, additional epigenetic mechanisms such as histone acetylation can be investigated to evaluate its effect on *VWF*.

Current *in vitro* expression is an artificial system not fully representative of *in vivo* expression. The isolation of BOEC from blood of type 1 VWD patients would provide valuable data about VWF biosynthesis, secretion and pathophysiology of VWD through culturing these cells in suitable media. Using these cells can assist the evaluation of VWF level, production, secretion and confocal imaging as they isolated from VWD patients reflecting the *in vivo* expression system. Experimental studies that have used BOEC cell lines isolated from VWD patients provided an ideal substrate for *ex vivo* experimentation. The level of released VWF was found to be decreased in types 1 and 2M VWD patients using BOEC isolated from their blood (Starke et al., 2013b). Moreover, investigation of derived BOEC from type 1 VWD patients

heterozygous for p.S1285P, p.L1307P and p.C2693Y showed VWF retention, reduced secreted level of VWF and abnormal morphology of WPB (Wang et al., 2013).

Almost 30% of investigated IC within the EU-cohort and other type 1 VWD cohorts were negative for mutations. The absence of identified genetic changes in these individuals in addition to variable penetrance and expressivity, and the variability in VWF levels observed in normal individuals and VWD patients suggest the contribution of other genetic loci rather than *VWF* could affect VWF levels. Also, among the remaining IC within the EU-cohort who remained negative for mutations, a large proportion of cases (77%) were blood group O in comparison with 38% of all EU HC. Also, the possibility of presence of mutations in other genes rather than *ABO* that may influence the levels of VWF has been discussed as contributing to the aetiology of VWD. Similar to the *ABO* locus, additional loci outside *VWF* have been reported to influence the level of plasma VWF. Smith et al (2010) detected a number of genetic loci outside *VWF* by genome wide association study (GWAS). These variants have been shown to correlate with VWF:Ag levels and include *STXBP5, STX2, STAB2, CLEC4M* and *SCARA5* (Smith et al., 2010). Therefore, SNP identified in genes from the CHARGE study could help to explain disease phenotype in IC with borderline VWF levels and pathogenic mutations in the same genes could possibly contribute to VWD phenotype.

The recent study within the MCMDM-1VWD on analysis the effect of *CLEC4M* on VWF level in the general population suggested variants in *CLEC4M* with a possible association with VWF level, although the association was not statistically significant (Mufti et al., 2013, Rydz et al., 2013).

Additionally, it was suggested that the *FUT3* locus may have an influence on VWF level through VWF glycosylation by an unknown mechanism (O'Donnell et al., 2002b). Hickson et al (2009) reported a 9% reduction of VWF level in individuals with the *FUT3* variant c.202T>C;p.W68R in individuals with the T reference allele in comparison to those with the C non-reference allele (Hickson et al., 2009b). Analysis of this gene for the presence of further genetic variants that is associated with abnormal phenotypes more severe than those associated with identified common SNP could be undertaken. The presence of these changes could contribute to bleeding symptoms in patients diagnosed with type 1 VWD.

One of the important issues relevant to the diagnosis of type 1 VWD is possible misdiagnosis. In all three cohort studies, a number of patients with a bleeding history may have been falsely diagnosed as having type 1 VWD. This false positive diagnosis could be due to the presence of a proportion of the normal population who have mild bleeding symptoms in the EU study being

indistinguishable from classical type 1 VWD or due to the wide distribution of the normal range of VWF (48-167 IU/dL). The EU study analysed a number of IC who had high BS with normal levels of VWF. This suggests the presence of other bleeding disorders rather than type 1 VWD that could explain the occurrence of bleeding symptoms observed in IC (Daly et al., 2009). Belen et al (2014) reported an overlap and similarities in bleeding symptoms among patients with VWD and platelet function disorders (Belen et al., 2014). The addition of platelet function tests such as platelet aggregation test using several agonists during the initial investigation of the patient could assist the accuracy of diagnosis. Platelet aggregation tests could define which platelet receptor, intracellular signalling or secretion pathway is influenced and enable further genetic investigation required for the associated genes (Watson et al., 2010).

The silent mutation p.L1382= identified in one IC within the MCMDM-1VWD study showed a significant effect of this variant on VWF expression. *In silico* prediction illustrated that this silent variant has no effect on splice donor or acceptor sites but may disrupt ESE sequences that may alter the splicing mechanism. However, in order to provide evidence that c.4146G>T could result in *VWF* mRNA alteration due to the exonic change predicted to disrupt an ESE, a minigene assay was planned to be established. pcDNA-Dup (SF2/ASF3x) was selected as the appropriate vector to investigate the effect of c.4146G>T on ESE. This vector contains three exons where the middle one is recognised if a functional ESE motif resides within the exon. This assay is based on the insertion of a short DNA segment (30 bp) of wild-type or mutant sequence corresponding to the sequence of interest including c.4146G>T and wild-type sequence. These constructs of mutant and wild-type sequences would be transiently transfected into the HEK293T cell line followed by extraction of mRNA 24 hr post transfection. mRNA is reverse transcribed into cDNA, amplified using PCR then RT-PCR products electrophoresed on polyacrylamide agarose gel. The size and number of minigene product bands of wild-type and mutant are compared to evaluate the effect of silent change on ESE and may also be sequenced (Gaildrat et al., 2012).

Within the group, we attempted to investigate the effect of c.4146G>T and other *VWF* SNP on ESE. A short pair of forward and reverse primers each of 30 bp sequences corresponding to the *VWF* region containing wild-type and mutant sequences surrounding c.4146 were designed to be inserted into the vector. The restriction and ligation steps to remove the existing middle exon from the minigene vector and to insert the desired 30bp oligonucleotides of interest of wild-type and mutant construct were unsuccessful after many attempts. With persistent failure using several different conditions, the work was discontinued due to limited time. In addition to the effect of c.4146G>T on protein expression, other work to determine how any impact on ESE could be investigated using either patients and HC RNA samples or using transfected cell line

DNA. The MCMDM-1VWD study did not historically collect RNA from IC and hence RNA analysis is not available. Collection of RNA samples from individuals harbouring the c.4146G>T variant may contribute to identify the disease causing mechanism. Therefore, completing these experiments using patients RNA or a minigene assay could confirm or exclude whether this silent change affects an ESE and the splicing mechanism and thereby contributes through this mechanism to bleeding symptoms observed in the affected members. Moreover, *in vitro* expression using vector lacking the entire exon 28 could be undertaken to evaluate the effect of exon 28 skipping resulting from improper splicing in rVWF and findings compared to phenotypes in the affected individuals.

In conclusion, this project has provided insight into the pathogenicity of type 1 VWD through identification and re-design of primers free of SNP in the primer binding regions, applicable to future VWF screening approaches utilising standard DNA sequencing. In addition, the identification of missed mutations has identified a further 3 IC that were originally mutation negative. *In vitro* analysis of these previously missed mutations has also shown that the type 1 VWD phenotype in the IC is likely to be a result of the missed mutations and hence has added information on the molecular mechanisms of type 1 VWD. Historically, the role of synonymous mutations within *VWF* have been dismissed as 'silent changes' unlikely to lead to disease phenotype. However, this thesis has provided insight into the pathogenic nature of such mutations through *in vitro* expression. This area of research is vastly under investigated in VWF genetics and some IC in the EU study who only have silent mutations in VWF might have VWD due to the nature of the silent synonymous changes. Throughout *VWF*, there have been number of synonymous changes reported and most are likely to remain as silent mutations, but this thesis has provided insight into a research area for synonymous mutation expression, *in silico* analysis and a potential novel type 1 VWD disease mechanism.

These investigations were an initial step to understand the genetics and molecular mechanisms of the disease better. Further investigations as suggested above will help to improve knowledge about this complex disease.

8. References

Abuzenadeh, A. M. 1998. Characterisation of the molecular basis of von Willebrand,s disease. *PhD thesis. University of Sheffield.*

Akashi, H. 1994. Synonymous codon usage in Drosophila melanogaster: natural selection and translational accuracy. *Genetics,* 136**,** 927-35.

Alexander, B. Goldstein, R. 1953. Dual hemostatic defect in pseudohemophilia. *Journal o fClinical Investigation,* 32**,** 551.

Allen, S., Abuzenadah, A. M., Blagg, J. L., Hinks, J., Nesbitt, I. M., Goodeve, A. C., Gursel, T., Ingerslev, J., Peake, I. R. Daly, M. E. 2000a. Two novel type 2N von Willebrand disease-causing mutations that result in defective factor VIII binding, multimerization, and secretion of von Willebrand factor. *Blood,* 95**,** 2000-7.

Allen, S., Abuzenadah, A. M., Hinks, J., Blagg, J. L., Gursel, T., Ingerslev, J., Goodeve, A. C., Peake, I. R. Daly, M. E. 2000b. A novel von Willebrand disease-causing mutation (Arg273Trp) in the von Willebrand factor propeptide that results in defective multimerization and secretion. *Blood,* 96**,** 560-8.

Bagnall, R. D., Waseem, N. H., Green, P. M., Colvin, B., Lee, C. Giannelli, F. 1999. Creation of a novel donor splice site in intron 1 of the factor VIII gene leads to activation of a 191 bp cryptic exon in two haemophilia A patients. *Br J Haematol,* 107**,** 766-71.

Baronciani, L., Cozzi, G., Canciani, M. T., Peyvandi, F., Srivastava, A., Federici, A. B. Mannucci, P. M. 2003. Molecular defects in type 3 von Willebrand disease: updated results from 40 multiethnic patients. *Blood Cells Mol Dis,* 30**,** 264-70.

Baronciani, L., Federici, A. B., Cozzi, G., La Marca, S., Punzo, M., Rubini, V., Canciani, M. T. Mannucci, P. M. 2008. Expression studies of missense mutations p.D141Y, p.C275S located in the propeptide of von Willebrand factor in patients with type 3 von Willebrand disease. *Haemophilia,* 14**,** 549-55.

Batlle, J., Lopez Fernandez, M. F., Lasierra, J., Fernandez Villamor, A., Lopez Berges, C., Lopez Borrasca, A., Ruggeri, Z. M. Zimmerman, T. S. 1986. von Willebrand disease type IIC with different abnormalities of von Willebrand factor in the same sibship. *Am J Hematol,* 21**,** 177-88.

Beacham, D. A., Wise, R. J., Turci, S. M. Handin, R. I. 1992. Selective inactivation of the Arg-Gly-Asp-Ser (RGDS) binding site in von Willebrand factor by site-directed mutagenesis. *J Biol Chem,* 267**,** 3409-15.

Belen, B., Kocak, U., Isik, M., Keskin, E. Y., Oner, N., Sal, E., Kaya, Z., Yenicesu, I. Gursel, T. 2014. Evaluation of Pediatric Bleeding Questionnaire in Turkish Children With Von Willebrand Disease and Platelet Function Disorders. *Clin Appl Thromb Hemost*.

Berber, E., James, P. D., Hough, C. Lillicrap, D. 2009. An assessment of the pathogenic significance of the R924Q von Willebrand factor substitution. *J Thromb Haemost,* 7**,** 1672-9.

Berget, S. M. 1995. Exon recognition in vertebrate splicing. *J Biol Chem,* 270**,** 2411-4.

Berliner, S., Seligsohn, U., Zivelin, A., Zwang, E. Sofferman, G. 1986. A relatively high frequency of severe (type III) von Willebrand,s disease in Israel. *Br J Haematol,* 62**,** 535-43.

Bernstein, B. E., Meissner, A. Lander, E. S. 2007. The mammalian epigenome. *Cell,* 128**,** 669-81.

Blencowe, B. J. 2000. Exonic splicing enhancers: mechanism of action, diversity and role in human genetic diseases. *Trends Biochem Sci,* 25**,** 106-10.

Blomback, B. 1958. studies on fibrinogen and antihaemophilic globulin,XII th conference of the protein foundation on blood cells and plasma proteins, Albany, NY, November 1957. *Vox Sang,* 3**,** 58.

Blomback, M., Blomback, B. Nilsson, I. M. 1964. Response to fractions in von Willebrand disease. In: Brinkhous KM (ed). *The Haemophilias***,** 286-294.

Bodo, I., Katsumi, A., Tuley, E. A., Eikenboom, J. C., Dong, Z. Sadler, J. E. 2001a. Type 1 von Willebrand disease mutation Cys1149Arg causes intracellular retention and degradation of heterodimers: a possible general mechanism for dominant mutations of oligomeric proteins. *Blood,* 98**,** 2973-9.

Bodo, I., Katsumi, A., Tuley, E. A., Eikenboom, J. C., Dong, Z. Sadler, J. E. 2001b. Type 1 von Willebrand disease mutation Cys1149Arg causes intracellular retention and degradation of heterodimers: a possible general mechanism for dominant mutations of oligomeric proteins. *Blood,* 98**,** 2973-9.

Borchiellini, A., Fijnvandraat, K., Ten Cate, J. W., Pajkrt, D., Van Deventer, S. J., Pasterkamp, G., Meijer-Huizinga, F., Zwart-Huinink, L., Voorberg, J. Van Mourik, J. A. 1996. Quantitative analysis of von Willebrand factor propeptide release in vivo: effect of experimental endotoxemia and administration of 1-deamino-8-D-arginine vasopressin in humans. *Blood,* 88**,** 2951-8.

Bosshart, H., Humphrey, J., Deignan, E., Davidson, J., Drazba, J., Yuan, L., Oorschot, V., Peters, P. J. Bonifacino, J. S. 1994. The cytoplasmic domain mediates localization of furin to the trans-Golgi network en route to the endosomal/lysosomal system. *J Cell Biol,* 126**,** 1157-72.

Bowen, D. J. 2003. An influence of ABO blood group on the rate of proteolysis of von Willebrand factor by ADAMTS13. *J Thromb Haemost,* 1**,** 33-40.

Bowen, D. J. 2004. Increased susceptibility of von Willebrand factor to proteolysis by ADAMTS13: should the multimer profile be normal or type 2A? *Blood,* 103**,** 3246.

Bowen, D. J. Collins, P. W. 2004. An amino acid polymorphism in von Willebrand factor correlates with increased susceptibility to proteolysis by ADAMTS13. *Blood,* 103**,** 941-7.

Bowman, M., Hopman, W. M., Rapson, D., Lillicrap, D. James, P. 2010. The prevalence of symptomatic von Willebrand disease in primary care practice. *J Thromb Haemost,* 8**,** 213-6.

Bowman, M., Mundell, G., Grabell, J., Hopman, W. M., Rapson, D., Lillicrap, D. James, P. 2008. Generation and validation of the Condensed MCMDM-1VWD Bleeding Questionnaire for von Willebrand disease. *J Thromb Haemost,* 6**,** 2062-6.

Bowman, M., Tuttle, A., Notley, C., Brown, C., Tinlin, S., Deforest, M., Leggo, J., Blanchette, V. S., Lillicrap, D., James, P. Sociation of Hemophilia Clinic Directors Of, C. 2013. The genetics of Canadian type 3 von Willebrand disease: further evidence for co-dominant inheritance of mutant alleles. *J Thromb Haemost,* 11**,** 512-20.

Brodsky, J. L. Mccracken, A. A. 1997. ER-associated and proteasomemediated protein degradation: how two topologically restricted events came together. *Trends Cell Biol,* 7**,** 151-6.

Budde, U. 2008. Diagnosis of von Willebrand disease subtypes: implications for treatment. *Haemophilia,* 14 Suppl 5**,** 27-38.

Budde, U., Schneppenheim, R., Eikenboom, J., Goodeve, A., Will, K., Drewke, E., Castaman, G., Rodeghiero, F., Federici, A. B., Batlle, J., Perez, A., Meyer, D., Mazurier, C., Goudemand, J., Ingerslev, J., Habart, D., Vorlova, Z., Holmberg, L., Lethagen, S., Pasi, J., Hill, F. Peake, I. 2008a. Detailed von Willebrand factor multimer analysis in patients with von Willebrand disease in the European study, molecular and clinical markers for the diagnosis and management of type 1 von Willebrand disease (MCMDM-1VWD). *J Thromb Haemost,* 6**,** 762-71.

Budde, U., Schneppenheim, R., Eikenboom, J., Goodeve, A., Will, K., Drewke, E., Castaman, G., Rodeghiero, F., Federici, A. B., Batlle, J., Perez, A., Meyer, D., Mazurier, C., Goudemand, J., Ingerslev, J., Habart, D., Vorlova, Z., Holmberg, L., Lethagen, S., Pasi, J., Hill, F. Peake, I. 2008b. Detailed von Willebrand factor multimer analysis in patients with von Willebrand disease in the European study, molecular and clinical markers for the diagnosis and management of type 1 von Willebrand disease (MCMDM-1VWD). *J Thromb Haemost,* 6**,** 762-71.

Cakir, B., Heiss, G., Pankow, J. S., Salomaa, V., Sharrett, A. R., Couper, D. Weston, B. W. 2004. Association of the Lewis genotype with cardiovascular risk factors and subclinical carotid atherosclerosis: the Atherosclerosis Risk in Communities (ARIC) study. *J Intern Med,* 255**,** 40-51.

Campos, M., Sun, W., Yu, F., Barbalic, M., Tang, W., Chambless, L. E., Wu, K. K., Ballantyne, C., Folsom, A. R., Boerwinkle, E. Dong, J. F. 2011. Genetic determinants of plasma von Willebrand factor antigen levels: a target gene SNP and haplotype analysis of ARIC cohort. *Blood,* 117**,** 5224-30.

Canis, K., Mckinnon, T. A., Nowak, A., Panico, M., Morris, H. R., Laffan, M. Dell, A. 2010. The plasma von Willebrand factor O-glycome comprises a surprising variety of structures including ABH antigens and disialosyl motifs. *J Thromb Haemost,* 8**,** 137-45.

Caron, C., Ternisien, C., Wolf, M., Fressinaud, E., Goudemand, J. Veyradier, A. 2009. An accurate and routinely adapted enzyme-linked immunosorbent assay for type 2N von Willebrand disease diagnosis. *Br J Haematol,* Abstract of Congress of international society for haemostasis and thrombosis PP-MO-626.

Cartegni, L., Chew, S. L. Krainer, A. R. 2002. Listening to silence and understanding nonsense: exonic mutations that affect splicing. *Nat Rev Genet,* 3**,** 285-98.

Cartwright, A., Hampshire, D., Bloomer, C., Albuhairan, A., Vijzelaar, R., Budde, U., Eikenboom, J., Schneppenheim, R., Peake, I. Goodeve, A. 2013. Characterisation of large in-frame deletions contributing to type 1 VWD pathogenesis in the MCMDM-1 VWD study. *Thrombosis and Haemostasis,* 11 (Suppl.2)**,** 117-118.

Casais, P., Carballo, G. A., Woods, A. I., Kempfer, A. C., Farias, C. E., Grosso, S. H. Lazzari, M. A. 2006. R924Q substitution encoded within exon 21 of the von Willebrand factor gene related to mild bleeding phenotype. *Thromb Haemost,* 96**,** 228-30.

Casana, P., Martinez, F., Haya, S., Espinos, C. Aznar, J. A. 2001. Significant linkage and non-linkage of type 1 von Willebrand disease to the von Willebrand factor gene. *Br J Haematol,* 115**,** 692-700.

Casonato, A., Pontara, E., Sartorello, F., Cattini, M. G., Sartori, M. T., Padrini, R. Girolami, A. 2002. Reduced von Willebrand factor survival in type Vicenza von Willebrand disease. *Blood,* 99**,** 180-4.

Castaman, G., Federici, A. B., Rodeghiero, F. Mannucci, P. M. 2003. Von Willebrand's disease in the year 2003: towards the complete identification of gene defects for correct diagnosis and treatment. *Haematologica,* 88**,** 94-108.

Castaman, G., Giacomelli, S. H., Jacobi, P., Obser, T., Budde, U., Rodeghiero, F., Haberichter, S. L. Schneppenheim, R. 2010a. Homozygous type 2N R854W von Willebrand factor is poorly secreted and causes a severe von Willebrand disease phenotype. *J Thromb Haemost,* 8**,** 2011-6.

Castaman, G., Tosetto, A., Cappelletti, A., Goodeve, A., Federici, A. B., Batlle, J., Meyer, D., Goudemand, J., Eikenboom, J. C., Schneppenheim, R., Budde, U., Ingerslev, J., Lethagen, S., Hill, F., Peake, I. R. Rodeghiero, F. 2010b. Validation of a rapid test (VWF-LIA) for the quantitative determination of von Willebrand factor antigen in type 1 von Willebrand disease diagnosis within the European multicenter study MCMDM-1VWD. *Thromb Res,* 126**,** 227-31.

Castaman, G., Tosetto, A. Rodeghiero, F. 2009. Reduced von Willebrand factors survival in von Willebrand disease: pathophysiologic and clinical relevance. *J thromb Haemost,* (Suppl 1)**,** 71-4.

Cattaneo, M., Simoni, L., Gringeri, A. Mannucci, P. M. 1994. Patients with severe von Willebrand disease are insensitive to the releasing effect of DDAVP: evidence that the DDAVP-induced increase in plasma factor VIII is not secondary to the increase in plasma von Willebrand factor. *Br J Haematol,* 86**,** 333-7.

Chamary, J. V., Parmley, J. L. Hurst, L. D. 2006. Hearing silence: non-neutral evolution at synonymous sites in mammals. *Nat Rev Genet,* 7**,** 98-108.

Chang, Y. F., Imam, J. S. Wilkinson, M. F. 2007. The nonsense-mediated decay RNA surveillance pathway. *Annu Rev Biochem,* 76**,** 51-74.

Chapeville, F., Lipmann, F., Von Ehrenstein, G., Weisblum, B., Ray, W. J., Jr. Benzer, S. 1962. On the role of soluble ribonucleic acid in coding for amino acids. *Proc Natl Acad Sci U S A,* 48**,** 1086-92.

Chen, M. Manley, J. L. 2009. Mechanisms of alternative splicing regulation: insights from molecular and genomics approaches. *Nat Rev Mol Cell Biol,* 10**,** 741-54.

Clark, S. J., Statham, A., Stirzaker, C., Molloy, P. L. Frommer, M. 2006. DNA methylation: bisulphite modification and analysis. *Nat Protoc,* 1**,** 2353-64.

Corrales, I., Catarino, S., Ayats, J., Arteta, D., Altisent, C., Parra, R. Vidal, F. 2012. High-throughput molecular diagnosis of von Willebrand disease by next generation sequencing methods. *Haematologica,* 97**,** 1003-7.

Corrales, I., Ramirez, L., Altisent, C., Parra, R. Vidal, F. 2011. The study of the effect of splicing mutations in von Willebrand factor using RNA isolated from patients' platelets and leukocytes. *J Thromb Haemost,* 9**,** 679-88.

Crick, F. H. 1966. Codon--anticodon pairing: the wobble hypothesis. *J Mol Biol,* 19**,** 548-55.

Cumming, A., Grundy, P., Keeney, S., Lester, W., Enayat, S., Guilliatt, A., Bowen, D., Pasi, J., Keeling, D., Hill, F., Bolton-Maggs, P. H., Hay, C. Collins, P. 2006. An investigation of the von Willebrand factor genotype in UK patients diagnosed to have type 1 von Willebrand disease. *Thromb Haemost,* 96**,** 630-41.

Daidone, V., Gallinaro, L., Grazia Cattini, M., Pontara, E., Bertomoro, A., Pagnan, A. Casonato, A. 2011. An apparently silent nucleotide substitution (c.7056C>T) in the von Willebrand factor gene is responsible for type 1 von Willebrand disease. *Haematologica,* 96**,** 881-7.

Daly, M. E., Dawood, B. B., Lester, W. A., Peake, I. R., Rodeghiero, F., Goodeve, A. C., Makris, M., Wilde, J. T., Mumford, A. D., Watson, S. P. Mundell, S. J. 2009. Identification and characterization of a novel P2Y 12 variant in a patient diagnosed with type 1 von Willebrand disease in the European MCMDM-1VWD study. *Blood,* 113**,** 4110-3.

Darst, R. P., Pardo, C. E., Ai, L., Brown, K. D. Kladde, M. P. 2010. Bisulfite sequencing of DNA. *Curr Protoc Mol Biol,* Chapter 7**,** Unit 7 9 1-17.

Davies, J. A., Collins, P. W., Hathaway, L. S. Bowen, D. J. 2007. Effect of von Willebrand factor Y/C1584 on in vivo protein level and function and interaction with ABO blood group. *Blood,* 109**,** 2840-6.

Davies, J. A., Collins, P. W., Hathaway, L. S. Bowen, D. J. 2008. von Willebrand factor: evidence for variable clearance in vivo according to Y/C1584 phenotype and ABO blood group. *J Thromb Haemost,* 6**,** 97-103.

De Smet, C. Loriot, A. 2013. DNA hypomethylation and activation of germline-specific genes in cancer. *Adv Exp Med Biol,* 754**,** 149-66.

Den Dunnen, J. Antonarakis, E. 2001. nomenclature for the description of human sequence variations. *Hum Genet,* 109**,** 121-124.

Desseyn, J. L., Aubert, J. P., Van Seuningen, I., Porchet, N. Laine, A. 1997. Genomic organization of the 3' region of the human mucin gene MUC5B. *J Biol Chem,* 272**,** 16873-83.

Dong, Z., Thoma, R. S., Crimmins, D. L., Mccourt, D. W., Tuley, E. A. Sadler, J. E. 1994. Disulfide bonds required to assemble functional von Willebrand factor multimers. *J Biol Chem,* 269**,** 6753-8.

Donner, M., Holmberg, L. Nilsson, I. M. 1987. Type IIB von Willebrand's disease with probable autosomal recessive inheritance and presenting as thrombocytopenia in infancy. *Br J Haematol,* 66**,** 349-54.

Duan, J., Wainwright, M. S., Comeron, J. M., Saitou, N., Sanders, A. R., Gelernter, J. Gejman, P. V. 2003. Synonymous mutations in the human dopamine receptor D2 (DRD2) affect mRNA stability and synthesis of the receptor. *Hum Mol Genet,* 12**,** 205-16.

Dumas, J. J., Kumar, R., Mcdonagh, T., Sullivan, F., Stahl, M. L., Somers, W. S. Mosyak, L. 2004. Crystal structure of the wild-type von Willebrand factor A1-glycoprotein Ibalpha complex reveals conformation differences with a complex bearing von Willebrand disease mutations. *J Biol Chem,* 279**,** 23327-34.

Eikenboom, J., Federici, A. B., Dirven, R. J., Castaman, G., Rodeghiero, F., Budde, U., Schneppenheim, R., Batlle, J., Canciani, M. T., Goudemand, J., Peake, I., Goodeve, A. Group, M.-V. S. 2013a. VWF propeptide and ratios between VWF, VWF propeptide, and FVIII in the characterization of type 1 von Willebrand disease. *Blood,* 121**,** 2336-9.

Eikenboom, J., Federici, A. B., Dirven, R. J., Castaman, G., Rodeghiero, F., Budde, U., Schneppenheim, R., Batlle, J., Canciani, M. T., Goudemand, J., Peake, I., Goodeve, A. Group, M.-V. S. 2013b. VWF propeptide and ratios between VWF, VWF propeptide, and FVIII in the characterization of type 1 von Willebrand disease. *Blood,* 121**,** 2336-9.

Eikenboom, J., Hilbert, L., Ribba, A. S., Hommais, A., Habart, D., Messenger, S., Al-Buhairan, A., Guilliatt, A., Lester, W., Mazurier, C., Meyer, D., Fressinaud, E., Budde, U., Will, K., Schneppenheim, R., Obser, T., Marggraf, O., Eckert, E., Castaman, G., Rodeghiero, F., Federici, A. B., Batlle, J., Goudemand, J., Ingerslev, J., Lethagen, S., Hill, F., Peake, I. Goodeve, A. 2009. Expression of 14 von Willebrand factor mutations identified in patients with type 1 von Willebrand disease from the MCMDM-1VWD study. *J Thromb Haemost,* 7**,** 1304-12.

Eikenboom, J., Van Marion, V., Putter, H., Goodeve, A., Rodeghiero, F., Castaman, G., Federici, A. B., Batlle, J., Meyer, D., Mazurier, C., Goudemand, J., Schneppenheim, R., Budde, U., Ingerslev, J., Vorlova, Z., Habart, D., Holmberg, L., Lethagen, S., Pasi, J., Hill, F. Peake, I. 2006. Linkage analysis in families diagnosed with type 1 von Willebrand disease in the European study, molecular and clinical markers for the diagnosis and management of type 1 VWD. *J Thromb Haemost,* 4**,** 774-82.

Eikenboom, J. C., Matsushita, T., Reitsma, P. H., Tuley, E. A., Castaman, G., Briet, E. Sadler, J. E. 1996. Dominant type 1 von Willebrand disease caused by mutated cysteine residues in the D3 domain of von Willebrand factor. *Blood,* 88**,** 2433-41.

Eikenboom, J. C., Reitsma, P. H. Briet, E. 1994. Seeming homozygosity in type-IIB von Willebrand's disease due to a polymorphism within the sequence of a commonly used primer *Ann Hematol,* 68**,** 139-41.

Ellgaard, L., Molinari, M. Helenius, A. 1999. Setting the standards: quality control in the secretory pathway. *Science,* 286**,** 1882-8.

Enayat, M. S., Guilliatt, A. M., Surdhar, G. K., Jenkins, P. V., Pasi, K. J., Toh, C. H., Williams, M. D. Hill, F. G. 2001. Aberrant dimerization of von Willebrand factor as the result of mutations in the carboxy-terminal region: identification of 3 mutations in members of 3 different families with type 2A (phenotype IID) von Willebrand disease. *Blood,* 98**,** 674-80.

Eng, C., Brody, L. C., Wanger, T. M., Devilee, P., Vijg, J. Al., E. 2001. Interpreting epidemiological research: blinded comparison of methods used to estimate the prevalence of inherited mutations in BRCA1. *J Med Genet,* 38(12)**,** 824-33.

Fairbrother, W. G., Yeh, R. F., Sharp, P. A. Burge, C. B. 2002. Predictive identification of exonic splicing enhancers in human genes. *Science,* 297**,** 1007-13.

Favaloro, E. J. 2001. Appropriate laboratory assessment as a critical facet in the proper diagnosis and classification of von Willebrand disorder. *Best Pract Res Clin Haematol,* 14**,** 299-319.

Federici, A. B. 2004. Clinical diagnosis of von Willebrand disease. *Haemophilia,* 10 Suppl 4**,** 169-76.

Flood, V. H., Gill, J. C., Christopherson, P. A., Bellissimo, D. B., Friedman, K. D., Haberichter, S. L., Lentz, S. R. Montgomery, R. R. 2012. Critical von Willebrand factor A1 domain residues influence type VI collagen binding. *J Thromb Haemost,* 10**,** 1417-24.

Flood, V. H., Gill, J. C., Friedman, K. D., Bellissimo, D. B., Haberichter, S. L. Montgomery, R. R. 2011. Von Willebrand disease in the United States: a perspective from Wisconsin. *Semin Thromb Hemost,* 37**,** 528-34.

Franchini, M., Capra, F., Targher, G., Montagnana, M. Lippi, G. 2007. Relationship between ABO blood group and von Willebrand factor levels: from biology to clinical implications. *Thromb J,* 5**,** 14.

Frontroth, J. P., Hepner, M., Sciuccati, G., Feliu Torres, A., Pieroni, G. Bonduel, M. 2010. Prospective study of low-dose ristocetin-induced platelet aggregation to identify type 2B von Willebrand disease (VWD) and platelet-type VWD in children. *Thromb Haemost,* 104**,** 1158-65.

Fujikawa, K., Suzuki, H., Mcmullen, B. Chung, D. 2001. Purification of human von Willebrand factor-cleaving protease and its identification as a new member of the metalloproteinase family. *Blood,* 98**,** 1662-6.

Fung, K. L. Gottesman, M. M. 2009. A synonymous polymorphism in a common MDR1 (ABCB1) haplotype shapes protein function. *Biochim Biophys Acta,* 1794**,** 860-71.

Gadisseur, A. P., Vrelust, I., Vangenechten, I., Schneppenheim, R. Van Der Planken, M. 2007. Identification of a novel candidate splice site mutation (0874 + 1G > A) in a type 3 von Willebrand disease patient. *Thromb Haemost,* 98**,** 464-6.

Gaildrat, P., Krieger, S., Di Giacomo, D., Abdat, J., Revillion, F., Caputo, S., Vaur, D., Jamard, E., Bohers, E., Ledemeney, D., Peyrat, J. P., Houdayer, C., Rouleau, E., Lidereau, R., Frebourg, T., Hardouin, A., Tosi, M. Martins, A. 2012. Multiple sequence variants of BRCA2 exon 7 alter splicing regulation. *J Med Genet,* 49**,** 609-17.

Gallinaro, L., Cattini, M. G., Sztukowska, M., Padrini, R., Sartorello, F., Pontara, E., Bertomoro, A., Daidone, V., Pagnan, A. Casonato, A. 2008. Ashorter von Willebrand factor survival in O blood group subjects explains how

ABO determinants influence plasma von Willebrand factor. *Blood* 111**,** 3540-3545.

Gavazova, S., Gill, J. C., Scott, J. P., Hillery, C. A., Friedman, K. D., Wetzel, N., Jozwiak, M. A., Haberichter, S. L., Christopherson, P. Montgomery, R. R. 2002. a mutation in the D4 domain of von willebrand factor (VWF) result in a variant type von willebrand disease with accelerated in vivo VWF clearance. *Blood,* 100**,** 128a.

Ghosh, K. Shetty, S. 2011. Epidemiology, diagnosis, and management of von Willebrand disease in India. *Semin Thromb Hemost,* 37**,** 595-601.

Giblin, J. P., Hewlett, L. J. Hannah, M. J. 2008. Basal secretion of von Willebrand factor from human endothelial cells. *Blood,* 112**,** 957-64.

Gill, J. C., Endres-Brooks, J., Bauer, P. J., Marks, W. J., Jr. Montgomery, R. R. 1987. The effect of ABO blood group on the diagnosis of von Willebrand disease. *Blood,* 69**,** 1691-5.

Ginsburg, D. Bowie, E. J. 1992. Molecular genetics of von Willebrand disease. *Blood,* 79**,** 2507-19.

Ginsburg, D., Handin, R. I., Bonthron, D. T., Donlon, T. A., Bruns, G. A., Latt, S. A. Orkin, S. H. 1985. Human von Willebrand factor (vWF): isolation of complementary DNA (cDNA) clones and chromosomal localization. *Science,* 228**,** 1401-6.

Ginsburg, D. Sadler, J. E. 1993. von Willebrand disease: a database of point mutations, insertions, and deletions. For the Consortium on von Willebrand Factor Mutations and Polymorphisms, and the Subcommittee on von Willebrand Factor of the Scientific and Standardization Committee of the International Society on Thrombosis and Haemostasis. *Thromb Haemost,* 69**,** 177-84.

Goldberg, A. D., Allis, C. D. Bernstein, E. 2007. Epigenetics: a landscape takes shape. *Cell,* 128**,** 635-8.

Goodeve, A. 2010. The genetic basis of von Willebrand disease. *Blood Rev*.

Goodeve, A., Eikenboom, J., Castaman, G., Rodeghiero, F., Federici, A. B., Batlle, J., Meyer, D., Mazurier, C., Goudemand, J., Schneppenheim, R., Budde, U., Ingerslev, J., Habart, D., Vorlova, Z., Holmberg, L., Lethagen, S., Pasi, J., Hill, F., Hashemi Soteh, M., Baronciani, L., Hallden, C., Guilliatt, A., Lester, W. Peake, I. 2007. Phenotype and genotype of a cohort of families historically diagnosed with type 1 von Willebrand disease in the European study, Molecular and Clinical Markers for the Diagnosis and Management of Type 1 von Willebrand Disease (MCMDM-1VWD). *Blood,* 109**,** 112-21.

Goodeve, A., Peake, I., Hashemi, M., Al-Buhairan, A., Castman, G. Al., E. 2003. Mutation analysis in type 1 von Willebrand disease patients entered in the multicenter MCMDM-1VWD study. *Thromb Haemost,* Supplement 1**,** OC075.

Goodeve, A. C., Eikenboom, J. C., Ginsburg, D., Hilbert, L., Mazurier, C., Peake, I. R., Sadler, J. E. Rodeghiero, F. 2001. A standard nomenclature for von Willebrand factor gene mutations and polymorphisms. On behalf of the ISTH SSC Subcommittee on von Willebrand factor. *Thromb Haemost,* 85**,** 929-31.

Goodeve, A. C., Reitsma, P. H., Mcvey, J. H., Working Group on Nomenclature of The, S., Standardisation Committee of the International Society On, T. Haemostasis 2011. Nomenclature of genetic variants in hemostasis. *J Thromb Haemost,* 9**,** 852-5.

Graham, F. L., Smiley, J., Russell, W. C. Nairn, R. 1977. Characteristics of a human cell line transformed by DNA from human adenovirus type 5. *J Gen Virol,* 36**,** 59-74.

Graham, J. B. 1959. The inheritance of vascular hemophilia; a new and interesting problem in human genetics. *J Med Educ,* 34**,** 385-96.

Gu, J., Jorieux, S., Lavergne, J. M., Ruan, C., Mazurier, C. Meyer, D. 1997. A patient with type 2N von Willebrand disease is heterozygous for a new mutation: Gly22Glu. Demonstration of a defective expression of the second allele by the use of monoclonal antibodies. *Blood,* 89**,** 3263-9.

Gupta, P. K., Saxena, R., Adamtziki, E., Budde, U., Oyen, F., Obser, T. Schneppenheim, R. 2008. Genetic defects in von Willebrand disease type 3 in Indian and Greek patients. *Blood Cells Mol Dis,* 41**,** 219-22.

Haberichter, S. L., Balistreri, M., Christopherson, P., Morateck, P., Gavazova, S., Bellissimo, D. B., Manco-Johnson, M. J., Gill, J. C. Montgomery, R. R. 2006. Assay of the von Willebrand factor (VWF) propeptide to identify patients with type 1 von Willebrand disease with decreased VWF survival. *Blood,* 108**,** 3344-51.

Haberichter, S. L., Castaman, G., Budde, U., Peake, I., Goodeve, A., Rodeghiero, F., Federici, A. B., Batlle, J., Meyer, D., Mazurier, C., Goudemand, J., Eikenboom, J., Schneppenheim, R., Ingerslev, J., Vorlova, Z., Habart, D., Holmberg, L., Lethagen, S., Pasi, J., Hill, F. G. Montgomery, R. R. 2008. Identification of type 1 von Willebrand disease patients with reduced von Willebrand factor survival by assay of the VWF propeptide in the European study: molecular and clinical markers for the diagnosis and management of type 1 VWD (MCMDM-1VWD). *Blood,* 111**,** 4979-85.

Haberichter, S. L., Fahs, S. A. Montgomery, R. R. 2000. von Willebrand factor storage and multimerization: 2 independent intracellular processes. *Blood,* 96**,** 1808-15.

Hamasaki-Katagiri, N., Salari, R., Simhadri, V. L., Tseng, S. C., Needlman, E., Edwards, N. C., Sauna, Z. E., Grigoryan, V., Komar, A. A., Przytycka, T. M. Kimchi-Sarfaty, C. 2012. Analysis of F9 point mutations and their correlation to severity of haemophilia B disease. *Haemophilia,* 18**,** 933-40.

Hampshire, D. J., Burghel, G. J., Goudemand, J., Bouvet, L. C., Eikenboom, J., Schneppenheim, R., Budde, U., Peake, I. Goodeve, A. 2010. Polymorphic variation within the VWF gene contributes to tha failure to detect mutations in patients historically diagnosed with type 1 VWD from the MCMDM-1VWD cohort. *Haematologica,* 95(12)**,** 2163-65.

Hampshire, D. J. Goodeve, A. C. 2011. The international society on thrombosis and haematosis von Willebrand disease database: an update. *Semin Thromb Hemost,* 37**,** 470-9.

Hampshire, D. J. Goodeve, A. C. 2013. p.P2063S: a neutral VWF variant masquerading as a mutation. *Ann Hematol*.

Hampton, R. Y. 2002. ER-associated degradation in protein quality control and cellular regulation. *Curr Opin Cell Biol,* 14**,** 476-82.

Harteveld, C. L., Losekoot, M., Haak, H., Heister, G. A., Giordano, P. C. Bernini, L. F. 1994. A novel polyadenylation signal mutation in the alpha 2-globin gene causing alpha thalassaemia. *Br J Haematol,* 87**,** 139-43.

Hastings, M. L. Krainer, A. R. 2001. Pre-mRNA splicing in the new millennium. *Curr Opin Cell Biol,* 13**,** 302-9.

Hershberg, R. Petrov, D. A. 2008. Selection on codon bias. *Annu Rev Genet,* 42**,** 287-99.

Hickson, D., Hampshire, D., Winship, D., James, P., Peake, I., Goode, A. Group, O. B. O. T. E.-V. a. Z.-V. S. 2009a. Fut3 gene determining Lewis blood groupantigen expression influencesVWF:Ag levels in plasma [abstract]. *J Thromb Haemos. 7,* (Suppl. 1), abst PP-TH-639

Hickson, N., Hampshire, D., Winship, P., Goudemand, J., Schneppenheim, R., Budde, U., Castaman, G., Rodeghiero, F., Federici, A. B., James, P., Peake, I., Eikenboom, J., Goodeve, A., Mcmdm, V. W. D. Groups, Z.-V. S. 2010. von Willebrand factor variant p.Arg924Gln marks an allele associated with reduced von Willebrand factor and factor VIII levels. *J Thromb Haemost,* 8**,** 1986-93.

Hickson, N., Hampshire, D. J., Winship, P. R., James, P. D., Peake, I. R., Goodeve, A. C. Eu-Study&Groups, A. Z. V. S. 2009b. FUT3 gene determining Lewis blood group antigen.

Hilbert, L., Gaucher, C. Mazurier, C. 1995. Identification of two mutations (Arg611Cys and Arg611His) in the A1 loop of von Willebrand factor (vWF) responsible for type 2 von Willebrand disease with decreased platelet-dependent function of vWF. *Blood,* 86**,** 1010-8.

Hilbert, L., Jorieux, S., Proulle, V., Favier, R., Goudemand, J., Parquet, A., Meyer, D., Fressinaud, E., Mazurier, C. Disease, I. N. O. M. a. I. V. W. 2003. Two novel mutations, Q1053H and C1060R, located in the D3 domain of von Willebrand factor, are responsible for decreased FVIII-binding capacity. *Br J Haematol,* 120**,** 627-32.

Hinks, J. L., Winship, P. R., Makris, M., Preston, F. E., Peake, I. R. Al., E. 1999. A rapid method for haemophilia B mutation detection using conformation sensitive gel electrophoresis. *Br J Haematol,* 104(4)**,** 915-18.

Holmberg, L. Nilsson, I. M. 1972. Genetic variants of von Willebrand's disease. *Br Med J,* 3**,** 317-20.

Hommais, A., Stepanian, A., Fressinaud, E., Mazurier, C., Meyer, D., Girma, J. P. Ribba, A. S. 2006a. Mutations C1157F and C1234W of von Willebrand factor cause intracellular retention with defective multimerization and secretion. *J Thromb Haemost,* 4**,** 148-57.

Hommais, A., Stepanian, A., Fressinaud, E., Mazurier, C., Pouymayou, K., Meyer, D., Girma, J. P. Ribba, A. S. 2006b. Impaired dimerization of von Willebrand factor subunit due to mutation A2801D in the CK domain results in a recessive type 2A subtype IID von Willebrand disease. *Thromb Haemost,* 95**,** 776-81.

Houdayer, C., Dehainault, C., Mattler, C. Al., E. 2008. Evaluation of in silico splice tools for decision-making in molecular diagnosis. *Hum Mutat,* 29**,** 975-982.

Huizinga, E. G., Tsuji, S., Romijn, R. A., Schiphorst, M. E., De Groot, P. G., Sixma, J. J. Gros, P. 2002. Structures of glycoprotein Ibalpha and its complex with von Willebrand factor A1 domain. *Science,* 297**,** 1176-9.

Hurst, L. D. 2011. Molecular genetics: The sound of silence. *Nature,* 471**,** 582-3.

Hurtley, S. M. Helenius, A. 1989. Protein oligomerization in the endoplasmic reticulum. *Annu Rev Cell Biol,* 5**,** 277-307.

Jacobi, P. M., Gill, J. C., Flood, V. H., Jakab, D. A., Friedman, K. D. Haberichter, S. L. 2012. Intersection of mechanisms of type 2A VWD through defects in VWF multimerization, secretion, ADAMTS-13 susceptibility, and regulated storage. *Blood,* 119**,** 4543-53.

Jaffe, E. A., Hoyer, L. W. Nachman, R. L. 1974. Synthesis of von Willebrand factor by cultured human endothelial cells. *Proc Natl Acad Sci U S A,* 71**,** 1906-9.

James, P. Lillicrap, D. 2006. Genetic testing for von Willebrand disease: the Canadian experience. *Semin Thromb Hemost,* 32**,** 546-52.

James, P. D., Notley, C., Hegadorn, C., Leggo, J., Tuttle, A., Tinlin, S., Brown, C., Andrews, C., Labelle, A., Chirinian, Y., O'brien, L., Othman, M., Rivard, G., Rapson, D., Hough, C. Lillicrap, D. 2007. The mutational spectrum of type 1 von Willebrand disease: Results from a Canadian cohort study. *Blood,* 109**,** 145-54.

James, P. D., O'brien, L. A., Hegadorn, C. A., Notley, C. R., Sinclair, G. D., Hough, C., Poon, M. C. Lillicrap, D. 2004. A novel type 2A von Willebrand factor mutation located at the last nucleotide of exon 26 (3538G>A) causes skipping of 2 nonadjacent exons. *Blood,* 104**,** 2739-45.

James, P. D., Paterson, A. D., Notley, C., Cameron, C., Hegadorn, C., Tinlin, S., Brown, C., O'brien, L., Leggo, J. Lillicrap, D. 2006. Genetic linkage and association analysis in type 1 von Willebrand disease: results from the Canadian type 1 VWD study. *J Thromb Haemost,* 4**,** 783-92.

Jokela, V., Lassila, R., Szanto, T., Joutsi-Korhonen, L., Armstrong, E., Oyen, F., Schneppenheim, S. Schneppenheim, R. 2013. Phenotypic and genotypic characterization of 10 Finnish patients with von Willebrand disease type 3: discovery of two main mutations. *Haemophilia*.

Jorieux, S., Fressinaud, E., Goudemand, J., Gaucher, C., Meyer, D. Mazurier, C. 2000. Conformational changes in the D' domain of von Willebrand factor induced by CYS 25 and CYS 95 mutations lead to factor VIII binding defect and multimeric impairment. *Blood,* 95**,** 3139-45.

Jorieux, S., Gaucher, C., Goudemand, J. Mazurier, C. 1998. A novel mutation in the D3 domain of von Willebrand factor markedly decreases its ability to bind factor VIII and affects its multimerization. *Blood,* 92**,** 4663-70.

Kadir, R. A., Economides, D. L., Sabin, C. A., Owens, D. Lee, C. A. 1999. Variations in coagulation factors in women: effects of age, ethnicity, menstrual cycle and combined oral contraceptive. *Thromb Haemost,* 82**,** 1456-61.

Karp, G. 2008. Cell and Molecular Biology. *Wiley,* 5th Ed.

Katsumi, A., Tuley, E. A., Bodo, I. Sadler, J. E. 2000. Localization of disulfide bonds in the cystine knot domain of human von Willebrand factor. *J Biol Chem,* 275**,** 25585-94.

Keeney, S., Bowen, D., Cumming, A., Enayat, S., Goodeve, A. Hill, M. 2008. The molecular analysis of von Willebrand disease: a guideline from the UK Haemophilia Centre Doctors' Organisation Haemophilia Genetics Laboratory Network. *Haemophilia,* 14**,** 1099-111.

Keeney, S. Cumming, A. M. 2001. The molecular biology of von Willebrand disease. *Clin Lab Haematol,* 23**,** 209-30.

Kenny, D., Morateck, P. A. Montgomery, R. R. 2002. The cysteine knot of platelet glycoprotein Ib beta (GPIb beta) is critical for the interaction of GPIb beta with GPIX. *Blood,* 99**,** 4428-33.

Khelifi, M. M., Ishmukhametova, A., Khau Van Kien, P., Thorel, D., Mechin, D., Perelman, S., Pouget, J., Claustres, M. Tuffery-Giraud, S. 2011. Pure intronic rearrangements leading to aberrant pseudoexon inclusion in dystrophinopathy: a new class of mutations? *Hum Mutat,* 32**,** 467-75.

Kimchi-Sarfaty, C., Simhadri, V. L., Kopelman, D. B., Friedman, A., Edwards, N. C., Javaid, A., Okunji, C., Komar, A. A., Sauna, Z. E. Katagir, N. H. 2011. The Synonymous V107V Mutation In Factor IX Is Not So Silent and May Cause Hemophilia B In Patients. . *53rd ASH Annual Meeting and Exposition.,* Oral and Poster Abstracts, Poster Board Number: II-77.

Kinoshita, S., Harrison, J., Lazerson, J. Abildgaard, C. F. 1984. A new variant of dominant type II von Willebrand's disease with aberrant multimeric pattern of factor VIII-related antigen (type IID). *Blood,* 63**,** 1369-71.

Klumpp, S., Dong, J. Hwa, T. 2012. On ribosome load, codon bias and protein abundance. *PLoS One,* 7**,** e48542.

Knobe, K. E., Sjorin, E. Ljung, R. C. 2008. Why does the mutation G17736A/Val107Val (silent) in the F9 gene cause mild haemophilia B in five Swedish families? *Haemophilia,* 14**,** 723-8.

Komar, A. A., Lesnik, T. Reiss, C. 1999. Synonymous codon substitutions affect ribosome traffic and protein folding during in vitro translation. *FEBS Lett,* 462**,** 387-91.

Kornfeld, R. Kornfeld, S. 1985. Assembly of asparagine-linked oligosaccharides. *Annu Rev Biochem,* 54**,** 631-64.

Kudla, G., Murray, A. W., Tollervey, D. Plotkin, J. B. 2009. Coding-sequence determinants of gene expression in Escherichia coli. *Science,* 324**,** 255-8.

Laffan, M., Brown, S. A., Collins, P. W., Cumming, A. M., Hill, F. G., Keeling, D., Peake, I. R. Pasi, K. J. 2004. The diagnosis of von Willebrand disease: a guideline from the UK Haemophilia Centre Doctors' Organization. *Haemophilia,* 10**,** 199-217.

Lak, M., Peyvandi, F. Mannucci, P. M. 2000. Clinical manifestations and complications of childbirth and replacement therapy in 385 Iranian patients with type 3 von Willebrand disease *Br J Haematol,* 111**,** 1236-9.

Lanke, E., Johansson, A. M., Hallden, C. Lethagen, S. 2005. Genetic analysis of 31 Swedish type 1 von Willebrand disease families reveals incomplete linkage to the von Willebrand factor gene and a high frequency of a certain disease haplotype. *J Thromb Haemost,* 3**,** 2656-63.

Larrieu, M. J., Caen, J. P., Meyer, D. O., Vainer, H., Sultan, Y. Bernard, J. 1968. Congenital bleeding disorders with long bleeding time and normal platelet count. II. Von Willebrand's disease (report of thirty-seven patients). *Am J Med,* 45**,** 354-72.

Larrieu, M. J. Soulier, J. P. 1953. Deficiency of antihemophilic factor A in a girl associated with bleeding disorder. *Rev Hematol,* 8**,** 361-70.

Lavner, Y. Kotlar, D. 2005. Codon bias as a factor in regulating expression via translation rate in the human genome. *Gene,* 345**,** 127-38.

Legendre, P., Navarrete, A. M., Rayes, J., Casari, C., Boisseau, P., Ternisien, C., Caron, C., Fressinaud, E., Goudemand, J., Veyradier, A., Denis, C. V., Lenting, P. J. Christophe, O. D. 2013. Mutations in the A3 domain of von Willebrand factor inducing combined qualitative and quantitative defects in the protein. *Blood,* 121**,** 2135-43.

Lemmerhirt, H. L., Broman, K. W., Shavit, J. A. Ginsburg, D. 2007. Genetic regulation of plasma von Willebrand factor levels: quantitative trait loci analysis in a mouse model. *J Thromb Haemost,* 5**,** 329-35.

Lenting, P. J., Pegon, J. N., Christophe, O. D. Denis, C. V. 2010. Factor VIII and von Willebrand factor--too sweet for their own good. *Haemophilia,* 16 Suppl 5**,** 194-9.

Lester, W., Guilliatt, A., Grundy, P., Enayat, S., Millar, C., Hill, F., Cumming, T. Collins, P. 2008. Is VWF R924Q a benign polymorphism, a marker of a null allele or a factor VIII-binding defect? The debate continues with results from the UKHCDO VWD study. *Thromb Haemost,* 100**,** 716-8.

Lethagen, S. (ed.) 2007. *Classification and Diagnostic Criteria of von Willebrand Disease*: Medicom Group.

Lethagen, S., Isaksson, C., Schaedel, C. Holmberg, L. 2002a. Von Willebrand's disease caused by compound heterozygosity for a substitution mutation (T1156M) in the D3 domain of the von Willebrand factor and a stop mutation (Q2470X). *Thromb Haemost,* 88**,** 421-6.

Lethagen, S., Isaksson, C., Schaedel, C. Holmberg, L. 2002b. Von Willebrand's disease caused by compound heterozygosity for a substitution mutation (T1156M) in the D3 domain of the von Willebrand factor and a stop mutation (Q2470X). *Thromb Haemost,* 88**,** 421-6.

Levy, G. G., Nichols, W. C., Lian, E. C., Foroud, T., Mcclintick, J. N., Mcgee, B. M., Yang, A. Y., Siemieniak, D. R., Stark, K. R., Gruppo, R., Sarode, R., Shurin, S. B., Chandrasekaran, V., Stabler, S. P., Sabio, H., Bouhassira, E. E., Upshaw, J. D., Jr., Ginsburg, D. Tsai, H. M. 2001. Mutations in a member of the ADAMTS gene family cause thrombotic thrombocytopenic purpura. *Nature,* 413**,** 488-94.

Lodish, H. F. 1988. Transport of secretory and membrane glycoproteins from the rough endoplasmic reticulum to the Golgi. A rate-limiting step in protein maturation and secretion. *J Biol Chem,* 263**,** 2107-10.

Lorson, C. L. Androphy, E. J. 2000. An exonic enhancer is required for inclusion of an essential exon in the SMA-determining gene SMN. *Hum Mol Genet,* 9**,** 259-65.

Lykke-Andersen, J., Shu, M. D. Steitz, J. A. 2000. Human Upf proteins target an mRNA for nonsense-mediated decay when bound downstream of a termination codon. *Cell,* 103**,** 1121-31.

Lyons, S. E., Bruck, M. E., Bowie, E. J. Ginsburg, D. 1992. Impaired intracellular transport produced by a subset of type IIA von Willebrand disease mutations. *J Biol Chem,* 267**,** 4424-30.

Mancuso, D. J., Kroner, P. A., Christopherson, P. A., Vokac, E. A., Gill, J. C. Montgomery, R. R. 1996. Type 2M:Milwaukee-1 von Willebrand disease: an in-frame deletion in the Cys509-Cys695 loop of the von Willebrand factor A1 domain causes deficient binding of von Willebrand factor to platelets. *Blood,* 88**,** 2559-68.

Mancuso, D. J., Tuley, E. A., Westfield, L. A., Lester-Mancuso, T. L., Le Beau, M. M., Sorace, J. M. Sadler, J. E. 1991. Human von Willebrand factor gene and pseudogene: structural analysis and differentiation by polymerase chain reaction. *Biochemistry,* 30**,** 253-69.

Mancuso, D. J., Tuley, E. A., Westfield, L. A., Worrall, N. K., Shelton-Inloes, B. B., Sorace, J. M., Alevy, Y. G. Sadler, J. E. 1989. Structure of the gene for human von Willebrand factor. *J Biol Chem,* 264**,** 19514-27.

Mannucci, P. M., Bloom, A. L., Larrieu, M. J., Nilsson, I. M. West, R. R. 1984. Atherosclerosis and von Willebrand factor. I. Prevalence of severe von Willebrand's disease in western Europe and Israel. *Br J Haematol,* 57**,** 163-9.

Markoof, A., Sormbroen, H., Bogdanova, N., Preisler-Adams, S., Ganev, V. Al., E. 1998. Comparison of conformation-sensitive gel electrophoresis and single-strand conformation polymorphism analysis for detection of mutations in the BRCA1 gene using optimized conformation analysis protocols. *Eur J Hum Genet,* 6(2)**,** 145-50.

Marti, T., Rosselet, S. J., Titani, K. Walsh, K. A. 1987. Identification of disulfide-bridged substructures within human von Willebrand factor. *Biochemistry,* 26**,** 8099-109.

Matsui, T., Titani, K. Mizuochi, T. 1992. Structures of the asparagine-linked oligosaccharide chains of human von Willebrand factor. Occurrence of blood group A, B, and H(O) structures. *J Biol Chem,* 267**,** 8723-31.

Matsushita, T., Meyer, D. Sadler, J. E. 2000. Localization of von willebrand factor-binding sites for platelet glycoprotein Ib and botrocetin by charged-to-alanine scanning mutagenesis. *J Biol Chem,* 275**,** 11044-9.

Matsuyama, S., Ueda, T., Crain, P. F., Mccloskey, J. A. Watanabe, K. 1998. A novel wobble rule found in starfish mitochondria. Presence of 7-methylguanosine at the anticodon wobble position expands decoding capability of tRNA. *J Biol Chem,* 273**,** 3363-8.

Mayadas, T. N. Wagner, D. D. 1989. In vitro multimerization of von Willebrand factor is triggered by low pH. Importance of the propolypeptide and free sulfhydryls. *J Biol Chem,* 264**,** 13497-503.

Mayadas, T. N. Wagner, D. D. 1992. Vicinal cysteines in the prosequence play a role in von Willebrand factor multimer assembly. *Proc Natl Acad Sci U S A,* 89**,** 3531-5.

Mazurier, C. 1992. von Willebrand disease masquerading as haemophilia A. *Thromb Haemost,* 67**,** 391-6.

Mazurier, C., Dieval, J., Jorieux, S., Delobel, J. Goudemand, M. 1990a. A new von Willebrand factor (vWF) defect in a patient with factor VIII (FVIII) deficiency but with normal levels and multimeric patterns of both plasma and platelet vWF. Characterization of abnormal vWF/FVIII interaction. *Blood,* 75**,** 20-6.

Mazurier, C., Gaucher, C., Jorieux, S., Parquet-Gernez, A. Goudemand, M. 1990b. Evidence for a von Willebrand factor defect in factor VIII binding in three members of a family previously misdiagnosed mild haemophilia A and haemophilia A carriers: consequences for therapy and genetic counselling. *Br J Haematol,* 76**,** 372-9.

Mazurier, C., Goudemand, J., Hilbert, L., Caron, C., Fressinaud, E. Meyer, D. 2001. Type 2N von Willebrand disease: clinical manifestations, pathophysiology, laboratory diagnosis and molecular biology. *Best Pract Res Clin Haematol,* 14**,** 337-47.

Mazurier, C. Hilbert, L. 2005. Type 2N von Willebrand disease. *Curr Hematol Rep,* 4**,** 350-8.

Mazurier, C. Meyer, D. 1996. Factor VIII binding assay of von Willebrand factor and the diagnosis of type 2N von Willebrand disease--results of an international survey. On behalf of the Subcommittee on von Willebrand Factor of the Scientific and Standardization Committee of the ISTH. *Thromb Haemost,* 76**,** 270-4.

Mcdonald, N. Q. Hendrickson, W. A. 1993. A structural superfamily of growth factors containing a cystine knot motif. *Cell,* 73**,** 421-4.

Mcgrath, R. T., Mcrae, E., Smith, O. P. O'donnell, J. S. 2010. Platelet von Willebrand factor--structure, function and biological importance. *Br J Haematol,* 148**,** 834-43.

Mckinnon, T. A., Goode, E. C., Birdsey, G. M., Nowak, A. A., Chan, A. C., Lane, D. A. Laffan, M. A. 2010. Specific N-linked glycosylation sites modulate synthesis and secretion of von Willebrand factor. *Blood,* 116**,** 640-8.

Mercier, B., Gaucher, C. Mazurier, C. 1991. Characterisation of 98 alleles in 105 unrelated individuals in the F8VWF gene. *Nucleic Acids Res,* 19**,** 4800.

Meyer, D., Fressinaud, E., Gaucher, C., Lavergne, J. M., Hilbert, L., Ribba, A. S., Jorieux, S. Mazurier, C. 1997. Gene defects in 150 unrelated French cases with type 2 von Willebrand disease: from the patient to the gene. INSERM Network on Molecular Abnormalities in von Willebrand Disease. *Thromb Haemost,* 78**,** 451-6.

Meyer, D., Fressinaud, E., Hilbert, L., Ribba, A. S., Lavergne, J. M. Mazurier, C. 2001. Type 2 von Willebrand disease causing defective von Willebrand factor-dependent platelet function. *Best Pract Res Clin Haematol,* 14**,** 349-64.

Meyer, D. Larrieu, M. J. 1970. Von Willebrand factor and platelet adhesiveness. *J Clin Pathol,* 23**,** 228-31.

Michaux, G., Abbitt, K. B., Collinson, L. M., Haberichter, S. L., Norman, K. E. Cutler, D. F. 2006. The physiological function of von Willebrand's factor depends on its tubular storage in endothelial Weibel-Palade bodies. *Dev Cell,* 10**,** 223-32.

Miller, C. H., Lenzi, R. Breen, C. 1987. Prevalence ofvon Willebrand disease among US adults. *Blood,* 69**,** 454-459.

Mitarai, N. Pedersen, S. 2013. Control of ribosome traffic by position-dependent choice of synonymous codons. *Phys Biol,* 10**,** 056011.

Mitarai, N., Sneppen, K. Pedersen, S. 2008. Ribosome collisions and translation efficiency: optimization by codon usage and mRNA destabilization. *J Mol Biol,* 382**,** 236-45.

Moake, J. L., Turner, N. A., Stathopoulos, N. A., Nolasco, L. H. Hellums, J. D. 1986. Involvement of large plasma von Willebrand factor (vWF) multimers and unusually large vWF forms derived from endothelial cells in shear stress-induced platelet aggregation. *J Clin Invest,* 78**,** 1456-61.

Mohlke, K. L., Nichols, W. C., Westrick, R. J., Novak, E. K., Cooney, K. A., Swank, R. T. Ginsburg, D. 1996. A novel modifier gene for plasma von Willebrand factor level maps to distal mouse chromosome 11. *Proc Natl Acad Sci U S A,* 93**,** 15352-7.

Mohlke, K. L., Purkayastha, A. A., Westrick, R. J., Smith, P. L., Petryniak, B., Lowe, J. B. Ginsburg, D. 1999. Mvwf, a dominant modifier of murine von Willebrand factor, results from altered lineage-specific expression of a glycosyltransferase. *Cell,* 96**,** 111-20.

Montgomery, R. R. 2005. von Willebrand disease--the relevance of history. *J Thromb Haemost,* 3**,** 2617-8.

Mufti, A., Lillcrap, D., Peake, I., Goodeve, A. Hampshire, A. 2013. Investigation of the effect of CLEC4M on plasma von willebrand factor level in the general population. *Abstract,* ISTH.

Nachman, R., Levine, R. Jaffe, E. A. 1977. Synthesis of factor VIII antigen by cultured guinea pig megakaryocytes. *J Clin Invest,* 60**,** 914-21.

Nackley, A. G., Shabalina, S. A., Tchivileva, I. E., Satterfield, K., Korchynskyi, O., Makarov, S. S., Maixner, W. Diatchenko, L. 2006. Human catechol-O-methyltransferase haplotypes modulate protein expression by altering mRNA secondary structure. *Science,* 314**,** 1930-3.

Nakamura, Y., Gojobori, T. Ikemura, T. 2000. Codon usage tabulated from international DNA sequence databases: status for the year 2000. *Nucleic Acids Res,* 28**,** 292.

Nesbitt, I. M., Hampton, K. K., Preston, F. E., Peake, I. R. Goodeve, A. C. 1999. A common splice site mutation is shared by two families with different type 2N von Willebrand disease mutations. *Thromb Haemost,* 82**,** 1061-4.

Neugebauer, B. M., Goy, C., Budek, I. Seitz, R. 2002. Comparison of two von Willebrand factor collagen-binding assays with different binding affinities for low, medium, and high multimers of von Willebrand factor. *Semin Thromb Hemost,* 28**,** 139-48.

Nichols, W. C. Ginsburg, D. 1997. von Willebrand disease. *Medicine (Baltimore),* 76**,** 1-20.

Nichols, W. L., Hultin, M. B., James, A. H., Manco-Johnson, M. J., Montgomery, R. R., Ortel, T. L., Rick, M. E., Sadler, J. E., Weinstein, M. Yawn, B. P. 2008a. von Willebrand disease (VWD): evidence-based diagnosis and management guidelines, the National Heart, Lung, and Blood Institute (NHLBI) Expert Panel report (USA). *Haemophilia,* 14**,** 171-232.

Nichols, W. L., Hultin, M. B., James, A. H., Manco-Johnson, M. J., Montgomery, R. R., Ortel, T. L., Rick, M. E., Sadler, J. E., Weinstein, M. Yawn, B. P. 2008b. von Willebrand disease (VWD): evidence-based diagnosis and management guidelines, the National Heart, Lung, and Blood Institute (NHLBI) Expert Panel report (USA). *Haemophilia,* 14**,** 171-232.

Nielsen, K. B., Sorensen, S., Cartegni, L., Corydon, T. J., Doktor, T. K., Schroeder, L. D., Reinert, L. S., Elpeleg, O., Krainer, A. R., Gregersen, N., Kjems, J. Andresen, B. S. 2007. Seemingly neutral polymorphic variants may confer immunity to splicing-inactivating mutations: a synonymous SNP in exon 5 of MCAD protects from deleterious mutations in a flanking exonic splicing enhancer. *Am J Hum Genet,* 80**,** 416-32.

Nilsson, I. M. Holmberg, L. 1979. Von Willebrand's disease today. *Clin Haematol,* 8**,** 147-68.

Nishino, M., Girma, J. P., Rothschild, C., Fressinaud, E. Meyer, D. 1989. New variant of von Willebrand disease with defective binding to factor VIII. *Blood,* 74**,** 1591-9.

Nishino, M., Nishino, S., Sugimoto, M., Shibata, M., Tsuji, S. Yoshioka, A. 1996. Changes in factor VIII binding capacity of von Willebrand factor and factor VIII coagulant activity in two patients with type 2N von Willebrand disease after hemostatic treatment and during pregnancy. *Int J Hematol,* 64**,** 127-34.

Nitu-Whalley, I. C., Riddell, A., Lee, C. A., Pasi, K. J., Owens, D., Enayat, M. S., Perkins, S. J. Jenkins, P. V. 2000. Identification of type 2 von Willebrand disease in previously diagnosed type 1 patients: a reappraisal using phenotypes, genotypes and molecular modelling. *Thromb Haemost,* 84**,** 998-1004.

Noe, D. A. 1996. A mathematical model of coagulation factor VIII kinetics. *Haemostasis,* 26**,** 289-303.

Nossent, A. Y., V, V. a. N. M., Nh, V. a. N. T., Rosendaal, F. R., Bertina, R. M., Ja, V. a. N. M. Eikenboom, H. C. 2006. von Willebrand factor and its propeptide: the influence of secretion and clearance on protein levels and the risk of venous thrombosis. *J Thromb Haemost,* 4**,** 2556-62.

O'brien, L. A., James, P. D., Othman, M., Berber, E., Cameron, C., Notley, C. R., Hegadorn, C. A., Sutherland, J. J., Hough, C., Rivard, G. E., O'shaunessey, D. Lillicrap, D. 2003. Founder von Willebrand factor haplotype associated with type 1 von Willebrand disease. *Blood,* 102**,** 549-57.

O'brien, S. H. 2012. Bleeding scores: are they really useful? *Hematology Am Soc Hematol Educ Program,* 2012**,** 152-6.

O'donnell, J., Boulton, F. E., Manning, R. A. Laffan, M. A. 2002a. Amount of H antigen expressed on circulating von Willebrand factor is modified by ABO blood group genotype and is a major determinant of plasma von Willebrand factor antigen levels. *Arterioscler Thromb Vasc Biol,* 22**,** 335-41.

O'donnell, J., Boulton, F. E., Manning, R. A. Laffan, M. A. 2002b. Genotype at the secretor blood group locus is a determinant of plasma von Willebrand factor level. *Br J Haematol,* 116**,** 350-6.

Othman, M., Chirinian, Y., Brown, C., Notley, C., Hickson, N., Hampshire, D., Buckley, S., Waddington, S., Parker, A. L., Baker, A., James, P. Lillicrap, D. 2010. Functional characterization of a 13-bp deletion (c.-1522_-1510del13) in the promoter of the von Willebrand factor gene in type 1 von Willebrand disease. *Blood,* 116**,** 3645-52.

Pagliari, M. T., Baronciani, L., Garcia Oya, I., Solimando, M., La Marca, S., Cozzi, G., Stufano, F., Canciani, M. T. Peyvandi, F. 2013. A synonymous (c.3390C>T) or a splice-site (c.3380-2A>G) mutation causes exon 26 skipping in four patients with von Willebrand disease (2A/IIE). *J Thromb Haemost,* 11**,** 1251-9.

Pan, Q., Shai, O., Lee, L. J., Frey, B. J. Blencowe, B. J. 2008. Deep surveying of alternative splicing complexity in the human transcriptome by high-throughput sequencing. *Nat Genet,* 40**,** 1413-5.

Paulin, C. N. Henikoff, S. 2006. Prediction the effects of Amino Acid Substitutions on Protein Function. *Annual Review of Genomics and Human Genetics,* 7**,** 61-80.

Pezeshkpoor, B., Zimmer, N., Marquardt, N., Nanda, I., Haaf, T., Budde, U., Oldenburg, J. El-Maarri, O. 2013. Deep intronic 'mutations' cause hemophilia A: application of next generation sequencing in patients without detectable mutation in F8 cDNA. *J Thromb Haemost,* 11**,** 1679-87.

Prior, J. F., Lim, E., Lingam, N., Raven, J. L. Finlayson, J. 2007. A moderately severe alpha-thalassemia condition resulting from a combination of the alpha2 polyadenylation signal (AATAAA-->AATA- -) mutation and a 3.7 Kb alpha gene deletion in an Australian family. *Hemoglobin,* 31**,** 173-7.

Rabinowitz, I., Tuley, E. A., Mancuso, D. J., Randi, A. M., Firkin, B. G., Howard, M. A. Sadler, J. E. 1992. von Willebrand disease type B: a missense mutation selectively abolishes ristocetin-induced von Willebrand factor binding to platelet glycoprotein Ib. *Proc Natl Acad Sci U S A,* 89**,** 9846-9.

Randi, A. M., Rabinowitz, I., Mancuso, D. J., Mannucci, P. M. Sadler, J. E. 1991. Molecular basis of von Willebrand disease type IIB. Candidate mutations cluster in one disulfide loop between proposed platelet glycoprotein Ib binding sequences. *J Clin Invest,* 87**,** 1220-6.

Rehemtulla, A. Kaufman, R. J. 1992. Preferred sequence requirements for cleavage of pro-von Willebrand factor by propeptide-processing enzymes. *Blood,* 79**,** 2349-55.

Reininger, A. J. 2008. Function of von Willebrand factor in haemostasis and thrombosis. *Haemophilia,* 14 Suppl 5**,** 11-26.

Ribba, A. S., Loisel, I., Lavergne, J. M., Juhan-Vague, I., Obert, B., Cherel, G., Meyer, D. Girma, J. P. 2001. Ser968Thr mutation within the A3 domain of von Willebrand factor (VWF) in two related patients leads to a defective binding of VWF to collagen. *Thromb Haemost,* 86**,** 848-54.

Rodeghiero, F. 2002. von Willebrand disease: still an intriguing disorder in the era of molecular medicine. *Haemophilia,* 8**,** 292-300.

Rodeghiero, F., Castaman, G. Dini, E. 1987. Epidemiological investigation of the prevalence of von Willebrand's disease. *Blood,* 69**,** 454-9.

Rodeghiero, F., Tosetto, A., Abshire, T., Arnold, D. M., Coller, B., James, P., Neunert, C., Lillicrap, D., Vwf, I. S. J. Perinatal/Pediatric Hemostasis Subcommittees Working, G. 2010. ISTH/SSC bleeding assessment tool: a standardized questionnaire and a proposal for a new bleeding score for inherited bleeding disorders. *J Thromb Haemost,* 8**,** 2063-5.

Ronneberg, T. A., Landweber, L. F. Freeland, S. J. 2000. Testing a biosynthetic theory of the genetic code: fact or artifact? *Proc Natl Acad Sci U S A,* 97**,** 13690-5.

Rosenberg, J. B., Haberichter, S. L., Jozwiak, M. A., Vokac, E. A., Kroner, P. A., Fahs, S. A., Kawai, Y. Montgomery, R. R. 2002. The role of the D1 domain of the von Willebrand factor propeptide in multimerization of VWF. *Blood,* 100**,** 1699-706.

Ruggeri, Z. M. 1999. Structure and function of von Willebrand factor. *Thromb Haemost,* 82**,** 576-84.

Ruggeri, Z. M. 2001. Structure of von Willebrand factor and its function in platelet adhesion and thrombus formation. *Best Pract Res Clin Haematol,* 14**,** 257-79.

Ruggeri, Z. M., Nilsson, I. M., Lombardi, R., Holmberg, L. Zimmerman, T. S. 1982. Aberrant multimeric structure of von Willebrand factor in a new variant of von Willebrand's disease (type IIC). *J Clin Invest,* 70**,** 1124-7.

Ruggeri, Z. M. Zimmerman, T. S. 1980. Variant von Willebrand's disease: characterization of two subtypes by analysis of multimeric composition of factor VIII/von Willebrand factor in plasma and platelets. *Journal of Clinical Investigation,* 65**,** 1318-1325.

Ruggeri, Z. M. Zimmerman, T. S. 1987. von Willebrand factor and von Willebrand disease. *Blood,* 70**,** 895-904.

Rydz, N., Swystun, L. L., Notley, C., Paterson, A. D., Riches, J. J., Sponagle, K., Boonyawat, B., Montgomery, R. R., James, P. D. Lillicrap, D. 2013. The C-type lectin receptor CLEC4M binds, internalizes, and clears von Willebrand factor and contributes to the variation in plasma von Willebrand factor levels. *Blood,* 121**,** 5228-37.

Sadler, J. E. 1994. A revised classification of von Willebrand disease. For the Subcommittee on von Willebrand Factor of the Scientific and Standardization Committee of the International Society on Thrombosis and Haemostasis. *Thromb Haemost,* 71**,** 520-5.

Sadler, J. E. 1998. Biochemistry and genetics of von Willebrand factor. *Annu Rev Biochem,* 67**,** 395-424.

Sadler, J. E. 2007. Interesting variations on how a disease is defined: comparisons of von Willebrand disease and Glanzmann thrombasthenia. Reply to a rebuttal. *J Thromb Haemost,* 5**,** 649-651.

Sadler, J. E. 2009. von Willebrand factor assembly and secretion. *J Thromb Haemost,* 7 Suppl 1**,** 24-7.

Sadler, J. E., Budde, U., Eikenboom, J. C., Favaloro, E. J., Hill, F. G., Holmberg, L., Ingerslev, J., Lee, C. A., Lillicrap, D., Mannucci, P. M., Mazurier, C., Meyer, D., Nichols, W. L., Nishino, M., Peake, I. R., Rodeghiero, F., Schneppenheim, R., Ruggeri, Z. M., Srivastava, A., Montgomery, R. R. Federici, A. B. 2006. Update on the pathophysiology and classification of von Willebrand disease: a report of the Subcommittee on von Willebrand Factor. *J Thromb Haemost,* 4**,** 2103-14.

Sadler, J. E., Mannucci, P. M., Berntorp, E., Bochkov, N., Boulyjenkov, V., Ginsburg, D., Meyer, D., Peake, I., Rodeghiero, F. Srivastava, A. 2000. Impact, diagnosis and treatment of von Willebrand disease. *Thromb Haemost,* 84**,** 160-74.

Salzman, E. W. 1963. Measurement of Platelet Adhesiveness. A Simple in Vitro Technique Demonstrating an Abnormality in Von Willebrand's Disease. *J Lab Clin Med,* 62**,** 724-35.

Sanger, F., Nicklen, S. Coulson, A. R. 1977. DNA sequencing with chain-terminating inhibitors. *Proc Natl Acad Sci U S A,* 74(12)**,** 5463-5467.

Sauna, Z. E. Kimchi-Sarfaty, C. 2011. Understanding the contribution of synonymous mutations to human disease. *Nat Rev Genet,* 12**,** 683-91.

Savage, B., Saldivar, E. Ruggeri, Z. M. 1996. Initiation of platelet adhesion by arrest onto fibrinogen or translocation on von Willebrand factor. *Cell,* 84**,** 289-97.

Schlammadinger, A., Kerenyi, A., Muszbek, L. Boda, Z. 2000. Comparison of the O'Brien filter test and the PFA-100 platelet analyzer in the laboratory diagnosis of von Willebrand's disease. *Thromb Haemost,* 84**,** 88-92.

Schneppenheim, R., Brassard, J., Krey, S., Budde, U., Kunicki, T. J., Holmberg, L., Ware, J. Ruggeri, Z. M. 1996. Defective dimerization of von Willebrand factor subunits due to a Cys-> Arg mutation in type IID von Willebrand disease. *Proc Natl Acad Sci U S A,* 93**,** 3581-6.

Schneppenheim, R. Budde, U. 2005. Phenotypic and genotypic diagnosis of von Willebrand disease: a 2004 update. *Semin Hematol,* 42**,** 15-28.

Schneppenheim, R., Budde, U., Obser, T., Brassard, J., Mainusch, K., Ruggeri, Z. M., Schneppenheim, S., Schwaab, R. Oldenburg, J. 2001a. Expression and characterization of von Willebrand factor dimerization defects in different types of von Willebrand disease. *Blood,* 97**,** 2059-66.

Schneppenheim, R., Budde, U. Ruggeri, Z. M. 2001b. A molecular approach to the classification of von Willebrand disease. *Best Pract Res Clin Haematol,* 14**,** 281-98.

Schneppenheim, R., Federici, A. B., Budde, U., Castaman, G., Drewke, E. Al., E. 2000. von Willebrand disease type 2M (Vicenza) in Italian and German patients: identification of the first candidate mutation (G3864A; R1205H) in 8 families. *Thromb Haemost,* 83 (1)**,** 136-40.

Schneppenheim, R., Michiels, J. J., Obser, T., Oyen, F., Pieconka, A., Schneppenheim, S., Will, K., Zieger, B. Budde, U. 2010. A cluster of mutations in the D3 domain of von Willebrand factor correlates with a distinct subgroup of von Willebrand disease: type 2A/IIE. *Blood*.

Schneppenheim, R., Thomas, K. B., Krey, S., Budde, U., Jessat, U., Sutor, A. H. Zieger, B. 1995. Identification of a candidate missense mutation in a family with von Willebrand disease type IIC. *Hum Genet,* 95**,** 681-6.

Schooten, C. J., Tjernberg, P., Westein, E., Terraube, V., Castaman, G., Mourik, J. A., Hollestelle, M. J., Vos, H. L., Bertina, R. M., Berg, H. M., Eikenboom, J. C., Lenting, P. J. Denis, C. V. 2005. Cysteine-mutations in von Willebrand factor associated with increased clearance. *J Thromb Haemost,* 3**,** 2228-37.

Schwachtgen, J. L., Janel, N., Barek, L., Duterque-Coquillaud, M., Ghysdael, J., Meyer, D. Kerbiriou-Nabias, D. 1997. Ets transcription factors bind and transactivate the core promoter of the von Willebrand factor gene. *Oncogene,* 15**,** 3091-102.

Sellner, L. N. Taylor, G. R. 2004. MLPA and MAPH: new techniques for detection of gene deletions. *Hum Mutat,* 23**,** 413-9.

Shabalina, S. A., Ogurtsov, A. Y. Spiridonov, N. A. 2006. A periodic pattern of mRNA secondary structure created by the genetic code. *Nucleic Acids Res,* 34**,** 2428-37.

Shabalina, S. A., Spiridonov, N. A. Kashina, A. 2013. Sounds of silence: synonymous nucleotides as a key to biological regulation and complexity. *Nucleic Acids Res,* 41**,** 2073-94.

Shah, J. H., Maguire, D. J., Munce, T. B. Cotterill, A. 2008. Alanine in HI: a silent mutation cries out! *Adv Exp Med Biol,* 614**,** 145-50.

Shahbazi, S., Baniahmad, F., Zakiani-Roudsari, M., Raigani, M. Mahdian, R. 2012. Nonsense mediated decay of VWF mRNA subsequent to c.7674-7675insC mutation in type3 VWD patients. *Blood Cells Mol Dis,* 49**,** 48-52.

Sharp, P. M., Averof, M., Lloyd, A. T., Matassi, G. Peden, J. F. 1995. DNA sequence evolution: the sounds of silence. *Philos Trans R Soc Lond B Biol Sci,* 349**,** 241-7.

Shavit, J. A., Manichaikul, A., Lemmerhirt, H. L., Broman, K. W. Ginsburg, D. 2009. Modifiers of von Willebrand factor identified by natural variation in inbred strains of mice. *Blood,* 114**,** 5368-74.

Shelton-Inloes, B. B., Titani, K. Sadler, J. E. 1986. cDNA sequences for human von Willebrand factor reveal five types of repeated domains and five possible protein sequence polymorphisms. *Biochemistry,* 25**,** 3164-71.

Shima, M., Fujimura, Y., Nishiyama, T., Tsujiuchi, T., Narita, N., Matsui, T., Titani, K., Katayama, M., Yamamoto, F. Yoshioka, A. 1995. ABO blood group genotype and plasma von Willebrand factor in normal individuals. *Vox Sang,* 68**,** 236-40.

Silwer, J. 1973. von Willebrand's disease in Sweden. *Acta Paediatr Scand Suppl,* 238**,** 1-159.

Smith, N. L., Chen, M. H., Dehghan, A., Strachan, D. P., Basu, S., Soranzo, N., Hayward, C., Rudan, I., Sabater-Lleal, M., Bis, J. C., De Maat, M. P., Rumley, A., Kong, X., Yang, Q., Williams, F. M., Vitart, V., Campbell, H., Malarstig, A., Wiggins, K. L., Van Duijn, C. M., Mcardle, W. L., Pankow, J. S., Johnson, A. D., Silveira, A., Mcknight, B., Uitterlinden, A. G., Aleksic, N., Meigs, J. B., Peters, A., Koenig, W., Cushman, M., Kathiresan, S., Rotter, J. I., Bovill, E. G., Hofman, A., Boerwinkle, E., Tofler, G. H., Peden, J. F., Psaty, B. M., Leebeek, F., Folsom, A. R., Larson, M. G., Spector, T. D., Wright, A. F., Wilson, J. F., Hamsten, A., Lumley, T., Witteman, J. C., Tang, W. O'donnell, C. J. 2010. Novel associations of multiple genetic loci with plasma levels of factor VII, factor VIII, and von Willebrand factor: The CHARGE (Cohorts for Heart and Aging Research in Genome Epidemiology) Consortium. *Circulation,* 121**,** 1382-92.

Solimando, M., Baronciani, L., La Marca, S., Cozzi, G., Asselta, R., Canciani, M. T., Federici, A. B. Peyvandi, F. 2012. Molecular characterization, recombinant protein expression, and mRNA analysis of type 3 von Willebrand disease: Studies of an Italian cohort of 10 patients. *Am J Hematol,* 87**,** 870-4.

Sorensen, M. A. Pedersen, S. 1991. Absolute in vivo translation rates of individual codons in Escherichia coli. The two glutamic acid codons GAA and GAG are translated with a threefold difference in rate. *J Mol Biol,* 222**,** 265-80.

Souto, J. C., Almasy, L., Muniz-Diaz, E., Soria, J. M., Borrell, M., Bayen, L., Mateo, J., Madoz, P., Stone, W., Blangero, J. Fontcuberta, J. 2000. Functional effects of the ABO locus polymorphism on plasma levels of von Willebrand factor, factor VIII, and activated partial thromboplastin time. *Arterioscler Thromb Vasc Biol,* 20**,** 2024-8.

Souto, J. C., Almasy, L., Soria, J. M., Buil, A., Stone, W., Lathrop, M., Blangero, J. Fontcuberta, J. 2003. Genome-wide linkage analysis of von Willebrand factor plasma levels: results from the GAIT project. *Thromb Haemost,* 89**,** 468-74.

Sporn, L. A., Chavin, S. I., Marder, V. J. Wanger, D. D. 1985. Biosynthesis of von Willebrand protein by human megakaryocytes. *J Clin Invest,* 76**,** 1102-6.

Staden, R. 1979. A strategy of DNA sequencing employing computer programs. *Nucleic Acids Res,* 6**,** 2601-2610.

Staden, R. 1984. A computer program to enter DNA gel reading data into a computer. *Nucleic Acids Res,* 12**,** 499-503.

Starke, R. D., Paschalaki, K. E., Dyer, C. E., Harrison-Lavoie, K. J., Cutler, J. A., Mckinnon, T. A., Millar, C. M., Cutler, D. F., Laffan, M. A. Randi, A. M. 2013a. Cellular and molecular basis of von Willebrand disease: studies on blood outgrowth endothelial cells. *Blood*.

Starke, R. D., Paschalaki, K. E., Dyer, C. E., Harrison-Lavoie, K. J., Cutler, J. A., Mckinnon, T. A., Millar, C. M., Cutler, D. F., Laffan, M. A. Randi, A. M. 2013b. Cellular and molecular basis of von Willebrand disease: studies on blood outgrowth endothelial cells. *Blood,* 121**,** 2773-84.

Sunohara, T., Jojima, K., Yamamoto, Y., Inada, T. Aiba, H. 2004. Nascent-peptide-mediated ribosome stalling at a stop codon induces mRNA cleavage resulting in nonstop mRNA that is recognized by tmRNA. *RNA,* 10**,** 378-86.

Sutherland, M. S., Cumming, A. M., Bowman, M., Bolton-Maggs, P. H., Bowen, D. J., Collins, P. W., Hay, C. R., Will, A. M. Keeney, S. 2009a. A novel deletion mutation is recurrent in von Willebrand disease types 1 and 3. *Blood,* 114**,** 1091-8.

Sutherland, M. S., Keeney, S., Bolton-Maggs, P. H., Hay, C. R., Will, A. Cumming, A. M. 2009b. The mutation spectrum associated with type 3 von Willebrand disease in a cohort of patients from the north west of England. *Haemophilia,* 15**,** 1048-57.

Sztukowska, M., Gallinaro, L., Cattini, M. G., Pontara, E., Sartorello, F., Daidone, V., Padrini, R., Pagnan, A. Casonato, A. 2008. Von Willebrand factor propeptide makes it easy to identify the shorter Von Willebrand factor survival in patients with type 1 and type Vicenza von Willebrand disease. *Br J Haematol,* 143**,** 107-14.

Thomas, M. R., Cutler, J. A. Savidge, G. F. 2006a. Diagnostic and therapeutic difficulties in type 2A von Willebrand disease: resolution. *Clin Appl Thromb Hemost,* 12**,** 237-9.

Thomas, M. R., Cutler, J. A. Savidge, G. F. 2006b. Diagnostic and therapeutic difficulties in type 2A von Willebrand disease: resolution. *Clin Appl Thromb Hemost,* 12**,** 237-9.

Titani, K., Kumar, S., Takio, K., Ericsson, L. H., Wade, R. D., Ashida, K., Walsh, K. A., Chopek, M. W., Sadler, J. E. Fujikawa, K. 1986. Amino acid sequence of human von Willebrand factor. *Biochemistry,* 25**,** 3171-84.

Tjernberg, P., Castaman, G., Vos, H. L., Bertina, R. M. Eikenboom, J. C. 2006. Homozygous C2362F von Willebrand factor induces intracellular retention of mutant von Willebrand factor resulting in autosomal recessive severe von Willebrand disease. *Br J Haematol,* 133**,** 409-18.

Tjernberg, P., Vos, H. L., Castaman, G., Bertina, R. M. Eikenboom, J. C. 2004. Dimerization and multimerization defects of von Willebrand factor due to mutated cysteine residues. *J Thromb Haemost,* 2**,** 257-65.

Tosetto, A., Castaman, G. Rodeghiero, F. 2007. Assessing bleeding in von Willebrand disease with bleeding score. *Blood Rev,* 21**,** 89-97.

Tosetto, A., Rodeghiero, F., Castaman, G., Goodeve, A., Federici, A. B., Batlle, J., Meyer, D., Fressinaud, E., Mazurier, C., Goudemand, J., Eikenboom, J., Schneppenheim, R., Budde, U., Ingerslev, J., Vorlova, Z., Habart, D., Holmberg, L., Lethagen, S., Pasi, J., Hill, F. Peake, I. 2006. A quantitative analysis of bleeding symptoms in type 1 von Willebrand disease: results from a multicenter European study (MCMDM-1 VWD). *J Thromb Haemost,* 4**,** 766-73.

Tournier, I., Vezain, M., Martins, A., Charbonnier, F., Baert-Desurmont, S., Olschwang, S., Wang, Q., Buisine, M. P., Soret, J., Tazi, J., Frebourg, T. Tosi, M. 2008. A large fraction of unclassified variants of the mismatch repair genes MLH1 and MSH2 is associated with splicing defects. *Hum Mutat,* 29**,** 1412-24.

Van De Ven, W. J., Voorberg, J., Fontijn, R., Pannekoek, H., Van Den Ouweland, A. M., Van Duijnhoven, H. L., Roebroek, A. J. Siezen, R. J. 1990. Furin is a subtilisin-like proprotein processing enzyme in higher eukaryotes. *Mol Biol Rep,* 14**,** 265-75.

Van Schooten, C. J., Denis, C. V., Lisman, T., Eikenboom, J. C., Leebeek, F. W., Goudemand, J., Fressinaud, E., Van Den Berg, H. M., De Groot, P. G. Lenting, P. J. 2007. Variations in glycosylation of von Willebrand factor with O-linked sialylated T antigen are associated with its plasma levels. *Blood,* 109**,** 2430-7.

Verweij, C. L., De Vries, C. J., Distel, B., Van Zonneveld, A. J., Van Kessel, A. G., Van Mourik, J. A. Pannekoek, H. 1985. Construction of cDNA coding for human von Willebrand factor using antibody probes for colony-screening and mapping of the chromosomal gene. *Nucleic Acids Res,* 13**,** 4699-717.

Verweij, C. L., Hart, M. Pannekoek, H. 1987. Expression of variant von Willebrand factor (vWF) cDNA in heterologous cells: requirement of the pro-polypeptide in vWF multimer formation. *EMBO J,* 6**,** 2885-90.

Vlot, A. J., Koppelman, S. J., Meijers, J. C., Dama, C., Van Den Berg, H. M., Bouma, B. N., Sixma, J. J. Willems, G. M. 1996. Kinetics of factor VIII-von Willebrand factor association. *Blood,* 87**,** 1809-16.

Von Willebrand, E. A. 1926. Hereditar Pseudohemofili. *Finska Lakaresallsk Handle,* 68**,** 87-112.

Voorberg, J., Fontijn, R., Calafat, J., Janssen, H., Van Mourik, J. A. Pannekoek, H. 1991. Assembly and routing of von Willebrand factor variants: the requirements for disulfide-linked dimerization reside within the carboxy-terminal 151 amino acids. *J Cell Biol,* 113**,** 195-205.

Wagner, D. D., Fay, P. J., Sporn, L. A., Sinha, S., Lawrence, S. O. Marder, V. J. 1987. Divergent fates of von Willebrand factor and its propolypeptide (von Willebrand antigen II) after secretion from endothelial cells. *Proc Natl Acad Sci U S A,* 84**,** 1955-9.

Wagner, D. D., Mayadas, T. Marder, V. J. 1986. Initial glycosylation and acidic pH in the Golgi apparatus are required for multimerization of von Willebrand factor. *J Cell Biol,* 102**,** 1320-4.

Wagner, D. D., Olmsted, J. B. Marder, V. J. 1982. Immunolocalization of von Willebrand protein in Weibel-Palade bodies of human endothelial cells. *J Cell Biol,* 95**,** 355-60.

Wang, J. W., Bouwens, E. A., Pintao, M. C., Voorberg, J., Safdar, H., Valentijn, K. M., De Boer, H. C., Mertens, K., Reitsma, P. H. Eikenboom, J. 2013. Analysis of the storage and secretion of von Willebrand factor in blood outgrowth endothelial cells derived from patients with von Willebrand disease. *Blood,* 121**,** 2762-72.

Watson, S., Daly, M., Dawood, B., Gissen, P., Makris, M., Mundell, S., Wilde, J. Mumford, A. 2010. Phenotypic approaches to gene mapping in platelet function disorders - identification of new variant of P2Y12, TxA2 and GPVI receptors. *Hamostaseologie,* 30**,** 29-38.

Weiss, H. J., Ball, A. P. Mannucci, P. M. 1982. Incidence of severe von Willebrand disease (letter). *N Engl J Med,* 307**,** 127.

Weiss, H. J., Hoyer, L. W., Rickles, F. R., Varma, A. Rogers, J. 1973. Quantitative assay of a plasma factor deficient in von Willebrand's disease that is necessary for platelet aggregation. Relationship to factor VIII procoagulant activity and antigen content. *J Clin Invest,* 52**,** 2708-2716.

Weiss, H. J., Turitto, V. T. Baumgartner, H. R. 1991. Further evidence that glycoprotein IIb-IIIa mediates platelet spreading on subendothelium. *Thromb Haemost,* 65**,** 202-5.

Werner, E. J., Broxson, E. H., Tucker, E. L., Giroux, D. S., Shults, J. Abshire, T. C. 1993. Prevalence of von Willebrand disease in children: a multiethnic study. *J Pediatr,* 123**,** 893-8.

Whittock, N. V., Ashton, G. H., Mohammedi, R., Mellerio, J. E., Mathew, C. G. Al., E. 1999. Comparative mutation detection screening of type VII collagen gene (COL7A1) using the protein truncation test, fluorescent chemical cleavage of mismatch, and conformation sensitive gel electrophoresis. *J Invest Dermatol,* 113 (4)**,** 673-86.

Wise, R. J., Pittman, D. D., Handin, R. I., Kaufman, R. J. Orkin, S. H. 1988. The propeptide of von Willebrand factor independently mediates the assembly of von Willebrand multimers. *Cell,* 52**,** 229-36.

Woods, A. I., Kempfer, A. C., Sanchez-Luceros, A., Calderazzo, J. C., Grosso, S. H. Lazzari, M. A. 2013. Clinical profile of the association of P.R1205h and P.R924q in a patient with von Willebrand's disease. *Haemophilia,* 19**,** e180-1.

Yadegari, H., Driesen, J., Hass, M., Budde, U., Pavlova, A. Oldenburg, J. 2011. Large deletions identified in patients with von Willebrand disease using multiple ligation-dependent probe amplification. *J Thromb Haemost,* 9**,** 1083-6.

Yadegeri, H., Driesen, J., Pavlova, A., Biswas, A., Ivaskevicius, V., Klamroth, R. Oldenburg, J. 2013. Insights into pathological mechanisms of missense mutations in C-terminal domains of von Willebrand factor causing qualitative or quantitative von Willebrand disease. *Haematologica,* 98(8)**,** 1315-1323.

Zabaneh, D., Gaunt, T. R., Kumari, M., Drenos, F., Shah, S., Berry, D., Power, C., Hypponen, E., Shah, T., Palmen, J., Pallas, J., Talmud, P. J., Casas, J. P., Sofat, R., Lowe, G., Rumley, A., Morris, R. W., Whincup, P. H., Rodriguez, S., Ebrahim, S., Marmot, M. G., Smith, G. D., Lawlor, D. A., Kivimaki, M., Whittaker, J., Hingorani, A. D., Day, I. N. Humphries, S. E. 2011. Genetic variants associated with Von Willebrand factor levels in healthy men and women identified using the HumanCVD BeadChip. *Ann Hum Genet,* 75**,** 456-67.

Zatkova, A., Messiaen, L., Vandenbroucke, I., Wieser, R., Fonatsch, C., Krainer, A. R. Wimmer, K. 2004. Disruption of exonic splicing enhancer elements is the principal cause of exon skipping associated with seven nonsense or missense alleles of NF1. *Hum Mutat,* 24**,** 491-501.

Zhang, F., Saha, S., Shabalina, S. A. Kashina, A. 2010. Differential arginylation of actin isoforms is regulated by coding sequence-dependent degradation. *Science,* 329**,** 1534-7.

Zhang, Z. P., Blomback, M., Egberg, N., Falk, G. Anvret, M. 1994. Characterization of the von Willebrand factor gene (VWF) in von Willebrand disease type III patients from 24 families of Swedish and Finnish origin. *Genomics,* 21**,** 188-93.

Zheng, X., Chung, D., Takayama, T. K., Majerus, E. M., Sadler, J. E. Fujikawa, K. 2001. Structure of von Willebrand factor-cleaving protease (ADAMTS13), a metalloprotease involved in thrombotic thrombocytopenic purpura. *J Biol Chem,* 276**,** 41059-63.

Zhou, Y. F., Eng, E. T., Zhu, J., Lu, C., Walz, T. Springer, T. A. 2012. Sequence and structure relationships within von Willebrand factor. *Blood,* 120**,** 449-58.

Zimmerman, T. S., Dent, J. A., Ruggeri, Z. M. Nannini, L. H. 1986. Subunit composition of plasma von Willebrand factor. Cleavage is present in normal individuals, increased in IIA and IIB von Willebrand disease, but minimal in variants with aberrant structure of individual oligomers (types IIC, IID, and IIE). *J Clin Invest,* 77**,** 947-51.

Zimmerman, T. S., Ratnoff, O. D. Powell, A. E. 1971. Immunologic differentiation of classic hemophilia (factor 8 deficiency) and von Willebrand's dissase, with observations on combined deficiencies of antihemophilic factor and proaccelerin (factor V) and on an acquired circulating anticoagulant against antihemophilic factor. *J Clin Invest,* 50**,** 244-54.

Zimmerman, T. S. Ruggeri, Z. M. 1987. von Willebrand disease. *Hum Pathol,* 18**,** 140-52.

9. APPENDICES

Appendix 1 Sequences of M13 forward and reverse primers used for tailing PCR primers for DNA sequencing

Primer	Sequence	Complementary sequence for DNA sequencing
M13 F (5'-3')	dTGTAAAACGACGGCCAGT	dACATTTTGCTGCCGGTCA
M13 R (5'-3'):	dCAGGAAACAGCTATGACC	dGTCCTTTGTCGATACTGG

Appendix 2 Reaction mixture for conventional PCR using ReddyMix (Fisher Scientific, Loughborough, UK) with various concentration of $MgCl_2$

30 µl final volume	**[$MgCl_2$] mM**				
	1.5	**2**	**2.5**	**3**	**4**
Master mix	27	27	27	27	27
F primer	0.6	0.6	0.6	0.6	0.6
R primer	0.6	0.6	0.6	0.6	0.6
dH_2O	1.2	0.9	0.6	0.3	0
50mM $MgCl_2$	0	0.3	0.6	0.9	1.5

Appendix 3 PCR program for the amplification of *VWF*

Initiation	Cycling	Final extension
94 °C for 7 min	35 cycles	72 °C for 7 min
	94 °C for 1 min	
	n °C for 1 min*	
	72 °C for 1 min	

* See Appendices 4, 6, 11 and 12 for details of temperature used

Appendix 4 List of *VWF* PCR primers used within the EU study which did not require re-design

EXON	Primer sequence (5' to 3')*	Annealing temp °C	$MgCl_2$ conc (mM)
2F	GTCCATGTTCAAAGGGGAAA	59	3
2R	GGCAGGAATGAGAAATGGAG		
3F	GAGATCACCAGCCCAACCT	60	1.5
3R	CAGCCCTCCCTCTGAAGTC		
4F	GGTTACGTAGATAATGATTC	53	1.5
4R	AACATTTGCTTCCATTCTCT		
5F	AAGGTGGGAGAGACATCCAG	51	1.5
5R	AGTGAAGGTTTATGAGCAAG		
6F	ACCACCAGCAGACCTAGAAT	51	1.5
6R	TGGAAGGATATGAGACTGAG		
7F	AGGGAGACACTAACGGAGCA	59	1.5
7R	TGTGGTAAAGCCGCACATAC		
9F	ACCCAACCATTGTCCCTG	55	1.5
9R	AGGTCTCCCAGAGCACGC		
10F	GAGCTCTAAATCCATTTGC	51	1.5
10R	GGAGACGCCTCCCCGATT		
11F	CACCCTGCTTGCATATGCAT	51	1.5
11R	TCTGGAAGAGACCTCCCTCA		
13F	CCCAAATACATCTGCCTGCC	60	1.5
13R	TTCTTCTCCCACCACACAAA		
16F	AACCACAGTCCTTGCTGTCC	60	1.5
16R	CCCCAGCTCTGCTGTTTTAG		
17F	AGAGTGAGTGGGAGGTGAAG	59	1.5
17R	CCATTCCACACGTGAGGAAT		
19F	GGCTTTAGATCAGTCACTGTG	59	1.5
19R	GTGCACCCTCACTCCACCCGC		
21F	AATCTTCTGGTCTGGTGAGA	60	1.5
21R	CCTCATCCTCTTTAATGGCT		
22F	AGAGTGGAGGGAGGATCTGG	59	1.5
22R	TAGAGACCTACGATCAGGGA		
35F	GCATCCATCCTCTGCTTCTC	60	1.5
35R	CCTGACATTCTATTGCCTTACCA		
37F	CTGGTGAGGATCAAGAATGG	61	1.5
37R	AAGAATCTGGGGCACAGAGA		
38F	GTCTGATGATTAACCATGTTGA	55	1.5
38R	GGCCAATCACTGGTGAACAT		
39F	GAATTCTGGGCTTCGTACCT	55	1.5
39R	CAGTGTTTGAGTCTGCTCTG		
40F	CAAATCCCTCTGAGGCTGTC	59	1.5
40R	AGACACCTTTCAGCACCTTCA		
41F	GCATCCCACTCACAGGTAAT	55	1.5
41R	AACAGGAAATGACGTGATCT		
42F	GCACCCTATAGCATAGCTGA	55	1.5
42R	ATGGATGGGTGGATAGAAGG		
43F	CTTCTGTGTTAGTAGGTGCTAA	51	1.5
43R	TACCCTTCCTAAGATGCCCT		

Appendix 4 List of *VWF* PCR primers used within the EU study which did not require re-design cont

EXON	Primer sequence (5' to 3')*	Annealing temp °C	$MgCl_2$ conc (mM)
44F	TCTGCAGCTGATGTAAGACTTCG	62	1.5
44R	AAGGTCAACGCTGGTCCCTGG AGT		
45F	CCTGTGGTGGGACTTACATGTTA	63	1.5
45R	TCAGGAGCCAAAAGTGGAAAGAG		
46F	AGGAGGAGCCCCAAAGAGAG	60	1.5
46R	CTAGCCTGGGCTCCATGA		
47F	GGCTCATGGGAGCTATGG	59	1.5
47R	CAGTTTGGGTGGGTGATTTT		
48F	AGCCTACTTACAATTGGGAT	51	1.5
48R	AAAAGGAAGCAAGATGGTGA		
49F	ACCCACTCCTCTTTCCTTCC	60	1.5
49R	GAGAAATTATGCCGGAGCTG		
50F	TGGTCAGGTAGGGTGGTCA	58	1.5
50R	AGGAGCAAGCTGCAAAGAGC		
51F	CCAGCCAGTCCTCAAGTTTC	60	1.5
51R	CCAGCCCTTATTGAAGCAGA		
52F	CTACTGTCCTGGGTGCTTC	59	1.5
52R	TGACACTGAGGCTTGCAGA		

* All primers were tailed with the following sequences (M13) to facilitate DNA sequencing:
M13 F (5'-3'): dTGTAAAACGACGGCCAGT
M13 R (5'-3'): dCAGGAAACAGCTATGACC

Appendix 5 Internal primers used to sequence the long rang PCR product for exon 28

Primer	Primer sequence 5'-3'
28 AF	CTTGGATGTGGAATGGTCCA
28 AR	CTTCAGCAAGATCGACCGCC
28 BF	CAGCAGGCTACTGGACCTGG
28 BR	CGAGATCGTTAGCTACCTCTG
28 CF	CAAGCAGATCCGCCTCATCG
28 CR	GAGATCAAGAGGCTGCCTGG
28 DF	AACAGGACCAACACTGGGC
28 DR	CGACTCGGGTTCTAATCCTG

Appendix 6 List of promoter and exon-intron 1 region primers

EXON	Primer sequences (5' to 3')*	GC%	Tm °C	Optimised annealing Temp °C/Cycles	$MgCl_2$ conc (mM)	Product size (bp)
Promoter F	dCTGGCTGCTCTTCCATTTTT	45.0	55.0	57/28	1.5	3500
Promoter R	dGGGATCAGTCAGTCCTGCAT	55.0	59.0			
Intron 1F	dCTCATTTGCAGGGGAAGGTA	50.0	57.0	58/30	1.5	1427
Intron 1R	dGAGGCAACCAACAGCCTAAG	55.0	59.2			

* All primers were tailed with M13 sequences to facilitate DNA sequencing:

A 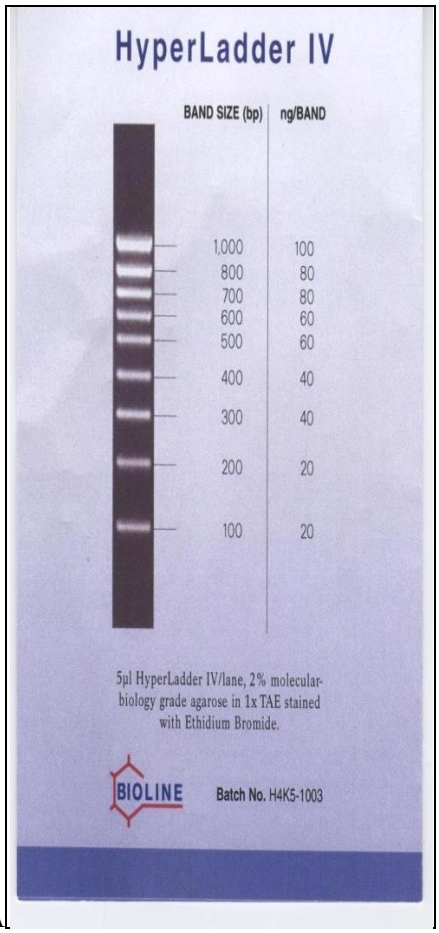

B 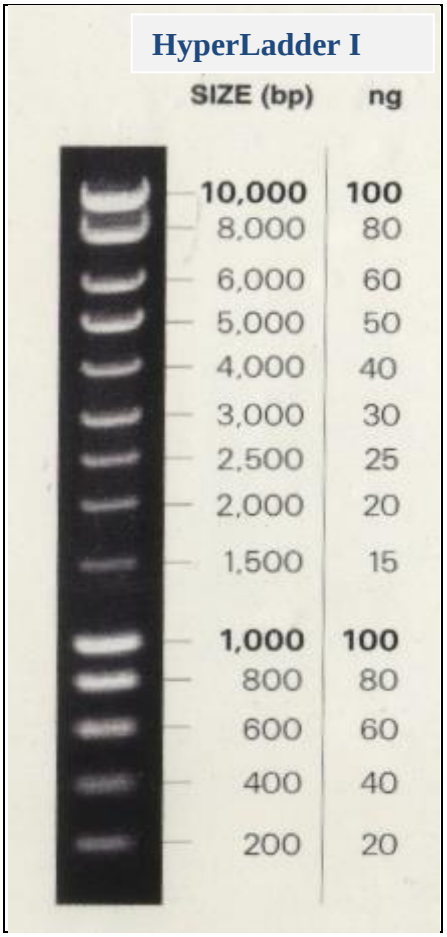

Appendix.7 A) Hyperladder IV. It includes 9 fragments ranging between 100-1000bp, **B)** Hyperladder I includes 14 fragments ranging between 200-10,000 bp (www.bioline.com).

Appendix 8 Mutagenic primers used to introduce mutation to the wild-type VWF construct

Mutation	Exon	Nucleotide change	Mutagenic primer
p.S539Lfs*38	14	c.1614del	DEL1614: ACTTCCTTACCCCTCTGGGCTGGCGG DEL1614-ANTISENSE: CCGCCAGCCCAGAGGGGTAAGGAAGT
p.R924Q	21	c.2771G>A	G2771A: AGTGAAATGCAAGAAACAGGTCACCATCCTGGTGG G2771A_ANTISENSE: CCACCAGGATGGTGACCTGTTTCTTGCATTTCACT
p.C1157R	26	c.3469T>C	T3469C: CCTGTCAAGTCACGCGTCAGCACCCTGAG T3469C_ANTISENSE: CTCAGGGTGCTGACGCGTGACTTGACAGG
p.L1382=	28	c.4146G>T	G4146T: CCGCATCGCCCTTCTCCTGATGGCC G4146T_ANTISENSE: GGCCATCAGGAGAAGGGCGATGCGG
p.L1382=	28	c.4146G>A	G4146T: CCGCATCGCCCTACTCCTGATGGCC G4146T_ANTISENSE: GGCCATCAGGAGTAGGGCGATGCGG
p.L1382=	28	c.4146G>C	G4146T: CCGCATCGCCCTCCTCCTGATGGCC G4146T_ANTISENSE: GGCCATCAGGAGGAGGGCGATGCGG
p.C1927R	34	c.5779T>C	T5779C: GCTGAGGCCTTCGCGCCCTAACAGCCA T5779C_ANTISENSE: TGGCTGTTAGGGCGCGAAGGCCTCAGC
p.W2271G	39	c.6811T>G	T6811G: TTCCTGGAAGCCGGGGTCCCGGACC T6811G_ANTISENSE: GGTCCGGGACCCCGGCTTCCAGGAA

Appendix 9 Primers designed for sequencing the full length *VWF* cDNA

Primer	Primer Sequence (5'-3')
PC1 (F)	TAATACGACTCACTATAGGG
PC2	CGGCAACTTTCAAGTCCTGCTGT
PC3	CAGTGTGCCCTGCTGGTATG
PC4	CAGCCTTGTGAAACTGAAGCATGG
PC5	CGAAAGGCCAGGTGTACCTGCAG
PC6	CTGGAGTGCATGAGCATGGGCTG
PC7	CATCATTCTGCTGCTGGGCAAAG
PC8	CAGAGCTGCGAGGAGAGGAATC
PC9	CTTTGTGGTGGACATGATGGAGC
PC10	CATGGCACAAGTCACTGTGGGC
P11	CTAATGCCAACGTGCAGGAGCTG
PC12	TCATCCTGGTCACGGACGTCTC
PC13	CAAGCTGACTGGCAGCTGTTCTT
PC14	CATCCTGGAGGAGCAGTGTCTTG
PC15	CACGTGTGGCCTGTGTGAAGTAG
PC16	CAGAAGCCCTGTGAGGACAGCT
PC17	CAAGGAAGAAAATAACACAGGTG
PC18 (R)	TAGAAGGCACAGTCGAGG

Appendix 10 Primer set previously used in the EU study with SNP or sequence error within primers sequences

Primer	Primer sequence (5'-3')	Allele	SNP Ref No	Origin	Distance from target exon	Reason for re-design
Exon 8 R	TGCTGGCAAGGTCT**C**TGATCTGT A	G/A	rs3213721	Ensembl	Close (22bp)	SNP found Close to target exon
Exon 12 F	TTGAGGCCTTTCTCTGATTA**A**	A/T	rs 61754008	SNPCheck	Acceptable (>50bp)	SNP found
Exon 14 R	GCCTTGCGTGACGTGATTA	N/A	N/A	SNPCheck	-	Sequence error: could not be located by BLAST
Exon 15 R	CACCGTGGA**C**GGATTTGGG	G/A	rs73264986	Ensembl	Close (38bp)	SNP found Close to target exon
Exon 18 R	CCTGCCTACAAGAAAA**C**TGAA	G/T	rs77372340	Ensembl	Close (33bp)	SNP found Close to target exon
Exon 20 R	AGATCCACAGAACCCAAC**C**T	G/T	rs73263045	Ensembl	Acceptable (>50bp)	SNP found
Exon 23 R	C**C**TTCCAGCCCCCATGAC	G/T	rs56068059	Ensembl	Acceptable (>50bp)	SNP found*
Exon 24 R	GCCAAGCCTTGGGACC**G**T	C/T	rs73051263	Ensembl	Close (30bp)	SNP found Close to target exon
Exon 25 F	CAGACTAAGAGCCAGAGTT**C**	C/T	rs4021577	Ensembl	Close (46bp)	SNP found Close to target exon
Exon 26 F	CAACATTATCTCCAGATGGC	del	rs140819	Ensembl	Acceptable (>50bp)	SNP found
Exon 26 R	TTGCAGGTCAGAGAT**A**GGAC	T/C	rs13054481	Ensembl	Acceptable (>50bp)	SNP found
Exon 27 R	ATCCAAAACCTAGTCTC TA	T/C	N/A	N/A	Acceptable (>50bp)	Sequence error
Exon 29 F	TA**G**GCCTGGTGGCCATTGTC	C/A	rs11613273	Ensembl	Close (43bp)	SNP found Close to target exon

*SNP will destabilise PCR product

Appendix 10 Primer set previously used in the EU study with presence of SNP or sequence error within their primers sequences cont

Primer	Primer sequence (5'-3')	Allele	SNP Ref No	Origin	Distance from target exon	Reason for re-design
Exon 30 R	GAGCAAAGTGACTGGCC**G**A	C/T	rs72613680	Ensembl	Acceptable (>50bp)	SNP found
Exon 31 F	ATCCACCGTTAAGACAGGGTGTC**G**	G/C	rs57349683	Ensembl	Close (46bp)	SNP found Close to target exon
Exon 32	TGAACATCTTCCTCATAGGGCTGA	-	-	-	Acceptable (>50bp)	No product
Exon 33R	CCCCAAACACATCTCTAA**C**C	G/A	rs55664929	Ensembl	Close (31bp)	SNP found Close to target exon
Exon 34 R	GAAAAGCAATTCTTC**C**TTCCA	G/A	Rs4764479	Ensembl	Acceptable (>50bp)	SNP found
Exon 36 F	CCT**A**GGATTCCTCATTGCTA	A/G	rs71579337	Ensembl	Close (33bp)	SNP found Close to target exon

Appendix 11 List of re-designed primers not in the *VWF* pseudogene region

EXON	Primer sequences (5' to 3')	GC%	Tm °C	Optimised annealing Temp °C/Cycles	$MgCl_2$ conc (mM)	Product size (bp)
8F	GTCAGAGTGGGCACGAGAG	63.1	59.5	60/35	1.5	300
8R	GTGGCCTTCATCTCACTTCC	55.0	59.6			
12F	AGCCTTCTTGCTGCACAACT	50.0	60.2	60/35	1.5	395
12R	GGTTGAGAAGGAGGGTGCTA	55.0	59.2			
14F	GTTTCACCCGGGGAACTT	55.5	59.7	60/35	1.5	374
14R	AACGCACTGCACTAATGTGG	50.0	59.7			
15F	CAGCACTGGGCTATTTCCAG	55.0	60.7	55/32	1.5	399
15R	GGAAACAACGCAGAGAAAGG	50.0	59.8			
18F	TAGGGGACCAAAGGACAGTG	55.0	59.9	60/35	1.5	349
18R	CCGTGTTTAGCCCTTGTTTC	50.0	59.6			
20F	CAGGTCCTCAACTTCCTTGG	55.0	59.6	60/35	1.5	389
20R	GACCCCAGAGTTGTTTCTGC	55.0	59.7			
36F	TTTGTGGCTGATGTTGCAGT	45.0	60.3	60/35	1.5	396
36R	AAGCATCCAAGAGCCTCAGA	50.0	60.1			

Appendix 12 List of re-designed primers showing mismatches between *VWF* and *VWFP*

Exon	Primer sequences (5' to 3')	Introduced mismatch	GC%	Tm °C	Optimised annealing Temp °C/Cycles	$MgCl_2$ conc (mM)	Product size (bp)
23F	GGGCATGTTGCCTCTCT--GT*		57.9	61.2	60/35	1.5	473
23R	TCCAGCCCCCATGACCAAT		55.5	62.3			
24F	GTCCCTCTGTCCCCATTGTC		60.0	61.7	60/35	1.5	343
24R	ACTCTGTGTCCATACCACCAG		52.4	57.5			
25F	CCTGGACCCCC-TTATCCTTA		55.0	60.1	60/35	1.5	400
25R	GCCATCCAGTCCC-TACTAA*		52.6	55.1			
26F	CAGTGACTCATACCTGTAATCC		45.5	58.4	60/32	1.5	865
26R	GCTGTACCATAGGATCGTGAC	**G>C**	52.4	59.8			
27F1	TTAGTTAAAAATGAGGCTTCCTC		34.7	56.1	62/35	2.5	260
27F2	AGGCTTGGGGAGGTGAGGTAGGG		65.0	62.0	60/35	1.5	427
27R	CCTGGAGAAGCAATAAGATTCA		40.9	58.4			
28F	GGCTATGTGTGTGTTTTGATGG	**T>G**	45.5	64.0	67/32	1.5	1673
28R	CTTGGCAGATGCATGTAGCAG	**G>C**	52.3	65.0			
29F	GCCTGGTGGCCATTGTCC		66.6	64.9	60/35	1.5	250
29R	TTATTTTGAATCAAGTAGAGCCA		30.4	55.9			
30F	GAGGCTCTTTTTGTGGCTCT		50.0	58.6	60/35	1.5	404
30R	CTTAAAAGCTGAATGATTCAGAA		30.4	55.6			
31F	GCAGTCAGTACTGACTTGGC		55.0	56.0	60/35	1.5	278
31R	AACATCCAAAAGTAACCCCAGC		45.4	61.4			
32F	CATCTTCCTCATAGGGCTGA		50.0	57.8	56/35	1.5	396
32R	CCTGGGGTCTCTTGAATAC		52.6	54.5			
33F	CAGGATGACCACCTCAGCCT		60.0	62.6	61/35	2.5	436
33R	GACCCCTAGAATTGAACTCA	**T>A**	45.0	55.0			
34F	CCTCCTTTGGTCTTAGTCCAGT		50.0	58.7	60/35	1.5	733
34R	CCACTGCTATACCCTGAATAGAC	**G>C**	47.8	57.7			

- **Bold red nucleotides represent mismatches between *VWF* and *VWFP*.**
- **Bold blue nucleotides represent introduced mismatches.**

***** **Indicates no nucleotides present to introduce mismatches between *VWF* and *VWFP***

Appendix 13 List of known SNP identified through DNA sequence analysis cont

SNP reference number	Affected nucleotide	SNP location Exon/Intron	SNP identified in IC
rs2286608	c.1-64C>T	Intron 1	P1F2II1,P2F13I3,P4F5I1,P4F7II1,P5F1II3,P6F4II1,P6F9II1,P7F8I2,P8F2II2, P8F3I2,P8F5II1,P9F14III1,P9F18I1,P10F5II2,P10F8II1,P10F9II3,P12F5II1
rs7980045	c.657+11A>C	Intron 6	P10F5II2,P12F5II1
rs3213721	c.997+32G>A	Intron 8	P7F8I2,P8F2II2,P8F3I2,P8F5II1,P9F14III1,P9F18I1,P10F8II1, P12F5II1
rs55907031	c.998-27C>T	Intron 9	P4F7II1P8F5II1,P10F9II3,P9F18I1
rs1800375	c.1173A>T	Exon 11	P4F7II1,P8F5II1,P9F18I1,P10F9II3
rs1800376	c.1182A>C	Exon 11	P4F7II1,P8F5II1,P9F18I1,P10F9II3
rs1800377	c.1411G>A	Exon 12	P1F2II1, P4F7II1,P8F3I2,P8F5II1,P9F18I1,P10F9II3
rs1800378	c.1451A>G	Exon 13	P1F2II1,P2F13I3,P4F5I1,P4F7II1,P5F1II3,P6F4II1,P6F9II1,P7F8I2,P8F2II2,P8F3I2, P8F5II1,P9F14III1,P9F18II,P10F5II2,P10F7II1, P10F8II1,P10F9II3,P12F5II1
rs7312411	c.1548T>C	Exon 14	P10F5II2, P2F13I3, P5F1II3
rs35365059	c.1626G>A	Exon 14	P8F5II1
rs61908661	c.1945+24C>T	Intron 15	P8F2II2,P9F14III1,P10F8II1
rS216293	c.2282-42C>A	Intron 17	P1F2II1,P2F13I3,P4F5I1,P10F7II1 P6F4II1,P6F9II1,P10F5II2,P10F9II3
rs1063856	c.2365A>G	Exon 18	P2F13I3, P5F1II3,P8F5II1,P9F18I1,P10F5II2,P10F8II1,P12F5II1
rs1063857	c.2385T>C	Exon 18	P2F13I3,P5F1II3,P8F5II1,P9F18I1,P10F5II2,P10F8II1,P12F5II1
rs216325	c.2546+25C>T	Intron 19	P1F2II1,P2F13I3,P4F5I1,P6F4II1,P6F9II1,P7F8I2,P8F2II2,P8F3I2 P9F14III1,P9F18I1,P10F5II2,P10F7II1, P10F9II3,P12F5II1
rs216321	c.2555A>G	Exon 20	P1F2II1,P2F13I3,P4F5I1,P5F1II3,P6F4II1,P6F9II1,P7F8I2, P8F2II2,P8F3I2, P8F5II1,P9F14III1,P9F18I1,P10F5II2,P10F7II1, P10F8II1,P10F9II3,P12F5II1

Appendix 13 List of known SNP identified through DNA sequence analysis cont

SNP reference number	Affected nucleotide	SNP location Exon/Intron	SNP identified in IC
rs1800380	c.2880G>A	Exon 22	P2F13I3, P5F1II3, P8F5II1,P9F18I1 P10F5II2,P10F8II1,P12F5II1
rs34877178	c.2968-53G>A	Intron 22	P2F13I3, P5F1II3,P8F5II1,P9F18I1, P10F5II2,P10F8II1,P12F5II1
rs3858686	c.2968-125C>T	Intron 22	P2F13I3,P5F1II3,P8F5II1,P9F18I1,P10F5II2,P10F8II1,P12F5II1
rs11063993	c.2968-154C>T	Intron 22	P6F4II1,P7F8I2
rs73051263	c.3222+31C>T	Intron 24	P2F13I3,P9F18I1,P10F5II2,P10F8II1,P12F5II1
rs56121649	c.3109-90G>C	Intron 23	P2F13I3, P5F1II3,P9F18I1,P10F5II2,P10F8II1,P12F5II1
rs56068059	c.3109-128G>T	Intron 23	P2F13I3, P5F1II3, P10F5II2
rs4008538	c.3414C>T	Exon 26	P6F9II1,P8F2II2,P8F3I2,P9F14III1,P10F5II2
rs216305	c.5665-118G>A	Intron 33	P1F2II1,P2F13I3,P4F5I1,P4F7II1,P6F4II1,P6F9II1, P10F5II2,P10F7II1, P10F9II3
rs216305	c.5664+175G>A	Intron 33	P1F2II1,P4F7II1,P6F4II1,P6F9II1,P10F5II2,P10F7II1, P10F9II3
rs216902	c.5844C>T	Exon 35	P4F5I1, P4F7II1, P6F4II1
rs71579337	c.6064-50A>G	Intron 35	P1F2II1,P8F3I2
rs17491334	c.6064-71C>T	Intron 35	P2F13I3,P5F1II3, P10F5II2, P10F9II3

Appendix 13 List of known SNP identified through DNA sequence analysis cont

SNP reference number	Affected nucleotide	SNP location Exon/Intron	SNP identified in IC
rs3741906	c.6063+25G>A	Intron 35	P6F4II1,P7F8I2
rs34230288	c.6532G>T	Exon 37	P9F14III1
rs177702	c.6799-14C>T	Intron 38	P1F2II1,P2F13I3,P4F5I1,P4F7II1,P5F1II3,P6F4II1,P6F9II1,P7F8I2,P8F2II2,P8F3I2, P8F5II1,P9F14III1,P9F18II,P10F5II2,P10F7II1, P10F8II1,P10F9II3,P12F5II1
rs10849371	c.6846A>G	Exon 39	P2F13I3, P5F1II3, P8F5II1,P10F5II2, P10F8II1,P10F9II3
rs2070885	c.6976+59C>T	Intron 40	P6F4II1,P7F8I2
rs55867239	c.6977-22C>T	Intron 40	P2F13I3, P5F1II3, P8F5II1,P10F5II2,P10F8II1,P10F9II3
rs2286937	c.7287+61C>T	Intron 42	P6F4II1
rs216867	c.7239T>C	Exon 42	P1F2II1,P2F13I3,P4F5I1,P4F7II1,P5F1II3,P6F4II1,P6F9II1,P7F8I2,P8F2II2,P8F3I2, P8F5II1,P9F14III1,P9F18II,P10F5II2,P10F7II1, P10F8II1,P10F9II3,P12F5II1
rs216868	c.7082-7C>T	Intron 42	P1F2II1, P4F5I1, P4F7II1, P6F4II1, P7F8I2,P8F2II2,P8F3I2,P8F5II1, P9F18I1,P10F8II1, P12F5II1
rs3819539	c.7288-21C>T	Intron 42	P6F4II1
rs3819540	c.7288-19C>T	Intron 42	P6F4II1
rs2270239	c.7549-59A>C	Intron 44	P2F13I3,P4F5I1,P5F1II3,P7F8I2,P8F2II2,P8F3I2,P8F5II1 P9F14II1,P10F5II2,P10F9II3,P12F5II1

Appendix 13 List of known SNP identified through DNA sequence analysis cont

SNP reference number	Affected nucleotide	SNP location Exon/Intron	SNP identified in IC
rs2286938	c.7082-48G>A	Intron 41	P6F4II1
rs11063962	c.7771-13C>T	Intron 46	P1F2II1, P5F1II3
rs55687637	c.7887+12T>C	Intron 47	P12F5II1
rs2286646	c.8115+66T>C	Intron 49	P6F9II1, P8F3I2,P8F5II1, P9F14III1,P9F18I1,P10F5II2,P10F8II1, P12F5II1
rs41276732	c.8079C>T	Exon 49	P2F13I3
rs7962217	c.8113G>A	Exon49	P8F5II1,P9F18I1,P10F8II1,P12F5II1
rs2270152	c.8116-20A>C	Intron 50	P8F3I2,P8F5II1,P9F14III1,P9F18I1,P10F8II1, P12F5II1
rs2270151	c.8155+50C>T	Intron 50	P6F9II1,P8F3I2,P9F14II1,P10F5II2,P10F8II1
rs2362483	c.8253+32T>C	Intron 51	P7F8I2,P8F2II2,P8F3I2,P8F5II1,P9F14III1,P9F18I1,P10F8II1,P12F5II1
rs7976955	c.8442+204C>T	3' untranslated region	P1F2II1, P2F13I3, P5F1II3, P6F9II1,P8F3I2, P8F5II1,P9F18I1,P10F8II1P12F5II1
rs216312	c.3675-75A>G	Intron 27	PIF2II1, P2F13I3,P4F5I1,P6F4II1,P6F9II1, P10F5II2, P10F7II1,P10F9II3
rs216311	c.4141A>G	Exon 28	PIF2II1, P2F13I3, P4F5I1, P6F4II1, P6F9II1, P10F5II2, P10F7II1,P10F9II3
rs216310	c.4641T>C	Exon 28	PIF2II1, P2F13I3, P4F5I1, P6F4II1, P6F9II1, P10F5II2, P10F7II1, P10F9II3
rs1800382	c.4196G>A	Exon 28	P4F5I1
rs1800383	c.4414G>C	Exon 28	P6F4II1
rs6127535	c.5049A>C	Exon 28	P5F1II3

Appendix 14 List of present identified mutations in the 18 IC

Index Case	Identified mutation	Copy number variation (CNV)
P1F2II:1		NT
P2F13I:3		No CNV
P4F5I:1		NT
P4F7II:1		NT
P5F1II:3	**p.[R854];[W2271G]**	No CNV
P6F4II:1		No CNV
P6F9II:1		No CNV
P7F8I:2		No CNV
P8F2II:2	**p.Q2544X**	No CNV
P8F3I:2		NT
P8F5II:1		NT
P9F14II:2	**p.[R924Q;C1927R]** **c.1533+1G>T**	NT
P9F18I:1	**p.[S539fs];[C1157R]**	No CNV
P10F5II:2	**p.L1382=**	NT
P10F7II:1		No CNV
P10F8II:1	**c.1432+1G>T; p.R816W**	NT
P10F9II:3		NT
P12F5II:1		NT

NT (not tested)

Appendix 15 Pedigree of family P5F1

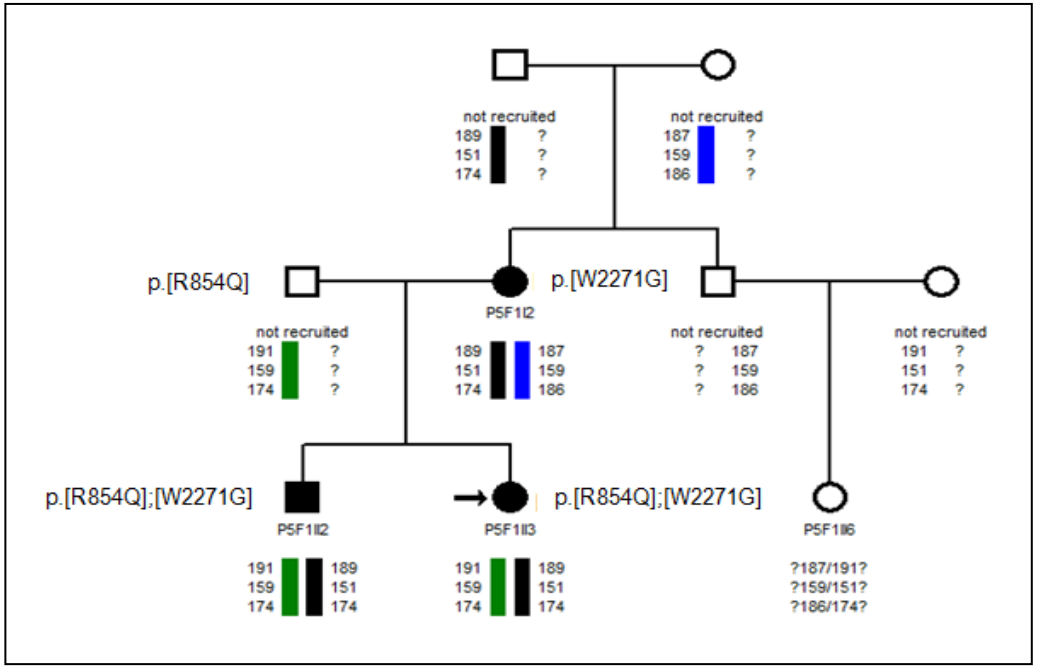

Phenotypic data for family P5F1

Family member	Status	BS	VWF:Ag IU/dL	VWF:RCo IU/dL	FVIII:C IU/dL	VWF:CB IU/dL	VWFpp	VWF:FVIIIB	Multimer profile	ABO genotype
I:2	AFM	7	38	37	85	NT*	71.3	1.185 Normal	Normal	O/A
II:2	AFM	-1	37	43	34	NT*	64.7	NT*	Normal	O/A
II:3	IC	2	37	32	28	43	66.8	0.313 (Heterozygous)	Normal	O/A
II:6	UFM	-2	73	59	91	NT*	96.3	NT*	Normal	O/A

*** Not tested**

Appendix 16 Pedigree of family P9F14

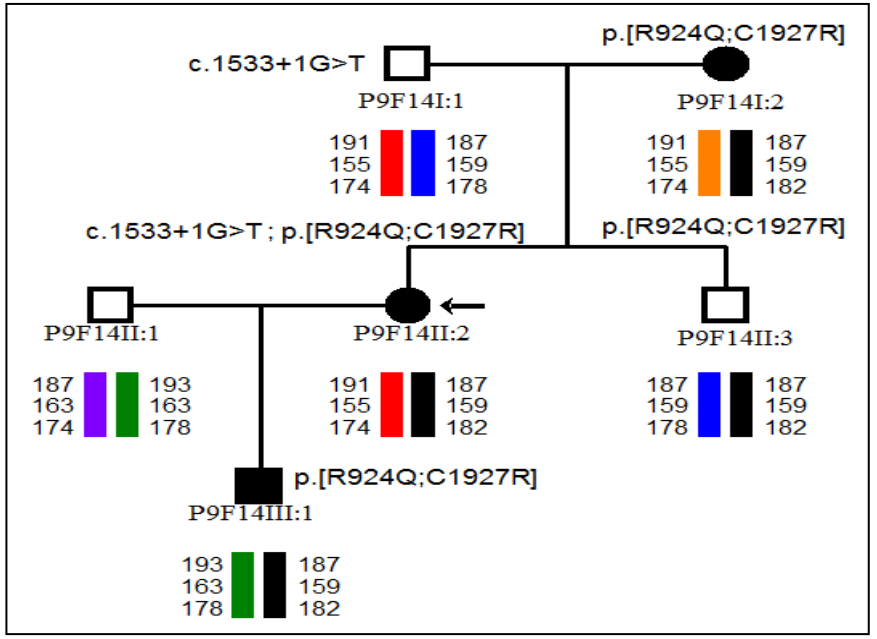

Phenotypic data for family P9F14

Family member	Status	BS	VWF:Ag IU/dL	VWF:RCO IU/dL	FVIII:C IU/dL	CB/Ag	Multimer pattern	ABO genotype
I:1	UFM	0	88	79	82	NT	Normal	O/O
I:2	AFM	4	57	58	63	NT	Normal	A/A
II:1	UFM	0	150	215	88	NT	Normal	O/A
II:2	IC	18	3	3	7	0.33	Abnormal	O/A
II:3	UFM	5	57	80	50	NT	Abnormal	A/B
III:1	AFM	1	19	18	25	0.63	Abnormal	O/O

Appendix 17 Pedigree of family P6F5

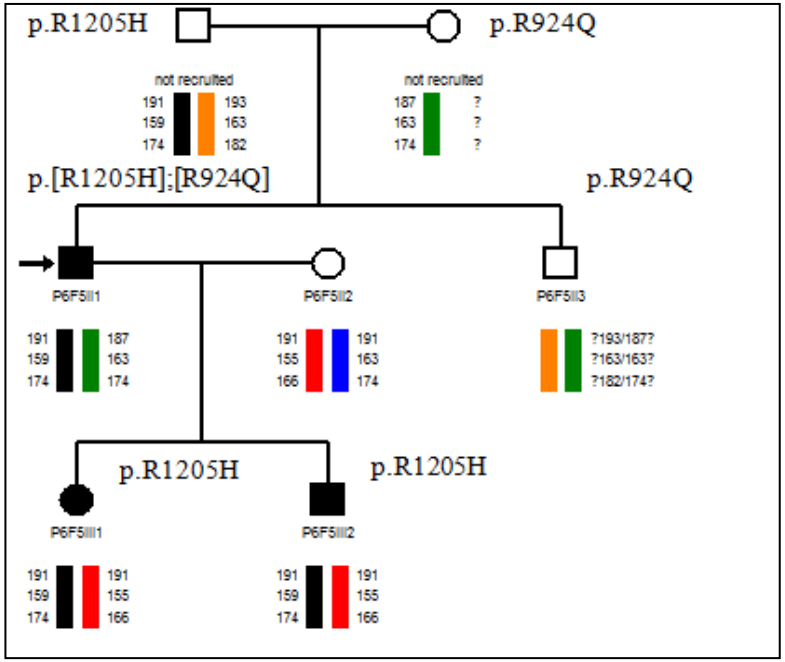

Phenotypic data for family P6F5

Family member	Status	BS	VWF:Ag IU/dL	VWF:RCO IU/dL	VWF:CB IU/dL	VWFpp	VWF:FVIIIB	pp/Ag ratio	FVIII:C IU/dL	Multimer profile	ABO genotype
II:1	IC	18	11	7	6	127.5	1.15 (Normal)	11.6 ↑	18	Normal	O/O
II:2	UFM	1	95	90	NT	142.8	NT	1.5	112	Normal	O/O
II:3	UFM	-1	131	95	NT	115.5	NT	0.9	107	Normal	O/A
III:1	AFM	3	15	17	NT	141.3	1.2 (Normal)	9.4↑	28	Normal	O/O
III:2	AFM	2	16	25	NT	172.6	1.32 (Normal)	10.8↑	44	Normal	O/O

Appendix 18 Pedigree of family P9F18

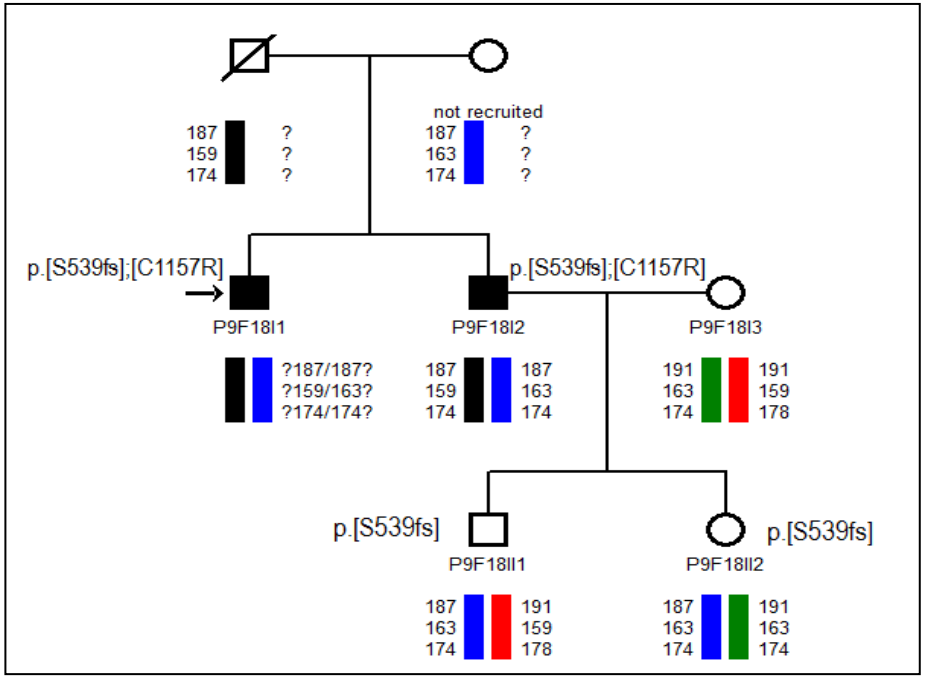

Phenotypic data for family P9F18

Family member	Status	BS	VWF:Ag IU/dL	VWF:RCO IU/dL	FVIII:C IU/dL	VWF:CB	VWFpp	VWF:FVIIIB	Multimer profile	ABO genotype
I:1	IC	9	3	3	3	0.7	NI*	NI*	Abnormal	O/O
I:2	AFM	10	3	3	3	NT	3.4	NI*	Abnormal	O/B
I:3	UFM	-2	48	45	41	NT	100.7	NT‡	Normal	O/A2
II:1	UFM	2	60	69	74	NT	100.1	NT‡	Normal	A2/B
II:2	UFM	0	53	50	75	NT	94.4	NT‡	Normal	O/B

*Not interpretable ‡Not tested

Appendix 19 Pedigree of family P10F5

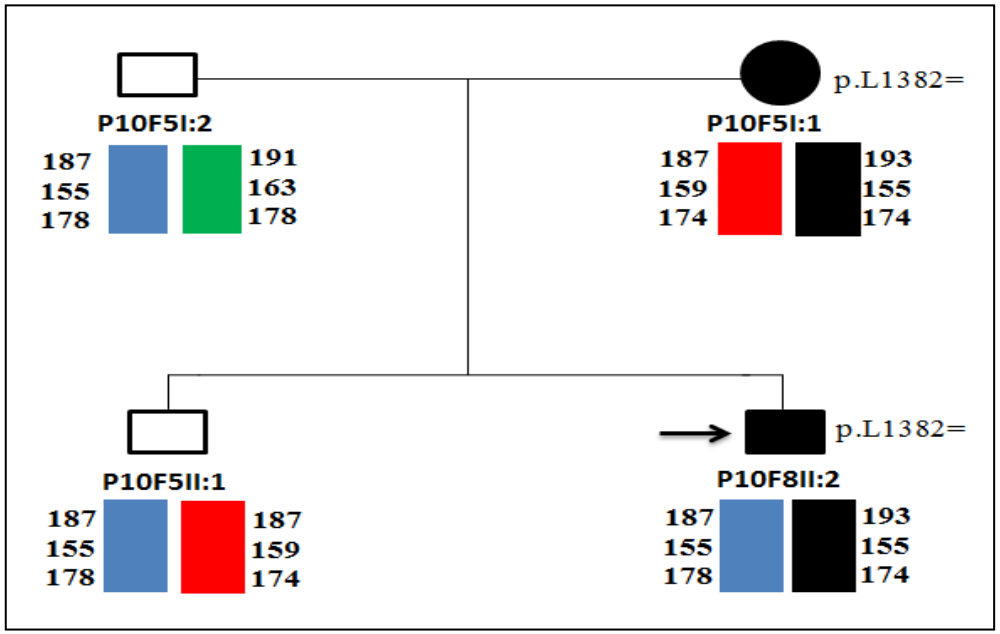

Phenotypic data for family P10F5

Family member	Status	BS	VWF:Ag IU/dL	VWF:RCO IU/dL	FVIII:C IU/dL	Multimer pattern	ABO genotype
I:1	AFM	6	54	61	87	Normal	O/O
I:2	UFM	-1	95	78	144	Normal	O/O
II:1	UFM	3	78	53	90	Normal	O/O
II:2	IC	4	48	41	84	Normal	O/O